

Institut de Biochimie  
Université de Fribourg (Suisse)

# Understanding Apoptosis involved in the Development and Treatment of Malignancies

THESE

présentée à la Faculté des Sciences de l'Université de Fribourg  
(Suisse) pour l'obtention du grade de *Doctor rerum naturalium*  
et réalisée à l'Université de California, San Diego (USA)

par

**Davide Genini**

de

Cresciano (TI)

Thèse Nr 1321

Tipo-Offset Jam SA, Prosito TI,  
Juin 2001



Acceptée par la Faculté des Sciences de l'Université de Fribourg (Suisse) sur la proposition du Prof. Sandro Rusconi (UNIFR), du Prof. Jean-Claude Martinou (UNI Lausanne) et du Prof. Lorenzo Leoni (UCSD, San Diego).

Fribourg, le 13 novembre 2000

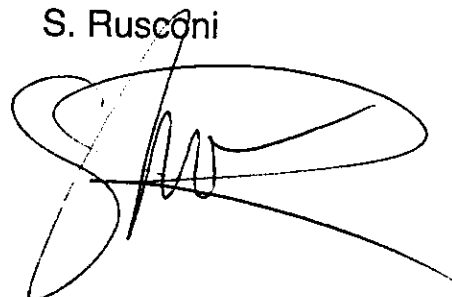
Le Doyen:

A. von Zelewsky

A handwritten signature in black ink, appearing to read 'A. von Zelewsky', written in a cursive style.

Le directeur de Thèse:

S. Rusconi

A handwritten signature in black ink, appearing to read 'S. Rusconi', written in a cursive style with a large loop.







## **ABSTRACTS**

**Apoptosis is a key event occurring in living organisms. In order to maintain tissue homeostasis, a comparable number of cells have to die to compensate for the cells produced by mitosis. However in many diseases this mechanism is altered. Once a malignancy is established, the conventional approach is to treat cells with drugs able to induce apoptosis. Although the execution of apoptosis is a common pathway leading to caspase activation, the triggering events are usually distinct for the different anti-cancer drugs.**

**In this report, we studied apoptosis in general and in specific situations like in HIV infection, we then applied our knowledge to comprehend how several drugs, mainly synthesized in our laboratory, may be effective in cancer therapy. We expose how nucleoside analogs, compounds commonly used for the treatment of Chronic Lymphocytic Leukemia (B-CLL), are able to damage DNA and, in some cases, can even directly affect mitochondria. We explain how the newly synthesized microtubule-disrupting agent indanocine is effective in the killing of multidrug-resistant cells and how etodolac, a nonsteroidal anti-inflammatory drug, may become a useful drug for the treatment of B-CLL.**

**Hopefully, the data reported in this thesis (13 works that have been or are being officially published) can be successfully translated into clinical applications for improved treatment of cancers.**

*L'apoptose (ou mort cellulaire programmée) est un processus cellulaire essentiel présent dans la majorité des organismes. Afin de préserver l'homéostasie des tissus, un nombre comparable de cellules doit mourir pour maintenir l'équilibre avec les cellules produites par mitose. Cependant, dans de nombreuses maladies (en particulier le cancer), ce mécanisme de mort cellulaire est altéré. Une fois la maladie établie, on traite généralement les cellules avec des médicaments capables d'induire l'apoptose.*

*Bien que le programme d'exécution de l'apoptose soit un mécanisme qui conduit en général à l'activation des caspases, les événements qui mènent à la libération du cytochrome C (un autre acteur important dans l'apoptose) sont différents pour chaque médicament.*

*Dans ce travail de thèse, nous avons essayé de comprendre le mécanisme de l'apoptose en général et dans certain cas spécifiques comme lors de l'infection par le virus du SIDA. Notre but est donc d'appliquer nos connaissances afin de comprendre comment certain médicaments, dont quelques uns ont été synthétisés dans notre laboratoire, peuvent être efficaces dans le traitement de certain cancer.*

*Nous démontrons comment des analogues de nucléosides, médicaments utilisés pour le traitement de la leucémie lymphocytaire chronique (B-CLL), sont capables d'endommager l'ADN et quelques fois aussi les mitochondries. Nous démontrons aussi comment un agent destructeur de microtubules (indanocine) est efficace pour tuer les cellules résistantes à plusieurs substances utilisées contre les cancers, et comment etodolac, un médicament anti-inflammatoire non-stéroïdale, réduit le nombre de cellules chez les patients B-CLL.*

*On espère que les résultats reportés dans cette thèse (treize travaux publiés ou en voie de publication) vont pouvoir être appliqués dans le domaine clinique pour l'amélioration des traitements contre le cancer.*





## ***ACKNOWLEDGMENTS***

I want to thank God for the chance He gave me to accomplish one of my dreams. Good and bad circumstances occurred to give me the chance to come to United States and achieve my Ph.D. Of course, I can't forget the courage of Professor Dennis Carson, who decided to consider the request of a Swiss undergraduate student to work in his laboratory. Lorenzo accepted me into his "group", helped me to find financial support, taught me how to work in a laboratory, survived my good and bad mood and was always there when I needed it. Charlie, who gracefully reviewed my Thesis. I can't forget the counterpart in Switzerland, Professor Sandro Rusconi, who allowed me to complete my Ph.D. as an external student and the whole faculty of Uni Fribourg, which technically accepted this situation.

I want to thank everybody in the laboratory, who helped me in the projects; Dennis and Jacques for the HIV collaboration, Rommel and Jessica for the technical support and for the patience they used to read and correct my Thesis and everybody else who tolerated my loud Swiss Italian behavior.

*Voglio dedicare questa tesi alla mia famiglia, che ha sempre accettato ogni mia decisione, anche se e' stato difficile per loro vedermi partire.*

I want to dedicate this Thesis to my family, which always accepted every decision I have taken in my life, even though it was difficult for them to let me go so far away: my mother Rosanna, my father Leardo, my sister Dania, her husband Tiziano, my niece Alexia, the baby inside my sister, and my grandmother Ines. I love you all.



## ***PROLOGUE***

When I first started my studies about ten years ago, the leading idea directing me to biology was that one day I might be able to discover the reason why so many diseases were afflicting human beings and maybe I would be able to go inside a cell and say "You! You villain! I blame you for all this damage".

Now, at the end of my Ph.D., I realize that this is a wonderful, magnificent utopia. In most of the cases, diseases are not the result of a single erroneous event, but rather several circumstances occurring at the same time usually causing sufferance to many people. Because different combinations of events can cause the same illness, it results in the complex task of finding the villain. Still more frustrating is that even if the cause is pinpointed, the identification of the bad guy does not give us the possibility to switch its status from bad into good, simply by snapping our fingers. Restoration of the damage is practically impossible. Maybe one day technology will be so powerful and our knowledge so great that the images seen in Star Trek will not be purely fiction, but we will have enough knowledge to repair DNA and fight any disease with the use of a single instrument. By that time, we will probably be traveling with Tele-transport or Quantum-transport. Presently, the most efficient approach to deal with diseases is not to repair the damage, but to prevent the malady or to kill the affected cells. Prevention can be obtained by vaccines or just by information campaigns with the purpose of warning the people of the danger. If the disease is already present in the body, the only solution is the treatment. Fortunately, in the past we were able to use natural and chemical products capable of fighting many diseases. Unfortunately, only some of the battles have been won, but not the war. Everyday new opponents appear on the enemy battlefield, threatening our health. Malignancy in most of the cases cannot be specifically treated and often side effects of the actual treatments are observed. The tendency is therefore to find new approaches that affect primarily the sick cells, without damaging healthy organs. New compounds are constantly synthesized, tested, and proofed against every kind of disorder. Usually, chance allows a new therapy to be discovered, without even knowing the mechanism of action used by the drug. The fascinating peculiarity of biology is to dig into the field, among the microscopic proteins contained in the cells and find out what is the target that mediates a positive response to the treatment.

This is exactly the idea that drove us to our research. Years ago Professor Dennis Carson and our chemist Dr. Howard Cottam synthesized one of the compound that is still currently used for the treatment of Chronic Lymphocytic Leukemia and Hairy Cell Leukemia, cladribine. The mechanism by which this drug induces lymphocyte depletion in patients was unknown. The cool thing was that this therapy was working in patients. Years later X. Wang and coworkers shed a new light on the intrinsic machinery of apoptosis in cells. Adding one plus one, Dr. Carson realized that the possible machinery we were looking for was somehow related to this discovery. This basically was the starting point of the path, which led us to climb the mountain. On my way I had the unique opportunity to see the whole development of drugs starting from synthesis, screening, application in vitro, and discovery of the biochemical pathway, to the clinical application with patients in phase II of clinical trial. With the increasing knowledge in the field we were then able to apply our understanding of cell death to other fields. And other fields are not so difficult to find: many cancers, infective diseases, neurodegenerative disorders (...) are present in the world and many more are about to be discovered. What we have to do is simply find the way to KILL these disordered pathogens. Kill them by inducing cell death. The plot will be destroying malignancies, featuring apoptosis in the leading role.







# CONTENTS

<b>AKNOWLEDGMENTS.....</b>	<b>IV</b>
<b>PROLOGUE .....</b>	<b>V</b>
<b>ABSTRACT .....</b>	<b>1</b>
<b>INTRODUCTION .....</b>	<b>3</b>
Genesis of death.....	3
Dysfunction of Programmed Cell Death Induces Debilitating Disorders.....	3
MALIGNANCIES CAUSED BY INEFFICIENT DEATH.....	3
DAMAGE INDUCED BY EXCESSIVE DEATH .....	3
Exploration of Death.....	4
THE PROGRAMMED CELL DEATH OR APOPTOSIS.....	4
INFLAMMATORY NECROSIS .....	4
DEATH OF ELDERLY CELLS, SENESENCE .....	5
Apoptosis Is A Complicated and Well-Regulated Process.....	5
THE DECISION IS TAKEN: CASPASE ACTIVATION.....	7
ACTIVATION OF THE CASPASES CASCADE BY GATHERING.....	8
THE APOPTOTIC PHENOTYPE IS CAUSED BY SPECIFIC PROTEIN CLEAVAGE .....	8
Caspases Activated by Signaling Events .....	10
THE RECEPTOR-MEDIATED EXTRINSIC PATHWAY .....	10
THE INTRINSIC PATHWAY .....	10
THE ESSENTIAL ROLE OF MITOCHONDRIA.....	10
RELEASE OF THE DEADLY CYTOCHROME C .....	13
THE TWO PATHWAYS COOPERATE TO ENHANCE THE POWER OF KILLING.....	13
Taking the Decision of Death .....	14
A GENE INVOLVED IN THE TRIGGERING OF APOPTOSIS: p53.....	14
COULD OTHER CELLULAR SIGNALS INDUCE APOPTOSIS?.....	16
Regulation of Apoptosis Prevents Undesired Surprises.....	16
BCL-2 FAMILY MEMBERS .....	16
IAPs.....	18
AKT.....	18
CLL: A Beautiful Primary System To Study Apoptosis.....	19
<b>DESCRIPTION AND SIGNIFICANCE OF THE PERSONAL CONTRIBUTIONS ...</b>	<b>21</b>
<b>ARTICLES .....</b>	<b>23</b>
<b>PAPERS.....</b>	<b>25</b>
<b>EPILOGUE.....</b>	<b>39</b>
<b>REFERENCES.....</b>	<b>41</b>
<b>APPENDIX .....</b>	<b>49</b>





## **ABSTRACT**

Thirty years ago, the term apoptosis was conceived to define a mechanism of cell death programmed by the cell itself. Since then, apoptosis has become one of the most studied events in the cell, because it has been correlated to several diseases. Cancers arise in some cases from the inability of a set of cells to undergo apoptosis. Other malignancies like immunodeficient diseases and neurodegenerative disorders often present a defect in regulation of apoptosis.

In this thesis I mostly present data on drug-induced and virus-mediated apoptosis. Novel drugs were synthesized and developed in our laboratory, tested for their cytotoxicity in tumor models and their mechanism of action was elucidated.

The antitumoral agents most commonly used in the clinical treatment of Chronic Lymphocytic Leukemia (B-CLL), are nucleoside analogs. Developed more than 20 years ago in the laboratory of Dr. Dennis Carson, Cladribine (2CdA) together with other analogs such as Fludarabine (F-ara-A) and CaFdA, were shown to reduce the count of B-CLL cells in the patients, but their complete mechanism of action was unresolved until a few years ago. In our research, we were able to demonstrate the ability of these compounds to induce DNA damage, activate the p53 pathway and induce cytochrome c release from mitochondria. We also demonstrated that the same compounds can also activate the complex downstream cytochrome c release of Apaf-1 and caspase-9 in a cell-free system. Interestingly, big differences were observed in the mitochondrial toxicity of the various purine nucleoside analogs. 2CdA and CaFdA were able to induce direct cytochrome c release by directly damaging mitochondria. F-ara-A on the other hand absolutely required a p53 intact pathway to kill B-CLL cells. We showed that CLL cells isolated from patients with non-functional p53 pathway were resistant to F-ara-A.

Indanocine, a novel microtubule-binding drug, was also developed in our laboratory. Indanocine was shown to induce apoptosis in multidrug-resistant cell lines by binding to tubulin and inducing its depolymerization. To better understand its mechanism of action, we selected and analyzed a resistant clone (CEM-178) from a T lymphoblastoid CCRF-CEM cell line.

B-CLL cells have been known to be hypersensitive to microtubule-binding antimetabolic agents, such as colchicine, for more than 30 years, but the mechanism of this cytotoxicity was never fully elucidated. For this reason, we tested indanocine on primary B-CLL cells, and demonstrated its potent and selective cytotoxicity. We carefully studied the anti-CLL activity of indanocine, and showed the activation of the intrinsic pathway of apoptosis. The anti-apoptotic molecule Bcl-2 was phosphorylated and this resulted in its dimerization, subcellular relocalization, and inactivation. In addition, indanocine treatment reduced the amount of cytosolic pro-apoptotic Bax, released cytochrome c from the mitochondria to the cytosol, and activated the caspases. Concomitantly with Bcl-2 phosphorylation activation of the JNK pathway was observed.

Etodolac, a non-steroidal anti-inflammatory drug already used in the clinic for the treatment of rheumatoid arthritis, was able to give relief to patients affected by B-CLL. Here I report the data about the mechanisms by which etodolac induces apoptosis in B-CLL cells, which include the down-regulation of the anti-apoptotic molecule Mcl-1, the reduction of the mitochondrial membrane potential and the activation the PPAR- $\gamma$  receptor, which is over-expressed in B-CLL. Etodolac also activated cell movement (chemotaxis) in B-CLL cells.

Depletion of CD4+ T lymphocytes is observed during infection by HIV-virus. In this thesis, we elucidated the mechanism of action by which CD4+ are depleted by HIV. We propose that, once cells are infected, the virus integrates in the genomic DNA, activating the intrinsic pathway of apoptosis, by phosphorylation of p53 at residue Ser15. The p53 phosphorylation results in the up-regulation of pro-apoptotic protein Bax, which causes the release of cytochrome c from the mitochondria and the activation of the caspase cascade.

The results reported in this thesis help us understand the mechanism of action of widely used and newly synthesized drugs. Application of these findings in the clinic will help lead to more affective treatment of cancer and AIDS. Moreover a deeper interpretation of the data and an aimed design of new compounds will result in the development of more potent and less toxic treatments.



# ***INTRODUCTION***

## **Genesis of death**

At the beginning there was only life! The biology of the cell was mainly development, metabolism and division. Then researchers realized one important thing: every second in the human body hundreds of thousands of cells were produced by mitosis. The dilemma was where those cells were ending up. Since the size of the human body is maintained and the number of cells is growing, an important event not previously considered had to be part of normal life. Hence death as a daily occurrence was recognized. Cell death is so important that more than 99.9% of the total number of cells generated during the course of a human lifetime go on to die (1).

Good and bad ways for cells to die exist. The “good” cell death is observed when cells silently die, vanishing without a trace, without any accompanying inflammatory response. This usually happens in normal development or tissue homeostasis. Cells shrink and condense, whereas the plasma membrane retains its integrity. Then the cells are rapidly phagocytosed by macrophages or degraded. Almost 30 years ago, this process was termed as “apoptosis” (2). The “bad” cell death usually occurs at the center of acute lesions such as traumas and ischemia, and lead to an inflammatory response. Those cells and their organelles tend to swell and disrupt, leaking their contents into the environment. This is also called “necrosis”.

The most shocking discovery for these scientists was that finally they could talk about death without fear. Death was no longer a taboo, the end of the human being, the constant impending threat, growing bigger with time, but rather it was something helping life. Cell death is used by multicellular organisms for development and morphogenesis to control cell number, as defensive strategy to remove infected, mutated or damaged cells. Apoptosis is important in the formation of the fetus (3, 4). It is involved in the formation of tubes, the separation of the digits, the remodeling of bones, and involution of the mammary gland (5).

## **Dysfunction of Programmed Cell Death Induces Debilitating Disorders**

Closer analysis however revealed that death was still playing a role in the termination of life. Dysfunction of cell death was leading to debilitating disorders. Predominance of cell survival over death or death over survival contributes to the pathogenesis of a number of human diseases, including cancer, viral infection, autoimmune disease, neurodegenerative disorders, and AIDS (6).

### ***MALIGNANCIES CAUSED BY INEFFICIENT DEATH***

Cell death is a strictly regulated process. Mediators of apoptosis are constitutively expressed in many cell types and these are controlled by the environment. Most normal cells are programmed to commit suicide if survival signals are not received from the environment (7). For example, in metastatic tumors cells have circumvented this homeostatic mechanism and can survive at sites distinct from the tissue in which they arose.

Clearly all tumors demonstrate this progress of life leading over death. A tumor is considered as an uncontrolled overgrowth of cells. Death mechanisms are not capable to compensate for cell overgrowth and usually the reason lays in the inability of genes and proteins that control apoptosis to give the right orders to induce apoptosis. It is now clear that some oncogenic mutations disrupt apoptosis, leading to tumor initiation, progression and metastasis (8).

Excessive survival is also observed in autoimmune diseases. During development of the immune system an abundant number of immune cells are produced. In healthy individuals auto-reactive cells and excessive cells are generally removed from the body. Failure of the apoptotic machinery promotes survival of cells that are shown to be autoimmune responsive during development of the disease.

Sometimes cell survival overcome cell death thanks to the help received from the exterior. During viral infections, cells usually undergo suicide as a cellular defense mechanism to prevent viral spread. Sometimes viral proteins help survival armies to circumvent the host defense, favoring virus replication and infection.

### ***DAMAGE INDUCED BY EXCESSIVE DEATH***

Excessive cell death is also a problem and can result from conditions that enhance the accumulation of signals that induce apoptosis.

In HIV-induced lymphocyte depletion, AIDS has been directly correlated with the CD4<sup>+</sup> T cell depletion. CD4<sup>+</sup> cells are involved in the immune response against viral infection. HIV virus can lead directly to apoptosis in defensive host cells, reducing the host defensive barrier to promote self-survival (9).

A wide variety of neurological diseases are characterized by the gradual loss of specific sets of neurons (10). Such disorders include Alzheimer's disease, Parkinson's disease, amyotrophic lateral sclerosis, retinitis pigmentosa, spinal muscular atrophy, and various forms of cerebellar degeneration. The cell loss in these diseases does not induce an inflammatory response, and apoptosis appears to be the mechanism of cell death (11).

Disorders of blood cell production, such as myelodysplastic syndrome and some forms of aplastic anemia are also associated with increased apoptotic cell death within the bone marrow (12). These disorders could result from the activation of genes that promote apoptosis, acquired deficiencies in stromal cells or hematopoietic survival factors.

## **Exploration of Death**

Aware that death was still to be feared, researchers started to explore cell death. This was the only way to face cell death disorders and fight them. Cell death was thus taken apart. Apoptosis and necrosis were analyzed in their small details. Scientists realized that there was no good and bad cell death. Apoptosis was not necessarily a good way to die and necrosis a bad way to die. Moreover, a distinct demarcation could not be designated between the two deaths (13). If damage is too violent, cells have no choice but to undergo the genetically uncontrolled necrotic form of death. On the other hand, when damage is subtler biochemical signals will decide whether the cell may continue to live or should die. In this case, death normally occurs through apoptosis. The reality is usually somewhere in the middle.

### ***THE PROGRAMMED CELL DEATH OR APOPTOSIS***

Navigation into meanders of cell death brought scientists to face a death process encoded by the organism for the sole purpose of killing its own cells. The great majority of our cells are destined to die by just such a physiological process. The programmed cell death that occurs as part of normal mammalian development was first observed nearly a century ago (14), but the idea that animal cells had a built-in death program was generally accepted only 20 years ago (15). Biologists started to appreciate that the regulation of apoptosis is just as complex as the regulation of cell proliferation only at the beginning of the nineties (16).

The evolution of multicellularity and cell specialization brought with it a need for the regulation of cell death by intracellular signaling (17). Genetic studies in the nematode *Caenorhabditis elegans* identified genes that seem dedicated to the death program and its control. Although diverse signals can induce apoptosis in a wide variety of cell types, a number of evolutionarily conserved genes regulate a final common cellular suicide pathway that is conserved from worm to human (18, 19).

Apoptosis results in cytoskeletal disruption, cell shrinkage, and membrane blebbing. Apoptosis also involves characteristic changes within the nucleus. The nucleus undergoes condensation as endonucleases are activated and begin to degrade nuclear DNA. In many cell types, DNA is degraded into DNA fragments the size of oligonucleosomes, whereas in others larger DNA fragments are produced. Apoptosis is also characterized by a loss of mitochondrial function. The dying cells maintain their plasma membrane integrity. However, alteration in the plasma membrane of apoptotic cells signals neighboring phagocytic cells with specific receptors (20) to engulf them and thus complete the degradation process. Cells not immediately phagocytosed break down into smaller membrane-bound fragments called apoptotic bodies (16, 21).

### ***INFLAMMATORY NECROSIS***

Another research route led to the study of inflammation-accompanied necrosis. Necrosis involves cytoplasmic blebbing, dilatation of the endoplasmic reticulum (ER), swelling of the cytosol, alteration of mitochondria, and dissolution of other organelles (22). Disruption of the cell membrane and release of cytosolic and nuclear proteins leads to an inflammatory response (23).

## DEATH OF ELDERLY CELLS, SENESENCE

In addition to apoptosis and necrosis, other types of cell death were also observed. Senescence is an irreversible program of cell-cycle arrest that is disrupted in many tumors or tumor-derived lines. Replicative senescence was originally defined by the observation that primary cells have a genetically determined limit to their proliferation potential in cell culture. Telomeres shorten during each cell division unless telomerase is expressed, and it is thought that some aspect of excessive telomere shortening activates cell-cycle arrest and other characteristics of senescence (24).

## Apoptosis Is A Complicated and Well-Regulated Process

Researchers started to dig into the apoptosis field by studying an animal, which usually digs into the ground. The worm *Caenorhabditis elegans* is a small (about 1 mm long) soil nematode found in temperate regions. In the 1960's, Sydney Brenner began using it to study the genetics of development and neurobiology (25). Since then, hundreds of scientists around the world have been working full time investigating the biology of *C. elegans*. *C. elegans* is a primitive organism, which shares many of the essential biological characteristics found also in human biology. The worm is conceived as a single cell, which undergoes a complex process of development, starting with embryonic cleavage, proceeding through morphogenesis and growth to the adult. It has a nervous system with a 'brain' (the circumpharyngeal nerve ring). It exhibits behavior and is even capable of rudimentary learning. It produces sperm and eggs, mates and reproduces. After reproduction it gradually ages, loses vigor and finally dies. Embryogenesis, morphogenesis, development, nerve function, behavior and aging, and how genes determine them: the list includes most of the fundamental mysteries of modern biology.

*C. elegans* has been used as a model system to study the genetics of apoptosis (26). Ced-3 was identified as the most important protein among the 14 gene products that have been characterized as important for the process of programmed cell death (27, 28). The discovery that the structure of Ced-3 was closely similar to Interleukin-1 $\beta$  Converting Enzyme (ICE), a cytoplasmic protease responsible for the cleavage of the inactive precursor cytokine IL-1 $\beta$  to the mature pro-inflammatory active cytokine in mononuclear cells, suggested that ICE might represent a mammalian counterpart of Ced-3 and therefore might play a role in apoptosis (29). IL-1 $\beta$  was cleaved at the Asp 116 residues by ICE, also called caspase-1, which was identified as the prototype of a new family of cytoplasmic endoproteases (30). Transfection of ICE into mammalian cells was shown to induce apoptosis through the Fas pathway (31). Cells without measurable ICE proteins were still able to undergo apoptosis induced by gamma-irradiation, viral infection, or addition of various drugs or biosynthetic inhibitors. This precluded the presence in the cells of enzymes similar to ICE, able to induce cell death (32).

A caspase family was then characterized. Caspases were recognized as the executioners of apoptosis. Once activated, cells are committed to death. Fourteen mammalian members of this protease family have been identified so far (Table 1) (33-35). Sequence analysis and X-ray crystallography data suggested that all caspases (Cysteiny ASPartate-specific proteASE) share common structures within three domains: An N-terminal prodomain, a large subunit containing the active site cysteine within a conserved QACXG motif, and a C-terminal small subunit. An aspartate cleavage site separates the prodomain from the large subunit, and an interdomain linker containing one or two aspartate cleavage sites separate the large and the small subunit (Figure 1). Activation involves proteolytic processing between small and large domains, followed by association of the large and small subunit to form heterodimer, usually accompanied by the removal of the prodomain. Homodimerization of two caspases will follow catalytic cleavage, where both homodimers contain an independent active site (Figure 2).

Zymogen	Size of prodomain and activated form (kDa)	Contained motif	Adaptor molecule	Tetrapeptide preference			
				P <sub>1</sub>	P <sub>2</sub>	P <sub>3</sub>	P <sub>4</sub>
<b>Apoptotic Initiators</b>							
Caspase-2	51 ý 20 / 12	CARD	RAIDD	D	Q	Q	D
Caspase-8	55 ý 18 / 11	DED	FADD	V	E	T	D
Caspase-9	45 ý 17 / 10	CARD	Apaf-1	P	E	P	D
Caspase-10	55 ý 17 / 12	DED	FADD	I	E	A	D
Granzyme B				I	E	T	D
<b>Apoptotic Executioners</b>							
Caspase-3	32 ý 17 / 12			I	E	T	D
Caspase-6	34 ý 18 / 11			T	E	V	D
Caspase-7	35 ý 20 / 12			I	Q	A	D
<b>Cytokine Processors</b>							
Caspase-1	45 ý 20 / 10	CARD		W	F	K	D
Caspase-4	43 ý 20 / 10	CARD		W	V	R	D
Caspase-5	48 ý 20 / 10			W	V	R	D
Caspase-11	42 ý 20 / 10						D
Caspase-12	50 ý 20 / 10						D
Caspase-13	43 ý 20 / 10						D
Caspase-14	30 ý 20 / 10						D
<b>Invertebrate Caspase</b>							
CED-3	56 ý 17 / 14	CARD	CED-4	D	S	V	D
DCP-1g	36 ý 22 / 13						D

Table 1 **Caspase family members**

14 mammalian members of this family have been identified. All these proteins have similar structure. The table describes the characteristics of the single caspases.

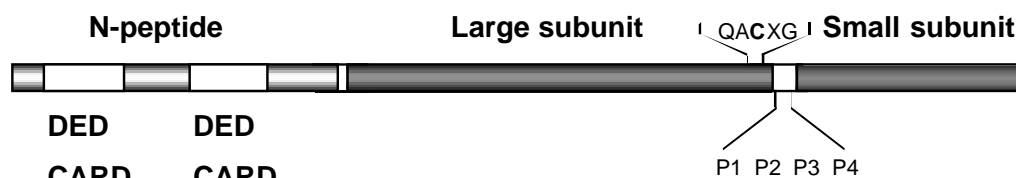


Figure 1 **Caspase Structure**

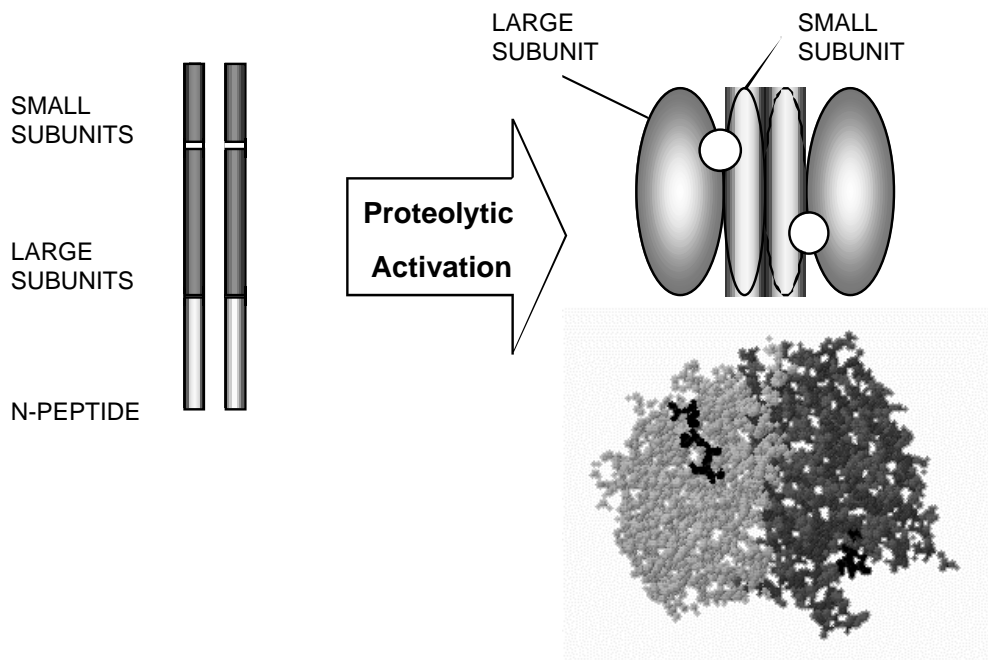


Figure 2 **Caspase activation by proteolysis and zymogenicity**

Pro-caspases are stored in the cells in an inactive zymogen form. Activation usually proceeds in all caspases by cleavage at the conserved Asp-297. The small and the large subunit associate and the functional active site is localized in the white circle. Frequently an N-terminal peptide is removed. For their activation caspases have to homodimerize. Both homodimers contain a substrate binding site (Black peptide in the 3D representation (36))

Caspases are the most specific proteases, with an absolute requirement for cleavage after aspartic acid. The recognition of a tetrapeptide pocket is also a necessary requirement for efficient catalysis. Substrate specificity of caspases has been extensively studied by using synthetic tetrapeptides (37) (Figure 1). The tertiary structure may also influence the substrate recognition. Cleavage of proteins by caspases is not only specific, but also highly efficient ( $K_{\text{cat}}/K_m > 10^6 \text{ M}^{-1}\text{S}^{-1}$ ). Caspase prodomains also vary in length and sequence. Long prodomains function as signal integrators and promote interactions with activator molecules. Caspases involved in apoptosis are divided into two groups: initiator caspases (2, 8, 9 and 10), which generally act upstream of the small prodomain apoptotic executioner caspases (3, 6 and 7) (38). By contrast caspase-1 and 11 function predominantly as cytokine processors (39, 40). Less is known about caspase 4, 5, 12, 13 and 14.

### **THE DECISION IS TAKEN: CASPASE ACTIVATION**

Caspases are the executioners in the apoptotic process. What is the triggering event inducing these slayers to kill? Caspases are constitutively expressed in living cells as inactive zymogens. Zymogenicity represents the ratio of activity of the cleaved form compared to the zymogen form (Table 2). Initiator caspases zymogenicity in fact is low, indicating that cleavage is not essential for their initiation, implying another mechanism for the cascade activation. In contrast executioner caspases requires processing for their activation. Evidence suggests caspase activation may proceed by autoactivation, transactivation or proteolysis by other proteinases (41).

Protease	Zymogenicity
Caspase-3	>10,000
Caspase-8	100
Caspase-9	10
Trypsin	>10,000

Table 2 **Zymogenicity** is defined as the ratio of the activity of a processed protease to the activity of the zymogen on any given substrate (42). Data for trypsin is taken from ref. (42).

According to these observations, caspase oligomerization is thought to be important for caspase activation. Vicinity allows autoactivation of the initiator caspases, which consequently activate the executioner caspases in the apoptotic cascade. Forced oligomerization of Caspase-9, -8 or Ced-3 has been shown to promote apoptosis (43-45).

In vivo adapter molecules mediate oligomerization of long prodomain caspases. The pro-caspases have been demonstrated to possess low but detectable proteolytic activity. Once activated, caspases transactivate other procaspases, providing the opportunity for cascade amplification and positive feedback. Caspase-8 efficiently activates caspase-3 ( $K_{cat}/K_m > 8.7 \times 10^5 \text{ M}^{-1}\text{S}^{-1}$ ) and caspase-3 in turn may activate procaspase-8 (46). Caspases can be activated also by non-caspase proteinases such as granzyme B, which is excreted by T cells in immunologic response (47). Granzyme B is also an aspartate-specific serine protease, which can activate several caspases and induce apoptosis (48).

### **ACTIVATION OF THE CASPASES CASCADE BY GATHERING**

In order to be efficient, caspases require adaptor molecules, which are essential to bring initiator caspases together to induce their activation by vicinity. Induction of the interaction is triggered by proapoptotic signals. Specific domains mediate the binding. Activation of caspase-8 requires association with its cofactor FADD (Fas-Associated protein with Death Domain) through death effector domains (DED), also found in caspase-10 (49, 50). Procaspase-9 activation involves the formation of a complex with cofactor Apaf-1 (APOptotic Activating Factor-1) through the CASpase Recruitment Domain (CARD), present also in procaspase-1, -2, -4, and -5 (51). Hydrophobic interactions are important for DED-DED binding, whereas electrostatic interactions are critical for CARD-CARD binding. The result in each case of caspase recruitment is the formation of a complex called "apoptosome", whose functions to mediate the activation of caspases (52).

Activation of initiator caspases by binding to cofactors and not by cleavage may play a role in the prevention of undesired activation of the cascade. Due to the intrinsic activity possessed by pro-caspases, unexpected activation by cleavage could happen. Association instead is more controllable, and the ability of adapter molecules to activate the caspases can be regulated by other proteins that appear to directly interact with the adapter or with the caspases itself, as for example the inhibitor of apoptosis IAP. Zymogenicity data on initiator caspases supports this hypothesis (41).

### **THE APOPTOTIC PHENOTYPE IS CAUSED BY SPECIFIC PROTEIN CLEAVAGE**

What is surprising in apoptosis is that the caspase pathway takes place in the interior of a cell. The fact that proteolytic activity inside the cell is responsible for its demise suggests that the main role of caspases is to destroy intracellular proteins in such a way that the cell would not be able to function (53). In fact, one of the roles of caspases is to inactivate proteins that protect living cells from apoptosis. Cleavage of DNA-Protein Kinase, U1 snRNP-70K, ATM, PARP, proteins involved in DNA repair, splicing and replication prevent the induction of repair in cells targeted to apoptosis (54, 55). Another example is the cleavage of I<sup>CAD</sup>/DFF 45, an inhibitor of the nuclease responsible for DNA fragmentation CAD (Caspase-Activated Deoxyribonuclease). CAD is usually present as an inactive complex with I<sup>CAD</sup>. During apoptosis, caspases cleave I<sup>CAD</sup> and release active



CAD enzyme, which promotes chromatin condensation (56, 57). Caspases also cleave structural proteins of the nucleus and cytoskeleton such as lamin, fodrin, keratin, and actin, thus promoting cellular packaging and subsequent engulfment and phagocytosis (58, 59). Also negative regulators of apoptosis are cleaved and inactivated, such as Bcl-2 family members (60). Cleavage appears not only to inactivate these proteins, but the products seem to promote apoptosis (61).

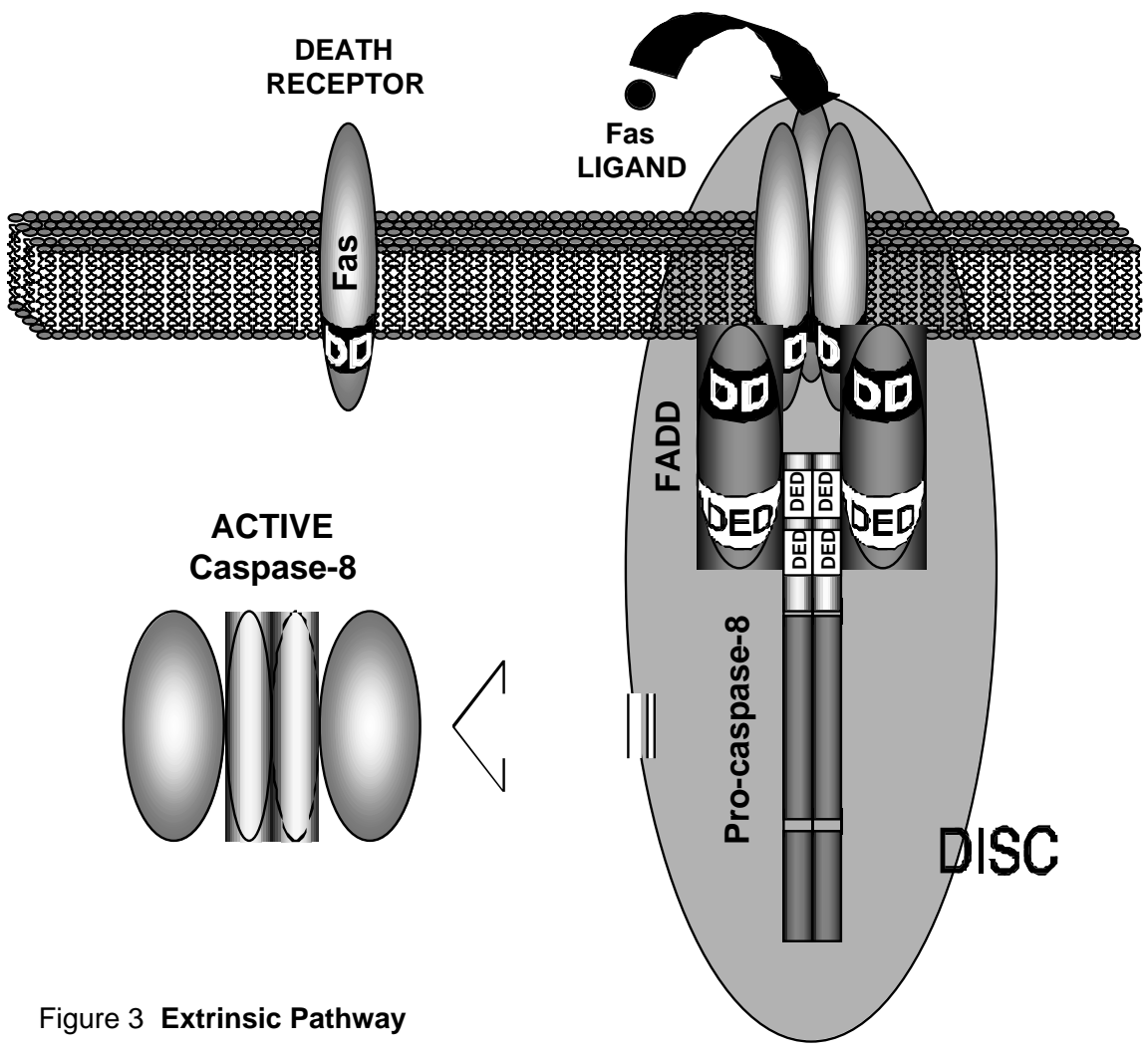


Figure 3 **Extrinsic Pathway**

Five death receptors have been characterized. This picture describes the most common and best known mechanism leading to cell death, the Fas/Fas ligand pathway. The ligand binds to the receptor, which trimerizes and gets activated. Interaction with docking molecule FADD through Death Domains (DD), allows activation of pro-caspase-8 by binding through Death Effector Domains (DED). Once activated caspase-8 dimerizes and can activate the apoptotic cascade. The Death Inducing Signaling Complex (DISC) was isolated with anti-Fas antibodies.

## Caspases Activated by Signaling Events

Many signaling pathways leading to apoptosis have been described. Extracellular and intracellular roads inducing activation of caspases have been characterized. What is common for all these pathways is the requirement of a death signal that activates apoptosis, leading to cytochrome c release or Fas ligand activation to induce the apoptosome formation and the subsequent caspase cascade activation.

### *THE RECEPTOR-MEDIATED EXTRINSIC PATHWAY*

As an extrinsic pathway, it is considered activation going through signals coming from the outside of the cell. This is the best-understood cell death pathway and it involves the binding of ligands to death receptors. Most of the progress in defining the extracellular signaling mechanism regulating apoptosis has been made by studying hematopoietic cells.

Five death receptors have been described so far in mammalian cells: Fas/CD95, TNFR1, DR3 (Apo-3/WS1/TRAMP/LARD), DR4, and DR5 (Apo 2R/TRIAL-R2/TRICK-2/KILLER), of the Tumor Necrosis Factor (TNF) receptor family, characterized by cystein-rich pseudorepeats in the N-terminal extracellular domain. The death-inducing receptors share a related intracellular sequence known as the death domain (DD) (38). After ligand binding, the receptor trimerizes and associates with cytoplasmic adapter molecules containing DD (62-64). Three of these proteins are known: FADD, RIP (Receptor Interacting Protein), and TRADD (TNFR1-Associated Death Domain). FADD and RIP interact directly with Fas, whereas TRADD appears to bind TNFR1. Overexpression of any of these proteins induces apoptosis. TNF engagement causes TNFR1 activation, binding to TRADD molecule and complex formation with FADD. FADD, as already mentioned, is able to activate caspase-8 (Figure 3) (65). Anti-Fas antibodies, which are able to trigger apoptosis, have been used to isolate the components of DISC (Death Inducing Signaling Complex), consisting of Fas receptor, FADD molecule and caspase-8 (43, 66). All these receptors, depending on the signals they receive from the environment, can determine whether to induce apoptosis or to send survival signals. For example, TNFR1/TRADD complex is able to induce NF- $\kappa$ B activation, which suppresses TNF- $\alpha$ -induced apoptosis (67).

### *THE INTRINSIC PATHWAY*

Similar to the extrinsic pathway, the intrinsic pathway requires a triggering event leading to caspase recruitment by the adapter molecule Apaf-1.

This triggering event has been identified as the release of cytochrome c from the mitochondria.

### *THE ESSENTIAL ROLE OF MITOCHONDRIA*

The principal function of mitochondria is to generate energy in the form of ATP by oxidative phosphorylation (Figure 4). However, mitochondria play a very important role in apoptosis. The oxidative phosphorylation proteins are located in the inner membrane of mitochondria. Electron-transport chain proteins, ATP synthase and adenine nucleotide translocator (ANT) oxidizes hydrogen from organic acid to generate H<sub>2</sub>O. Several respiratory complexes mediate the reaction and as an end-product two molecules of water are produced from a molecule of O<sub>2</sub>. The energy released is used to pump H<sup>+</sup> outside the inner membrane of the mitochondria to create a transmembrane potential ( $\Delta\Psi_m$ ). This leads to acidification of the intermembrane space of mitochondria and alkalization of the mitochondrial matrix. Depolarization of the membrane through F<sub>0</sub>/F<sub>1</sub> ATP synthase is used for the production of ATP. One of the components of this machinery is cytochrome c, located in the intermembrane space. Its function is to catalyze the electron transfer from complex III to complex IV in oxidative phosphorylation reaction (68).

Under certain conditions, such as a consequence of specific stimuli, cytochrome c is released into the cytoplasm and this event is sufficient to trigger caspase recruitment by Apaf-1 and activation of the caspase cascade. The importance of mitochondria in apoptosis was suggested by studies with a cell-free system in which nuclear condensation and DNA fragmentation were found to be dependent on the presence of mitochondria (69).

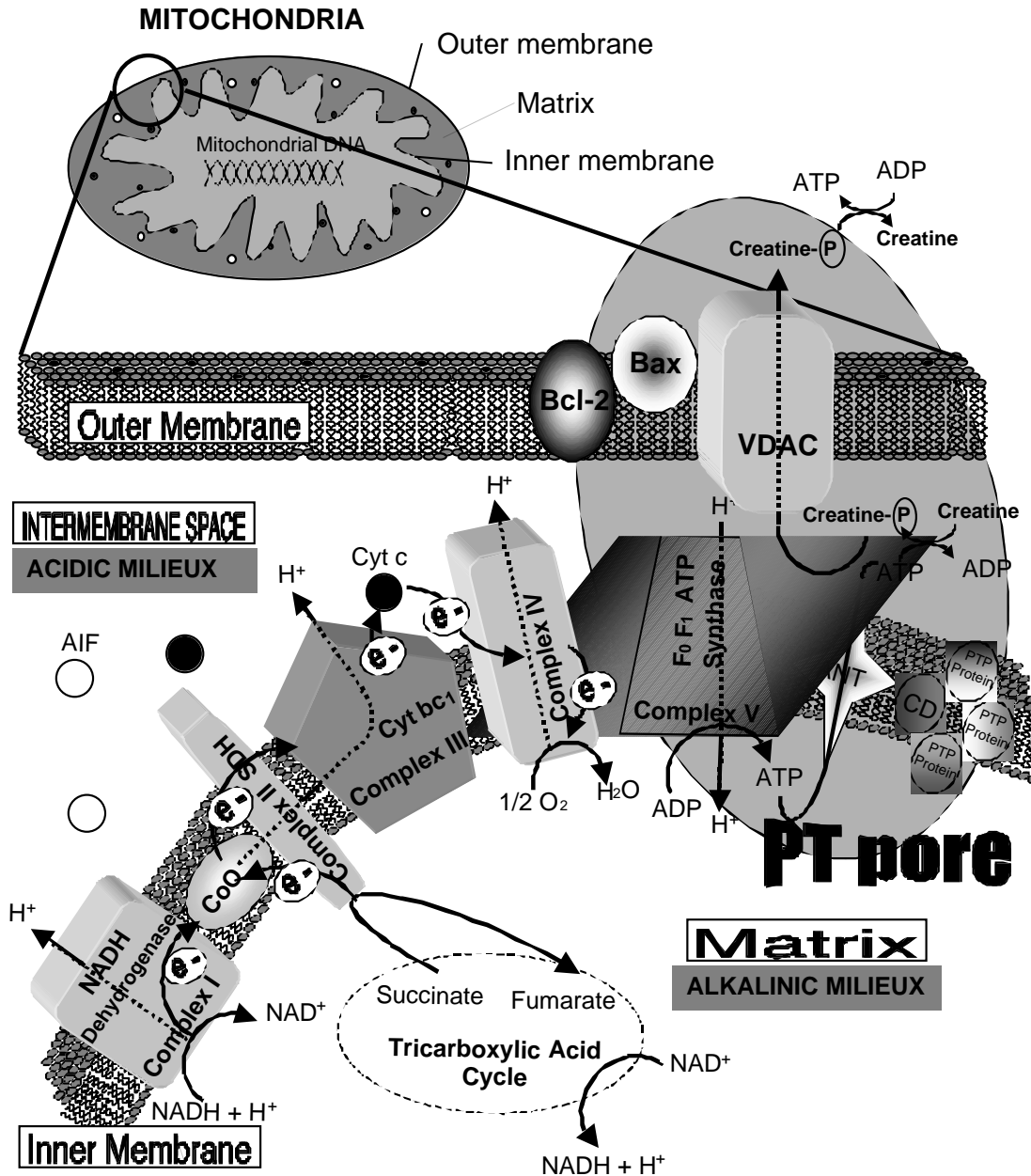


Figure 4 Mitochondria, Oxidative Phosphorylation, and PT pores

The key role of cytochrome c in the induction of caspase was again demonstrated in a cell-free system, where activation of caspase was triggered by the presence of cytochrome c and of deoxyadenosine triphosphate (70). Cytosolic cytochrome c binds to Apaf-1 (a chaperon-like protein), inducing a conformational change, allowing the binding of dATP to Apaf-1 (71) that further induces a conformational reorganization of the Apaf-1 molecule allowing recruitment of procaspase-9 in the apoptosome complex. This led to dATP hydrolysis-dependent caspase-9 autoactivation by cleavage, and the cascade proceeds through cleavage of caspase-3 (Figure 5) (72). The importance of cytochrome c in the apoptotic pathway was recently confirmed in cell lines derived from cytochrome c knockouts mice, where caspase-3 failed to be activated by different stimuli, such as UV-irradiation, serum starvation, and staurosporine (73).

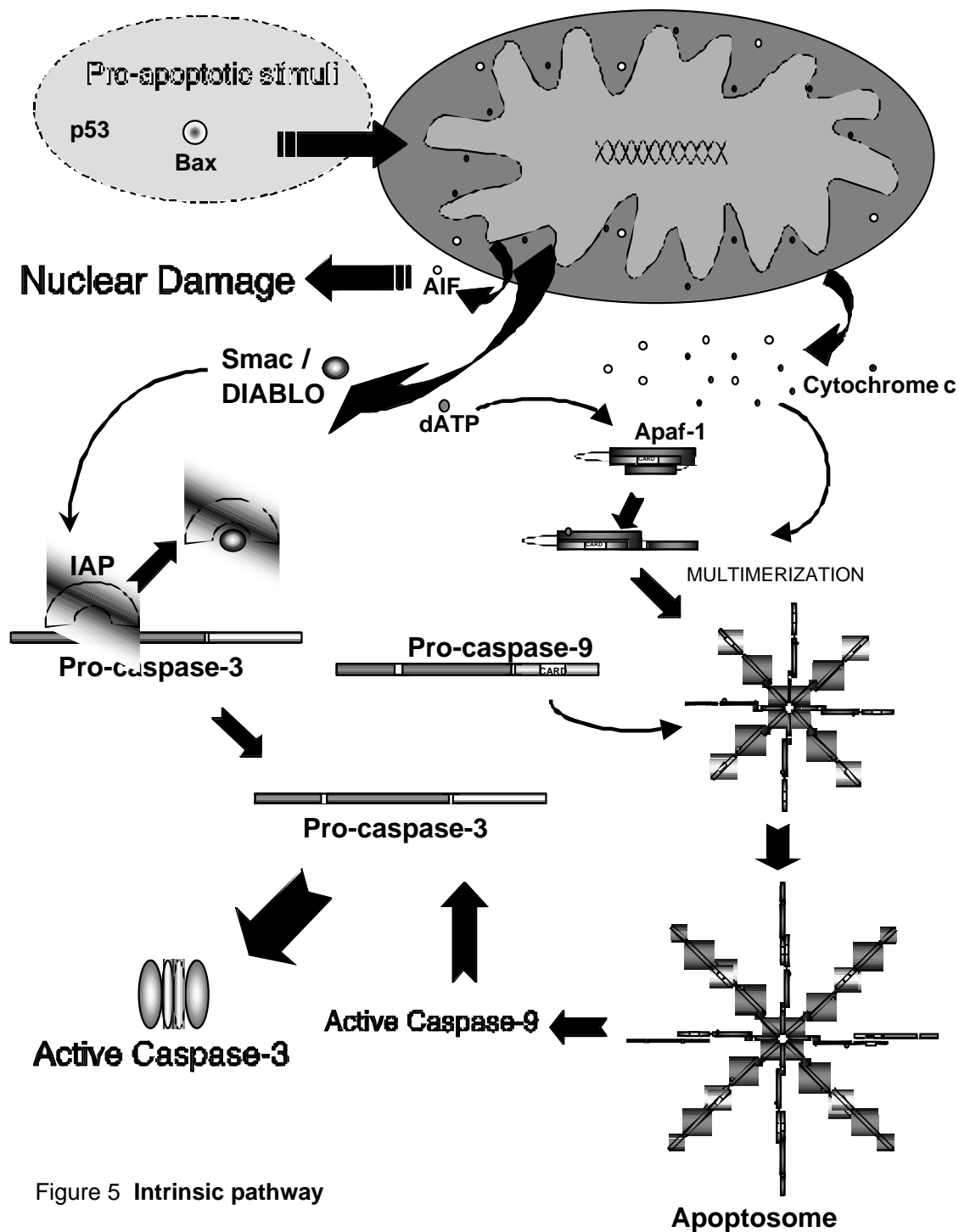


Figure 5 Intrinsic pathway

Cytochrome c release also disrupts the electron transport chain with consequent impairment of the production of energy. Although a drop in ATP production has been observed during apoptosis, it often occurs late in the process (71). This same event will increase the generation of reactive oxygen species, which are potent cytotoxic agents (74). With cytochrome c, other molecules are released from mitochondria during apoptosis. Apoptosis Inducing Factor (AIF) translocates to the nucleus and induces chromatin macrocondensation (75). Also procaspase-2 and -9 have been shown to be released during mitochondria damage (76).

Recently a novel molecule was found to be released from mitochondria during apoptosis, the so-called Smac (the Second Mitochondria-derived Activator of Caspases) (77) or DIABLO (Direct IAP Binding protein with low pI) (78). Smac/DIABLO is likely the functional equivalent of *Drosophila* Reaper, Hid, and Grim (79-81). It neutralizes the anti-apoptotic function of IAP molecules.

## RELEASE OF THE DEADLY CYTOCHROME C

Several mechanisms have been proposed for the release of cytochrome c from mitochondria. The main difference is the association of loss of membrane potential to the release of cytochrome c. Opening of the permeability transition (PT) pores and swelling produce a drop in the  $\Delta\Psi_m$ , whereas Bax-pores allow the release of cytochrome c without affecting the  $\Delta\Psi_m$ .

In general, small molecules can diffuse freely through the outer membrane of mitochondria. The inner membrane is impermeable to small ions. In many apoptotic scenarios, the mitochondrial inner transmembrane potential collapses, indicating the opening of the PT pores. The structure of the megachannels is still only partially defined. The PT pore is thought to be composed of several proteins, including hexokinases, mitochondrial creatine kinase, a voltage-dependent anion channel (VDAC) present on the outer membrane, and the inner membrane adenine nucleotide transferase (ANT) and the matrix cyclophilin D (CD). Finally, Bax was found to be part of this complex (Figure 4) (82).

Following PT pore opening, water and small solutes up to 1.5 kDa would enter the mitochondria. This allows a non selective movement of ions within matrix and intermembrane space of mitochondria, dissipating the  $H^+$  gradient, uncoupling the respiratory chain. The  $\Delta\Psi_m$  and the oxygen consumption drop. PT pore formation results in a volume deregulation of mitochondria, due to the hyperosmolarity of the matrix, and in swelling. Because of the flexibility of the inner membrane compared to the stiff outer membrane, expansion can cause the rupture of the outer membrane, releasing apoptotic-activating proteins (83).

Recent studies have provided evidence that cytochrome c release and caspase activation can occur prior to detectable loss of  $\Delta\Psi_m$ , implying that PT pore may open downstream of apoptosome-mediated caspase activation (84). Probably in these cells an excess of cytochrome c is present, so that enough cytochrome c remains docked to cytochrome c oxidase to maintain electron transport.

Cytochrome c release may also occur by a different mechanism. Bcl-2 family members have been demonstrated to insert in mitochondrial membranes (85). These molecules, with high structural affinity with some types of bacterial toxins, can form ion channels in membranes (86). Bax is a candidate for the formation of this channel in the outer membrane. Recently it was shown that addition of Bax or Bak to liposomes containing VDAC allows passage of cytochrome c through the VDAC channel (87). Mitochondrial ATP synthase was also shown to affect Bax activity. In addition oligomycin, an ATP synthase inhibitor, abrogates Bax killing. However it is not known if Bax induced cytochrome c release requires ATP synthase (88). Bax toxicity was reduced in yeast mutant strains lacking the ability to perform oxidative phosphorylation (89). Other molecules other than Bax and VDAC may constitute the putative cytochrome c channels.

## THE TWO PATHWAYS COOPERATE TO ENHANCE THE POWER OF KILLING

Intrinsic and extrinsic pathways are two distinct roads leading to cell death, but they can interact to increase the strength of apoptotic signals (Figure 6). It has been reported that caspase-8, once activated through Fas ligand binding to receptor, can cleave Bid, a Bcl-2 family member. Bid cleavage can directly induce cytochrome c release from mitochondria, activating caspase-9 (84). It has been demonstrated that in some experimental systems, the release of cytochrome c can be prevented with caspase inhibitors (90). It is controversial if the extrinsic pathway really requires the involvement of mitochondria. So the idea of two different cell types developed. In "type I" cells, death receptor signaling is not blocked by Bcl-2 and in "type II" cells it is (91). Bid is cleaved by active caspase-8, and the activated truncated Bid targets mitochondria to trigger Bax oligimerization and cytochrome c release (39). A new scenario was recently proposed where Bid induces the release of Smac/DIABLO molecule, which targets IAP and set the active caspase-3 free. Cytochrome c may not be relevant in this particular case (92).

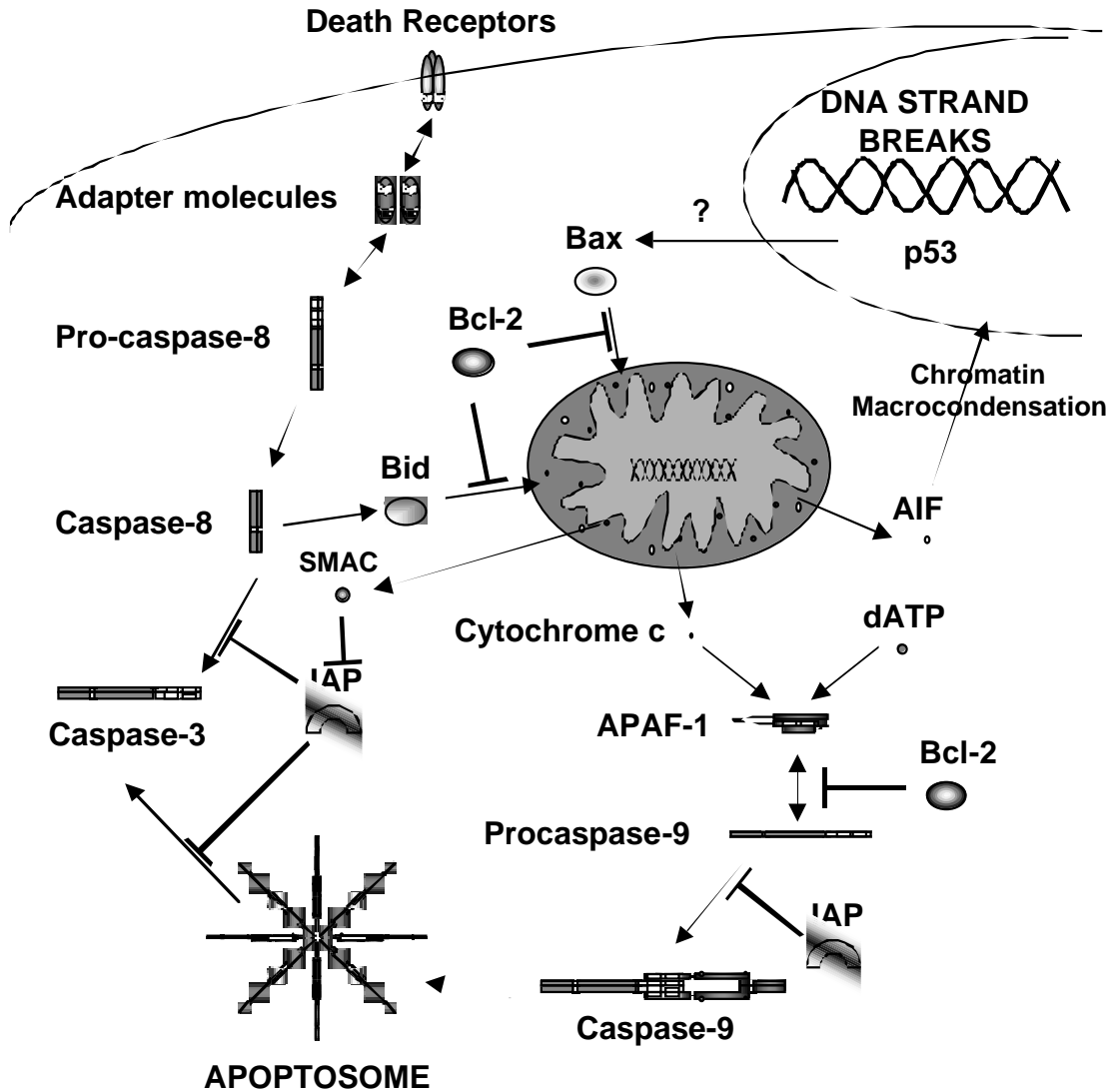


Figure 6 Apoptotic machinery

## Taking the Decision of Death

The extrinsic pathway can be triggered by any signal activating the death receptors. Intracellular mediators will decide if the cell has to undergo apoptosis or promote cell survival. The intrinsic pathway appears to be more complicated and is not fully understood. Several events may induce caspase activation within the cell. Growth factors, cytokines and DNA damage appear to signal cell death through the mitochondria, and this pathway is the target of many oncogenic mutations.

### A GENE INVOLVED IN THE TRIGGERING OF APOPTOSIS: p53

p53 was the first tumor suppressor gene related to apoptosis. p53 mutations occur in the majority of human tumors and are often associated with an advanced tumor stage and poor prognosis. p53 has a remarkable

number of biological activities including a central role in cell-cycle checkpoint, maintenance of genomic integrity, control of angiogenesis. However, p53 can also induce apoptosis (93). Growth arrest proceeds through induction of the cyclin-dependent kinase (Cdk) inhibitor p21 (94). In contrast, the mechanism by which p53 promotes apoptosis is more obscure. Nevertheless genes involved in cell death differ from those implementing growth arrest. One of the p53 targets implicated in apoptosis could be the Bcl-2 antagonist Bax (95).

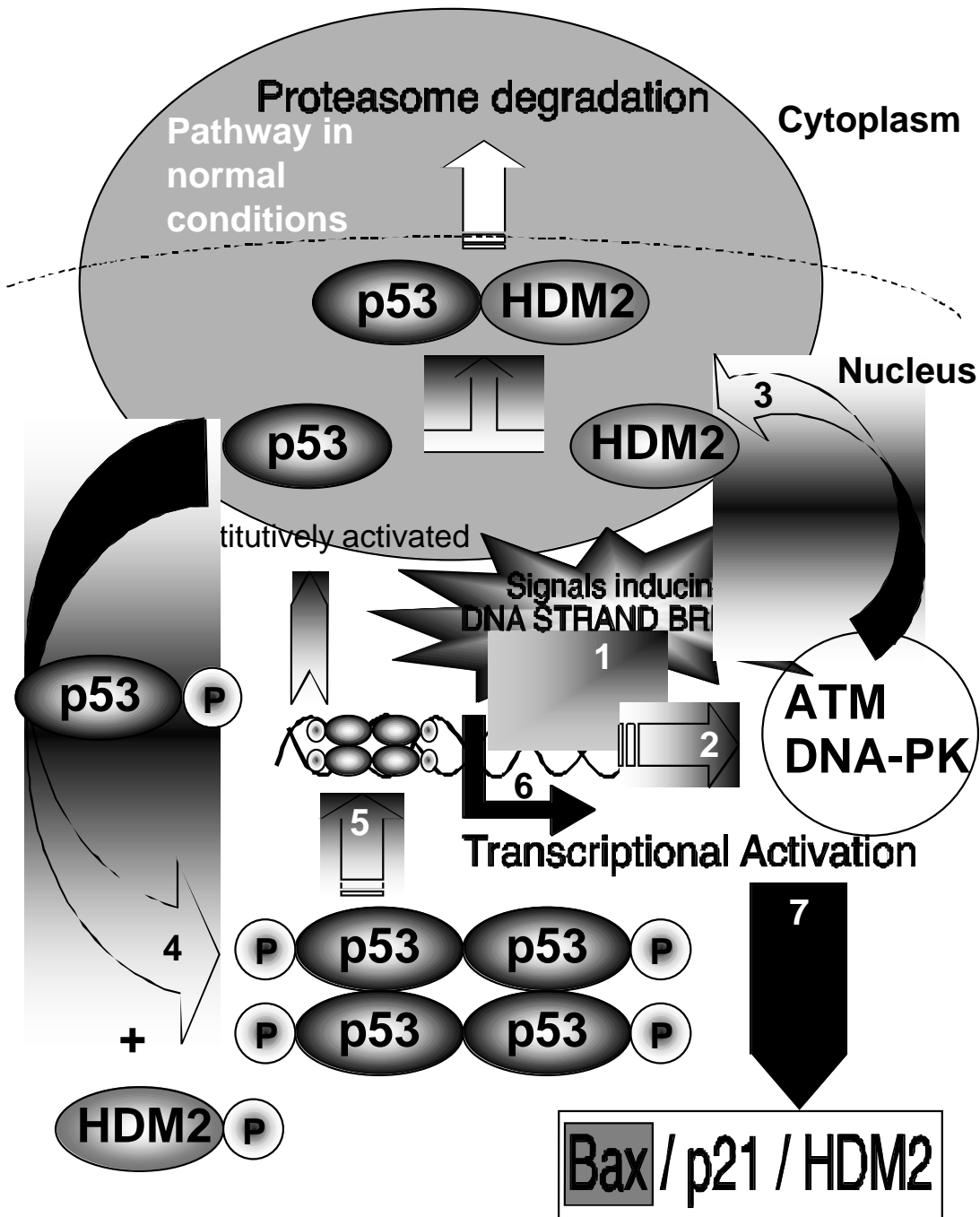


Figure 7 Induction of p53

p53 is implicated in cell responses to a variety of cellular insults: DNA damage, heat shock and expression of oncogenes such as *Myc* and E1A (96-98). When DNA damage occurs (1), the cell must decide to repair the damage or to undergo apoptosis. In both cases, DNA-PK (99), ATM (100) and other kinases are activated by DNA damage (2), and phosphorylate p53 and HDM2 (3) (101). p53 is a constitutively expressed gene and p53 protein is present at low levels in the nucleus of undamaged cells associated with HDM2, which targets p53 for proteasome degradation (102). After phosphorylation, p53 dissociates from HDM2, tetramerizes (4) and induces transcriptional activation of target genes, such as p21, HDM2 and GADD42 (5-7) (95, 99). One of these gene products, Bax, probably translocates to mitochondria and induces cytochrome c release (95).

### **COULD OTHER CELLULAR SIGNALS INDUCE APOPTOSIS?**

The extrinsic and the intrinsic pathways are the two most common routes leading to apoptosis. Nonetheless, in some cells different mechanisms could be used to activate apoptosis. Synthetic peptides containing the arginine-glycine-aspartate (RGD) motif used as an inhibitor of integrin-ligand interaction in studies of cell adhesion, migration, growth and differentiation, were shown to be able to directly induce apoptosis, without any requirement for integrin-mediated cell clustering or signals. RGD motif is an integrin-recognition motif found in many ligands. The peptides containing RGD enter cells and directly induce autoprocessing and enzymatic activity of procaspase-3. Procaspase-3 contains a potential RGD-binding motif, an aspartate-aspartate-methionine near its processing site. RGD probably induces apoptosis by triggering conformational changes in procaspase-3. After binding of RGD, a "safety catch" sequence in the small domain of procaspase-3 moves from its natural position, allowing caspase-3 auto-activation. Requirement of caspase-3 in RGD-mediated cell death was demonstrated with functional deletions of caspase-3 gene (103).

A pH-dependent mechanism of activation of procaspase-3 was also recently postulated. Low acidic pH (6) might be able to induce a conformational change in the structure of procaspase-3 inducing a N-terminus intermediate, which leads to its cleavage and to activation of caspase-3 (104).

## **Regulation of Apoptosis Prevents Undesired Surprises**

Apoptosis is a very important mechanism that must be strictly controlled to avoid undesired cell death or unprogrammed cell overgrowth. For these reasons the cells have evolved different checkpoints to regulate this event.

### **BCL-2 FAMILY MEMBERS**

The cloning and characterization of the Bcl-2 oncogene helped to establish the importance of apoptosis in tumor development. The first mammalian death regulator to be identified, Bcl-2, was discovered as a proto-oncogene in follicular B-cell lymphoma (105). A chromosome translocation affecting the Bcl-2 gene locus was found to allow cell survival of cytokine-dependent hematopoietic cells, in a quiescent state in the absence of cytokine (106). Further studies demonstrated that Bcl-2 promotes cell survival by blocking programmed cell death (107). Bcl-2 was found to be a functional and structural homologue to the *C. elegans* Ced-9 molecule (18). Bax (Bcl-2 Associated protein X) was the first pro-apoptotic member of the family discovered by coimmunoprecipitation with Bcl-2 (108). These genes were subsequently found to be part of a larger family, positively and negatively affecting apoptosis. The Bcl-2 family proteins constitute a critical intracellular checkpoint of apoptosis. The anti-apoptotic members of this family are Bcl-2, Bcl-X<sub>L</sub>, Mcl-1, Bcl-w, Boo, Baf, Bag and A1. The pro-apoptotic members so far identified are Bax, Bcl-X<sub>S</sub>, Bak, Bad, Bid, Bim, Bik, Bok, Blk, EGL-1, BNIP3, Noxa, and Harakiri. The Bcl-2 family has also homologues in DNA viruses: E1B-19K gene of adenovirus, BHRF1 gene of EBV, LMVS-HL genes of the African swine fever virus. The amino acid sequence homology between the Bcl-2 family members is low, and only confined to four specific regions called the Bcl-2 Homology (BH) domains. These domains control the ability to homodimerize and heterodimerize, which is an important feature in regulation of apoptosis (Figure 8) (108, 109). BH1 and BH2 are required for Bcl-2 and Bcl-X<sub>L</sub> interaction with Bax to suppress apoptosis (110). BH3 domain of pro-apoptotic proteins is sufficient for the binding to anti-apoptotic Bcl-2 and Bcl-X<sub>L</sub> to promote apoptosis (111). BH4 is found in the N-terminal region of anti-apoptotic proteins only. Mutants lacking BH4 lose their anti-apoptotic ability and also gain pro-apoptotic functions. Some of the Bcl-2 family members display a hydrophobic amino acid sequence at the C-terminus, probably involved in membrane interaction (61). The tri-dimensional structure of Bcl-X<sub>L</sub> and Bid has been



elucidated. It showed a structural homology to pore-forming domains of certain bacterial toxins, as colicins A and E1 (112-114). These bacteria toxins are pore-forming proteins that function as channels for ion and small proteins. As predicted by their structures, Bcl-2, Bcl-X<sub>L</sub>, and Bax can form ion-channels when they are added to synthetic membranes (85, 86, 115).

There is a pretty good evidence that Bcl-2 family proteins may play a role directly in the formation of the channels in mitochondrial membrane leading to release of cytochrome c, and this may explain their role in the regulation of apoptotic events (unpublished data). These proteins act as a checkpoint upstream of caspases and mitochondrial dysfunction. The multiconductive channels formed by Bcl-2 family proteins are pH sensitive, voltage-dependent, with poor ion selectivity. Bcl-2 and Bcl-X<sub>L</sub> channels are more prone to be cation selective and Bax channels anion selective at physiological pH. Bax can form pores at physiological pH, whereas Bcl-2 requires low pH. Bax pore forming ability depends on the membrane's lipid composition, and this could serve as a regulatory mechanism (116).

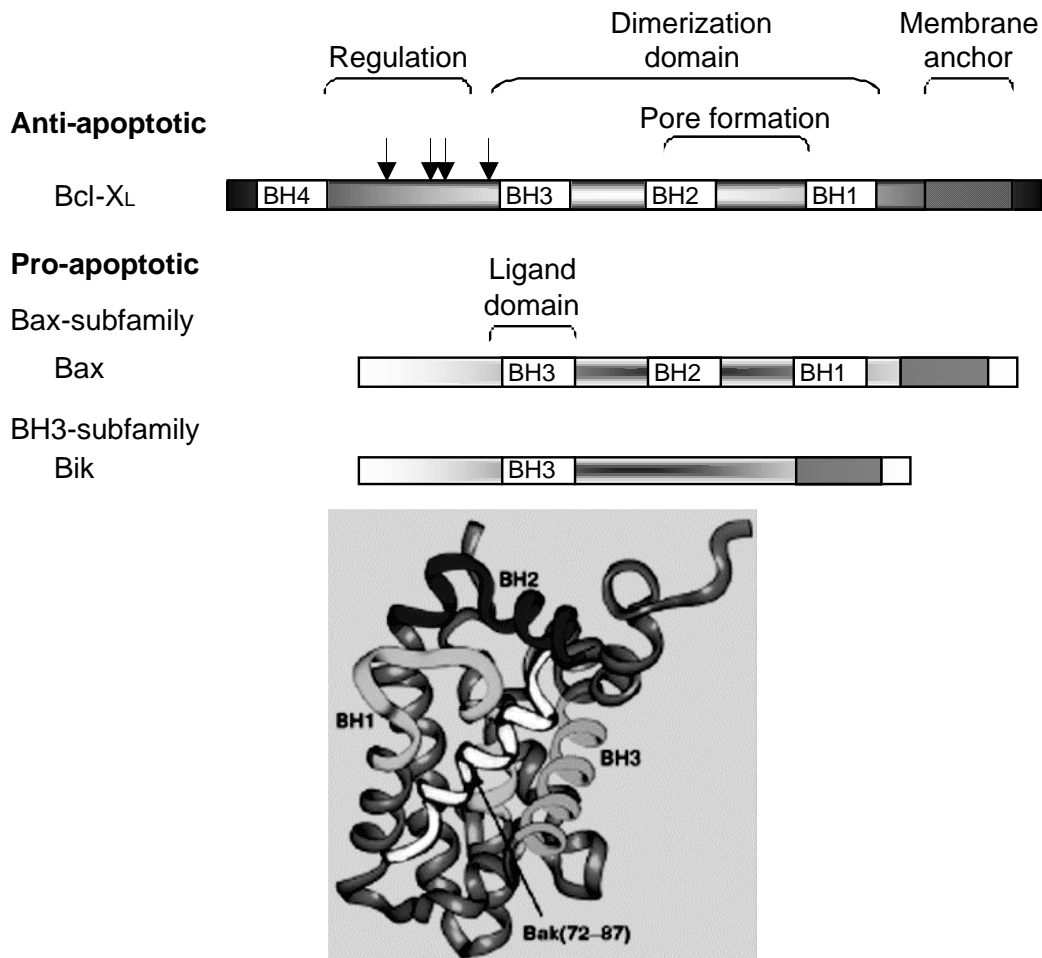


Figure 8 **Bcl-2 family members, BH domains**

Several Bcl-2 family members have been discovered and their structure has been characterized. The family has been divided in two major subfamilies, pro- and anti-apoptotic members. We can further divide the pro-apoptotic in Bax and BH3 subgroups. Bcl-2 homologous (BH) domains are characteristic for each subfamily. BH domains of Bcl-X<sub>L</sub> are represented in the 3D structure (117).

Bax can only form channels as an oligomer. Oligomerization results after a conformational change possibly triggered by Bid or by other BH3 domain containing proteins (116, 118, 119). Bax can directly induce

cytochrome c release from mitochondria, which can be prevented by Bcl-2. Bcl-2 may inhibit Bax insertion in mitochondria or may directly inhibit the Bax channel activity (120). Bcl-2 can also prevent PT pore opening by increasing proton efflux from matrix, inhibiting mitochondria respiration, which prevents free radical formation (121). This would explain the anti-toxicity properties attributed to Bcl-2 (122, 123). Because Bax homodimerization can lead to apoptotic death and Bcl-2 overexpression induces heterodimerization with Bax and death repression (108), the ratio Bcl-2/Bax is important in the determination of apoptosis susceptibility. Compartmentalization may also play a role in this process. Bcl-2 family members have been shown to be both membrane associated and cytosolic. A few years ago, the C-terminal domain of Bcl-2 family members, was thought to be responsible for the attachment to membranes, so that proteins containing this hydrophobic sequence were supposed to be membrane associated. New research demonstrated that this does not appear to be an absolute rule (124). Bcl-2 may also associated with ER, nuclear envelope and mitochondrial membranes, and Bcl-X<sub>L</sub> and Bax with C-terminal domains are found in the cytosol. Localization of Bcl-2 family proteins changes during apoptosis. It is possible that under normal conditions the hydrophobic domain is protected, localizing the molecule in the cytosol and after conformational change and exposure of the domain the protein translocate to mitochondrial membrane (118). Other modifications could induce relocation of these proteins. Phosphorylation and proteolysis regulate the activity of some Bcl-2 family members. Bcl-2 has been reported to undergo extensive phosphorylation, affecting its relocation and proteasome degradation in many occasions (125, 126). The kinase responsible for Bcl-2 phosphorylation has not been fully identified. A good candidate could be c-Jun N-terminal Kinase/stress-activated protein kinase (JNK), which is activated by several known stimuli (127). Other kinases such as Raf, ASK1, and ERK1/2, have been shown to phosphorylate Bcl-2 (128).

Bcl-2 family members can regulate apoptosis also at levels other than the mitochondria. For example, Bcl-X<sub>L</sub> may inhibit the association of Apaf-1 to procaspase-9 and prevent caspase-9 activation (129). Pro-apoptotic molecules like Bik may release Apaf-1 from the inhibition (130). Bcl-2 was also shown to protect cells after cytochrome c microinjection suggesting an inhibitory event at Apaf-1/procaspase-9 level (131).

## *IAPs*

IAPs are proteins that work as direct caspase inhibitors. IAPs were discovered during work on viruses. Very often, viruses attenuate apoptosis to circumvent the normal infection response. Three classes of viral inhibitors have been described: Crm A (132), p35 (124), and IAP family (Inhibitors of Apoptosis) (18). Crm A is a member of the serpin family that is a potent inhibitor of active initiator caspases involved in inflammation. The baculovirus p35 has no known homologies and its selectivity for caspases is not clearly defined (133). The IAP proteins are a large family that also has mammalian homologues. IAPs were first discovered in baculoviruses, a group of insect viruses. The IAP family is characterized by a novel ~70 amino acid domain containing Baculoviral IAP Repeat (BIR), up to three tandem copies (134). Another region of IAP, the RING domain, acts as a ubiquitin ligase, promoting the degradation of XIAP (135) and possibly any caspase it is bound to (92). The human c-IAP1 and c-IAP2 contain a CARD domain. Six IAP relatives have been defined in humans: XIAP, c-IAP1, c-IAP2, NAIP, Survivin, and BRUCE. Overexpression of IAPs has been shown to suppress apoptosis induced by a variety of stimuli, including TNF, staurosporin, taxol, and growth factor withdrawal. Several human IAPs directly inhibit caspases (136). Inhibition by IAPs may work by increasing the threshold that determines the concentration of active effector caspases required to initiate the cascade, thus preventing the consequence of accidental or spontaneous proenzyme activation (137), they may serve as endogenous "brakes" of apoptosis.

## *AKT*

Phosphorylation, which plays an important role in the regulation of Bcl-2 family members, may be involved in the regulation of the caspase cascade directly (1). The ability of endogenous factors to promote survival, for example nerve growth factor in sympathetic neurons, has been attributed partly to the phosphatidylinositol 3'-OH Kinase (PI3K)/c-Akt kinase cascade (138). Recent data have implicated PI3 kinases and their phospholipid products in promoting survival downstream of extracellular stimuli (139). PI3K was first implicated in the suppression of apoptosis in a study by Yao (140) in which Akt was identified as the general mediator of survival signals. Akt itself requires phosphorylation for its activity (141). Akt may target directly apoptotic molecules as caspase-9 and Bad inhibiting their pro-apoptotic activity (142, 143).

## CLL: A Beautiful Primary System To Study Apoptosis

Chronic lymphocytic leukemia (CLL) is a neoplasm of B-lymphocytes occurring predominantly in older persons with an average age between 60 and 70 years. In some cases (about 10 %) it has occurred in younger patients. B-CLL is classified along with indolent lymphoma. It is the most common leukemia in the Western World. Non-Hodgkin's lymphoma is a malignant (cancerous) growth of B or T cells in the lymph system. The Non-Hodgkin's lymphomas encompass over 29 types of lymphoma. The distinctions are based on the type of cancer cells. There are classification systems that group lymphomas by cell type and rate of growth. The US National Cancer Institute now splits lymphomas into aggressive (fast growing) and indolent (slow growing). /  $G_1$

CLL represents a perfect example of a human malignancy, which is caused primarily by defects in programmed cell death, rather than cell cycle deregulation. CLL patients typically accumulate  $CD5^+$ , non-responsive, growth-arrested B-cells that express little or no surface IgG. These mature circulating B-lymphocytes are largely quiescent  $G_0/ G_1$  phase cells, which accumulate not because they are dividing more rapidly than normal, but because they survive longer (144). Studies of apoptosis regulation in CLL may serve as a model not only for B-CLL, but also for eventually overcoming chemoresistance and inhibiting cancer cell survival in more common types of malignancies, including solid tumors.

The advantage of CLL is that the cells are essentially quiescent or very slowly proliferating. Therefore the cell cycle machinery, which is usually the conventional target of anti-cancer drugs, does not affect the study of drug-induced apoptosis. Primary B-CLL lymphocytes are used in our experiments as the system to analyze the apoptotic process.



## DESCRIPTION AND SIGNIFICANCE OF THE PERSONAL CONTRIBUTIONS

In this thesis we tried to characterize the mechanism of action of newly synthesized drugs, of old drugs whose mechanism was unknown or applied for the treatment of other diseases. The system we used is B-CLL, because these cells are a slowly proliferating primary system and because of the availability of millions of cells from a single patient.

The first set of drugs we started to analyze were the purine nucleoside analogs. For years cladribine and fludarabine were used for the clinical treatment of B-CLL, but their detailed mechanism of action was not fully understood. In a series of articles that were first published in 1995, Xiaodong Wang proposed a novel mechanism for the initiation and execution of apoptosis. He identified the partners forming the apoptosome complex (Apaf-1 / cytochrome c / caspase-9) and demonstrated that dATP or ATP was absolutely required for the activation of this apoptotic cascade (70). In our research, we demonstrated that 2CdATP was also able to activate in a cell-free system the apoptosome complex, substituting dATP, and that this activity is essential in the mechanism of action of cladribine in B-CLL cells **[Paper 1]**. We further investigated if other clinically relevant tri-phosphate versions of nucleoside analogs had the same ability to activate caspases in a cell free-system. We ranked several of these drugs for their “apoptosome activation” potency, determining their enzymatic kinetics for caspase activation. Interestingly we also found ADP and ATP to be inhibitors of the dATP-induced activation of the apoptosome complex **[Paper 2]**. To understand the mechanism of the ADP/ATP inhibition, we investigated the possible role of caspase-9 phosphorylation by Akt kinase (142). We determined, using <sup>35</sup>S-*in vitro* translation of caspase-9 experiments, that ATP acted exclusively as competitive inhibitor of the complex Apaf-1 / cytochrome c / caspase-9 and did not affect the Akt kinase. We also demonstrated that phosphorylation of caspase-9 protected the autocatalytic processing of caspase-9 but not the feed-back cleavage by caspase-3. We concluded that the phosphorylation of caspase-9 has no relevant effect on its activation, because the binding to Apaf-1 (and not its proteolytic cleavage) is the only essential step required for its activation **[Paper 3]**. Our interest in the mechanism of action of the nucleoside analogs didn't stop there. We were intrigued by the fact that, in whole cell assays, 2CdA was much more cytotoxic than fludarabine, whereas in a cell-free system, F-Ara-ATP was a more potent caspase activator. In order to understand this discrepancy, we measured the ability of several of purine deoxynucleoside analogs to induce DNA strand breaks by two methods: an alkaline unwinding assay to measure the total DNA strand breaks and the comet assay to measure single cell damage. We discovered that the DNA-damage activity of the drugs tested was comparable. We then compared their toxicity toward mitochondria by cytochrome c and AIF release assays, by mitochondrial membrane potential measurement in whole cells and in isolated mitochondria, and by immunohistochemical assays for cytochrome c release. We discovered that the two chlorinated analogs, 2CdA and CaFdA, were able to damage directly mitochondria. Direct microinjection of the nucleotide analogs in fibroblasts confirmed the mitochondria toxicity of the chlorinated analogs **[Paper 4]**. If F-Ara-A was killing the cells mainly through DNA damage, p53 had to be involved in its toxicity. Previous reports correlated multidrug-resistance of several cancers for DNA-damaging drugs to p53 status (145). In a further study, we identified a B-CLL sampler not expressing p53. We demonstrated that these cells were resistant to F-ara-A treatment. Further analysis confirmed that p53 appears to play a major role in B-CLL chemotherapy. In fact, not only is p53 required for an efficient response to F-ara-A treatment, but also its turnover in the cell appears to be distinct. We observed an unusual ubiquitous p53 localization in B-CLL cells, and this might be involved in the difference response to treatments compared to normal PBL **[Paper 5]**.

Indanocine is a novel microtubule-binding drug synthesized in our lab. Indanocine showed high affinity to colchicine, competing for its binding site on microtubule filaments. Indanocine showed higher toxicity for multidrug-resistant cell lines compared to the relative wild type **[Paper 6]**. Similar to colchicine, indanocine also was able to induce apoptosis in B-CLL cells. The study of indanocine-induced apoptosis revealed the activation of an intrinsic pathway, with a central role for mitochondria. The triggering event appeared to be the phosphorylation of the anti-apoptotic protein Bcl-2, resulting in its dimerization, subcellular relocalization, and inactivation. In addition, pro-apoptotic molecule Bax showed relocalization from cytosol to the membrane, release of cytochrome c, and consequent caspases cascade activation. Simultaneously with Bcl-2 phosphorylation, the activation of JNK kinase was observed. The kinase might be responsible for Bcl-2

phosphorylation [Paper 7]. To elucidate the mechanism of action of indanocine, we selected an indanocine-resistant clone (CEM-178), from a T lymphoblastoid CEM cell line. From polymerization and depolymerization assays it appeared that CEM-178 had mutated tubulin. In fact the resistant cell line presented cross-resistance to microtubule-disrupting agents such as colchicine and vinblastine. Fusion assays proved that the mutation was a codominant phenotype [Paper 8].

The non-steroidal anti-inflammatory drug etodolac, commonly used for the treatment of rheumatoid arthritis resulted to give relief to B-CLL patients. *In vivo* data showed the reduction of the circulating leukemic cell number when etodolac was administered to B-CLL patients. Additional study revealed that etodolac was able to induce apoptosis *in vitro* in B-CLL cells. Analysis of the pro-apoptotic mechanism of etodolac in B-CLL demonstrated that the nuclear receptor PPAR- $\gamma$ , expressed at unexpected high levels in B-CLL cells as compared to normal lymphocytes, was activated by etodolac. In addition, the anti-apoptotic molecule Mcl-1 was rapidly down-regulated in etodolac-treated B-CLL cells. This resulted in the activation of the intrinsic pathway of apoptosis. Etodolac is right now in a phase II clinical trial for the treatment of B-CLL, and the results are extremely promising [Paper 9].

HIV virus induces the depletion of CD4+ T lymphocytes in infected patients. The mechanism used by the virus to kill these cells was not clear. In particular, it was not clear whether the intrinsic pathway of apoptosis or the extrinsic Fas-mediated activation of apoptosis were responsible for the depletion of CD4+ cells. The enzymatic activity of caspases suggested the activation of the intrinsic pathway. We assessed if mitochondria were involved, by detecting cytochrome c and AIF release by immunohistochemistry and by measuring the mitochondrial membrane potential. After concluding that the intrinsic pathway was activated, the next step was to discover which triggering event was leading to mitochondria damage. The infection of the virus and its integration into the DNA suggested us that p53 could be involved in the activation. In fact, p53 was activated and this resulted in the up-regulation of pro-apoptotic molecule Bax. Bax has already been correlated with p53-mediated release of cytochrome c from mitochondria in different systems (95) [Paper 10]. In a collaborative study, we analyzed the HIV-induced gene expression of the infected cells using gene arrays. This novel technology allowed us to measure quantitatively and simultaneously the mRNA levels of more than 5,000 genes. The results confirmed our biochemical data, and indicated that HIV is capable of activating the p53-signaling pathway, and regulates mitochondrial-related genes that may be involved in apoptosis [Paper 11].

This thesis also contains other papers resulting from collaborations not directly related to the theme of the thesis.

The first publication is in the immunology field. Dr. Albani's group developed artificial antigen presenting cells (aAPC) to modulate immune response. Liposomes exposing MHC class II molecules were used to induce a response in T cells. Our expertise was essential in the imaging of the interaction between the aAPC and the target cells expressing the T cell receptor [Paper 12].

In another collaboration with the department of Bioengineering of UCSD, we analyzed the biological activity of particles released from orthopedic implants that play an essential role in the aseptic loosening of the prosthesis. Different materials are used for orthopedic implants, and the particles released can induce different response. We discovered that particles from different materials have an effect on the modulation of genes that code for inflammatory cytokines and for nucleus architecture. We also demonstrated that some of them can cause apoptosis in cells from bones (osteoblasts) [Paper 13].

## ARTICLES

### **PAPER 1:**

Leoni LM, Chao Q, Cottam HB, Genini D, Rosenbach M, Carrera CJ, Budihardjo I, Wang X, Carson DA.  
**“Induction of an apoptotic program in cell-free extracts by 2-chloro-2'-deoxyadenosine 5'-triphosphate and cytochrome c.”**  
*Proc Natl Acad Sci U S A.* 1998 Aug 4;95(16):9567-71.

### **PAPER 2:**

Genini D, Budihardjo I, Plunkett W, Wang X, Carrera CJ, Cottam HB, Carson DA, Leoni LM.  
**“Nucleotide requirements for the *in vitro* activation of the apoptosis protein-activating factor-1-mediated caspase pathway.”**  
*J Biol Chem.* 2000 Jan 7;275(1):29-34.

### **PAPER 3:**

Genini D, Reed J, Carson DA, Leoni LM.  
**“Ser196 phosphorylation of caspase-9 protects against autocatalytic cleavage”**

### **PAPER 4:**

Genini D, Adachi S, Chao Q, Rose DW, Carrera CJ, Cottam HB, Carson DA, Leoni LM.  
**“Deoxyadenosine analogs induce programmed cell death in chronic lymphocytic leukemia cells by damaging the DNA and by affecting directly the mitochondria.”**  
*Blood.* 2000 Nov 15;96(10):3537-3543

### **PAPER 5:**

Genini D, Tawato RI, Kipps TJ, Croce CM, Carson DA, Leoni LM.  
**“p53 status is involved in chronic lymphocytic leukemia-sensitivity to nucleosides analogs treatment.”**

### **PAPER 6:**

Leoni LM, Hamel E, Genini D, Shih H, Carrera CJ, Cottam HB, Carson DA:  
**“Indanocine, a microtubule-binding indanone and a selective inducer of apoptosis in multidrug-resistant cancer cells.”**  
*J Natl Cancer Inst.* 2000 Feb 2;92(3):217-24.

### **PAPER 7:**

Genini D, Tawatao RI, Sheeter D, Hua XH, Carson DA, Leoni LM.  
**“Selective induction of apoptosis in chronic lymphocytic leukemia by indanocine, a potent anti-mitotic drug.”**

**PAPER 8:**

*Genini D, Hua XH, Tawatao RI, Dell'Aquila M, Carson DA, Leoni LM.*

***“Establishment and characterization of a new indanocine-resistant cell line CEM-178.”***

**PAPER 9:**

*Adachi S, Welch J, Shinichi K, Pham-Mitchell NK, Tawato RI, Genini D, Cottam HB, Carrera CJ, Gottlieb RA, Reed JC, Glass CK, Amox DG, Carson DA, Leoni LM.*

***“Mechanism of Lymphocyte Depletion after Treatment of B-Chronic Lymphocytic Leukemia with Etodolac, a Non-steroidal Anti-inflammatory Agent.”***

**PAPER 10:**

*Genini D, Sheeter D, Rought S, Zaunders JJ, Susin SA, Kroemer G, Richman DD, Carson DA, Corbeil J, Leoni LM.*

***“HIV induces lymphocyte apoptosis by a p53-initiated, mitochondrial-mediated mechanism.”***

*FASEB, January 2001 6;15(1):5-*

**PAPER 11:**

*Corbeil J, Genini D, Sheeter S, Rought S, Leoni LM, Du P, Ferguson M, Masys DR, Welsh JB, Fink JL, Huang D, Drenkow J, Richman DD, Gingeras T.*

***“Temporal gene regulation during HIV-1 infection of human CD4+ T cells.”***

*Nature Genetics, In Press*

**PAPER 12:**

*Prakken B, Wauben M, Genini D, Samodal R, Barnett, Mendivil A, Leoni LM, and Albani S.*

***“Artificial J antigen presenting cells as a tool to exploit the immune synapse.”***

*Nature Medicine (2000). In Press*

**PAPER 13:**

*Pioletti PP, Leoni LM, Genini D, Takei H, Du P, Corbeil J.*

***“Functional Genomic Analysis of Osteoblasts Contacted by Orthopedic Implant Particles.”***



## ***PAPERS***



## Induction of an apoptotic program in cell-free extracts by 2-chloro-2'-deoxyadenosine 5'-triphosphate and cytochrome c

LORENZO M. LEONI\*<sup>†</sup>, QI CHAO\*, HOWARD B. COTTAM\*, DAVIDE GENINI\*, MICHAEL ROSENBAACH\*, CARLOS J. CARRERA\*, IMAWATI BUDIARDJO<sup>‡</sup>, XIAODONG WANG<sup>‡</sup>, AND DENNIS A. CARSON\*

\*Department of Medicine and The Sam and Rose Stein Institute for Research on Aging, University of California at San Diego, 9500 Gilman Drive, La Jolla, CA 92093-0663; and <sup>‡</sup>Howard Hughes Medical Institute, Department of Biochemistry, University of Texas Southwestern Medical Center, Dallas, TX 75235

Communicated by J. Edwin Seegmiller, University of California, San Diego, La Jolla, CA, May 21, 1998 (received for review March 17, 1998)

**ABSTRACT** Adenine deoxynucleosides, such as 2-chloro-2'-deoxyadenosine (2CdA) induce apoptosis in quiescent lymphocytes, and are thus useful drugs for the treatment of indolent lymphoproliferative diseases. However, it has remained puzzling why deoxyadenosine and its analogs are toxic to a cell that is not undergoing replicative DNA synthesis. The present experiments demonstrate that the 5'-triphosphate metabolite of 2CdA (2CdA-5'-triphosphate), similar to dATP, can cooperate with cytochrome c and Apaf-1 to activate caspase-3 in a cell free system. Chronic lymphocytic leukemia cells and normal peripheral blood lymphocytes expressed both caspase-3 and apoptotic protease activating factor 1. Incubation of the lymphocytes with 2CdA induced caspase-3 activation prior to DNA degradation and cell death. Stimulation of the caspase proteolytic cascade by 2CdA-5'-triphosphate, in the context of DNA strand break formation, may provide an explanation for the potent cytotoxic effects of 2CdA toward nondividing lymphocytes.

The effectiveness of cancer chemotherapy often depends upon the induction of apoptosis in malignant cells. Among antimetabolites, the 2'-deoxyadenosine congeners 2-chloro-2'-deoxyadenosine (2CdA, cladribine) and 9- $\beta$ -D-arabinofuranosyl-2-fluoroadenine (fludarabine) have the ability to induce apoptosis in nondividing lymphocytes, at concentrations that spare other cell types (1). For this reason, the deoxyadenosine analogs have achieved an important place in the treatment of indolent lymphoid malignancies, including hairy cell leukemia, chronic lymphocytic leukemia (CLL), and low grade lymphoma (2, 3).

The cytotoxicity of 2CdA depends mainly upon the selective and progressive accumulation of its 5'-triphosphate metabolite (2CdATP) in lymphocytes that have a high ratio of deoxycytidine kinase (EC 2.7.1.74) to cytosolic 5'-nucleotidase (EC 3.1.3.5), compared with other cell types (1, 4). However, why 2CdATP triggers apoptosis in non-dividing cells is unclear.

Various stimuli of apoptosis lead to the activation in the cytoplasm of cysteine proteases with specificity for aspartic acid residues, referred to as caspases. The activated caspases can cleave structural proteins and enzymes necessary for the survival of both proliferating and resting cells (reviewed in refs. 5–7). In addition, caspases have been shown to activate the endonuclease responsible for the internucleosomal cleavage of genomic DNA, a hallmark of apoptosis (8, 9).

One important component of the caspase cascade is caspase-3, which is activated by two sequential proteolytic events that cleave the 32-kDa precursor at aspartic acid residues to generate an active heterodimer of 20- and 12-kDa subunits (10). The activation can either be autocatalytic, or occur via a caspase cascade, similar to the serine protease cascade in the blood clotting process (7). In susceptible cells, caspase activation might amplify preex-

isting but sublethal apoptotic signals, leading to rapid and irreversible proteolysis.

Recently, Wang and coworkers established a cell free system in which caspase-3 activation in the cytosol is induced by the addition of dATP and cytochrome c (11–13). Three protein factors, designated apoptotic protease activating factors (Apafs), are necessary and sufficient to reconstitute dATP-dependent caspase-3 activation. Apaf-2 has been identified as cytochrome c, and Apaf-3 as caspase-9. Caspase-3 activation begins when caspase-9 (Apaf-3) binds to Apaf-1 in a reaction stimulated by cytochrome c and dATP (11). Because of the structural similarity between dATP and 2CdATP, and the important role of 2CdA in the treatment of indolent lymphoid malignancies, we designed experiments to address the possibility that 2CdATP directly induces caspase-3 proteolysis in a cell free system, and to verify that caspase-3 proteolytic activation occurs in viable lymphocytes and CLL cells exposed to 2CdA *in vitro*.

### MATERIALS AND METHODS

**Synthesis of 2CdATP.** 2-Chloro-2'-deoxyadenosine-5'-triphosphate (2CdATP) was prepared by a modification of the general procedure for nucleoside triphosphate synthesis (14). Briefly, unprotected (2-CdA) was phosphorylated with POCl<sub>3</sub> in trimethyl phosphate, followed by treatment of the 5'-phosphorodichloridate intermediate with tri-*n*-butylammonium pyrophosphate in dimethyl formamide. The reaction mixture was neutralized with cold 1.0 M of triethylammonium bicarbonate (pH 8.5) and was chromatographed on a DEAE-Sephadex A-25 column with water and then a linear gradient of triethylammonium bicarbonate. The 2-CdATP was eluted at about 0.8 M of triethylammonium bicarbonate, dried, and stored at –20°C.

**Cell Isolation and Analysis.** Heparinized peripheral blood samples from normal subjects, or patients with CLL containing at least 80% malignant cells, were fractionated by Ficoll/Hypaque sedimentation. Nonadherent mononuclear cells were resuspended in complete medium (RPMI 1640 medium supplemented with 10% fetal bovine serum) at a density of 1 to 2 × 10<sup>6</sup> per ml. Cells were incubated at 37°C in an atmosphere of 5% CO<sub>2</sub> with 1  $\mu$ M of 2CdA or 10  $\mu$ M of dexamethasone for up to 24 hr, as indicated.

**Preparation of HeLa and CLL Extracts.** Human HeLa S3 cells (American Type Culture Collection, Manassas, VA; CCL 2.2) were grown in complete medium (DMEM supplemented with 10% fetal bovine serum) at 37°C in an atmosphere of 5% CO<sub>2</sub> 95% air. At 80% confluence, the culture flasks were placed on ice, washed twice with ice-cold isotonic PBS (pH 7.4), and harvested using a cell scraper. CLL cells were isolated as de-

The publication costs of this article were defrayed in part by page charge payment. This article must therefore be hereby marked "advertisement" in accordance with 18 U.S.C. §1734 solely to indicate this fact.

© 1998 by The National Academy of Sciences 0027-8424/98/959567-5\$2.00/0  
PNAS is available online at www.pnas.org.

Abbreviations: 2CdA, 2-chloro-2'-deoxyadenosine; 2CdATP, 2-chloro-2'-deoxyadenosine 5'-triphosphate; CLL, chronic lymphocytic leukemia; Apaf, apoptotic protease activating factor;  $\Delta\psi_m$ , mitochondrial transmembrane potential; PI, propidium iodide; pNA, p-nitroanilide; DiOC<sub>6</sub>, 3,3' dihexyloxycarbocyanine iodide; DEVD, Asp-Glu-Val-Asp.

<sup>†</sup>To whom reprint requests should be addressed. e-mail: lleoni@ucsd.edu.

scribed above. Cells were then washed at 4°C and resuspended in a hypotonic extraction buffer (HEB; containing 50 mM Pipes/50 mM KCl/5 mM EGTA/2 mM MgCl<sub>2</sub>/1 mM DTT/0.1 mM phenylmethanesulfonyl fluoride). The cells were centrifuged at 1,000 × *g* to form a tight pellet, and the volume of the cell pellet was approximated. The supernatant was discarded and HEB buffer was added to a volume between 0.5 and 1× the pellet volume. The cells were allowed to swell for 20–30 min on ice and then lysed in a Dounce homogenizer with 100 strokes of a B-type pestle. The extent of lysis was monitored under the microscope by erythrosin B staining. The cell lysate was centrifuged for 30 min at 100,000 × *g*. The clarified supernatant was used immediately or stored in aliquots at –80°C. The cytoplasmic fraction did not contain microscopically visible whole cells, nuclei, or mitochondria.

**Immunoblot assay for Nucleotide-Induced Caspase-3 Activation.** HeLa and CLL extracts were prepared as described above. Ten microliter aliquots (100 μg of protein) were incubated with the indicated nucleotides, and 10 μM of cytochrome *c* from bovine heart, at 30°C for 1 h in 15 μl with HEB buffer. At the end of the incubation, 5 μl of 4× SDS sample buffer were added to each reaction. After boiling for 5 min, each sample was subjected to 14% Tris-glycine SDS/PAGE. Caspase-3 was revealed by immunoblotting as described below.

**Colorimetric Assay for Nucleotide-Induced Caspase-3 Activation.** HeLa extracts were clarified by 0.2 μm filtration, then 10 μl of extracts (100 μg protein) were incubated in a 96-well plate with the indicated nucleotides, 10 μM of cytochrome *c*, and 100 μM of DEVD-*p*-nitroanilide (pNA), at 37°C for 30–60 min, in 50 μl with HEB buffer. The hydrolysis of the substrate was followed spectrophotometrically at 405 nm, in a Molecular Devices MAXline Microplate Spectrophotometer (Menlo Park, CA). Baseline absorbance values from reactions without nucleotides were subtracted from each data point. The specificity of the assay was validated by using the caspase-3 inhibitor Ac-DEVD-CHO at 1 μM. DEVD-pNA [sequence; *N*-acetyl-Asp-Glu-Val-Asp-pNA (15)] and Ac-DEVD-CHO (16) were purchased from Calbiochem.

**Immunoblotting.** Washed cell pellets were lysed in 2× SDS/PAGE sample buffer containing 10 mM DTT, for 5 min at 100°C. Alternatively, washed cells were lysed in RIPA buffer [50 mM Tris-HCl/50 mM NaCl, pH 7.4/1 mM EGTA/0.5% (vol/vol) Nonidet P-40/1 μg/ml aprotinin/1 μg/ml leupeptin/1 mM phenylmethanesulfonyl fluoride]. Lysates were centrifuged at 15,000 × *g* for 10 min to remove nuclei and the protein content of supernatants was measured by using a modified Coomassie blue assay (Pierce). Proteins were resolved at 125 V on 14% gels and electrophoretically transferred to 0.2 μm of polyvinylidene fluoride membranes (Millipore) for 2 h at 125 V. Membranes were blocked overnight in I-Block blocking buffer (Tropix, Bedford, MA). Blots were then probed for 1 h with antibodies to caspase-3 (Transduction Laboratories, Lexington, KY), or to Apaf-1 (11). The blots were developed with species-specific antisera, and visualized by alkaline phosphatase-based enhanced chemiluminescence (Tropix, Bedford, MA), according to the manufacturer's instructions. The x-ray films were scanned, acquired in Adobe Systems (Mountain View, CA) PHOTOSHOP, and analyzed with National Institutes of Health IMAGE software.

**Measurement of DNA Fragmentation.** DNA fragmentation was assessed by flow cytometry and electrophoresis. Prior to analysis by flow cytometry, cells were fixed in ice-cold 70% ethanol, and incubated with 100 μg/ml of RNase A and 50 μg/ml PI for 1 h at 37°C. Hypodiploid cells were visualized using a Becton Dickinson FACScalibur, and the program MODFIT LT 2.0 (Verity Software House, Topsham, TX).

Prior to electrophoresis, cells were resuspended for 20 min in hypotonic lysis buffer containing 10 mM Tris-HCl, 50 mM NaCl, 10 mM EDTA and 0.2% Triton X-100 (pH 7.5). After centrifugation at 14,000 × *g* for 10 min, and proteinase K

digestion, DNA was precipitated at –20°C in 2 volumes of isopropanol and 0.5 M of NaCl. The pellet was washed and resuspended in 10 mM of Tris-HCl, 10 mM of EDTA, and the samples were then electrophoresed for 2 h at 60 V in 2% agarose with 0.5 μg/ml ethidium bromide. An *Hae*III digest of φX174 provided molecular mass standards. After electrophoresis, the gels were photographed on a UV transilluminator.

**Cytofluorimetric Analysis of Mitochondrial Transmembrane Potential ( $\Delta\psi_m$ ) by 3,3'-Dihexyloxacarbocyanine Iodide (DiOC<sub>6</sub>) and Cell Membrane Permeability by PI.** Cells were treated with the indicated amount of 2CdA and 10 μM of the cell-permeable caspase-3/caspase-7-selective inhibitor Ac-DEVD-fmk (sequence; *N*-acetyl-Asp-Glu-Val-Asp-fluoromethylketone, Enzyme Systems Products, Livermore, CA). Cells were then incubated for 10 min at 37°C in culture medium containing 40 nM of DiOC<sub>6</sub> (Molecular Probes, Eugene, OR) and 5 μg/ml PI (Molecular Probes), followed by analysis within 30 min of fluorochrome in a Becton Dickinson FACScalibur cytofluorometer. After suitable compensation, fluorescence was recorded at different wavelengths: DiOC<sub>6</sub> at 525 nm (FL-1) and PI at 600 nm (FL-3).

## RESULTS

**Caspase-3 Activation by 2CdATP.** Liu *et al.* have reported that the addition of cytochrome *c* and dATP to cytosolic extracts induces the processing of caspase-3 to active forms capable of inducing apoptotic cell death (12). To determine if 2CdATP was able to replace dATP, a similar cell free system was established using HeLa cells and CLL cells. The addition of cytochrome *c* (0.2 μg per reaction) and dATP was required for the activation of caspase-3 in both HeLa and CLL extracts (Fig. 1 *A* and *B*), as demonstrated by the disappearance of the 32-kDa band and the appearance of a 20-kDa band, which represent the cleaved active fragment of caspase-3. dATP alone was not enough to activate caspase-3, probably because during the preparation of the cytosolic extract, the mitochondria were not damaged and did not release sufficient cyto-

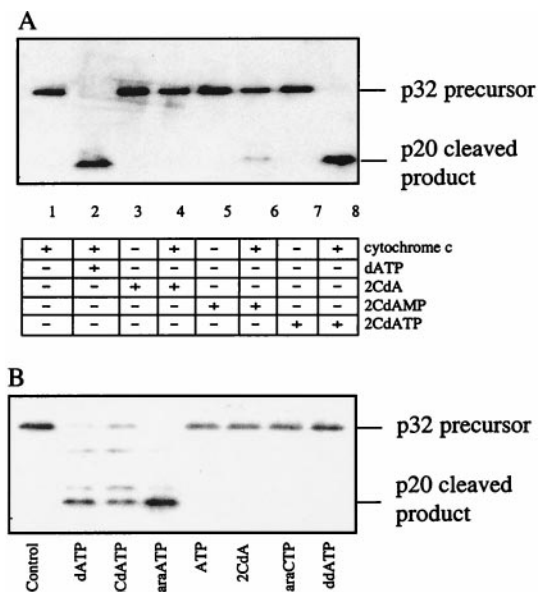


Fig. 1. Nucleotide-induced caspase-3 cleavage in cell free extracts. (*A*). Aliquots (10 μl) of HeLa cell extracts (100 μg) were incubated in the presence (lanes 1, 2, 4, 6, and 8) or absence (lanes 3, 5, and 7) of cytochrome *c* (10 μM) and various nucleotides (1 mM). Control lane (lane 1), dATP (lane 2), 2CdA (lane 3 and 4), 2CdAMP (lane 5 and 6), and 2CdATP (lane 7 and 8). (*B*) Aliquots (10 μl) of CLL cell extracts (100 μg) were incubated in absence (Control) or in the presence of cytochrome *c* (10 μM) and various nucleotides (1 mM), as indicated. Samples were subjected to SDS/PAGE, transferred to a polyvinylidene fluoride membrane, and probed with an anti-caspase-3 antibody.

chrome *c*. In the presence of cytochrome *c*, 2CdATP also induced caspase-3 cleavage, while 2CdA had no effect. The minimal activation of caspase-3 by 2CdAMP may be due to its conversion to 2CdATP by kinases present in the cell-free extracts, thus mimicking the process that occurs *in vivo* in cells exposed to 2CdA. Other nucleotides were also tested in the CLL extracts (Fig. 1B). 9- $\beta$ -D-Arabinofuranosyl ATP appeared to be the most potent inducer of caspase-3 activation, followed by dATP and 2CdATP. Under these conditions no caspase-3 cleavage was observed in extracts containing ATP, 2CdA, 9- $\beta$ -D-arabinofuranosyl-CTP and 2',3'-dideoxy ATP. The quantification of caspase-3 activation by the colorimetric enzyme assay (Fig. 2) showed that dATP is more potent than 2CdATP, especially at concentrations below 100  $\mu$ M. At concentrations of 1 mM and above, both nucleotides showed similar activities, and were more potent than ATP. The maximal caspase-3 activity induced by ATP was  $\approx$ 60% of the maximal activity induced by dATP and 2CdATP.

**Caspase-3 and Apaf-1 in Normal Lymphocytes and CLL.** In light of the results obtained in the cell free system, it was important to determine if caspase-3 and Apaf-1 were expressed in CLL cells and normal lymphocytes. Immunoblotting revealed that both components of the caspase cascade were detectable. The expression levels of Apaf-1 were approximately equivalent in the normal and malignant lymphocytes (Fig. 3B). In contrast, the expression level of caspase-3 was higher in CLL cells than in normal cells (Fig. 3A). Densitometric quantitation showed that the mean caspase-3 level in CLL cells was about twice that of normal peripheral blood lymphocytes.

**Caspase Activation by 2CdA in Normal Lymphocytes and CLL.** Previous work has shown that 2CdA induces internucleosomal DNA cleavage characteristic of apoptosis in sensitive CLL cells (17–19). To determine if the fragmentation was preceded by caspase-3 activation, cells from CLL patients were treated for 24 h with 1  $\mu$ M 2CdA, and the time courses of caspase-3 and DNA degradation were compared. Leukemic lymphocytes treated with 1  $\mu$ M 2CdA showed a gradual appearance of cells with a hypodiploid DNA content (Fig. 4). Agarose gel electrophoresis similarly demonstrated increasing amounts of the DNA fragments in an oligonucleosomal pattern (data not shown). Internucleosomal cleavage did not become prominent until 16 h of exposure. Untreated CLL cells also developed some spontaneous apoptosis after 24 h culture.

Immunoblotting experiments showed that freshly isolated CLL cells have already a small amount of cleaved caspase-3 (Fig. 4), as opposed to lymphocytes from normal donors, which did not show any detectable cleavage products (data not

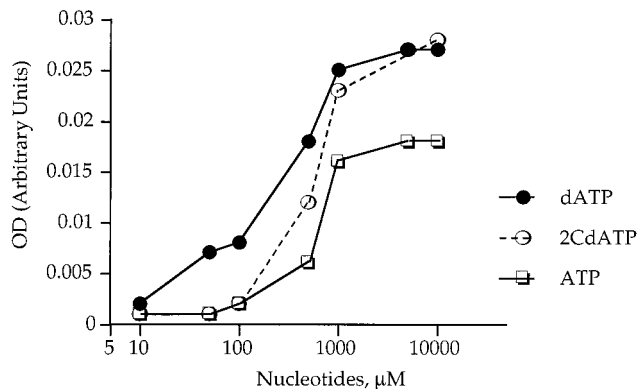


FIG. 2. Induction of caspase-3-like activity by nucleotides. Caspase-3-like activity was measured spectrophotometrically at 405 nm by hydrolysis of the colorimetric substrate DEVD-pNA. Aliquots (10  $\mu$ l) of HeLa cell extracts (100  $\mu$ g) were incubated at 37°C for 30 min, in the presence of DEVD-pNA (100  $\mu$ M), cytochrome *c* (10  $\mu$ M), and the indicated concentration of nucleotide. The data are representative of at least three independent experiments.

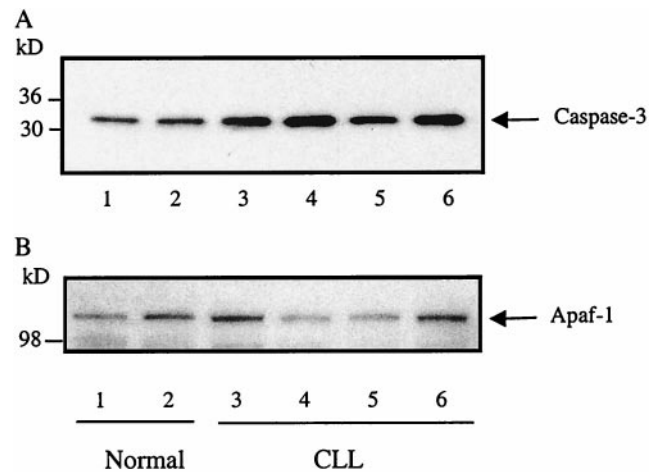


FIG. 3. Caspase-3 and Apaf-1 in normal and CLL lymphocytes. Extracts of CLL and normal lymphocytes were lysed in RIPA buffer for 1 h at 4°C, and lysates were centrifuged at 15,000  $\times$  g for 10 min. Equal amounts (50  $\mu$ g) of protein supernatants were electrophoresed on 14% Tris-glycine gels, subjected to SDS/PAGE, and transferred to polyvinylidene fluoride membranes. Caspase-3 and Apaf-1 were revealed by immunoblotting with enhanced chemiluminescent detection.

shown). 2CdA incubation substantially increased the caspase activation between 4 and 8 h of incubation, after the induction of DNA single strand breaks (20), but before endonuclease activation became prominent. Thus, significant cytoplasmic caspase-3 activation preceded nucleosomal degradation and cell death by 8 h in 2CdA-treated CLL cells.

**Effect of 2CdA on Mitochondria.** To determine the effect of 2CdA treatment on the  $\Delta\psi_m$  of freshly isolated CLL cells, the fluorochrome DiOC<sub>6</sub> was used. The reduction of  $\Delta\psi_m$  has been shown (21) to precede nuclear DNA fragmentation in lymphocyte apoptosis induced by dexamethasone. Either short-term treatment (24 h) of CLL cells with 1  $\mu$ M 2CdA or long-term (72 h) treatment with 50 nM 2CdA reduced the DiOC<sub>6</sub> fluorescence (Fig. 5 C and D). There was a concomitant increase in PI binding to DNA, reflecting a loss of membrane permeability and in the percentage of hypodiploid apoptotic cells. Untreated CLL cells incubated for 24 h had only 1% apoptotic cells, but 13% of low  $\Delta\psi_m$  cells and 8%

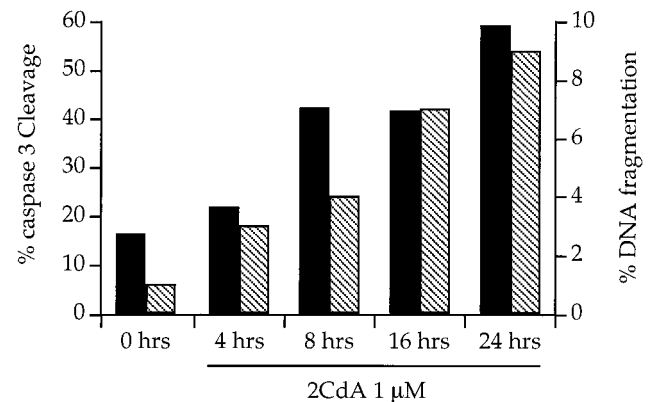


FIG. 4. Kinetics of caspase-3 activation and DNA fragmentation induced by 2CdA in CLL cells. Freshly isolated CLL cells were incubated for the times indicated with 1  $\mu$ M 2CdA, after which caspase-3 activation and DNA fragmentation were measured. Caspase-3 cleavage (■) was quantified by densitometry after immunoblotting, by comparing the relative intensities of the p32 caspase-3 precursor and the p20 cleaved product. DNA fragmentation (▨) was estimated by PI staining of ethanol-fixed cells and subsequent flow cytometry analysis. The results are representative of three independent replicates with different patient isolates.

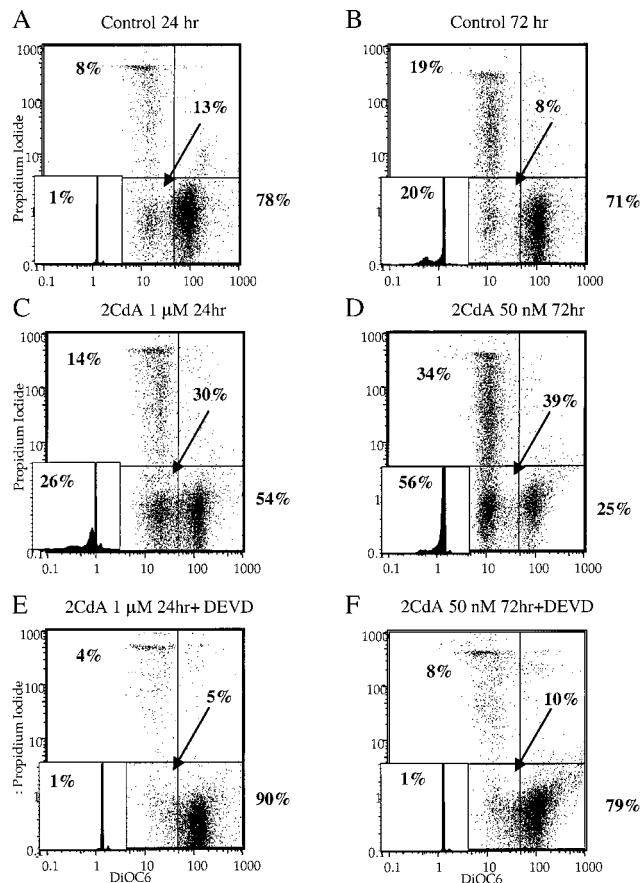


FIG. 5. Effect of 2CdA and caspase inhibitors on mitochondrial transmembrane potential and apoptosis. Freshly isolated CLL cells were incubated for the times indicated with 50 nM or 1  $\mu$ M 2CdA in the presence or absence of 10  $\mu$ M of the cell-permeable caspase-3/caspase-7-selective inhibitor Ac-DEVD-fmk. Cell membrane permeability and  $\Delta\psi_m$  were then assayed by incubating the unfixed cells for 10 min at 37°C in presence of 5  $\mu$ g/ml PI and 40 nM DiOC<sub>6</sub>. DNA fragmentation was estimated by flow cytometry after PI staining of fixed cells. In the large graphs, the x-axis is DiOC<sub>6</sub> (FL-1) fluorescence, and the y-axis is PI (FL-3) fluorescence. Numbers refer to the percentages of cells in the upper-left quadrant (dead cells), the lower-left quadrant (low  $\Delta\psi_m$ ), and the lower-right quadrant (normal cells). The small graphs (*Insets*) represent the DNA content of the cells from parallel cultures determined by PI staining of permeabilized cells, and the numbers refer to the percentages of hypodiploid (apoptotic) cells.

PI-positive cells (Fig. 5A). After 72 h of incubation, 20% of the untreated cells were apoptotic, 19% were PI-positive, and 8% showed a reduced  $\Delta\psi_m$  (Fig. 5B). Thus, a fall in DiOC<sub>6</sub> staining was a sensitive early marker of both drug-induced and spontaneous apoptosis in cultured CLL cells. The incubation of the cells with the cell-permeable caspase-3/caspase-7-selective inhibitor Ac-DEVD-fmk at 10  $\mu$ M inhibited completely the appearance of apoptotic cells (Fig. 5E and F). The loss of  $\Delta\psi_m$  was also noticeably reduced, but not blocked completely. Approximately 10% of cells treated with 50 nM 2CdA and with the caspase inhibitor still displayed a low  $\Delta\psi_m$ .

## DISCUSSION

The toxicity of 2CdA depends on its intracellular phosphorylation to CdATP by the tandem action of deoxycytidine kinase, AMP kinase, and nucleoside diphosphate kinase (22, 23). Because 2CdAMP is dephosphorylated back to the nucleoside by a cytosolic 5'-nucleotidase, both the *in vitro* sensitivity of cultured leukemic cells (1) and the *in vivo* response of patients with CLL to 2CdA (4) correlate with the ratio of deoxycytidine kinase to 5'-nucleotidase activities. Because CLL cells divide very slowly,

and cell volume remains stable, 2CdATP accumulates in cells with a high kinase to nucleotidase ratio until a new equilibrium is achieved, or death ensues. In patients given 2CdA orally (10 mg/m<sup>2</sup>) intracellular 2CdATP levels reached 10  $\mu$ M after 3 h, within cells cultured with 1  $\mu$ M 2CdA the intracellular 2CdATP levels reached 70  $\mu$ M (24).

How 2CdATP induces apoptosis in nondividing cells is not yet known. The nucleotide inhibits ribonucleoside diphosphate reductase (25), DNA polymerases  $\alpha$  and  $\beta$  (26), DNA ligase, and is incorporated into DNA (27). Together, these actions lead to the progressive accumulation of DNA single-strand breaks (20). The strand break formation by itself would not be expected to kill a noncycling cell. However, DNA strand breaks induce the activation of poly(ADP ribose)polymerase, with resultant consumption of NAD, and of total adenine nucleotides. The addition of nicotinamide to lymphocyte cultures exposed to 2CdA can delay the onset of cell death, by inhibiting poly(ADP ribose) formation, maintaining adenosine nucleotides, and replenishing NAD (20, 28).

In the present study, 2CdATP and cytochrome *c* initiated an apoptotic program in cell free cytosolic extracts, from both HeLa and CLL cells, as measured by the activation of caspase-3. Exposure of viable normal or CLL lymphocytes to 2CdA also induced caspase-3 activation. Time course analysis indicated that caspase activation occurred early, at the same time as DNA strand break formation, but before internucleosomal cleavage became prominent. The inhibition of caspase enzymatic activity by the cell-permeable caspase-3/caspase-7-selective inhibitor Ac-DEVD-fmk blocked 2CdA-induced apoptosis and partially prevented the 2CdA-induced reduction of the ( $\Delta\psi_m$ ) of freshly isolated CLL cells.

Recently, Liu and coworkers (8) identified in HeLa cytosol an heterodimeric protein of 45 kDa and 40 kDa, termed DNA fragmentation factor (DFF) that functions downstream of caspase-3 to trigger DNA fragmentation. A similar protein was found in the cytoplasm of mouse lymphocytes by Enari *et al.* (9). By cleavage of this inhibitor of caspase-activated DNase (ICAD), caspase-3 activates the caspase-activated DNase (CAD), enabling it to migrate to the nucleus and degrade DNA.

In most cell types, DNA strand break formation causes the activation of both poly(ADP ribose)polymerase and p53 dependent pathways (reviewed in refs. 29–32). In quiescent cells poly(ADP ribose)polymerase activation can induce an abrupt drop in NAD and in total adenine nucleotide pools (20). The activation of p53 has been shown to increase the synthesis of enzymes that generate or respond to oxidative stress (33). The combination of reduced adenine nucleotides and increased oxidative stress may impair the function of the F1F0-ATPase in the inner mitochondrial membrane, thereby promoting the release of cytochrome *c* into the cytoplasm (34, 35). The released cytochrome *c* could work together with Apaf-1, caspase-9, and increasing concentrations of adenine deoxynucleoside 5'-triphosphates to start a feed forward amplification cascade of caspase activation.

In summary, the data are consistent with the following mechanism of action of adenine deoxynucleosides in resting lymphocytes (Fig. 6). The deoxynucleoside enters cells and is converted progressively to its active 5'-triphosphate form, which causes DNA strand break formation, activating poly(ADP ribose)polymerase and p53. In consequence, NAD and total adenine nucleotides decrease, oxidative stress increases, and mitochondrial integrity wanes. In untreated cells, the concentrations of ATP and cytochrome *c* in the cytoplasm are insufficient to trigger the caspase cascade. However, the binding of Apaf-1 to caspase-9, and caspase-3, in the presence of high concentrations of adenine deoxynucleoside 5'-triphosphates and small amounts of released cytochrome *c*, leads to the cleavage of caspase-3, converting it to an active autocatalytic protease, in a process analogous to blood clot-

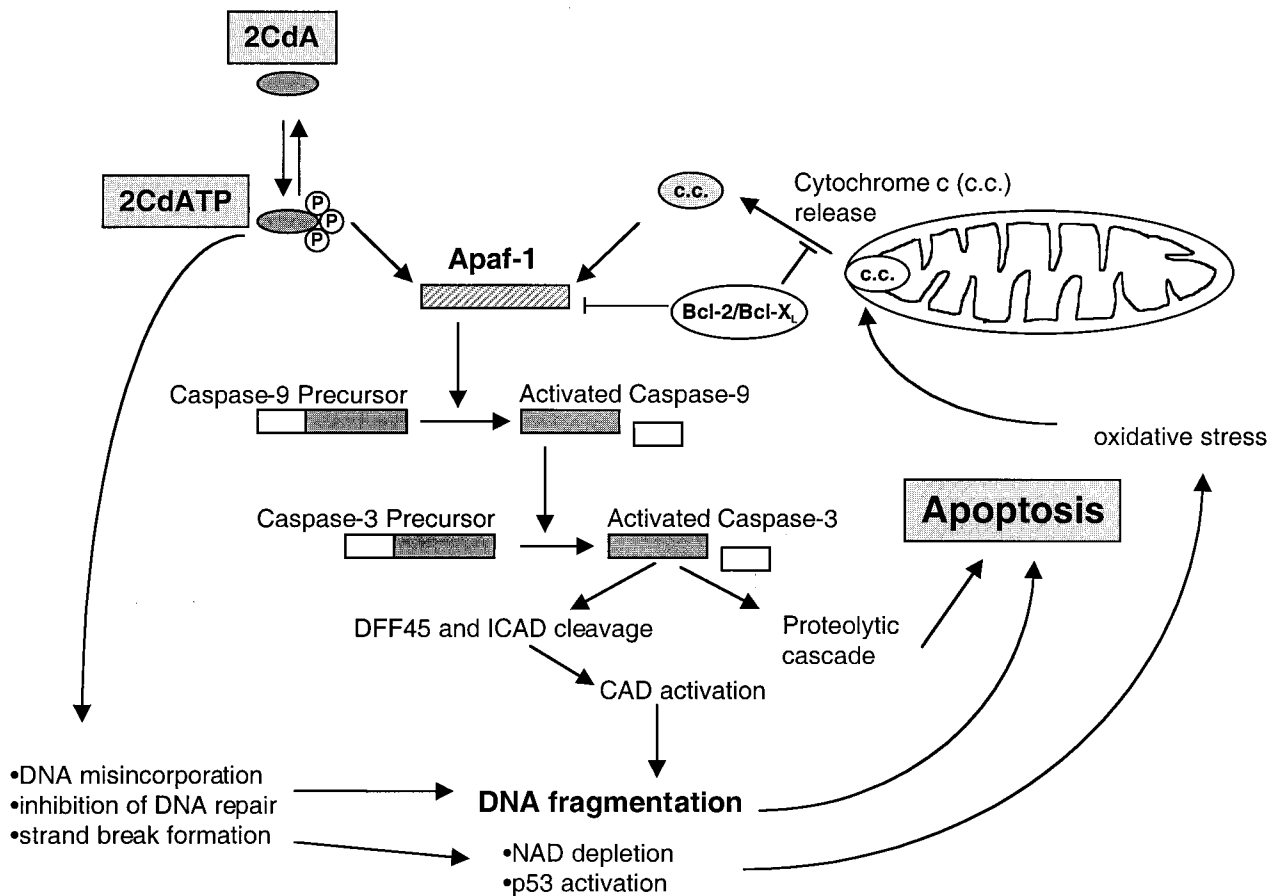


FIG. 6. Activation of the apoptotic pathway by adenine deoxynucleosides. An adenine deoxynucleoside, such as 2CdA, enters cells and is converted progressively to its active 2CdATP. The 2CdATP causes DNA strand break formation, activating poly(ADP ribose) polymerase and p53, with resultant depletion of NAD and adenine nucleotides, and a concomitant increase in oxidative stress. In untreated cells, the concentrations of ATP and cytochrome c (c.c.) in the cytoplasm are insufficient to trigger the caspase cascade. However, the binding of Apaf-1 to caspase-9, in the presence of 2CdATP and small amounts of released cytochrome c leads to the cleavage of caspase-3, converting it to an active autocatalytic protease, in a process analogous to the blood clotting. The active caspase-3 then stimulates, in turn, the CAD endonuclease that irreversibly degrades DNA.

ting. The active caspase-3 then stimulates, in turn, the CAD endonuclease that irreversibly degrades DNA. This model suggests that the baseline levels of caspase activation, in addition to the rate of adenine deoxynucleoside 5'-triphosphate formation, may be a factor that influences sensitivity to 2CdA, fludarabine, and deoxycoformycin chemotherapy. Malignant lymphocytes that display greatest sensitivity to the 2CdA, such as hairy cell leukemia cells, may undergo spontaneous apoptosis, due to a subthreshold level of caspase-3 activation in unmanipulated cells.

L.M.L. is supported by the Swiss Cancer League. This research was supported by National Institutes of Health Grants GM23200 and AR07567.

- Carson, D. A., Wasson, D. B., Taetle, R. & Yu, A. (1983) *Blood* **62**, 737-742.
- Carrera, C. J., Saven, A. & Piro, L. D. (1994) *Hematol. Oncol. Clin. North Am.* **8**, 357-381.
- Beutler, E. (1992) *Lancet* **340**, 952-956.
- Kawasaki, H., Carrera, C. J., Piro, L. D., Saven, A., Kipps, T. J. & Carson, D. A. (1993) *Blood* **81**, 597-601.
- Cohen, G. M. (1997) *Biochem. J.* **326**, 1-16.
- Salvesen, G. S. & Dixit, V. M. (1997) *Cell* **91**, 443-446.
- Nicholson, D. W. & Thornberry, N. A. (1997) *Trends Biochem. Sci.* **22**, 299-306.
- Liu, X., Zou, H., Slaughter, C. & Wang, X. (1997) *Cell* **89**, 175-184.
- Enari, M., Sakahira, H., Yokoyama, H., Iwamatsu, A. & Nagata, S. (1998) *Nature (London)* **391**, 43-50.
- Rotonda, J., Nicholson, D. W., Fazil, K. M., Gallant, M., Gareau, Y., Labelle, M., Peterson, E. P., Rasper, D. M., Ruel, R., Vaillancourt, J. P., *et al.* (1996) *Nat. Struct. Biol.* **3**, 619-625.
- Li, P., Nijhawan, D., Budihardjo, I., Srinivasula, S. M., Ahmad, M., Alnemri, E. S. & Wang, X. (1997) *Cell* **91**, 479-489.
- Liu, X., Kim, C. N., Yang, J., Jemmerson, R. & Wang, X. (1996) *Cell* **86**, 147-157.
- Zou, H., Henzel, W. J., Liu, X., Lutschg, A. & Wang, X. (1997) *Cell* **90**, 405-413.
- Seela, F. & Roling, A. (1992) *Nucleic Acids Res.* **20**, 55-61.
- Lazebnik, Y. A., Kaufmann, S. H., Desnoyers, S., Poirier, G. G. & Earnshaw, W. C. (1994) *Nature (London)* **371**, 346-347.
- Nicholson, D. W., Ali, A., Thornberry, N. A., Vaillancourt, J. P., Ding, C. K., Gallant, M., Gareau, Y., Griffin, P. R., Labelle, M., Lazebnik, Y. A., *et al.* (1995) *Nature (London)* **376**, 37-43.
- Carson, D. A., Carrera, C. J., Wasson, D. B. & Yamanaka, H. (1988) *Adv. Enzyme Regul.* **27**, 395-404.
- Robertson, L. E., Chubb, S., Meyn, R. E., Story, M., Ford, R., Hittelman, W. N. & Plunkett, W. (1993) *Blood* **81**, 143-150.
- Bellosillo, B., Dalmau, M., Colomer, D. & Gil, J. (1997) *Blood* **89**, 3378-3384.
- Seto, S., Carrera, C. J., Kubota, M., Wasson, D. B. & Carson, D. A. (1985) *J. Clin. Invest.* **75**, 377-383.
- Castedo, M., Hirsch, T., Susin, S. A., Zamzami, N., Marchetti, P., Macho, A. & Kroemer, G. (1996) *J. Immunol.* **157**, 512-521.
- Spasokoukotskaja, T., Arner, E. S., Brosjo, O., Gunven, P., Juliusson, G., Liliemark, J. & Eriksson, S. (1995) *Eur. J. Cancer* **31A**, 202-210.
- Wang, L., Karlsson, A., Arner, E. S. & Eriksson, S. (1993) *J. Biol. Chem.* **268**, 22847-22852.
- Reichelova, V., Albertioni, F. & Liliemark, J. (1996) *J. Chromatogr. B Biomed. Appl.* **682**, 115-123.
- Parker, W. B., Bapat, A. R., Shen, J. X., Townsend, A. J. & Cheng, Y. C. (1988) *Mol. Pharmacol.* **34**, 485-493.
- Hentosh, P., Koob, R. & Blakley, R. L. (1990) *J. Biol. Chem.* **265**, 4033-4040.
- Hentosh, P. & Grippo, P. (1994) *Mol. Pharmacol.* **45**, 955-962.
- Carson, D. A., Seto, S., Wasson, D. B. & Carrera, C. J. (1986) *Exp. Cell Res.* **164**, 273-381.
- Jeggo, P. A. (1998) *Curr. Biol.* **8**, R49-R51.
- Milner, J. (1995) *Nat. Med.* **1**, 879-880.
- Enoch, T. & Norbury, C. (1995) *Trends Biochem. Sci.* **20**, 426-430.
- Gotz, C. & Montenarh, M. (1996) *Rev. Physiol. Biochem. Pharmacol.* **127**, 65-95.
- Polyak, K., Xia, Y., Zweier, J. L., Kinzler, K. W. & Vogelstein, B. (1997) *Nature (London)* **398**, 300-305.
- Vander Heiden, M. G., Chandel, N. S., Williamson, E. K., Schumacker, P. T. & Thompson, C. B. (1997) *Cell* **91**, 627-637.
- Reed, J. C. (1997) *Cell* **91**, 559-562.





# Nucleotide Requirements for the *in Vitro* Activation of the Apoptosis Protein-activating Factor-1-mediated Caspase Pathway\*

(Received for publication, September 28, 1999)

Davide Genini‡§, Imawati Budihardjo¶, William Plunkett\*\*, Xiaodong Wang†, Carlos J. Carrera‡, Howard B. Cottam‡, Dennis A. Carson‡, and Lorenzo M. Leoni‡§§

From the ‡Department of Medicine and the Sam and Rose Stein Institute for Research on Aging, University of California San Diego, La Jolla, California 92093, ¶Howard Hughes Medical Institute, Department of Biochemistry, University of Texas Southwestern Medical Center, Dallas, Texas 75235, and the \*\*Department of Clinical Investigation, the University of Texas M. D. Anderson Cancer Center, Houston, Texas 77030

Adenine deoxynucleosides, such as 2-chlorodeoxyadenosine (2CdA) and fludarabine, induce apoptosis in quiescent lymphocytes, and are thus useful drugs for the treatment of indolent lymphoproliferative diseases. We previously demonstrated that the 5'-triphosphate metabolite of 2CdA (2CdATP), similar to dATP, can cooperate with cytochrome *c* and apoptosis protein-activating factor-1 (APAF-1) to trigger a caspase pathway in a HeLa cell-free system. We used a fluorometry-based assay of caspase activation to extend the analysis to several other clinically relevant adenine deoxynucleotides in B-chronic lymphocytic leukemia extracts. The nucleotide-induced caspase activation displayed typical Michaelis-Menten kinetics. As estimated by the  $V_{\max}/K_m$  ratios, the relative efficiencies of different nucleotides were Ara-ATP > 9-fluoro-9- $\beta$ -D-arabinofuranosyladenine 5'-triphosphate > dATP > 2CdATP > 9- $\beta$ -D-arabinofuranosylguanine 5'-triphosphate > dADP > ATP. In contrast to dADP, both ADP and its nonhydrolyzable  $\alpha,\beta$ -methylphosphonate analog were strong inhibitors of APAF-1-dependent caspase activation. The hierarchy of nucleotide activation was confirmed in a fully reconstituted system using recombinant APAF-1 and recombinant procaspase-9. These results suggest that the potency of adenine deoxynucleotides as co-factors for APAF-1-dependent caspase activation is due both to stimulation by the 5'-triphosphates and lack of inhibition by the 5'-diphosphates. The capacity of adenine deoxynucleoside metabolites to activate the apoptosome pathway may be an additional biochemical mechanism that plays a role in the chemotherapy of indolent lymphoproliferative diseases.

osine (cladribine or 2CdA), and 2'-deoxycoformycin are active to varying degrees in indolent lymphoproliferative diseases, including chronic lymphocytic leukemia (CLL), hairy cell leukemia, Waldenstrom's macroglobulinemia, and low grade lymphomas (1, 2). They are unique among nucleoside antimetabolites by virtue of their ability to induce apoptosis in nonproliferating cells.

The regulation of cell death by apoptosis is thought to play a fundamental role in the natural evolution of malignancy and in the response of tumors to chemotherapy. CLL is an attractive model to investigate the regulation of apoptosis, independent of cell cycle progression, because of its slow population doubling time and the ready accessibility of malignant cells. Previous studies have documented abnormalities in the expression of certain Bcl-2 family proteins in CLL (3–6). This family of proteins plays a critical role in controlling cellular responses to apoptotic stimuli, including those induced by many chemotherapeutic drugs (7). Some of the actions of Bcl-2 are mediated by its ability to control the response of mitochondria to factors in the cytoplasm that induce the release of cytochrome *c*.

The molecular details of the activation of the final steps of the apoptotic pathway have been recently investigated (8, 9). The cascade is initiated by cytochrome *c* binding to the apoptosis protein-activating factor APAF-1, which induces it to undergo a conformational change leading to the formation of APAF-1 multimers and to the recruitment of procaspase-9. The subsequent autocatalysis of procaspase-9 is followed by proteolytic activation of procaspase-3 and possibly procaspase-7. The entire multimeric complex has been defined as the functional apoptosome. Cytochrome *c* is normally sequestered inside mitochondria, between the inner and outer membranes of these organelles. However, it becomes released into the cytosol following exposure of cells to a variety of proapoptotic stimuli (10) (11–13). In addition to cytochrome *c*, the APAF-1-mediated *in vitro* activation of procaspase-9 and procaspase-3 requires dATP. Although ATP can supplant dATP, the deoxynucleotide is more active (12, 14). The peculiar preference of APAF-1 for dATP is unusual for energy-requiring processes not directly connected to DNA synthesis. In the present study, therefore, we designed experiments to compare the abilities of the purine deoxynucleoside analogs commonly used in the treatment of indolent lymphoproliferative diseases to activate the APAF-1-dependent apoptotic pathway and to define the kinetic parameters of the process.

The purine nucleoside analogs 9- $\beta$ -D-arabinofuranosyl-2-fluoradenine (fludarabine or F-Ara-A),<sup>1</sup> 2-chlorodeoxyaden-

\* This work was supported in part by National Institutes of Health Grants GM23200 and CA81534. The costs of publication of this article were defrayed in part by the payment of page charges. This article must therefore be hereby marked "advertisement" in accordance with 18 U.S.C. Section 1734 solely to indicate this fact.

‡ Supported by a grant from the Swiss National Science Foundation. ¶ Fellow of the Leukemia Society of America.

§§ Supported in part by a grant from the Swiss Cancer League. To whom all correspondence should be addressed. Tel.: 858-534-5408; Fax: 858-534-5399; E-mail: lleoni@ucsd.edu.

<sup>1</sup> The abbreviations used are: F-Ara-A or fludarabine, 2-fluoro-9- $\beta$ -D-arabinofuranosyladenine; CLL, chronic lymphocytic leukemia; APAF-1, apoptosis protein-activating factor-1; Ara-ATP, 9- $\beta$ -D-arabinofuranosyladenine 5'-triphosphate; F-Ara-ATP, 2-fluoro-9- $\beta$ -D-arabinofuranosyladenine 5'-triphosphate; CAFdATP, 2-chloro-9-(2-deoxy-2-fluoro- $\beta$ -D-arabinofuranosyl)adenine 5'-triphosphate; dATP, 2'-deoxyadenosine 5'-triphosphate; 2CdATP, 2-chloro-2'-deoxyadenosine 5'-triphosphate;

Ara-GTP, 9- $\beta$ -D-arabinofuranosylguanine 5'-triphosphate; 8-Cl-ATP, 8-chloroadenosine 5'-triphosphate; ADPcP,  $\beta,\gamma$ -methyleneadenosine 5'-triphosphate; AMPcP,  $\alpha,\beta$ -methyleneadenosine 5'-diphosphate; Ara-A, 9- $\beta$ -D-arabinofuranosyladenine; HEB, hypotonic extraction buffer; PIPES, 1,4-piperazinediethanesulfonic acid; AMC, Ac-DEVD-7-amino-4-methylcoumarin; AFC, Ac-LEHD-7-amino-4-trifluoromethylcoumarin; PAGE, polyacrylamide gel electrophoresis.

## MATERIALS AND METHODS

**Nucleotides**—Nucleosides were purchased from Sigma or Calbiochem. When nucleotides were unavailable commercially, they were synthesized by standard methods (15, 16) and checked for purity by TLC or high pressure liquid chromatography. The triphosphates studied included those of 9- $\beta$ -D-arabinofuranosyladenine 5'-triphosphate (Ara-ATP), 2-fluoro-9- $\beta$ -D-arabinofuranosyladenine 5'-triphosphate (F-Ara-ATP), 2-chloro-9-(2-deoxy-2-fluoro- $\beta$ -D-arabinofuranosyl)adenine 5'-triphosphate (CAFdATP), 2-chloro-2'-deoxyadenosine (2CdATP), 9- $\beta$ -D-arabinofuranosylguanine 5'-triphosphate (Ara-GTP), and 8-chloroadenosine 5'-triphosphate (8-Cl-ATP).

**Cell Isolation**—Heparinized peripheral blood samples from patients with CLL containing at least 80% malignant cells, were fractionated by Ficoll/Hypaque sedimentation. Nonadherent mononuclear cells were resuspended in complete medium (RPMI 1640 supplemented with 10% fetal bovine serum) at a density of  $1-2 \times 10^6$  cells/ml.

**Cell-free Extract Preparation**—CLL cells were isolated as described above. Cells were then washed at 4 °C and resuspended in a hypotonic extraction buffer (HEB; containing 50 mM PIPES, 50 mM KCl, 5 mM EGTA, 2 mM MgCl<sub>2</sub>, 1 mM dithiothreitol, 0.1 phenylmethanesulfonyl fluoride). The cells were centrifuged at  $1000 \times g$  to form a tight pellet, and the volume of the cell pellet was approximated. The supernatant was discarded, and HEB buffer was added to a volume between 0.5 and 1 times the pellet volume. The cells were allowed to swell for 20–30 min on ice and then lysed in a Dounce homogenizer with 100 strokes of a B-type pestle. The extent of lysis was monitored under the microscope by erythrosin B staining. The cell lysates were centrifuged for 60 min at  $100,000 \times g$ . The clarified supernatants were used immediately or stored in aliquots at  $-80$  °C. The cytoplasmic fractions did not contain microscopically visible whole cells, nuclei, or mitochondria.

**Cell-free Assays for Caspase Activity**—CLL extracts were clarified by 0.2- $\mu$ m filtration, and then 5–10  $\mu$ l of extracts (100–200  $\mu$ g of protein) were incubated in a 96-well plate with the indicated nucleotides, 2  $\mu$ M of cytochrome *c* from bovine heart, and either 50  $\mu$ M Ac-DEVD-7-amino-4-methylcoumarin (AMC) or 50  $\mu$ M of Ac-LEHD-7-amino-4-trifluoromethylcoumarin (AFC) at 37 °C for 30–60 min in 50  $\mu$ l with HEB buffer. The hydrolysis of the substrate was followed fluorometrically at 380 nm (excitation) and 460 nm (emission) for the caspase-3 substrate Ac-DEVD-AMC and at 400 nm and 505 nm for the caspase-9 substrate Ac-LEHD-AFC in a CytoFluor fluorescence plate reader (PerSeptive Biosystems, Framingham, MA). Base-line fluorescence values from reactions without nucleotides were subtracted from each data point. The specificity of the assay was validated using the caspase-3 inhibitor Ac-DEVD-CHO (aldehyde) at 1  $\mu$ M. Ac-DEVD-AMC (sequence, *N*-acetyl-Asp-Glu-Val-Asp-AMC (17)), Ac-DEVD-CHO (18), and Ac-LEHD-AFC (sequence, *N*-acetyl-Leu-Glu-His-Asp-AFC (19)) were purchased from Calbiochem.

**Immunoblotting**—10  $\mu$ l of CLL extracts were incubated at the indicated time points with the nucleotides and cytochrome *c* (2  $\mu$ M) in a volume of 20  $\mu$ l in HEB buffer at 37 °C. Proteins were resolved at 125 V on 14% gels and electrophoretically transferred to 0.2- $\mu$ m polyvinylidene fluoride membranes (Millipore Corp., Bedford, MA) for 2 h at 125 V. Membranes were blocked overnight in I-Block blocking buffer (Tropix, Bedford, MA). Blots were then probed for 1 h with antibodies to procaspase-3 (Transduction Laboratories, Lexington, KY) or to caspase-9 (provided by X. Wang). The blots were developed with species-specific antisera and visualized by alkaline phosphatase-based enhanced chemiluminescence (ECL; Tropix), according to the manufacturer's instructions. The x-ray films were scanned, acquired in Adobe Photoshop, and analyzed with NIH Image software.

**In Vitro Caspase-9 and Caspase-3 Assay**—Cytosolic extracts were prepared as described above and stored at  $-80$  °C. Human caspase-9 and caspase-3 expression plasmids were kindly provided by Dr. John Reed (Burnham Institute, La Jolla, CA). The respective procaspases were translated *in vitro* in the presence of [<sup>35</sup>S]methionine with a Promega (Madison, WI) TNT transcription/translation kit and purified from radioactive methionine and ATP through a desalting column (Bio-Rad).

**Reconstituted System**—The APAF-1/caspase-9 reconstituted system was recently described (20). Briefly, aliquots of 0.5  $\mu$ l (0.2  $\mu$ g) of His-tagged baculovirus-expressed recombinant procaspase-9 and 5  $\mu$ l (0.8  $\mu$ g) of baculovirus-expressed recombinant APAF-1 were incubated in the presence or absence of 10 ng/ml cytochrome *c* and the indicated nucleotides and 1 mM additional MgCl<sub>2</sub> at 30 °C for 1 h in a final volume of 20  $\mu$ l of buffer A (20 mM HEPES-KOH, pH 7.5, 10 mM KCl, 1.5 mM MgCl<sub>2</sub>, 1 mM NaEDTA, 1 mM NaEGTA, 1 mM dithiothreitol, 0.1 mM phenylmethylsulfonyl fluoride) (20). After incubation, the samples were

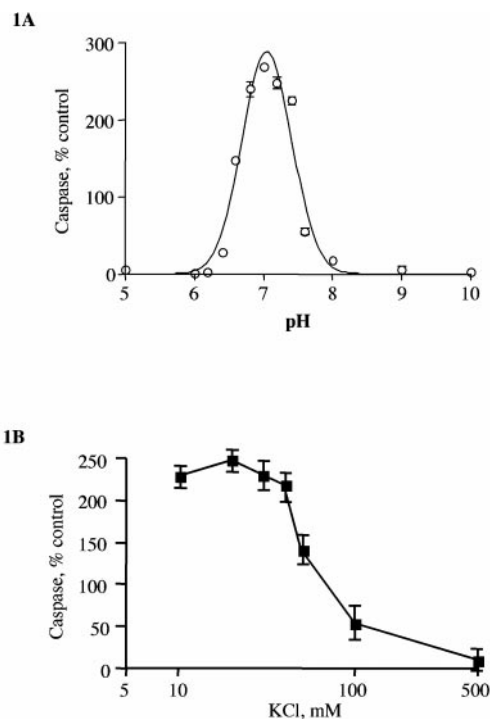


**FIG. 1. Characterization of nucleotide and cytochrome *c*-induced caspase activation in cell-free extracts: pH and salt dependence.** Caspase-3-like activity was measured fluorometrically by hydrolysis of the fluorogenic substrate DEVD-AMC (excitation, 380 nm; emission, 460 nm). Aliquots (10  $\mu$ l) of HeLa cell extracts (100  $\mu$ g) were incubated at 37 °C for 30 min, in the presence of DEVD-AMC (100  $\mu$ M), cytochrome *c* (2  $\mu$ M), and 0.5 mM dATP. HEB buffer was prepared for each of the indicated pH and KCl conditions. The y axis represents the percentage of caspase activity from the controls without dATP. The data are representative of at least three independent experiments.

subjected to a 15% SDS-PAGE and transferred to a nitrocellulose filter, which was blotted with anticaspase-9 antibody. Procaspase-3 was translated and purified as described above. A 1- $\mu$ l aliquot of *in vitro* translated caspase-3 was incubated with the mixture of procaspase-9 activation reaction as described above. The samples were subjected to a 15% SDS-PAGE, and then the gel was transferred to a nitrocellulose filter, which was subsequently exposed to a phosphor imaging plate and visualized in a Fuji BAS-1500 phosphor imager.

## RESULTS

**Characterization of the Assay Conditions**—We have previously demonstrated that the addition of cytochrome *c* and purine nucleotide analogs to HeLa and B-CLL cytosolic extracts induces the processing of procaspase-3 to active forms capable of inducing apoptotic cell death (14). To further investigate the details of this nucleotide-induced apoptotic pathway, the kinetic parameters were determined using a caspase-3-specific fluorogenic Ac-DEVD-AMC substrate. The results obtained using the Ac-LEHD-AFC substrate, which has a better affinity for caspase-9 (19), were very similar to those obtained with Ac-DEVD-AMC (data not shown). No cleavage of the caspase-1 substrate Ac-YVAD-AFC was observed in our experimental system (data not shown), thus confirming that caspase-1 is not activated by cytochrome *c* and nucleotides (21).

Nucleotide-induced caspase activation was optimal at pH 7.0 (Fig. 1A). This finding is in agreement with previous results showing that intracellular acidification is an early event in the apoptosis program in a variety of systems (22, 23). The optimum pH for caspase-3 activity has been reported to be pH 7.5 (24), indicating that the observed acidic optimum pH is determined by either caspase-9 activity or by cytochrome *c* and nucleotide-induced APAF-1 activation.

We used KCl in the range of 0–0.5 M in HEB buffer to

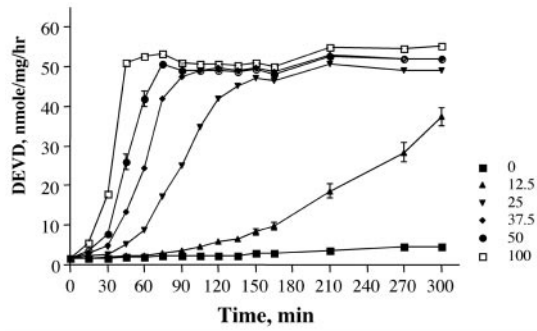


FIG. 2. Time course of nucleotide and cytochrome *c*-induced caspase activation in CLL extracts. Caspase-3-like activity was measured fluorometrically as described in Fig. 1. Various concentrations of dATP were used (12.5  $\mu\text{M}$  ( $\blacktriangle$ ), 25  $\mu\text{M}$  ( $\blacktriangledown$ ), 37.5  $\mu\text{M}$  ( $\blacklozenge$ ), 50  $\mu\text{M}$  ( $\bullet$ ), 100  $\mu\text{M}$  ( $\square$ ), and no ATP ( $\blacksquare$ ), and the fluorometric values at the indicated times were converted to nmol/mg using a standard curve of AMC.

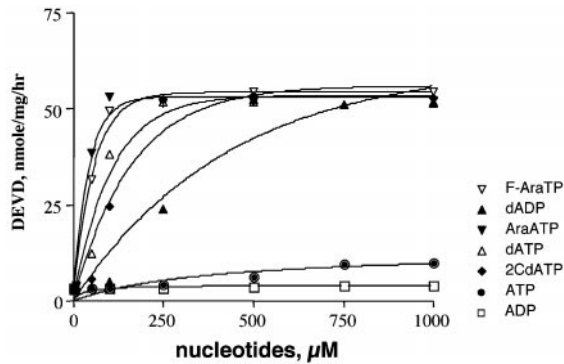


FIG. 3. Kinetics of nucleotides and cytochrome *c*-induced caspase activation in CLL extracts. Caspase-3-like activity was measured fluorometrically as described in the legends to Figs. 1 and 2 using DEVD-AMC. The nucleotides (F-Ara-ATP ( $\nabla$ ), dADP ( $\blacktriangle$ ), Ara-ATP ( $\blacktriangledown$ ), dATP ( $\triangle$ ), 2CdATP ( $\blacklozenge$ ), ATP ( $\bullet$ ), and ADP ( $\square$ )) were added at the indicated concentrations in the presence of 2  $\mu\text{M}$  cytochrome *c* in HEB buffer, and fluorescence was then measured after a 30-min incubation at 37  $^{\circ}\text{C}$ . Caspase-3-like activity was then expressed as nmol of AMC cleaved from the DEVD substrate per mg of CLL extract per 1 h of incubation (nmol/mg/h) using an AMC standard curve.

address the effect of ionic strength on nucleotide-induced caspase activation. Interestingly, although caspase-3 activity is not affected by high salt concentrations (24), nucleotide-induced caspase activity was maximal at 20 mM KCl (Fig. 1B) and was 20% of maximal activity at 150 mM KCl. These results indicate that the intracellular ionic strength may play an important role in restraining APAF-1-mediated caspase activation.

**Time Course of Nucleotide and Cytochrome *c*-Induced Caspase Activation**—In the presence of 2  $\mu\text{M}$  cytochrome *c*, but without the exogenous addition of dATP, no activation of caspase-3 pathway in CLL extracts was detectable (Fig. 2). In contrast, 12.5  $\mu\text{M}$  of dATP was sufficient to trigger the activation of the caspase after 15 min of incubation. The immunodepletion of caspase-9, APAF-1, or both, using specific polyclonal antibodies, completely abolished the nucleotide/cytochrome *c*-induced caspase activation (data not shown). These results indicate that caspase-9 and APAF-1 are critical for nucleotide/cytochrome *c*-initiated caspase-3 activation and cannot be substituted for by other caspases or CED-4 homologs present in the CLL extract.

In order to determine the possible role of intracellular nucleotides and low molecular weight compounds present in the CLL cell-free extracts, we dialyzed the extracts and repeated the caspase assays in the presence of exogenous cytochrome *c* and various concentrations of nucleotides. Dialysis did not prevent

TABLE I  
Kinetic parameters of cytochrome *c* and nucleotide-induced caspase-3 activation in a CLL cell-free system

B-CLL extracts (100  $\mu\text{g}$ ) were incubated at 37  $^{\circ}\text{C}$  with 2  $\mu\text{M}$  cytochrome *c* and concentrations of nucleotides ranging from 10 to 1000  $\mu\text{M}$ . A fluorometric based assay was used to monitor caspase-3 enzymatic activity at 20, 30, 40, and 60 min of incubation. The data collected were analyzed using nonparametric curve fitting to obtain the enzymatic kinetic values (Prism, GraphPad Software, San Diego, CA).

Nucleotide	$K_m$ $\mu\text{M}$	$V_{\max}$ nmol/mg/h	Efficiency ( $V_{\max}/K_m$ )	Relative efficiency
Ara-ATP	30 $\pm$ 13	53 $\pm$ 9	1.767	50
F-Ara-ATP	39 $\pm$ 11	54 $\pm$ 2	1.385	39
CaFdATP	59 $\pm$ 15	54 $\pm$ 8	0.915	26
dATP	65 $\pm$ 18	52 $\pm$ 4	0.897	25
2CdATP	199 $\pm$ 30	56 $\pm$ 5	0.281	8
Ara-GTP	220 $\pm$ 30	59 $\pm$ 7	0.268	8
8-Cl-ATP	252 $\pm$ 25	50 $\pm$ 5	0.198	6
dADP	298 $\pm$ 35	49 $\pm$ 11	0.164	5
ATP	374 $\pm$ 89	13 $\pm$ 5	0.035	1

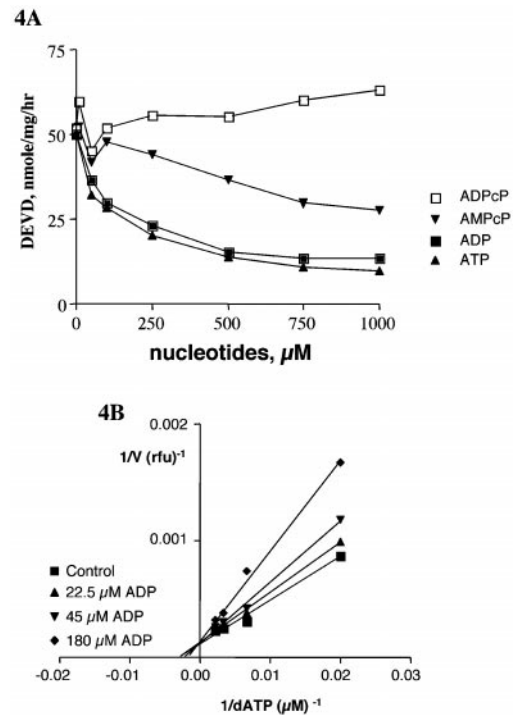


FIG. 4. Nucleotide inhibition of dATP and cytochrome *c*-induced caspase activation. A, CLL extracts were incubated in HEB buffer with DEVD-AMC, 250  $\mu\text{M}$  dATP, and 2  $\mu\text{M}$  cytochrome *c* and with the indicated concentrations of competing nucleotides (ADPcP ( $\square$ ), AMPcP ( $\blacktriangledown$ ), ADP ( $\blacksquare$ ), and ATP ( $\blacktriangle$ )). After 30 min at 37  $^{\circ}\text{C}$ , fluorescence was measured. B, "primary" double reciprocal plot (Lineweaver-Burk plot) for dATP and cytochrome *c*-induced caspase activation in HeLa extracts. dATP concentrations were varied between 50 and 500  $\mu\text{M}$ , while ADP was at different fixed concentrations (0  $\mu\text{M}$  ( $\blacksquare$ ), 25  $\mu\text{M}$  ( $\blacktriangle$ ), 50  $\mu\text{M}$  ( $\blacktriangledown$ ), and 200  $\mu\text{M}$  ( $\blacklozenge$ )). Each line was obtained by an unweighted least-squares fit to a hyperbola (Prism, GraphPad).

cytochrome *c* and nucleotide-induced caspase activation. However, the preparation of CLL and HeLa cell-free extracts by manual homogenization led predictably to the release of small amounts of cytochrome *c* from mitochondria that could be visualized by immunoblotting (data not shown). In order to address the role of the released cytochrome *c*, immunodepletion experiments using anticypochrome *c* (native form) antibodies were carried out. The removal of the endogenous cytochrome *c* did not alter the observed nucleotide kinetics. In the immunodepleted extracts, exogenous cytochrome *c* was required to initiate procaspase-9 and procaspase-3 cleavage (results

TABLE II

Inhibition constants of nucleotides for cytochrome *c*- and dATP-induced caspase-3 activation in a CLL cell-free system (100 ng)

CLL extracts were incubated at 37 °C with 2  $\mu$ M cytochrome *c* and 250  $\mu$ M dATP, and the activation of caspase-3 was assessed at nucleotide concentrations from 50 to 1000  $\mu$ M. The calculated  $K_i$  values are shown.

Nucleotide	$K_i$
	$\mu$ M
2',3'-ddATP	89 $\pm$ 6
ADP	133 $\pm$ 5
ATP	163 $\pm$ 16
AMPcP	1536 $\pm$ 250
3'-dATP (cordycepin)	1685 $\pm$ 302
ADPcP	NA <sup>a</sup>
dADP	NA

<sup>a</sup> NA, no inhibitory activity.

not shown).

**Kinetic Parameters of Nucleotide Activators in CLL Extracts**—A fluorometry-based assay was used to compare the effects of different nucleotides on APAF-1-dependent caspase activation in B-CLL cell extracts (Fig. 3). Caspase activation followed Michaelis-Menten kinetics, with a hyperbolic relationship between initial velocity and nucleotide concentrations. The ratio of  $K_m$  to  $V_{max}$ , calculated by a nonlinear least-squares fit method, revealed the relative efficiencies of the different nucleotides (Table I). The most active compounds were as follows: Ara-ATP > F-Ara-ATP > CAFdATP > dATP > 2CdATP > Ara-GTP > dADP > ATP. ATP was a very weak activator, with a relative efficiency 25-fold smaller than dATP and 50-fold smaller than Ara-ATP. We also tested nucleotides and deoxynucleotides based on other bases (C, G, U, T, and I), but none activated caspases in CLL extracts, with the notable exception of Ara-GTP (Table I). These results confirmed the energetic requirement for APAF-1-mediated caspase activation and indicated that arabinofuranosyl nucleotides are more active than deoxynucleotides.

**Kinetic Parameters of Nucleotide Inhibitors in CLL Extracts**—In addition to studying the activation of APAF-1 by purine nucleoside 5'-triphosphate substrates, it also was important to determine if the 5'-diphosphates were product inhibitors. Both ADP and ATP dose-dependently inhibited dATP-induced caspase activation in CLL extracts (Fig. 4). The determination of the  $K_i$  values (Table II) showed ADP ( $K_i = 133 \mu$ M) and ATP ( $K_i = 163$ ) to be nearly equipotent inhibitors. However, while a nonhydrolyzable  $\alpha,\beta$ -methylphosphonate analog of ADP (AMPcP) was also an inhibitor, a nonhydrolyzable analog of ATP (ADPcP) was ineffective (Fig. 4A). Hence, it is likely that the inhibitory action of ATP is due partly to its rapid conversion into ADP. It is noteworthy that dADP at concentrations up to 1 mM had no significant inhibitory effect on optimal dATP-induced caspase activation. The nonphysiological nucleotides 2',3'-ddATP and cordycepin (3'-dATP) showed an inhibitory capacity toward dATP-induced caspase activation.

**Immunoblotting**—Immunoblotting with anticaspase-3 and anticaspase-9 antibodies verified the time course of the nucleotide and cytochrome *c*-induced proteolytic activation of the procaspases in B-CLL extracts (Fig. 5). The results demonstrated that maximal procaspase-9 cleavage preceded maximal procaspase-3 proteolytic processing. Similarly, the depletion of caspase-9 was more rapid than that of caspase-3. After 20 min of incubation with 2  $\mu$ M cytochrome *c* and 0.25 mM dATP (lane 2) both caspase-3 and caspase-9 appeared to be cleaved. After 40 min, no visible procaspase-9 was detectable in the extract. In contrast, 120 min of incubation were needed to fully deplete procaspase-3. The immunoblotting also confirmed the ATP/ADP inhibition. The addition of 0.5 mM ATP reduced the intensity of the dATP-activated procaspase-3 band (lane 7). The

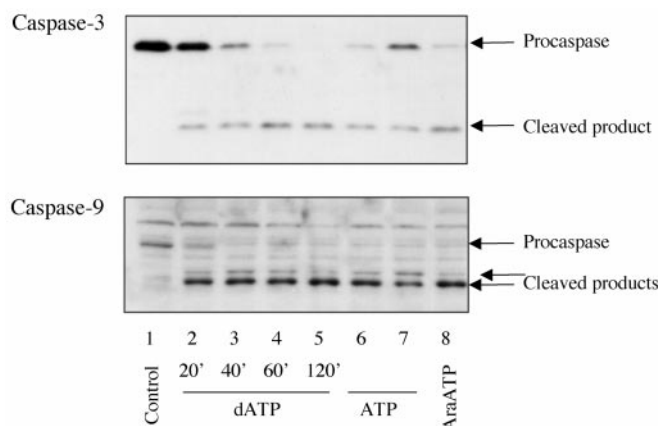


**FIG. 5. Nucleotide-induced procaspase-9 and procaspase-3 cleavage in cell-free CLL extracts.** Aliquots (10  $\mu$ l) of CLL cell extracts (100  $\mu$ g) were incubated in the presence of cytochrome *c* (2  $\mu$ M) and 250  $\mu$ M dATP (lanes 2–7) or 250  $\mu$ M Ara-ATP. Lane 1, control without any nucleotide; lanes 6 and 7, 100 and 500  $\mu$ M ATP. Lanes 1, 4, 6, 7, and 8 were incubated for 60 min, lane 2 for 20 min, lane 3 for 40 min, and lane 5 for 120 min at 37 °C. Samples were subjected to SDS-PAGE, transferred to a polyvinylidene difluoride membrane, and probed with an anticaspase-3 antibody (top) and an anticaspase-9 antibody (bottom).

inhibitory effect of ATP/ADP on dATP-induced procaspase-9 activation was less visible, but the intensity of the lower band that corresponded to the activated caspase-9 was also reduced. The immunoblotting of caspase-9 showed two bands of cleaved products, which probably correspond to the p35 and p37 fragments resulting from cleavage at the processing sites D315 (p35) and D330 (p37). The p35 fragment, which is the result of the autocatalytic cleavage of procaspase-9, was more abundant in the immunoblot than the p37 fragment, which is thought to be the result of feedback cleavage of caspase-9 by caspase-3 (25).

**Cleavage of *in Vitro* Translated Caspase-9 and Caspase-3**—To support further the data obtained by immunoblotting, the proteolysis of *in vitro* translated procaspase-9 was studied (Fig. 6). The results confirmed the dose dependence of dATP-induced procaspase-9 degradation. In agreement with the fluorometric assays, F-Ara-ATP and Ara-ATP were more potent than dATP, while 2CdATP was slightly less effective. These data also confirmed the inhibitory properties of ADP, which almost completely inhibited dATP-induced procaspase-9 cleavage.

**Nucleotide Effects in a Reconstituted System**—To rule out any possible effects of contaminants on nucleotide-induced caspase activation, we utilized a recently described reconstituted system, based on highly purified cytochrome *c*, recombinant APAF-1, and recombinant procaspase-9 and -3 (20). The results were similar to those obtained with CLL extracts (Fig. 7). Visible procaspase-3 and procaspase-9 cleavage was observed with as little as 10  $\mu$ M of F-Ara-ATP and dATP. The ranking of the tested nucleotides was the same as shown in Table I: F-Ara-ATP > CAFdATP > dATP > 2CdATP > ATP.

## DISCUSSION

These results indicate that various nucleotides can have markedly different effects on APAF-1-mediated caspase activation. Although other reports have elucidated carefully the mechanism of activation of caspase-9 by APAF-1, the role of the nucleotides in the process has not been quantified (9, 20, 21, 25). It is important to address this issue because of the known ability of certain purine deoxynucleoside analogs to induce apoptosis in nondividing cells.

The purine analogues fludarabine or cladribine are active in CLL patients resistant to classical alkylating agents (2, 26). Other nucleosides that are capable of killing nondividing

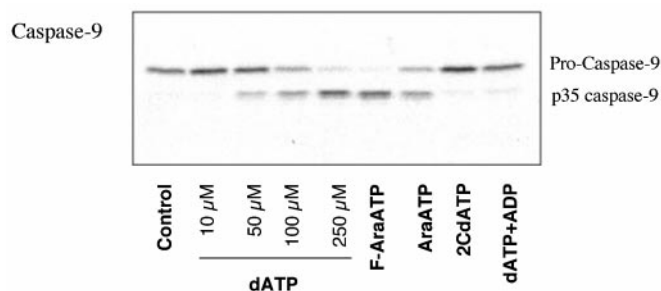


FIG. 6. Aliquots (10  $\mu$ l) of CLL cell extracts (100  $\mu$ g) were incubated in the presence of *in vitro* translated (rabbit reticulocyte)  $^{35}$ S-labeled procaspase-9 (3  $\mu$ l) and cytochrome *c* (2  $\mu$ M) and the indicated concentrations of nucleotides. Lane 1, control without any nucleotides; lanes 2–5, 10–250  $\mu$ M dATP; lanes 6–8, 100  $\mu$ M F-Ara-ATP, Ara-ATP, and 2CdATP; lane 9, 100  $\mu$ M dATP and 250  $\mu$ M ADP. Samples were subjected to SDS-PAGE, transferred to a polyvinylidene fluoride membrane, and exposed to x-ray films using an amplifying screen (Biomax Transcreen LE, Eastman Kodak Co.).

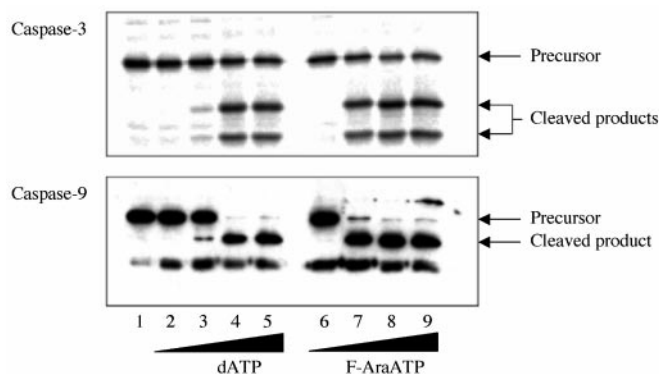


FIG. 7. Reconstituted purified recombinant APAF-1 and procaspase-9 system for nucleotide-induced activation of caspase-3 and -9. *Top panel*, caspase-3. Recombinant APAF-1 and procaspase-9 were prepared as described under "Materials and Methods." Aliquots of recombinant procaspase-9 (2  $\mu$ g), recombinant APAF-1 (0.8  $\mu$ g), and cytochrome *c* (0.2  $\mu$ g) were incubated in the presence (lanes 2 and 6, 10  $\mu$ M; lanes 3 and 7, 50  $\mu$ M; lanes 4 and 8, 100  $\mu$ M; lanes 5 and 9, 1000  $\mu$ M) or absence (lane 1) of the indicated nucleotides with 1  $\mu$ l of  $^{35}$ S-labeled affinity-purified procaspase-3 at 30  $^{\circ}$ C for 1 h in a final volume of 20  $\mu$ l of buffer A. The samples were then subjected to 15% SDS-PAGE, transferred to a nitrocellulose filter, and exposed to a phosphor imaging plate for 12 h at room temperature. *Lower panel*, caspase-9. The same procedure and conditions were used in the lower panel, except for the addition of the labeled procaspase-3. After the nucleotide incubation, the samples were subjected to 15% SDS-PAGE and transferred to a nitrocellulose filter. The filter was probed with a rabbit antibody against caspase-9. The antigen-antibody complexes were visualized by an ECL method.

lymphoid cells include 2'-deoxyadenosine, 2'- $\beta$ -D-arabinofuranosyladenine (27), 2-chloro-2'- $\beta$ -D-arabinofluoro-2'-deoxyadenosine (28), and 2'- $\beta$ -D-arabinofuranosylguanine (29). The cytotoxicity of these nucleoside analogs in lymphocytes depends mainly upon the selective and progressive accumulation of the 5'-triphosphate metabolites because of the high ratio of deoxycytidine kinase (EC 2.7.1.74) to cytosolic 5'-nucleotidase (EC 3.1.3.5) in lymphocytes, compared with other cell types (30, 31). The nucleoside 5'-triphosphates inhibit DNA polymerization and ligation and are incorporated into DNA (32). This leads to the progressive accumulation of DNA single strand breaks (33), followed by the activation of poly(ADP-ribose) polymerase, with resultant consumption of NAD and depletion of total adenine nucleotides.

Recently, we reported that 2CdATP was able to replace dATP in the activation of the procaspase-9/APAF-1 death pathway in HeLa cell extracts (14). In this paper, we demonstrate that 5'-triphosphate metabolites of the same nucleosides with

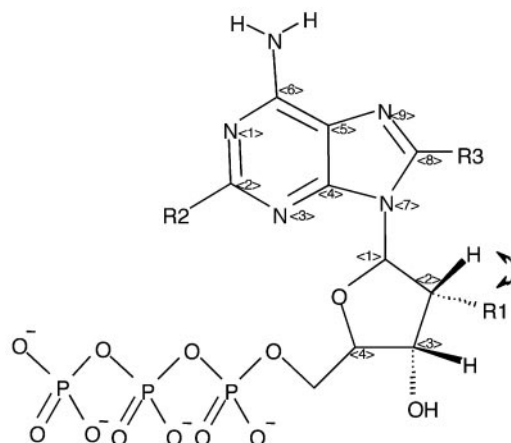


FIG. 8. Structure activity relationship for nucleotide-induced caspase activation. Schematic representation of the prototypic nucleotide activator of the apoptosome.

*in vitro* and *in vivo* cytotoxicity against indolent lymphoproliferative diseases are able to promote apoptosome activation both in CLL extracts and in a reconstituted "pure" system. The kinetics of nucleotide activation suggest that the apoptosome apoptotic pathway may play a relevant role *in vivo*. In fact, the concentrations of F-Ara-ATP in CLL lymphocytes of leukemic patients undergoing chemotherapy reach 30–60  $\mu$ M (34), near or above the  $K_m$  for the F-Ara-ATP-induced caspase cleavage (39  $\mu$ M).

In the CLL extracts, the arabinofuranosyl-based adenine nucleotides were the most potent activators, although Ara-GTP also had some activity (Table I). Furthermore, dATP was 25 times more effective than ATP in promoting apoptosome activation. A 2'-fluoro substitution of Ara-ATP slightly reduced its potency as compared with Ara-ATP, whereas the 2'-arabinofluoro substitution of CAFdATP increased its caspase activating capacity compared with 2CdATP. In other experiments, 8-Cl-ATP had 2-fold greater efficiency than ATP, whereas 2',3'-ddATP was devoid of caspase activating ability. Fig. 8 shows the structural features of nucleotides that appear to be optimal for APAF-1 activation of the apoptosome pathway: 1) a purine base (adenine > guanine), possibly with an 8-chloro substitution (R2), but without 2-halogenic substitutions (R3); 2) a ribofuranoside sugar with either no 2'-hydroxy group (R1) or a 2'-hydroxy or 2'-fluoro group in the "up" position and a 3'-hydroxy group in the "down" position; and 3) three 5'-hydrolyzable phosphate groups. Only a few proteins have been reported to show a preference for dATP as compared with ATP. These include DNA polymerases  $\alpha$ ,  $\beta$ , and  $\gamma$  as well as DNA primase (35, 36). Interestingly, 2-fluoro-2'-deoxyadenosine 5'-triphosphate was able to completely substitute for dATP using DNA polymerases  $\alpha$  and  $\gamma$ , whereas the 2-chloro and 2-bromo analogs substituted poorly (35).

Recent evidence suggests that the intracellular levels of purine nucleotides may play an important role in the modulation of apoptotic and necrotic cell death signals (37). Adenine nucleotide depletion has been shown to induce apoptosis, which was prevented by the antiapoptotic protein Bcl-2 (38). In our system, ADP was a good inhibitor of APAF-1-dependent caspase activation, with a  $K_i$  of 133  $\mu$ M. Thus, earlier reports showing that ATP was an inefficient activator of the APAF-1-mediated caspase pathway are difficult to interpret due to its progressive conversion into ADP. In addition, our findings showed that a nonhydrolyzable analog of ADP (AMPcP) was a good inhibitor, while a nonhydrolyzable analog of ATP (ADPcP) was not. Normal lymphocytes and CLL cells have been reported to have average cell volumes of 200 and 160 femtoliters

and ADP contents of 1127 and 873 pmol/10<sup>7</sup> cells, respectively (39–41). These values yield an estimated ADP concentration of about 400  $\mu$ M, 3-fold higher than the  $K_i$  of ADP for apoptosome activation. Taken together, The data appear to indicate that ADP may work as a physiological intracellular inhibitor of the cytochrome *c* and APAF-1-mediated caspase pathway in both normal lymphocytes and CLL cells.

The correlation between the clinical relevance of the nucleosides and the capacities of their corresponding 5-triphosphate derivatives to activate the apoptosome pathway underscores the relevance of these effects in the chemotherapy of indolent lymphoproliferative diseases. However, the capacity of nucleotide analogs to activate directly the apoptosome pathway does not fully explain their diverse cytotoxicities toward CLL cells, both *in vitro* and *in vivo*. It is well known that 2CdA is more toxic than F-Ara-A when tested in purified CLL cells (42), and the *in vivo* dosage of F-Ara-A is approximately 5 times higher than 2CdA (43). In contrast, our results showed that F-Ara-ATP was more effective than 2CdATP in activating caspases. Therefore, there must be additional mechanisms involved in the nucleoside cytotoxicity toward CLL cells. One contributing parameter may be DNA strand break formation, which triggers the consumption of adenine nucleotide pools for poly(ADP-ribose) synthesis and reduces ADP constraints on caspase activation. It is also possible that various nucleotide analogs may interfere with adenine nucleotide translocation in mitochondria, leading to the release of cytochrome *c*. Thus, deoxynucleotides may be able to modulate several different biochemical targets in lymphocytes that ultimately induce apoptotic death through caspase activation.

## REFERENCES

- Juliusson, G., Christiansen, I., Hansen, M. M., Johnson, S., Kimby, E., Elmhorn-Rosenborg, A., and Liliemark, J. (1996) *J. Clin. Oncol.* **14**, 2160–2166
- Johnson, S., Smith, A. G., Loffler, H., Osby, E., Juliusson, G., Emmerich, B., Wyld, P. J., and Hiddemann, W. (1996) *Lancet* **347**, 1432–1438
- Kitada, S., Andersen, J., Akar, S., Zapata, J. M., Takayama, S., Krajewski, S., Wang, H. G., Zhang, X., Bullrich, F., Croce, C. M., Rai, K., Hines, J., and Reed, J. C. (1998) *Blood* **91**, 3379–3389
- Hanada, M., Delia, D., Aiello, A., Stadtmayer, E., and Reed, J. C. (1993) *Blood* **82**, 1820–1828
- Pepper, C., Hoy, T., and Bentley, D. P. (1997) *Br. J. Cancer* **76**, 935–938
- Robertson, L. E., Plunkett, W., McConnell, K., Keating, M. J., and McDonnell, T. J. (1996) *Leukemia* **10**, 456–459
- Reed, J. C. (1997) *Semin. Hematol.* **34**, Suppl. 5, 9–19
- Zou, H., Henzel, W. J., Liu, X., Lutschg, A., and Wang, X. (1997) *Cell* **90**, 405–413
- Hu, Y., Benedict, M. A., Ding, L., and Nunez, G. (1999) *EMBO J.* **18**, 3586–3595
- Krippner, A., Matsuno-Yagi, A., Gottlieb, R. A., and Babior, B. M. (1996) *J. Biol. Chem.* **271**, 21629–21636
- Kluck, R. M., Bossy-Wetzell, E., Green, D. R., and Newmeyer, D. D. (1997) *Science* **275**, 1132–1136
- Liu, X., Kim, C. N., Yang, J., Jemmerson, R., and Wang, X. (1996) *Cell* **86**, 147–157
- Wang, X., and Studzinski, G. P. (1997) *Exp. Cell Res.* **235**, 210–217
- Leoni, L. M., Chao, Q., Cottam, H. B., Genini, D., Rosenbach, M., Carrera, C. J., Budihardjo, I., Wang, X., and Carson, D. A. (1998) *Proc. Natl. Acad. Sci. U. S. A.* **95**, 9567–9571
- Hoard, D. E., and Ott, D. G. (1965) *J. Am. Chem. Soc.* **87**, 1785–1788
- Moffatt, J. G. (1965) *Can. J. Chem.* **42**, 599–604
- Lazebnik, Y. A., Kaufmann, S. H., Desnoyers, S., Poirier, G. G., and Earnshaw, W. C. (1994) *Nature* **371**, 346–347
- Nicholson, D. W., Ali, A., Thornberry, N. A., Vaillancourt, J. P., Ding, C. K., Gallant, M., Gareau, Y., Griffen, P. R., Labelle, M., Lazebnik, Y. A., Munday, N. A., Raju, S. M., Smulson, M. E., Ting-Ting, Y., Yu, V. L., and Miller, D. K. (1995) *Nature* **376**, 37–43
- Thornberry, N. A., Rano, T. A., Peterson, E. P., Rasper, D. M., Timkey, T., Garcia-Calvo, M., Houtzager, V. M., Nordstrom, P. A., Roy, S., Vaillancourt, J. P., Chapman, K. T., and Nicholson, D. W. (1997) *J. Biol. Chem.* **272**, 17907–17911
- Zou, H., Li, Y., Liu, X., and Wang, X. (1999) *J. Biol. Chem.* **274**, 11549–11556
- Slee, E. A., Harte, M. T., Kluck, R. M., Wolf, B. B., Casiano, C. A., Newmeyer, D. D., Wang, H. G., Reed, J. C., Nicholson, D. W., Alnemri, E. S., Green, D. R., and Martin, S. J. (1999) *J. Cell Biol.* **144**, 281–292
- Meisenholder, G. W., Martin, S. J., Green, D. R., Nordberg, J., Babior, B. M., and Gottlieb, R. A. (1996) *J. Biol. Chem.* **271**, 16260–16262
- Gottlieb, R. A., Giesing, H. A., Zhu, J. Y., Engler, R. L., and Babior, B. M. (1995) *Proc. Natl. Acad. Sci. U. S. A.* **92**, 5965–5968
- Stennicke, H. R., and Salvesen, G. S. (1997) *J. Biol. Chem.* **272**, 25719–25723
- Srinivasula, S. M., Ahmad, M., Fernandes-Alnemri, T., and Alnemri, E. S. (1998) *Mol. Cell* **1**, 949–957
- Juliusson, G., and Liliemark, J. (1996) *Ann. Oncol.* **7**, 373–379
- Bajaj, S., Insel, J., Quagliata, F., Hirschhorn, R., and Silber, R. (1983) *Blood* **62**, 75–80
- Carson, D. A., Wasson, D. B., Esparza, L. M., Carrera, C. J., Kipps, T. J., and Cottam, H. B. (1992) *Proc. Natl. Acad. Sci. U. S. A.* **89**, 2970–2974
- Shewach, D. S., and Mitchell, B. S. (1989) *Cancer Res.* **49**, 6498–6502
- Carson, D. A., Wasson, D. B., Taetle, R., and Yu, A. (1983) *Blood* **62**, 737–743
- Kawasaki, H., Carrera, C. J., Piro, L. D., Saven, A., Kipps, T. J., and Carson, D. A. (1993) *Blood* **81**, 597–601
- Hentosh, P., Koob, R., and Blakley, R. L. (1990) *J. Biol. Chem.* **265**, 4033–4040
- Seto, S., Carrera, C. J., Kubota, M., Wasson, D. B., and Carson, D. A. (1985) *J. Clin. Invest.* **75**, 377–383
- Gandhi, V., Kemena, A., Keating, M. J., and Plunkett, W. (1993) *Leuk. Lymphoma* **10**, 49–56
- Parker, W. B., Bapat, A. R., Shen, J. X., Townsend, A. J., and Cheng, Y. C. (1988) *Mol. Pharmacol.* **34**, 485–491
- Kunkel, T. A., and Alexander, P. S. (1986) *J. Biol. Chem.* **261**, 160–166
- Eguchi, Y., Shimizu, S., and Tsujimoto, Y. (1997) *Cancer Res.* **57**, 1835–1840
- Marton, A., Mihalik, R., Bratincsák, A., Adleff, V., Peták, I., Végh, M., Bauer, P. I., and Krajcsi, P. (1997) *Eur. J. Biochem.* **250**, 467–475
- Liebes, L. F., Krigel, R. L., Conklyn, M., Nevrla, D. R., and Silber, R. (1983) *Cancer Res.* **43**, 5608–5617
- Carlucci, F., Rosi, F., Di Pietro, C., Marinello, E., Pizzichini, M., and Tabucchi, A. (1997) *Biochim. Biophys. Acta* **1360**, 203–210
- Kuse, R., Schuster, S., Schutte, H., Dix, S., and Hausmann, K. (1985) *Blut* **50**, 243–248
- Robertson, L. E., Chubb, S., Meyn, R. E., Story, M., Ford, R., Hittelman, W. N., and Plunkett, W. (1993) *Blood* **81**, 143–150
- O'Brien, S., del Giglio, A., and Keating, M. (1995) *Blood* **85**, 307–318

## Ser196 Phosphorylation of Caspase-9 Protects Against Autocatalytic Cleavage

Davide Genini<sup>1</sup>, John C. Reed<sup>2</sup>, Dennis A. Carson<sup>1</sup>, Lorenzo M. Leoni<sup>1</sup>.

<sup>1</sup> Department of Medicine and The Sam and Rose Stein Institute for Research on Aging, University of California at San Diego, <sup>2</sup> The Burnham Institute, Cancer Research Center.

Correspondence should be addressed to L.M.L.;

Leoni M. Lorenzo, Dept. Medicine, UCSD-0663, Stein Clinical Res. 126D, 9500 Gilman Drive, LA JOLLA, CA-92093, USA. Tel: 858-534-5442, Fax: 858-534-5399, email: lleoni@ucsd.edu

This work was supported in part by grants GM23200, CA81534, AR07567, RR00833 and RR00827 from the National Institutes of Health, and grant number DAMD17-99-1-9100 from the U.S. Army Medical Research and Material Command.

Key words: Apoptosis, caspase-9, caspase-3, anticancer drugs.

### SUMMARY

**Caspase-9 is a cysteine protease that plays a central role in mitochondrial-mediated programmed cell death. Association with APAF-1 activates procaspase-9 in a cytochrome c- and dATP-dependent manner. Akt, a kinase that suppresses apoptosis, phosphorylates caspase-9, thereby preventing activation of this protease. Using a cell-free system obtained from B-chronic lymphocytic leukemia cells, we demonstrate that the phosphorylation at Serine 196 (S196) protects caspase-9 from autocatalytic activation induced by Apaf-1/cytochrome c, but not from caspase-3 cleavage. Moreover, we observed that deoxyadenosine triphosphate (dATP) hydrolysis is required for autocatalytic processing of caspase-9, but not for caspase-3 cleavage. Transfection of either human leukemic Jurkat or of breast cancer MCF-7 cells with mutant procaspase-9 (S196) did not alter their susceptibility to a variety of apoptotic-inducing anticancer drugs. These findings suggest therefore that autocatalytic cleavage of caspase-9 is not an essential requirement for an effective apoptosis pathway.**

### INTRODUCTION

Apoptosis is an evolutionary conserved process involved in tissue homeostasis of multicellular organisms (1,2). A wide variety of genetic and biochemical studies have revealed that apoptosis is caused by caspases, a family of cysteine (3-5). Usually present as zymogen pro-forms, caspases require proteolysis at conserved aspartic acids for activation. Because active caspases cleave substrate proteins at aspartic acid residues, these proteases are capable of activating themselves and each other through trans-proteolytic mechanisms and cascades of sequential proteolysis.

Caspases involved in apoptosis can be divided into two groups: apical caspases such as caspases-2, -8, -9, and -10 and executioner caspases such as -3, -6, and -7 (6,7). Once activated, the apical caspases transmit an apoptotic signal to

the executioners through proteolytic cleavage, activating a cascade, which leads to apoptosis. The apical zymogens contain large N-terminal prodomains, which mediate interactions with caspase-activating proteins. One of these prodomain structures is the CARD domain (Caspase Recruitment Domain), which is found in several initiator caspases. The CARD domain of procaspase-9 binds Apaf-1 (Apoptotic Protease activating factor-1) in a cytochrome c-dependent manner in a mitochondrial pathway of cell death (8).

Granzyme B is the only other mammalian protease with specificity for Asp, playing a role in lymphocyte granule-mediated apoptosis for protection from pathogens and tumor cells (9,10). It is able to activate most caspase zymogens, except for caspase-1 (7).

UV light, -irradiation and chemotherapeutic drugs induce apoptosis largely through cytochrome c release from mitochondria, resulting in activation of procaspase-9 (11-13). Using purified components, several of the steps in this mechanism have been elucidated. First cytochrome c binding to Apaf-1, in conjunction with dATP, allows self-oligomerization of Apaf-1, and induces a conformational change in Apaf-1 structure leading to the exposure of its CARD domain, thus permitting binding to the CARD domain of procaspase-9. Closely juxtaposed caspase-9 zymogens assemble on the Apaf-1 oligomeric complex, then trans-proteolyze each other, resulting in cleavage of procaspase-9 molecules at amino acid residue 315. Procaspase-3 is then recruited in this complex, called the "apoptosome", and activated by caspase-9-mediated cleavage (14,15). Active caspase-3 then cleaves apoptosome-associated caspase-9 at aspartic acid residue 330 (16).

The regulation of the "apoptosome" pathway can occur at different levels. We previously demonstrated that the 5'-triphosphate metabolites of adenine deoxynucleosides, similar to dATP, can cooperate with cytochrome c and APAF-1 to trigger a caspase pathway in a chronic lymphocytic leukemia cell-free system (17). In the same experimental system, ATP and ADP were shown to act as inhibitors, but the inhibitory mechanism remained unclear.

Post-translational modifications have also been reported to regulate the apoptosome pathway. Phosphorylation of caspase-9 and its proform at residue Ser196 by the kinase Akt (also known as protein kinase B or PKB) was recently shown to inhibit its protease activity, interfering with cytochrome c-mediated activation of caspases (18). In this study we analyzed the role of Ser-196 phosphorylation in both the autocatalytic and caspase-3-induced cleavage of procaspase-9, and the effect of Ser-196 phosphorylation on the susceptibility of cells to undergo programmed cell death triggered by a variety of anti-cancer agents.

In this study, we analyzed the role of caspase-9 phosphorylation on the cytochrome c/dATP-induced apoptosome activation, and reevaluated the inhibitory activity of ATP and ADP.

## EXPERIMENTAL PROCEDURES

### Cell-Free Extract Preparation

Heparinized peripheral blood samples from patients with CLL containing at least 80% malignant cells were fractionated by Ficoll/Hypaque sedimentation. Cells were then washed at 4°C and resuspended in a hypotonic extraction buffer (HEB; containing 50 mM PIPES/ 50 mM KCl/5 mM EGTA/2 mM MgCl<sub>2</sub>/1 mM DTT/0.1 phenylmethanesulfonyl fluoride). The cells were centrifuged at 1000 g to form a tight pellet, and the volume of the cell pellet was approximated. The supernatant was discarded and HEB buffer was added to a volume between 0.5 and 1× the pellet volume. The cells were allowed to swell for 20-30 minutes on ice and then lysed in a Dounce homogenizer with 100 strokes of a B-type pestle. The extent of lysis was monitored under the microscope by erythrosin B staining. The cell lysate was centrifuged for 60 minutes at 100,000 g. The clarified supernatant was used immediately or stored in aliquots at -80°C. The cytoplasmic fraction did not contain microscopically visible whole cells, nuclei, or mitochondria.

### *In vitro* caspase-9 and caspase-3 assay

Full-length human Procaspase-9 wild-type (WT) and S196A expression plasmids (18), were subcloned into pcDNA3 (Invitrogen, San Diego, CA). The respective procaspases were *in vitro* translated in presence of [<sup>35</sup>S]-methionine with a Promega (Madison, WI) TNT transcription/translation kit and purified from radioactive methionine and ATP through a p-10 desalting column (Bio-Rad, Richmond, CA). The recombinant caspases were incubated 30 minutes at 37 °C with the cytosolic extract in presence of the indicated amount of nucleotide triphosphates. Inhibition assays were performed after activation with 250 μM dATP and inhibition with different concentrations of ATP.

### Assays for the characterization of the D315 and D330 cleavage site

For the characterization of the two cleavage sites, the caspase-3 D330 and the caspase-9 D315, recombinant [<sup>35</sup>S]-caspase-9 wild-type (WT) and mutants were treated with 20 μM recombinant active caspase-3 (provided by G.S. Salvesen, Burnham Institute, La Jolla, CA), 200 ng granzyme

B (provided by D.R. Green, La Jolla Institute for Allergy and Immunology), or activated in a cell-free system with 250 μM dATP. Specific caspases were inhibited with DEVD-CHO (Molecular Probes, Eugene, OR), z-VAD-fmk (Calbiochem, San Diego, CA) or depleted with specific monoclonal antibodies for caspase-3 (Transduction Laboratories, Lexington, KY) and polyclonal for caspase-9, kindly provided by X. Wang (Howard Hughes Medical Institute, Dallas, TX).

### Selection of the transfected clones of MCF-7

Full-length human procaspase-9 WT and S196A expression plasmids, which contain neomycin-selectable markers, were transfected into human breast adenocarcinoma MCF-7 cell line (ATCC HTB 22) and human T cell leukemia Jurkat cell line (ATCC TIB 152) with liposome-mediated Effectene reagent (Qiagen, Valencia, CA) according to the manufacturer's instructions. Efficiency of transfection was quantified by concomitant transfection of a plasmid encoding for the GFP protein (kindly provided by Jacques Corbeil, VA Medical Center San Diego, CA) followed by flow cytometry analysis of the cells after 48 h. Selection of stable transformants was performed in the presence of 1 mg/ml (Jurkat) and 0.5 mg/ml (MCF-7) geneticin (Sigma, St. Louis, MO). Individual clones were obtained by limiting dilution.

### Cytotoxicity assays

Forty-eight hours after transient transfection with the mutant caspase-9 vectors, MCF-7 cells were tested against staurosporine, paclitaxel (Taxol), cladribine (2CdA), and indanocine (19) at different concentrations chosen according to the IC<sub>50</sub> of the untransfected cells. For assays using stable transfectants, cells were grown under continuous neomycin selection (1 mg/ml) until two days before the assay. Cells were then washed and resuspended in neomycin-free medium for two days, before various concentrations of the indicated drugs were added. Cells were cultured for three days in presence of the indicated drugs and cytotoxicity was measured with an MTT assay and monitored with a spectrophotometer (20). The data collected for the single drugs were analyzed using non-parametric curve fitting to obtain the IC<sub>50</sub> values (Prism, GraphPad Software, San Diego, CA).

### Whole Cell Assay for Caspase Activity

MCF-7 transfected cells were treated with 1 μM 2CdA or 1 μM staurosporine for 24 hours at 37 °C to induce caspase-9 activation. Cells were washed twice with PBS and the pellets were resuspended in caspase buffer (50 mM Hepes, pH 7.4, 100 mM NaCl, 1 mM EDTA, 0.1% Chaps, and 5 mM dithiothreitol) for 30 min at 4 °C. Lysates (10-20 μg of total protein) were mixed with 50 μl aliquots of caspase buffer, and reactions were initiated by addition of 50 μM of the specific substrate. After 1 hour incubation at 37°C, caspase-9-like protease activity was measured with the substrate Ac-LEHD-AFC (sequence; N-acetyl-Leu-Glu-His-Asp-AFC (21)). Activity was measured by the release of 7-amino-4-trifluoromethylcoumarin (AFC) monitoring fluorescence at excitation and emission wavelengths of 400 and 505 nm, respectively.



## RESULTS

### Comparison of wild-type and mutant S196A caspase-9 activation in a cell-free system

Recombinant wild-type (WT) or S196A mutant procaspase-9 was translated *in vitro* in the presence of [<sup>35</sup>S]-methionine. When added to extracts prepared from CLL cells, the combination of dATP and cytochrome c induced cleavage of both WT and S196A procaspase-9. The proteolytic cleavage was equivalent for wild-type and Ser196A caspase-9 (Fig. 1a). Interestingly, the cleavage of wild-type caspase-9 resulted in a single large-subunit fragment with a molecular weight of about 37 kDa (p37), while the Ser196A caspase-9 protein produced p37 plus an additional fragment with a smaller molecular weight (p35).

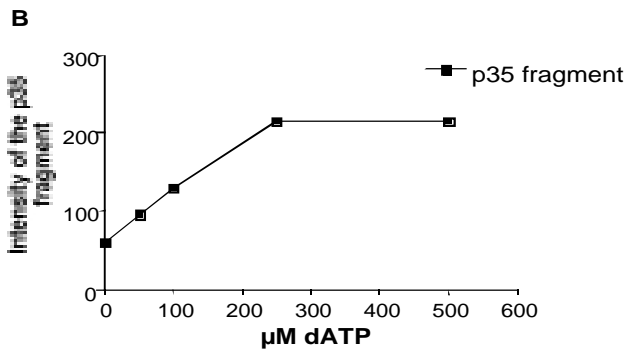
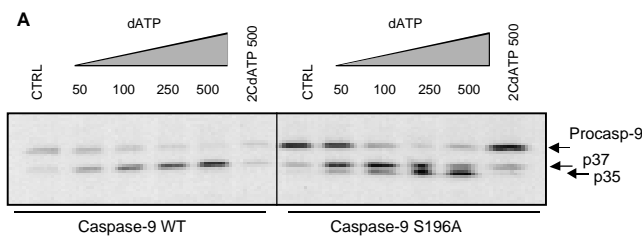


**Figure 1.** Comparison of dATP-induced procaspase-9 cleavage in wild type (WT) and mutant non-phosphorable (S196A) procaspase-9. **Fig 1A.** CLL S-100 extracts (100 μg) were incubated with *in vitro* translated <sup>35</sup>S-Caspase-9 WT or S196A (3 μl) and cytochrome c (2 μM) and the indicated amount of nucleotide triphosphates for 30 minutes at 37°C. Samples were separated in a 4-20% SDS-gel, transferred to a PVDF membrane and exposed to X-ray films using an amplifying screen (Biomax Transcreen LE, Kodak). **Fig 1B.** Quantification of the dATP-induced p35 caspase-9 cleaved fragment. The intensity of the p35 caspase-9 fragment was determined by quantitative phosphorimager analysis using a PhosphorImager™ (Molecular Dynamics). The results are representative of 3 independent experiments using S100 extracts from different CLL patients.

### Cytochrome c-induced processing of S196A procaspase-9 is regulated by dATP concentration

Increasing the dATP concentrations in cell extracts with mutated S196A procaspase-9 dose-dependently increased intensity of the p35 fragment (Fig 1A). At low dATP concentrations, or using the less efficient analogue 2CdATP, the p37 fragment is predominantly expressed. Increasing dATP concentrations induces the disappearance of p37 and the appearance of p35 (Fig. 1B).

### Inhibition of the caspases by addition of ATP does not go through Caspase-9 phosphorylation

We previously demonstrated that ATP can act as an inhibitor of the apaf-1/caspase-9 pathway in cell-free extracts (11). One possible explanation for this result is that addition of ATP activated Akt kinase and enhanced the phosphorylation of caspase-9, which could explain the observed inhibitory activity. To test this hypothesis we compared the ATP inhibitory activity in the dATP-activated cell-free system using the WT and S196A caspase-9. No differences were observed between the wild-type and mutant caspases in terms of the ATP inhibitory activity (Fig. 2).

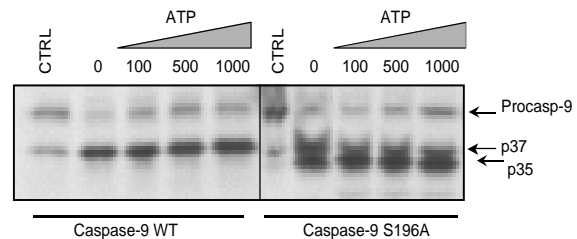


**Figure 2.** Comparison of the ATP-inhibitory activity on cytochrome c/dATP-induced caspase-9 cleavage. CLL S100 extracts (100 μg) were incubated with *in vitro* translated <sup>35</sup>S-caspase-9 WT or S196A (3 μl) and cytochrome c (2 μM) and the caspase pathway was activated with 250 μM of dATP. Inhibition assays were performed with addition of different ATP concentrations for 30 minutes at 37°C. Samples were fractionated in a 4-20% SDS-gel, transferred on a PVDF membrane and exposed to X-ray films.

### Characterization of the two bands of caspase-9

The activated caspase-9 fragment p37 is known to be the result of the cleavage by caspase-3 at Asp 330, and the fragment p35 is the product of the autocatalytic processing at Asp 315 (22). To identify the nature of the observed caspase-9 fragments, we used the following approaches: (a) treatment with specific caspase inhibitors; (b) incubation with recombinant active forms of caspase-3 and granzyme B; and (c) immunodepletion with specific anti-caspase antibodies. Inhibition of caspase-3 by the specific inhibitor DEVD-CHO, in the cell-free system activated by 250 μM dATP, blocked the appearance of the p37 fragment of caspase-9 S196A and almost reduced completely the activation of the wild-type caspase (Fig. 3A lanes 1 and 2). Depletion of caspase-3 by immunoprecipitation with monoclonal anti-caspase-3 antibody, resulted in the removal of the p37 fragment, leaving behind the smaller p35 (Fig. 3B lanes 1 and 2). Incubation of the recombinant caspases with active recombinant caspase-3 resulted in the cleavage of both types of caspase-9, but only at D 330 resulting in the fragment p37 (Fig. 3A lanes 5 and 6). Granzyme B treatment produced both bands (Fig. 3A lanes 3 and 4), but resulted in the cleavage only at the expected Asp 315 when caspases were inhibited with zVAD-fmk (Fig. 3B lane 5).

### Experiments with transfected MCF-7 and Jurkat cells

The human T lymphoblastoid cell line Jurkat and the human breast cancer cell line MCF-7, were used to assess the role of the

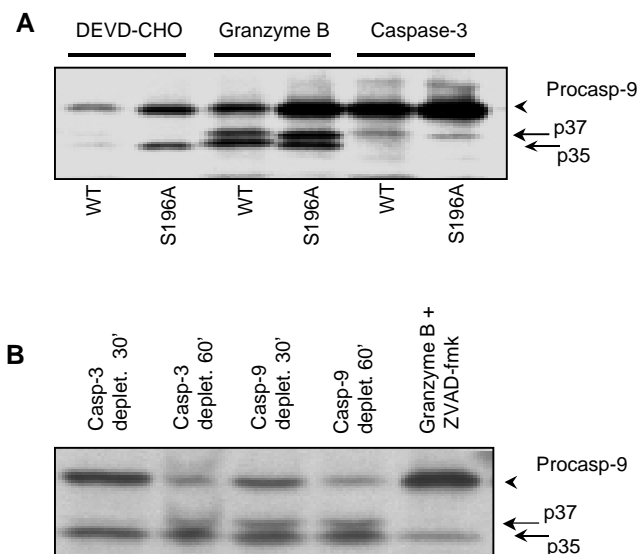


**Figure 3.** Determination of the cleavage fragments of WT and S196A procaspase-9. **Fig. 3A** Recombinant caspase-9 (3  $\mu$ l) was incubated with CLL extract (100  $\mu$ g), activated with 250  $\mu$ M dATP in presence of cytochrome c (2  $\mu$ M) and caspase-3 was inhibited by the specific inhibitor DEVD-CHO at 1  $\mu$ M (lanes 1 and 2). In lanes 3 and 4 recombinant caspase-9 was incubated with 200 ng granzyme B and in lanes 5 and 6 with 20  $\mu$ M active recombinant caspase-3, all at 37  $^{\circ}$ C for 30'. **Fig. 3B** 3  $\mu$ l of  $^{35}$ S-Caspase-9 S196A was incubated with 100  $\mu$ g of CLL extract, 2  $\mu$ M cytochrome c and 250  $\mu$ M dATP for 30' and 60' respectively, after immunodepletion of caspase-3 (lanes 1 and 2) and immunodepletion of caspase-9 (lanes 3 and 4) with specific antibodies. In lane 5 recombinant caspase-9 S196A was incubated with 200 ng of granzyme B in presence of 1  $\mu$ M ZVAD-fmk for 30' at 37 $^{\circ}$ C. All the samples were electrophorated in a 4-20% SDS-gel, transferred to a PVDF membrane and exposed to X-ray films, as described in the previous figures. The results are representative of 3 independent experiments.

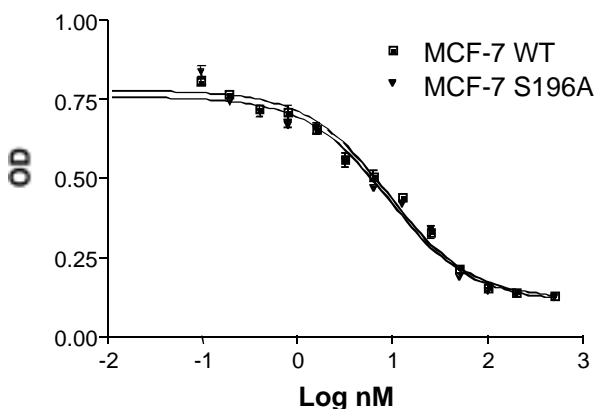
phosphorylation mutation of caspase-9 on susceptibility to drug-induced apoptosis. Cells transiently or stably expressing wild-type and S196A mutant procaspase-9 were generated, and their susceptibilities to apoptosis were tested using the following cytotoxic drugs: staurosporine (23), taxol (24), 2CdA (17), and indanocine (19). To confirm the presence of the plasmid in the cells, we performed PCR analysis for exon 2 and 3 of caspase-9 (data not shown). Serial-dilution of the drugs was performed to determine their IC<sub>50</sub> values on the tested cell lines. No difference was observed in the toxicity of the four compounds tested in the stably transfected Jurkat or MCF-7 cells (Fig. 4). Transiently transfected cell lines also exhibited the same apoptotic responses to these drugs (data not shown). Caspase activity analysis was performed using lysates from drug-tested cells by fluorometric analysis with specific caspase-3 and -9 substrates. No difference was detected in the intensity or kinetics of drug-induced caspases activation, comparing WT and S196A transfected cells (data not shown).

## DISCUSSION

Phosphorylation of procaspase-9 by Akt was reported to inhibit its activation and to down-regulate apoptosis in cells (18). We showed in a previous report that ADP is an endogenous inhibitor of the dATP-mediated activation of

APAF-1/cytochrome c apoptotic pathway, probably through competitive inhibition of the binding of dATP to APAF-1 (11).

In this study, we analyzed the role of procaspase-9 phosphorylation on nucleotide-induced caspase activation. For this reason, mutants of caspase-9 at the phosphorylation site Ser 196 were employed. We observed a difference in cleavage between the wild-type and the mutant S196A procaspase-9 after activation with dATP, with mutant procaspase-9 S196A exhibiting a smaller p35 cleaved fragment. Procaspase-9 is known to possess two different cleavage site at aspartic acid residues 330 and 315. The first is believed to be specific for feedback activation by caspase-3, and the second is the autocatalytic site and cleavage site for granzyme B (22). To identify the fragments observed in our blots, several approaches were taken, including (a) cleavage with granzyme B; (b) recombinant active caspase-3; and (c) depletion or inhibition of specific caspases with specific antibodies. Our results indicate that the two bands observed represent the previously described fragments. The activated caspase-9 produced the p37 fragment, reflecting cleavage at D330, the cleavage site of caspase-3. In contrast the mutant S196A was cleaved at both sites, D330 and D315. Therefore it appears that phosphorylation at S196 protects procaspase-9 from its autocatalytic processing. This result explains previous observations that Akt-mediated phosphorylation of procaspase-9 prevents activation of the protease by cytochrome c (18).



	IC50 MCF-7 WT (nM)	IC 50 MCF-7 S196A (nM)
STAUROSPORIN	8.5	8.9
TAXOL	2.3	3.1
2CdA	15.8	19
INDANOCINE	6.3	8.9

**Figure 4.** Chemosensitivity of MCF-7 cells stably transfected with full-length human procaspase-9 and mutated caspase-9 S196A. Cytotoxic assays were performed as indicated in the experimental procedures section after 72 hours drugs exposure by MTT reduction. Cells were grown under continuous neomycin selection until two days before the assay. Cells were then washed and resuspended in neomycin-free medium, for two days before different concentrations of the indicated drugs were added. The top panel represents the MTT assay for staurosporine. The y-axis is optical density measured at 570 nm. The x-axis indicates the various concentrations of staurosporine, expressed in Log<sub>10</sub> nM. The lower panel represents the results of the assays performed with the indicated drugs. The IC<sub>50</sub> was calculated using non-parametric curve fitting software (Prism, Graphpad, San Diego). The results are representative of 4 independent experiments.

Hu et. al. recently reported that energy is required for the activation of procaspase-9 in the APAF-1-mediated pathway (25). ATP-analog hydrolysis is a requisite for the assembly of APAF-1 molecules (11). Our data suggest that energy is also needed for the autocatalytic cleavage of procaspase-9. Titration of dATP in the S196A mutated system induces a linear appearance of the p35 fragment of caspase-9.

We investigated the possibility that previously observed ATP inhibition of the dATP-induced caspase activation (11) was mediated by the phosphorylation of procaspase-9 by an activated upstream kinase, such as Akt. The results obtained in this report seem to exclude this hypothesis. In fact, the ATP-based inhibitory activity for both wild-type and mutated S196A recombinant procaspase-9 was similar. Therefore ATP inhibition appears occur by a phosphorylation-independent mechanism. Finally, stable or transient transfected cell lines showed no difference in the response to cytotoxic drugs nor in caspase activation *in vivo*. We can not exclude the possibility that the endogenous procaspase-9 present in the cells may

still be functional, and that the "dominant negative" overexpression approach used in our experiments is not sufficient to completely block its function. Nevertheless, the data suggest that phosphorylation of Ser 196 does not greatly influence the apoptotic cascade *in vivo*. We speculate that the Ser196 residue of caspase-9 may be constitutively phosphorylated *in vivo* and, as already reported (16), and thus its cleavage may not be a crucial step. Phosphorylation may play a role in the prevention of undesired spontaneous apoptosis, by blocking the apical caspase autoactivation. Association of procaspase-9 with the cofactor APAF-1 appears to be more important than its cleavage for the activation of the apoptotic cascade, and phosphorylation of procaspase-9 may interfere with this protein interaction.

## REFERENCES

- Martin, S. J., and Green, D. R. (1995) *Cell* **82**(3), 349-52
- Miura, M., Zhu, H., Rotello, R., Hartweg, E. A., and Yuan, J. (1993) *Cell* **75**(4), 653-60
- Green, D. R. (1998) *Cell* **94**(6), 695-8
- Horvitz, H. R., Shaham, S., and Hengartner, M. O. (1994) *Cold Spring Harb Symp Quant Biol* **59**, 377-85
- Miller, D. K. (1997) *Semin Immunol* **9**(1), 35-49
- Froelich, C. J., Dixit, V. M., and Yang, X. (1998) *Immunol Today* **19**(1), 30-6
- Salvesen, G. S., and Dixit, V. M. (1997) *Cell* **91**(4), 443-6
- Susin, S. A., Zamzami, N., Castedo, M., Daugas, E., Wang, H. G., Geley, S., Fassy, F., Reed, J. C., and Kroemer, G. (1997) *J Exp Med* **186**(1), 25-37
- Darmon, A. J., Nicholson, D. W., and Bleackley, R. C. (1995) *Nature* **377**(6548), 446-8
- Froelich, C. J., Orth, K., Turbov, J., Seth, P., Gottlieb, R., Babior, B., Shah, G. M., Bleackley, R. C., Dixit, V. M., and Hanna, W. (1996) *J Biol Chem* **271**(46), 29073-9
- Genini, D., Budihardjo, I., Plunkett, W., Wang, X., Carrera, C. J., Cottam, H. B., Carson, D. A., and Leoni, L. M. (2000) *Journal of Biological Chemistry* **275**(1), 29-34
- Hakem, R., Hakem, A., Duncan, G. S., Henderson, J. T., Woo, M., Soengas, M. S., Elia, A., de la Pompa, J. L., Kagi, D., Khoo, W., Potter, J., Yoshida, R., Kaufman, S. A., Lowe, S. W., Penninger, J. M., and Mak, T. W. (1998) *Cell* **94**(3), 339-52
- Yoshida, H., Kong, Y. Y., Yoshida, R., Elia, A. J., Hakem, A., Hakem, R., Penninger, J. M., and Mak, T. W. (1998) *Cell* **94**(6), 739-50
- Qin, H., Srinivasula, S. M., Wu, G., Fernandes-Alnemri, T., Alnemri, E. S., and Shi, Y. (1999) *Nature* **399**(6736), 549-57
- Zou, H., Li, Y., Liu, X., and Wang, X. (1999) *J Biol Chem* **274**(17), 11549-56
- Stennicke, H. R., Deveraux, Q. L., Humke, E. W., Reed, J. C., Dixit, V. M., and Salvesen, G. S. (1999) *J Biol Chem* **274**(13), 8359-62
- Leoni, L. M., Chao, Q., Cottam, H. B., Genini, D., Rosenbach, M., Carrera, C. J., Budihardjo, I., Wang, X., and Carson, D. A. (1998) *Proc Natl Acad Sci U S A* **95**(16), 9567-71
- Cardone, M. H., Roy, N., Stennicke, H. R., Salvesen, G. S., Franke, T. F., Stanbridge, E., Frisch, S., and Reed, J. C. (1998) *Science* **282**(5392), 1318-21
- Leoni, L. M., Hamel, E., Genini, D., Shih, H., Carrera, C. J., Cottam, H. B., and Carson, D. A. (2000) *Journal of the National Cancer Institute* **92**(3), 217-24
- Mosmann, T. (1983) *J Immunol Methods* **65**(1-2), 55-63
- Thornberry, N. A., Rano, T. A., Peterson, E. P., Rasper, D. M., Timkey, T., Garcia-Calvo, M., Houtzager, V. M., Nordstrom, P. A., Roy, S., Vaillancourt, J. P., Chapman, K. T., and Nicholson, D. W. (1997) *J Biol Chem* **272**(29), 17907-11
- Srinivasula, S. M., Ahmad, M., Fernandes-Alnemri, T., and Alnemri, E. S. (1998) *Mol Cell* **1**(7), 949-57
- O'Brian, C. A., and Ward, N. E. (1990) *J Natl Cancer Inst* **82**(22), 1734-5
- Blagosklonny, M. V., and Fojo, T. (1999) *Int J Cancer* **83**(2), 151-6
- Hu, Y., Benedict, M. A., Ding, L., and Nunez, G. (1999) *Embo J* **18**(13), 3586-95



# Deoxyadenosine analogs induce programmed cell death in chronic lymphocytic leukemia cells by damaging the DNA and by directly affecting the mitochondria

Davide Genini, Souichi Adachi, Qi Chao, David W. Rose, Carlos J. Carrera, Howard B. Cottam, Dennis A. Carson, and Lorenzo M. Leoni

**Adenine deoxynucleosides induce apoptosis in quiescent lymphocytes and are thus useful drugs for the treatment of indolent lymphoproliferative diseases. To explain why deoxyadenosine and its analogs are toxic to a cell that is not undergoing replicative DNA synthesis, several mechanisms have been proposed, including the direct binding of dATP to the pro-apoptotic factor Apaf-1 and the activation of the caspase-9 and -3 path-**

**ways. In this study it is shown, by means of several assays on whole cells and isolated mitochondria, that 2-chloro-2'-deoxyadenosine (2CdA) and 2-chloro-2'-ara-fluoro-deoxyadenosine (CaFdA) disrupt the integrity of mitochondria from primary chronic lymphocytic leukemia (B-CLL) cells. The nucleoside-induced damage leads to the release of the pro-apoptotic mitochondrial proteins cytochrome c and apoptosis-induc-**

**ing factor. The other adenine deoxynucleosides tested displayed comparable DNA-damaging potency but did not affect mitochondrial function. Interference with mitochondrial integrity, thus, may be a factor in the potent cytotoxic effects of 2CdA and CaFdA toward nondividing lymphocytes. (Blood. 2000;96:3537-3543)**

© 2000 by The American Society of Hematology

## Introduction

The deoxynucleoside analogs 2'-deoxyadenosine (dAdo), 2-chloro-2'-deoxyadenosine (2CdA, cladribine), 9- $\beta$ -D-arabinofuranosyl-2-fluoroadenine (F-ara-A, fludarabine), and 2-chloro-2'-fluorodeoxyadenosine (CaFdA) have achieved an important role in the treatment of indolent lymphoid malignancies, including hairy cell leukemia (HCL), chronic lymphocytic leukemia (CLL), and low-grade lymphoma, because of their ability to kill nondividing cells. The cytotoxicity of these drugs depends mainly on the accumulation of their triphosphate metabolites (dATP, 2CdATP, F-araATP, CaFdATP) in lymphocytes because of the high deoxycytidine kinase levels and the low 5'-deoxynucleotidase activities in these cells.<sup>1</sup> Different concentrations of the 2 enzymes in malignant cells may explain resistance between patients.<sup>2</sup> Once transformed into the triphosphate form, adenine deoxynucleosides can induce DNA damage<sup>2,3</sup> and trigger the apoptotic cascade.<sup>4</sup>

Apoptosis is characterized by the activation of cysteine proteases called caspases, which cleave proteins essential for the survival of the cell. Furthermore, these caspases have been shown to activate the endonuclease responsible for the internucleosomal cleavage of genomic DNA.<sup>5</sup>

Mitochondria play a key role in the events leading to caspase activation in cells undergoing apoptosis. Alteration of their functions can induce the release of cytochrome c and apoptosis-inducing factor (AIF) from the intermembrane space into the cytosol, triggering activation of caspases and endonucleases.<sup>6-8</sup> Bcl-2 family members, some of which are located in the mitochondria, control those events, by either inducing (eg, Bax, Bad, Bak, Bid, Bim) or inhibiting (eg, Bcl-2, Bcl-X<sub>L</sub>, Mcl-1) apoptosis.<sup>9,10</sup>

Cytochrome c released by the mitochondria and a cytosolic apoptosis protease activating factor (Apaf-1) oligomerize into a large multi-

meric complex, called the apoptosome.<sup>7</sup> This complex itself is sufficient to recruit and activate procaspase-9. Once activated, caspase-9 cleaves the downstream caspases, such as caspase-3, and activates the programmed cell death cascade.<sup>11</sup> In addition to cytochrome c, AIF is normally confined to mitochondria. The release of AIF to the cytosol is followed by its relocalization to the nucleus. Recombinant AIF causes chromatin condensation in isolated nuclei and large-scale fragmentation of DNA.<sup>12</sup>

Several anticancer drugs induce DNA damage, which can lead to the phosphorylation of p53 and the subsequent transcriptional activation of p53-dependent proteins such as p21, Bax, and Hdm-2, leading to growth arrest, repair, or apoptosis. One of the target genes involved in p53-dependent programmed cell death might be Bax, a pro-apoptotic Bcl-2 family member protein. Bax overexpression has been linked to cytochrome c release from the mitochondria<sup>13</sup> and can induce apoptosis.<sup>14</sup>

The assembly of the apoptosome requires dATP, which binds to Apaf-1. In a previous study, we compared several clinically relevant adenine deoxynucleotide analogs for their capacity to bind APAF-1 and to activate caspase-9.<sup>15</sup> In this study we analyzed and compared the effect of the corresponding nucleosides on both mitochondrial function and DNA integrity.

## Materials and methods

### Cell lines and drugs

Human fibroblasts HS-68 (ATCC CRL 1635) and human leukemia T lymphoblast CEM cell lines stably transfected with pZipneo vector (CEM/Neo) or with vector encoding BCL2 (CEM/Bcl-2)<sup>16</sup> were cultured in

From the Department of Medicine and The Sam and Rose Stein Institute for Research on Aging and the Department of Medicine/Division of Endocrinology and Metabolism, Whittier Diabetes Program, University of California, San Diego, La Jolla, CA.

Submitted May 11, 2000; accepted July 17, 2000.

Supported in part by National Institutes of Health grants GM23200 and CA81534 and by a grant from the DOD Breast Cancer Research Program (L.M.L.).

**Reprints:** Lorenzo M. Leoni, Dept of Medicine, University of California San Diego, 9500 Gilman Dr, La Jolla, CA 92093-0663; e-mail: lleoni@ucsd.edu.

The publication costs of this article were defrayed in part by page charge payment. Therefore, and solely to indicate this fact, this article is hereby marked "advertisement" in accordance with 18 U.S.C. section 1734.

© 2000 by The American Society of Hematology

complete medium (RPMI-1640 supplemented with 10% fetal bovine serum). The deoxynucleoside analogs dAdo and fludarabine were from Sigma (St Louis, MO); cladribine and CaFdA were synthesized by published procedure.<sup>17</sup> F-AraATP and CaFdATP were kind gifts of Dr W. Plunkett (University of Texas M. D. Anderson Cancer Research Center, Houston, TX), and 2CdATP was synthesized in our laboratory by Dr Q. Chao.<sup>18</sup>

### Cell isolation and analysis

Written informed consent was obtained to procure peripheral blood from all patients. Patients had to have B-CLL according to National Cancer Institute criteria of any Rai stage. Criteria for requiring therapy were as follows: disease-related symptoms; anemia, thrombocytopenia, or both; bulky lymphadenopathy, clinically relevant splenomegaly, or both. Heparinized peripheral blood samples from different patients with CLL and containing at least 90% malignant cells were fractionated by Ficoll-Hypaque sedimentation. Nonadherent mononuclear cells were resuspended in complete medium (RPMI-1640 supplemented with 10% fetal bovine serum) at a density of 1 to  $2 \times 10^6$ /mL. Cells were incubated at 37°C in an atmosphere of 5% CO<sub>2</sub> with the indicated drugs. In some experiments, frozen cells were used. dAdo was used in cells that were pretreated for 1 hour with 50 μmol/L of the adenosine deaminase inhibitor deoxycytosine.

### Cellular assay for caspase activity

At the indicated time points, CLL cells were washed twice with phosphate-buffered saline (PBS), and the pellet was resuspended in caspase buffer (50 mmol/L HEPES, pH 7.4, 100 mmol/L NaCl, 1 mmol/L EDTA, 0.1% Chaps, and 5 mmol/L dithiothreitol [DTT]) for 10 minutes at 4°C. Lysates were then stored at -80°C. The caspase enzymatic assays were carried out in 96-well plates. Lysates (10-20 μg total protein) were mixed with 50 μL HEB buffer (PIPES 50 mmol/L, KCl 20 mmol/L, EGTA 5 mmol/L, MgCl<sub>2</sub> 2 mmol/L, and DTT 1 mmol/L, pH 7), and reactions were initiated by the addition of 100 μmol/L of the specific substrate. After a 1-hour incubation at 37°C, caspase-3-like protease activity was measured with the substrate Ac-DEVD-AMC, and caspase-9-like activity was measured using Ac-LEHD-AFC. Activity was measured by the release of 7-amino-4-trifluoromethylcoumarin (AFC) or 7-amino-4-methyl-coumarin (AMC), monitoring fluorescence at excitation and emission wavelengths of 400 and 505 nm, and 380 and 460 nm respectively.

### Cytofluorometric analysis of mitochondrial transmembrane potential ( $\Delta\Psi_m$ ) by DiOC6 and cell membrane permeability by PI

CLL cells were treated with the indicated amount of the drugs either alone or with 50 μmol/L of the cell-permeable caspase inhibitor Z-VAD-fmk (Z-Val-Ala-Asp(Ome)-CH<sub>2</sub>F; Biomol, Plymouth Meeting, PA). Cells were then incubated for 10 minutes at 37°C in culture medium containing 40 nmol/L 3,3' dihexyloxycarbocyanine iodide (DiOC6; Molecular Probes, Eugene, OR) and 5 μg/mL propidium iodide (PI; Molecular Probes), followed by analysis within 30 minutes of fluorochrome in a Becton Dickinson FACScalibur cytofluorometer. After suitable compensation, fluorescence was recorded at different wavelengths: DiOC6 at 525 nm (FL-1) and PI at 600 nm (FL-3).

### Measurement of alkali-sensitive sites in DNA

DNA damage was assessed by alkaline unwinding and ethidium bromide fluorescence as previously described.<sup>19</sup> Because ethidium bromide preferentially binds to double-strand DNA (ds-DNA) in alkali, the relative amounts of nonbroken ds-DNA and broken single-strand DNA can be assessed. Fluorescence was determined with a CytoFluor fluorescence plate reader (PerSeptive Biosystems, Framingham, MA) with excitation at 520 nm and emission at 585 nm. Results are expressed as [% ds-DNA = [(F - F<sub>min</sub>) / (F<sub>max</sub> - F<sub>min</sub>)] × 100], where F is the fluorescence of the experimental condition, F<sub>min</sub> is the background ethidium bromide fluorescence determined after conversion of all DNA into single-strand form by sonication, and F<sub>max</sub> is the fluorescence determined after the addition of the mercaptoethanol solution before the alkaline solution to maintain the pH at 11.0,

which is well below that needed to augment unwinding of single-strand DNA. The amount of single-strand DNA in alkali after sonication is proportional to the number of DNA-strand breaks (either single or double), which varies directly as a function of the extent of DNA unwinding.

### Neutral comet assay of double-strand DNA breaks

The single-cell comet electrophoresis assay was performed according to the Trevigen CometAssay (Trevigen, Gaithersburg, MD) reagent kit. CLL cells were suspended in complete medium (RPMI-1640 supplemented with 10% fetal bovine serum) at a density of  $1 \times 10^6$ /mL and treated with the indicated drugs for 6 hours at 37°C. Then, 0.5 mL aliquots of 0.5% low melting point agarose in PBS (Sigma, St Louis, MO) at 42°C were added to tubes containing 50 μL each of the cell suspensions. Fifty μL of the mixture was quickly pipetted onto a microscope slide, precured with 0.5% agarose, and allowed to solidify at 4°C. Slides were immersed for 30 minutes in prechilled lysis buffer (2.5 mol/L sodium chloride, 100 mmol/L EDTA, pH 10, 10 mmol/L Tris base, 1% sodium lauryl sarcosinate, 0.01% Triton X-100) at 4°C. After lysis, slides were incubated for 30 minutes in alkali buffer (0.3 mol/L NaOH, 1 mmol/L EDTA). TBE washed slides were placed in horizontal gel electrophoresis chambers containing 1 L 90 mmol/L Tris/90 mmol/L boric acid/2 mmol/L EDTA buffer (TBE) at 1 V/cm for 10 minutes. DNA was stained after SYBR green was added to the slides. A Zeiss Axioscope microscope (Carl Zeiss, Thornwood, NY) attached to a camera and image analysis system was used to quantify the different parameters of the comets. At least 100 cells were analyzed per slide. Results were expressed in terms of percentage of comet cells divided by total amount of cells.

### Mitochondria isolation

The CLL cells were washed in ice-cold Dulbecco's phosphate-buffered saline for disruption by nitrogen cavitation.<sup>20</sup> All subsequent steps were carried out on ice or at 4°C. The cells were washed with MA buffer (100 mmol/L sucrose, 1 mmol/L EGTA, 20 mmol/L MOPS pH 7.4, 1 g/L bovine serum albumin) then resuspended at  $2 \times 10^8$  cells/mL in MB buffer (MA buffer plus 10 mmol/L triethanolamine, 5% Percoll, 1 mmol/L phenylmethylsulfonyl fluoride, and an antiprotease mixture consisting of aprotinin, pepstatin A, and leupeptin, each at 10 μmol/L). The cells were then disrupted by cavitation, after which lysates were centrifuged twice at 2500g for 5 minutes to remove nuclei and unbroken cells then at 25 000g for 30 minutes to isolate mitochondria. The mitochondria were suspended in MC buffer (identical to MA buffer except that the sucrose concentration was 300 mmol/L and an antiprotease mixture was included that consisted of aprotinin, pepstatin A, and leupeptin, each at 10 μmol/L) and used for measuring membrane potential alterations with DiOC<sub>6</sub>.

### Flow cytometry analysis of AIF release

Nondividing CLL cells were treated with the nucleosides as indicated. Cells were washed and permeabilized by 0.03% digitonin treatment for 15 minutes at room temperature. The concentration of digitonin used was obtained by titration and is enough to permeabilize the outer membrane of the cells without affecting the mitochondrial membrane. Cells were then fixed with 2% paraformaldehyde and incubated with the primary antibody to AIF (a kind gift from G. Kroemer, Institut Gustave Roussy, Villejuif, France), washed, and stained with the fluorescent-labeled secondary antibody (Alexa 488; Molecular Probes). An isotype-matched primary antibody was used as control. Cells were postfixed by resuspending the pellet in 2% paraformaldehyde and analyzed by flow cytometry.

### Immunocytochemistry

One hundred microliters of the CLL cells at a concentration of  $2 \times 10^6$ /mL, treated for 24 hours with the indicated drugs, was stained for the detection of the mitochondrial membrane potential with 150 nmol/L Mitotracker Orange (Molecular Probes) for 30 minutes at 37°C. Then  $2 \times 10^5$  cells were pelleted at 300g for 5 minutes on a slide. The cells were fixed for 10 minutes in 4% paraformaldehyde, washed in PBS, and incubated for 2 hours with the antibodies specific for AIF (supplied by G. Kroemer) and cytochrome c

(clone 6H2.B4; Pharmingen, San Diego, CA), at a concentration of 2 to 10  $\mu\text{g}/\text{mL}$  in I-Block blocking buffer (Tropix, Bedford, MA) supplemented with 0.05% Triton X-100. Alexa 488 (green) and Alexa 568 (red) served as species-specific secondary antibodies. The nuclear DNA was stained using DAPI. Coverslips were washed successively in PBS and deionized  $\text{H}_2\text{O}$  for 5 minutes and mounted in Fluoromount (Fisher, CA). Images were obtained with a Zeiss Axioscope microscope.

### Microinjection

HS-68 cells were grown on glass coverslips (Fisher, Pittsburgh, PA). The triphosphate forms of the nucleosides analogs were dissolved at a concentration of 5 mmol/L in microinjection buffer consisting of 5 mmol/L sodium phosphate and 100 mmol/L KCl (pH 7.4) containing a Dextran-FITC or Dextran-TRITC fluorescent dye (Sigma). Approximately 100 cells/analog were microinjected using glass capillary needles. The estimated final concentration in the cells was 500  $\mu\text{mol}/\text{L}$ , based on an estimated injection volume of 50 fL. Cells were stained as described above.

## Results

### Cytotoxicity of the nucleoside analogs on CLL cells

For this study, we first screened 20 patients for their sensitivities to the nucleoside analogs 2CdA, F-Ara-A, CaFdA and dAdo (plus deoxycoformycin). We used equimolar concentrations of the nucleosides because the principal aim was to compare their effects on DNA and mitochondria integrity. CLL cells that were completely resistant to the nucleoside toxicity after 24 hours of incubation at 10  $\mu\text{mol}/\text{L}$  (less than 20% specific killing) were excluded from analysis because these cells did not accumulate the active triphosphate analog intracellularly.<sup>21</sup> Five of 20 patients with CLL were thus excluded. In the nucleoside-susceptible CLL populations, loss of viability measured by dye exclusion was already visible after a few hours (Figure 1A). Analysis of the apoptotic mechanisms triggered by the different nucleosides showed distinct peculiarities. Mitochondrial membrane potential measured by flow cytometry decreased in CLL cells treated with 2CdA and CaFdA already after 12 hours, but not after similar treatment with dAdo and F-Ara (Figure 1B). Similarly, the kinetics of enzymatic activation of caspase-9 and -3 (Figure 1C,D) were different: 2CdA and CaFdA were able to activate the caspases already after 12 hours, whereas 24-hour incubation was required to see induction of the caspase activity by F-Ara-A. The intensity of caspase-3 (Figure 1C) and caspase-9 (Figure 1D) activation by F-AraA at 24 hours was also reduced by at least 2-fold when compared to 2CdA or CaFdA.

### DNA damage analysis

We used 2 different methods to study nucleoside effects on DNA integrity, alkaline unwinding and comet assay. As assessed by the unwinding assay, 2CdA, F-Ara-A and CaFdA at 10  $\mu\text{mol}/\text{L}$  generate approximately equivalent DNA breaks after 12 hours (Figure 2A). The broad-spectrum caspase inhibitor z-VAD-fmk did not protect the cells from early DNA damage (data not shown). dAdo was less potent. To confirm these results, single-cell analysis was performed. After 6 hours of continuous incubation with 10  $\mu\text{mol}/\text{L}$  nucleoside, cells were placed on the slides in an agarose layer and lysed. Current was applied for 10 minutes, and DNA was stained with SYBR green. Damaged DNA migrated from the lysed cell membrane, forming a DNA tail in a comet shape (Figure 2C). Approximately 100 cells were counted, and the percentages of the cells displaying comets were enumerated (Figure 2B). More than 20%

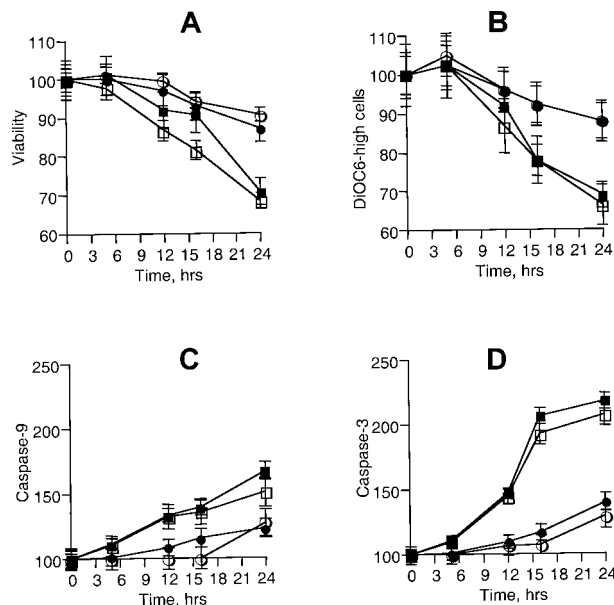


**Figure 1. Nucleoside cytotoxicity on B-CLL cells.** (A) B-CLL cells were treated with 2CdA (■), CaFdA (□), F-Ara-A (●), and dAdo (○) at 10  $\mu\text{mol}/\text{L}$  for the indicated time points. Viability was assessed by counting the cells after staining with erythrosin B and is represented as percentage of the control. (B) The same cells were tested for mitochondria membrane potential by flow cytometry analysis of incorporation of DiOC<sub>6</sub>. (C) Cells were lysed in caspase buffer and incubated with 100  $\mu\text{mol}/\text{L}$  of fluorometric substrate, and caspase-9 activity was measured by fluorometric analysis. (D) Caspase-3 enzymatic activity. These data ( $\pm$  SD) were obtained from a single patient studied in duplicate and are representative of 6 different patients.

of the cells exposed to 2CdA, F-Ara-A, and CaFdA displayed a comet shape, whereas dAdo was able to affect only 12% of the cells.

### Mitochondrial damage

Mitochondria are known to contain their own deoxynucleoside kinases.<sup>22</sup> Mitochondria were isolated by cavitation from CLL cells and treated for 10 minutes with different concentrations of the nucleoside analogs. Both 2CdA and CaFdA were able to affect the membrane potential of the mitochondria by reducing the incorporation of the dye DiOC<sub>6</sub> (Figure 3A). dAdo and F-Ara-A at the highest concentrations tested (1000  $\mu\text{mol}/\text{L}$ ) did not affect the membrane potential. We then analyzed the damage to mitochondria in whole CLL cells by measuring the cytoplasmic fluorescence of AIF, after treatment with 10  $\mu\text{mol}/\text{L}$  of the analogs for 8 hours. Apparent relocation of AIF was detected by flow cytometric analysis after permeabilization of the cells with 0.03% digitonin. This concentration of digitonin used had been shown in preliminary experiments to permeabilize the outer membrane of the cells without affecting the mitochondrial membrane. Only treatment with 2CdA, but not F-AraA, increased AIF fluorescence (Figure 3B). CaFdA behaved as 2CdA (data not shown). We believe that the increased AIF fluorescence is a result of its relocation from mitochondria to the cytosol, as immunocytochemistry results also seem to indicate (data not shown). Pre-incubation of the CLL cells with 100  $\mu\text{mol}/\text{L}$  Z-VAD-fmk did not alter the 2CdA-induced AIF relocation.

Overexpression of the anti-apoptotic protein bcl-2 protects cells from direct mitochondrial damage.<sup>23</sup> The CEM cell line overexpressing bcl-2 (CEM/Bcl-2) and the control mock-transfected cells (CEM/NES) were treated with 1  $\mu\text{mol}/\text{L}$  2CdA, CaFdA, and F-Ara-A. At different time points mitochondrial membrane potential and caspase activation were measured. There was no significant difference in the toxicity of F-Ara-A toward the 2 cell lines. In contrast, Bcl-2 overexpression significantly protected against early caspase activation and mitochondrial transmembrane alterations induced by 2CdA after 4 and 8 hours

(Figure 3C). The protection was lost after 24 hours of incubation. CaFdA behaved like 2CdA (data not shown).

### Immunocytochemistry

To corroborate the biochemical results, we performed immunocytochemical analysis of nucleoside-treated CLL cells. The effect of the nucleoside analogs on B-CLL mitochondria was analyzed after only 8 hours to exclude secondary effects related to caspase activation. Alteration of the mitochondria membrane potential was assessed by the incorporation of Mitotracker orange (MT orange)

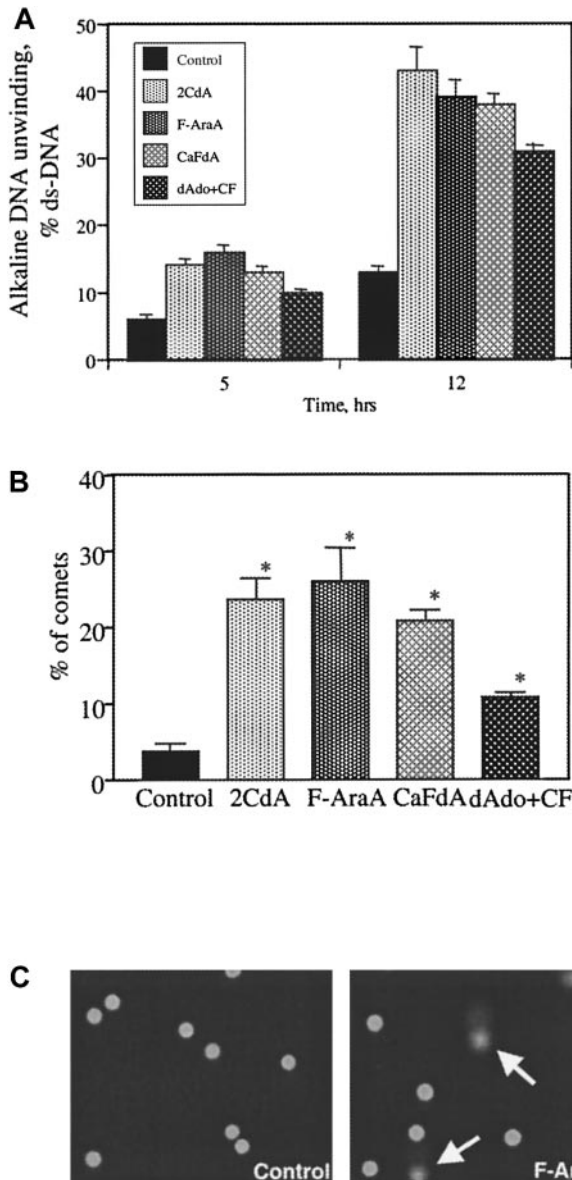


**Figure 2. Nucleoside-induced DNA damage of B-CLL cells.** (A) B-CLL cells from 4 different patients were treated at the indicated time points with 10  $\mu\text{mol/L}$  of 2CdA, CaFdA, F-Ara-A, and dAdo. DNA damage by alkaline unwinding was assessed. Data are reported as percentage ds-DNA. (B) Single-cell DNA damage (comet assay) was performed after 6-hour treatment with 10- $\mu\text{mol/L}$  concentrations of the drugs. Cells were plated on a slide in low-melting point agarose and lysed, and current was applied for 10 minutes at 1 V/cm. At least 100 cells were counted, and the percentages of the comets were determined. Columns represent the mean and error bars the standard deviation obtained from 4 patients. (\*) Statistically increased from control untreated cells;  $P < .05$  by the nonparametric Mann-Whitney test. (C) Example of comets after treatment with F-Ara-A compared to control cells. These data were obtained from a single patient and are representative for 4 patients.

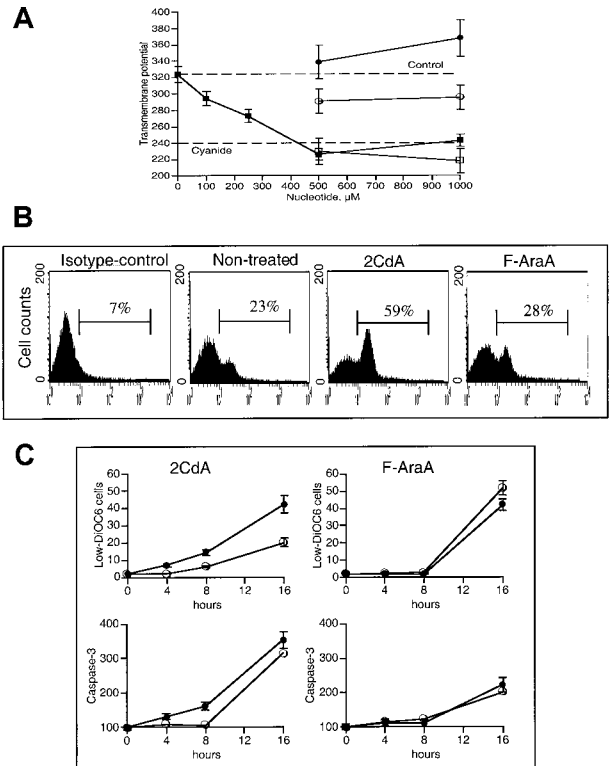


**Figure 3. Mitochondrial damage by nucleosides in B-CLL cells.** (A) Mitochondria from B-CLL cells were nitrogen isolated by cavitation, treated for 10 minutes with the indicated concentrations of 2CdATP (■), CaFdATP (□), F-Ara-ATP (●), and dATP (○), stained with 40 nmol/L DiOC<sub>6</sub> for 10 minutes at room temperature, and rapidly analyzed by flow cytometry. (B) B-CLL cells were treated with 10  $\mu\text{mol/L}$  of the nucleosides for 8 hours, then permeabilized with 0.03% of digitonin and fixed with 4% paraformaldehyde. AIF release was detected by staining with specific antibody and with fluorescence-labeled secondary Alexa 488 and measured by flow cytometry. (C) Human leukemia T-lymphoblastoid CEM cell lines, transfected with bcl-2-expressing vector (CEM/bcl-2) (○) or control vector (CEM/NEO) (●), were treated with 1  $\mu\text{mol/L}$  of the nucleosides. Membrane potential analyses and caspase analysis were performed at the indicated time points. Error bars represent the SD obtained from 3 independent experiments.

and the release of cytochrome c. In control cells, cytochrome c and MT orange colocalized in the mitochondria (Figure 4A). After treatment with 2CdA, the mitochondrial cytochrome c signal was strongly reduced, but the MT orange fluorescence remained constant, indicating that the mitochondria may have released cytochrome c but maintained the transmembrane potential (Figure 4B). F-Ara-A and dAdo did not visibly affect the mitochondria (Figure 4C; dAdo data not shown). Finally, experiments performed using the pan-specific caspase inhibitor Z-VAD-fmk indicated that the nucleoside-induced release of cytochrome c was not caspase dependent (data not shown).

### Microinjection

To confirm, in a separate system, the direct role of nucleotides in mitochondrial damage, we microinjected triphosphates into human fibroblasts. Because of their size, HS-68 cells were relatively easy to microinject. The results show that the triphosphates of 2CdA (and CaFdA; data not shown) induced a change in the subcellular distribution of mitochondria (Figure 5). To detect the mitochondria in the cells, both MT orange staining and labeling using cytochrome c antibodies were used, but only results using MT orange are shown. The microinjected cells were identified by the coinjection of fluorigenically labeled dextran (in green). The mitochondria were arranged along microtubules, forming a fibrillar array



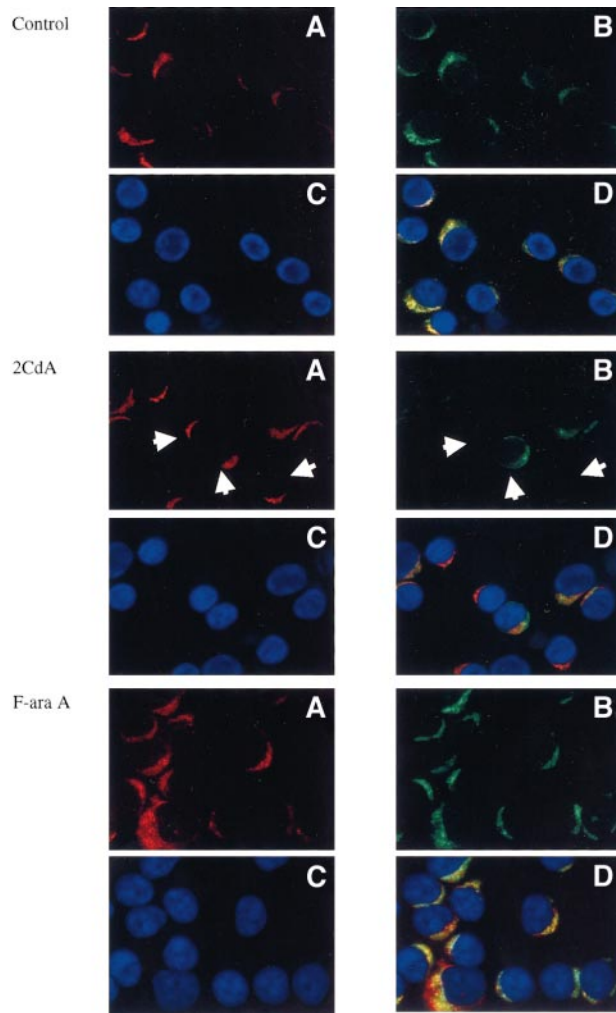


**Figure 4. Immunocytochemistry of mitochondrial damage.** B-CLL cells were treated with the indicated drugs for 8 hours. Cells were stained for mitochondria membrane potential with MT orange (red, A) for 30 minutes, pelleted on a slide at 300g, fixed in 4% paraformaldehyde, and stained for cytochrome c (green, B) with monoclonal antibody and secondary antibody Alexa 488. DNA was visualized with DAPI (blue, C). (D) Composite image. Arrows show cells affected by the drug, where cytochrome c release is noticeable. Images were obtained with a Zeiss Axioscope microscope, with CCD camera.

radiating toward the cell periphery. After microinjection with 2CdA (Figure 5C,D), but not with F-AraA (Figure 5E,F), the mitochondria retracted from the cell periphery and clumped around the nucleus. Interestingly, this mitochondrial redistribution was not accompanied by a dramatic change in cell shape or by cytoplasmic cytochrome c release.

## Discussion

Adenine deoxynucleoside analogs, such as F-Ara-A and 2CdA, are used for the treatment of B-CLL. However, the mechanisms of action of these drugs are not understood precisely. In this study, we confirm with 2 different assays that all the cytotoxic adenine deoxynucleosides induce DNA damage in CLL, as previously reported.<sup>24,25</sup> At equimolar concentrations, the DNA strand break formation was comparable, and was at the early time points, when the damage was a result of the direct effect of the drugs on DNA. After 24 hours, a big difference between 2CdA/CaFdA and F-Ara-A was observed. This was probably a consequence of the

activation of the caspases, leading to endonuclease-mediated cleavage of the DNA,<sup>26</sup> because caspase activity at 24 hours was higher in 2CdA- and CaFdA-treated cells.

The data indicate that 2CdA/CaFdA and F-Ara-A have distinct effects on mitochondria. Time-course analyses of mitochondrial membrane potential in whole cells, release of AIF by flow cytometry, cytochrome c release by immunofluorescence, and studies of purified mitochondria demonstrated that 2CdA/CaFdA, but not F-Ara-A, disrupted the mitochondrial integrity. These conclusions were supported by analyses of fibroblasts microinjected with the respective triphosphates.

Only 2CdA and CaFdA reduced the incorporation of DiOC<sub>6</sub> in mitochondria at 8 to 12 hours, induced AIF release (probably as a consequence of the opening of the PT pore<sup>12</sup>), stimulated the release of cytochrome c, and disrupted the structural filamentous arrangement of mitochondria, leaving the organelles dispersed in the cytoplasm. The immunofluorescence images suggest that both cytochrome c and AIF release preceded the loss of mitochondrial transmembrane potential. Caspase activation also anticipated the loss of the mitochondrial membrane potential, suggesting that the 2

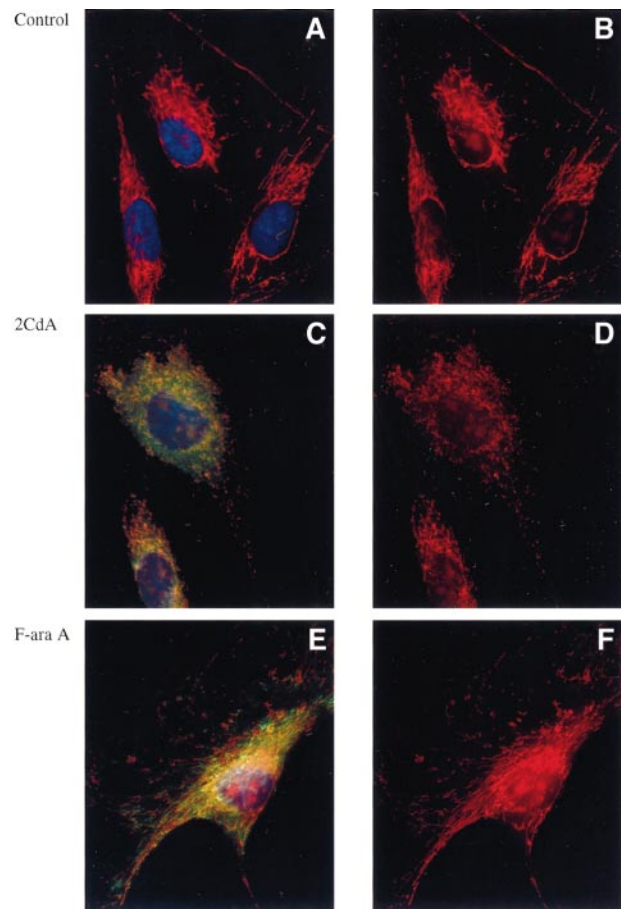


**Figure 5. Nucleotide microinjection experiments.** Human HS-68 fibroblasts were grown on coverslips. Nucleotide triphosphates were microinjected at an estimated final concentration of 500  $\mu$ mol/L. To identify the microinjected cells, fluorescein isothiocyanate-labeled dextran was co-injected with the nucleotides; therefore, the microinjected cells appear in green (C, E). Cells were incubated with 150 nmol/L MT orange (red stain) for 30 minutes to stain for mitochondria membranes, and fixed in 4% paraformaldehyde, and DNA was dyed with DAPI stain (blue, A, C, E). Left panels represent composite pictures that include DNA (blue), mitochondria (red), and dextran (green for microinjected cells). Right panels (B, D, F) represent the stained mitochondria alone. Cells treated with 2CdATP show a rearrangement of the mitochondria. Cells treated with the same concentration of F-AraATP do not display the same morphologic changes. Images were obtained with a Zeiss Axioscope microscope, equipped with CCD camera, using a 40  $\times$  1.3-na oil objective.

events may be independent, as already demonstrated in staurosporine-treated human tumor cells.<sup>27</sup>

Several explanations are possible for the severe and apparently direct mitochondrial damage observed with 2CdA- and CaFdA-treated CLL cells. First, the corresponding nucleotides could directly bind to proteins that are known to regulate mitochondrial functions, such as the F<sub>1</sub>-F<sub>0</sub> ATPase (mitochondrial adenosine triphosphate [ATP] synthase or complex V) or the adenine nucleotide translocator (ANT). Both proteins are situated on the mitochondrial inner membrane and are actively involved in the process of oxidative phosphorylation that produces most of the cellular energy. The F<sub>1</sub>-F<sub>0</sub> ATPase contains ATP and adenosine diphosphate binding sites, and it has been shown to bind dATP with an affinity similar to that of ATP.<sup>28</sup> We recently demonstrated that the nucleotide analogs can substitute for dATP in Apaf-1-mediated caspase-9 activation,<sup>29</sup> and it is thus conceivable that these analogs could also bind the F<sub>1</sub>-F<sub>0</sub> ATPase. The ANT, with the voltage-dependent anion channel (VDAC, or porin), Bax, and cyclophilin D, are thought to come together at the mitochondrial inner and outer membrane contact points to create the mitochondrial permeability transition pore (mtPTP).<sup>30,31</sup> Recently, the mtPTP and VDAC alone have been associated with the release of cytochrome c and AIF that precedes caspase activation.<sup>32</sup> It is conceivable that the adenine nucleotide analogs, by binding to ANT, could affect the opening of the mtPTP, allowing the release of AIF and cytochrome c. Results with purified mitochondria indicate that the mitochondrial transmembrane potential is rapidly reduced. Unfortunately, our analysis of AIF and cytochrome c release from isolated mitochondria produced inconsistent results (data not shown), but dATP-induced cytochrome c release from isolated mitochondria has been demonstrated.<sup>33</sup> The hypothesis of nucleotide-induced mtPTP opening is also consistent with the protection observed in Bcl-2-overexpressing cells, early after incubation with the 2CdA and CaFdA.

A second explanation for the observed mitochondrial damage may be the intramitochondrial accumulation of the triphosphate analogs, leading to mitochondrial DNA damage followed by a breakdown of metabolic functions. 2CdATP and CaFdATP may accumulate more rapidly than F-AraATP in the mitochondria because they are converted to their triphosphate forms with a 10-fold higher efficiency by the mitochondrial deoxyguanosine kinase.<sup>34</sup> Mitochondrial deoxyguanosine kinase-overexpressing cells showed increased sensitivity to 2CdA compared to untransfected cells.<sup>35</sup> It is also conceivable that the 2-chloro derivatives are slightly more hydrophobic than the corresponding 2-fluoro derivatives and therefore may be able to insert more easily into the mitochondrial membrane, affecting their integrity.

F-Ara-A also affected mitochondria, but only as a late event, suggesting an indirect mechanism. DNA damage is known to activate the p53 pathway by inducing phosphorylation of p53 and transcriptional activation of pro-apoptotic genes. This leads to the

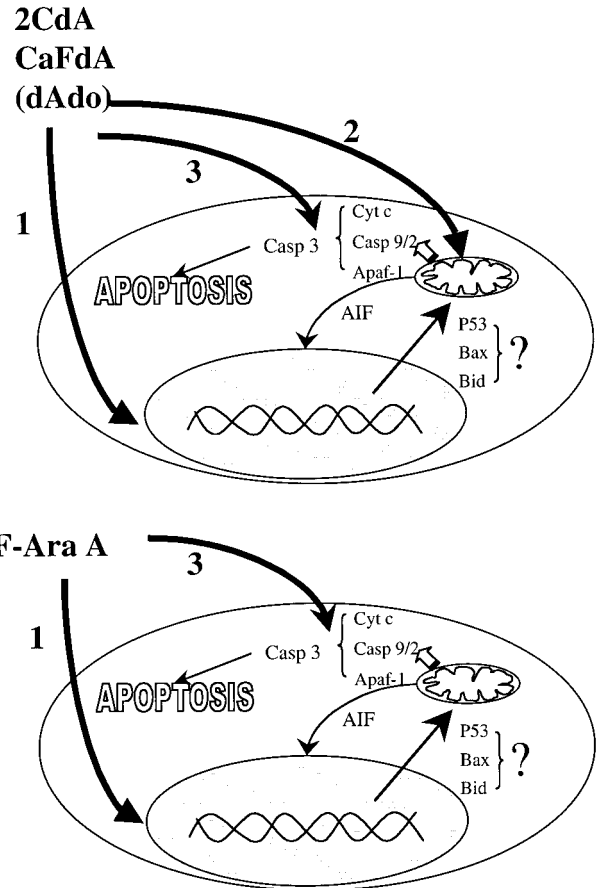


**Figure 6. Mechanisms of action.** There are 3 modes of action of the adenine deoxynucleoside analogs in nonproliferating CLL cells. In the cells the drugs are transformed into their triphosphate form, which induce DNA damage, mitochondrial dysfunction, and binding to APAF-1 and activation of the caspase pathway. F-ara-A kills cells mainly by DNA damage and Apaf-1 activation. 2CdA and CaFdA also interfere with mitochondrial function. The different effects of the adenine deoxynucleosides in various lymphoid malignancies may reflect the relative importance of the 3 mechanisms in apoptosis regulation.

release of cytochrome c and the activation of the intrinsic apoptotic machinery, resulting in caspase activation.<sup>13,36</sup>

In a previous study,<sup>29</sup> we demonstrated that F-Ara-ATP is the most potent nucleotide activator of Apaf-1, as assessed by pro-caspase-9 and -3 cleavage. The current study indicates that APAF-1 binding is not the only determinant in the adenosine deoxynucleoside cytotoxicity pathway in B-CLL cells. 2CdA and CaFdA are much more toxic to CLL cells than F-Ara-A, and only the chlorinated analogs cause direct mitochondrial damage. Thus, the mitochondrial effects of 2CdA and CaFdA may explain why these drugs are toxic to CLL cells at concentrations 5- to 10-fold lower than F-Ara-A. The different mechanisms for the toxicity of the nucleoside analogs are summarized in Figure 6.

## References

- Beutler E, Carson DA. 2-Chlorodeoxyadenosine: hairy cell leukemia takes a surprising turn. *Blood Cells*. 1993;19:559-568; discussion 569-572.
- Carson DA, Wasson DB, Taetle R, Yu A. Specific toxicity of 2-chlorodeoxyadenosine toward resting and proliferating human lymphocytes. *Blood*. 1983;62:737-743.
- Matsumoto SS, Yu AL, Bleeker LC, Bakay B, Kung FH, Nyhan WL. Biochemical correlates of the differential sensitivity of subtypes of human leukemia to deoxyadenosine and deoxycytosine. *Blood*. 1982;60:1096-1102.
- Carson DA, Wasson DB, Esparza LM, Carrera CJ, Kipps TJ, Cottam HB. Oral antilymphocyte activity and induction of apoptosis by 2-chloro-2'-arabino-fluoro-2'-deoxyadenosine. *Proc Natl Acad Sci U S A*. 1992;89:2970-2974.
- Salvesen GS, Dixit VM. Caspases: intracellular signaling by proteolysis. *Cell*. 1997;91:443-446.
- Kroemer G, Zamzami N, Susin SA. Mitochondrial control of apoptosis. *Immunol Today*. 1997;18:44-51.
- Li P, Nijhawan D, Budihardjo I, et al. Cytochrome c and dATP-dependent formation of Apaf-1/caspase-9 complex initiates an apoptotic protease cascade. *Cell*. 1997;91:479-489.
- Petit PX, Zamzami N, Vayssières JL, Mignotte B, Kroemer G, Castedo M. Implication of mitochondria in apoptosis. *Mol Cell Biochem*. 1997;174:185-188.
- Eskes R, Antonsson B, Osen-Sand A, et al. Bax-induced cytochrome C release from mitochondria is independent of the permeability transition pore

- but highly dependent on Mg<sup>2+</sup> ions. *J Cell Biol.* 1998;143:217-224.
10. Yang J, Liu X, Bhalla K, et al. Prevention of apoptosis by Bcl-2: release of cytochrome c from mitochondria blocked [see comments]. *Science.* 1997;275:1129-1132.
  11. Zou H, Li Y, Liu X, Wang X. An APAF-1-cytochrome c multimeric complex is a functional apoptosome that activates procaspase-9. *J Biol Chem.* 1999;274:11549-11556.
  12. Susin SA, Lorenzo HK, Zamzami N, et al. Molecular characterization of mitochondrial apoptosis-inducing factor [see comments]. *Nature.* 1999;397:441-446.
  13. Evan G, Littlewood T. A matter of life and cell death. *Science.* 1998;281:1317-1322.
  14. Bargou RC, Wagener C, Bommert K, et al. Overexpression of the death-promoting gene bax-alpha which is downregulated in breast cancer restores sensitivity to different apoptotic stimuli and reduces tumor growth in SCID mice [see comments]. *J Clin Invest.* 1996;97:2651-2659.
  15. Leoni LM, Chao Q, Cottam HB, et al. Induction of an apoptotic program in cell-free extracts by 2-chloro-2'-deoxyadenosine 5'-triphosphate and cytochrome c. *Proc Natl Acad Sci U S A.* 1998;95:9567-9571.
  16. Meisenholder GW, Martin SJ, Green DR, Nordberg J, Babior BM, Gottlieb RA. Events in apoptosis: acidification is downstream of protease activation and BCL-2 protection. *J Biol Chem.* 1996;271:16260-16262.
  17. Kazmierczuk Z, Cottam HB, Revankar GR, Robins RK. Synthesis of 2'-deoxytubercidin, 2'-deoxyadenosine, and related 2'-deoxynucleosides via a novel direct stereospecific sodium salt glycosylation procedure. *J Am Chem Soc.* 1984;106:6379-6382.
  18. Seela F, Roling A. 7-Deazapurine containing DNA: efficiency of NdTP incorporation during PCR-amplification and protection from endonuclease hydrolysis. *Nucleic Acids Res.* 1992;20:55-61.
  19. Birnboim HC, Jevcak JJ. Fluorometric method for rapid detection of DNA strand breaks in human white blood cells produced by low doses of radiation. *Cancer Res.* 1981;41:1889-1892.
  20. Adachi S, Gottlieb RA, Babior BM. Lack of release of cytochrome C from mitochondria into cytosol early in the course of Fas-mediated apoptosis of Jurkat cells. *J Biol Chem.* 1998;273:19892-19894.
  21. Kawasaki H, Carrera CJ, Piro LD, Saven A, Kipps TJ, Carson DA. Relationship of deoxycytidine kinase and cytoplasmic 5'-nucleotidase to the chemotherapeutic efficacy of 2-chlorodeoxyadenosine. *Blood.* 1993;81:597-601.
  22. Wang L, Hellman U, Eriksson S. Cloning and expression of human mitochondrial deoxyguanosine kinase cDNA. *FEBS Lett.* 1996;390:39-43.
  23. Green DR, Reed JC. Mitochondria and apoptosis. *Science.* 1998;281:1309-1312.
  24. Bromidge TJ, Howe DJ, Johnson SA, Phillips MJ. Adaptation of the TdT assay for semi-quantitative flow cytometric detection of DNA strand breaks. *Cytometry.* 1995;20:257-260.
  25. Huang P, Robertson LE, Wright S, Plunkett W. High molecular weight DNA fragmentation: a critical event in nucleoside analogue-induced apoptosis in leukemia cells. *Clin Cancer Res.* 1995;1:1005-1013.
  26. Liu X, Zou H, Slaughter C, Wang X. DFF, a heterodimeric protein that functions downstream of caspase-3 to trigger DNA fragmentation during apoptosis. *Cell.* 1997;89:175-184.
  27. Bossy-Wetzell E, Newmeyer DD, Green DR. Mitochondrial cytochrome c release in apoptosis occurs upstream of DEVD-specific caspase activation and independently of mitochondrial transmembrane depolarization. *EMBO J.* 1998;17:37-49.
  28. Okamoto M, Hiratani N, Arai K, Ohkuma S. Properties of H(+)-ATPase from rat liver lysosomes as revealed by reconstitution into proteoliposomes. *J Biochem (Tokyo).* 1996;120:608-615.
  29. Genini D, Budihardjo I, Plunkett W, et al. Nucleotide requirements for the in vitro activation of the apoptosis protein-activating factor-1-mediated caspase pathway. *J Biol Chem.* 2000;275:29-34.
  30. Woodfield K, Ruck A, Brdiczka D, Halestrap AP. Direct demonstration of a specific interaction between cyclophilin-D and the adenine nucleotide translocase confirms their role in the mitochondrial permeability transition. *Biochem J.* 1998;336:287-290.
  31. Beutner G, Ruck A, Riede B, Brdiczka D. Complexes between porin, hexokinase, mitochondrial creatine kinase and adenylate translocator display properties of the permeability transition pore: implication for regulation of permeability transition by the kinases. *Biochim Biophys Acta.* 1998;1368:7-18.
  32. Shimizu S, Narita M, Tsujimoto Y. Bcl-2 family proteins regulate the release of apoptogenic cytochrome c by the mitochondrial channel VDAC [see comments]. *Nature.* 1999;399:483-487.
  33. Yang JC, Cortopassi GA. dATP causes specific release of cytochrome C from mitochondria. *Biochem Biophys Res Commun.* 1998;250:454-457.
  34. Sjoberg AH, Wang L, Eriksson S. Substrate specificity of human recombinant mitochondrial deoxyguanosine kinase with cytostatic and antiviral purine and pyrimidine analogs. *Mol Pharmacol.* 1998;53:270-273.
  35. Zhu C, Johansson M, Permert J, Karlsson A. Enhanced cytotoxicity of nucleoside analogs by overexpression of mitochondrial deoxyguanosine kinase in cancer cell lines. *J Biol Chem.* 1998;273:14707-14711.
  36. Shieh SY, Ikeda M, Taya Y, Prives C. DNA damage-induced phosphorylation of p53 alleviates inhibition by MDM2. *Cell.* 1997;91:325-334.



# p53 Status is Involved in Chronic Lymphocytic Leukemia-Sensitivity to Nucleosides Analogs Treatment

Davide Genini<sup>1</sup>, Rommel I. Tawato<sup>1</sup>, Maria Dell'Aquila<sup>2</sup>, Thomas J. Kipps<sup>1</sup>, Carlo M. Croce<sup>3</sup>, Dennis A. Carson<sup>1</sup>, Lorenzo M. Leoni<sup>1</sup>

<sup>1</sup>Department of Medicine and The Sam and Rose Stein Institute for Research on Aging, University of California at San Diego, <sup>2</sup>Department of Biology, Center for Molecular Genetics, University of California, San Diego, 9500 Gilman Drive, La Jolla, CA 92093, <sup>3</sup>Wistar Institute of Anatomy and Biology, Philadelphia, PA 19104

Correspondence should be addressed to L.M.L.:

Leoni M. Lorenzo, Dept. Medicine, UCSD-0663, Stein Clinical Res. 126D, 9500 Gilman Drive, LA JOLLA, CA-92093, USA. Tel: 858-534-5442, Fax: 858-534-5399, e-mail: [leoni@ucsd.edu](mailto:leoni@ucsd.edu)

## ABSTRACT

**Deoxyadenosine nucleosides are commonly used for the treatment of Chronic Lymphocytic Leukemia (B-CLL), their anti-cancer activity has been previously correlated with mutations of the p53 gene. Disruption of p53 function may even be involved in the disease progression, by reducing apoptosis, increasing cell survival and producing multidrug-resistant phenotype. In this study we show that upon DNA damage by nucleosides such as fludarabine, p53 can be phosphorylated and activated, leading to the transcriptional activation of Hdm2 and p21, but not Bax. The activation of p53 is followed by cytochrome c and AIF cytoplasmic release, catalytic activation of caspase-9 and 3, downregulation of the endogenous caspase inhibitor XIAP, and subcellular relocalization of p53. These events occur in less than 24 hours post-treatment, and are completely blocked by cell-permeable peptidic inhibitors of caspases, suggesting the activation of programmed cell death or apoptosis. After screening of 25 CLL patients we identified a subset of CLL patients displaying a non-functional p53 pathway that were resistant from fludarabine-induced apoptosis. When incubated with fludarabine, the cells isolated from the p53-null patients showed loss of viability over a period of 3 days, that was not prevented by caspase inhibitors, and did not display all the biochemical indicators of apoptosis. We therefore demonstrate that p53 is essential in fludarabine-induced cell death of CLL cells, and that the activation of the caspase-9/apaf-1 apoptosome is important in the execution of apoptosis.**

## INTRODUCTION

Chronic lymphocytic Leukemia (CLL) malignancy is thought to be caused by a defect in the normal mechanism of cell death, increasing abnormally the number of cells in the patients blood (1, 2).

CLL treatments, including chlorambucil (CLB) and nucleosides analogs, such as fludarabine (F-ara-A) and 2-chlorodeoxyadenosine (2CdA), induce DNA damage in CLL cells. The nitrogen mustard alkylating agent CLB can bind to a variety of cellular structures comprehending DNA, RNA and proteins, however DNA crosslinking appears to be most

important for antitumor activity (3). In previous published data we demonstrated that the cytotoxic mechanism of nucleoside analogs involves direct damage of mitochondria, inducing release of cytochrome c and apoptosis-inducing factor AIF (4) and the binding and subsequent activation of caspase-9/APAF-1 complex (5, 6). Purine deoxynucleosides can also be incorporated into cellular DNA resulting in DNA damage (7, 8).

DNA-damage response involves stimulation of protein kinases, distantly related to the intracellular signaling molecule phosphatidylinositol 3-kinase (PI 3-kinase), of which the prototypes are ATM (9) and DNA-dependent protein kinase (DNA-PK) (10). Activation of these kinases triggers a cellular response that includes growth arrest, damage repair and apoptosis. The tumor suppressor protein p53 has been shown to be a substrate of ATM and DNA-PK (11). p53 is a transcription factor normally maintained at low levels through interaction with several regulatory proteins, such as Hdm-2 that target it to proteasome degradation (12). DNA-damage induces phosphorylation of p53, release from the Hdm-2 protein, multimerization into active tetramers, translocation to DNA, and transcription activation of various proteins like p21, Bax, Hdm-2, and others (10, 11).

The activation of p53 through DNA damage can lead to cell-cycle arrest and apoptosis. The cyclin dependent kinase (CDK) inhibitor p21 plays a major role on the p53-mediated cell growth arrest. In contrast, the mechanism by which p53 induce apoptosis is still obscure. One of the target genes might be Bax, a Bcl-2 family member protein capable of triggering cytochrome c release from the mitochondria (11). Recent evidence suggests that caspase-9, and its cofactor Apaf-1, are essential downstream components of p53-mediated apoptosis (13).

Sensitivity in treatment of CLL with CLB and nucleosides analogs has been correlated with p53 gene mutations (14, 15). Disruption of p53 function may be involved in the disease progression, by reducing apoptosis, increasing cell survival and producing multidrug-resistant phenotype (16). Multidrug resistance in CLL has been observed in patients with mutated p53, but has also observed in patients displaying a normal p53 genotype, suggesting multiple mechanism of drug resistance (15).

In this article we tested the hypothesis that the p53 pathway, including the upstream kinases, and the downstream p53-induced genes, is an important regulator of the cytotoxicity of some, but not all, ourine nucleoside analogs.

We show that upon DNA damage by nucleosides such as fludarabine, p53 can be phosphorylated and activated, leading to the transcriptional activation of Hdm2 and p21, but not Bax. The activation of p53 is followed by cytochrome c and AIF cytoplasmic release, catalytic activation of caspase-9 and 3, downregulation of the endogenous caspase inhibitor XIAP, and subcellular relocalization of p53. All of these events occur in less than 24 hours post-treatment, and are completely blocked by cell-permeable peptidic inhibitors of caspases, suggesting the activation of programmed cell death or apoptosis. Our screening allowed the identification of a subset of CLL patients displaying a non-functional p53 pathway that were completely resistant from fludarabine-induced apoptosis. When incubated with fludarabine, the cells isolated from the p53-null patients showed loss of viability over a period of 3 days, that was not prevented by caspase inhibitors, and did not display all the biochemical indicators of apoptosis. We therefore demonstrate that p53 is essential in fludarabine-induced cell death of CLL cells, and that the activation of the caspase-9/apaf-1 apoptosome is important in the execution of apoptosis.

## MATERIALS AND METHODS

### Cell isolation and analysis

Heparinized peripheral blood samples from 15 different patients with CLL containing at least 90% malignant cells, were fractionated by Ficoll/Hypaque sedimentation. Non adherent mononuclear cells were resuspended in complete medium (RPMI-1640 supplemented with 10% fetal bovine serum) at a density of 1 to 2 x 10<sup>6</sup> per ml. Cells were incubated at 37°C in an atmosphere of 5% CO<sub>2</sub> with the deoxynucleoside analogs with or without the cell-permeable caspases inhibitor IDUN 1965 (17) or z-VAD-fmk (Z-Val-Ala-Asp(Ome)-CH<sub>2</sub>F, Biomol, Plymouth Meeting, PA) 9-β-D-arabinofuranosyl-2-fluoroadenine (F-ara-A, fludarabine) came from Sigma (St. Louis, MO); 2-chloro-2'-deoxyadenosine (2CdA, Cladribine) was synthesized by published procedure (18).

### Immunoblotting

Washed CLL cell were lysed in 2 X SDS-PAGE sample buffer containing 10 mM DTT, for 5 minutes at 100°C. Alternatively, washed cells were lysed in Lysis buffer (25 mM Tris, pH 7.4, 150 mM KCl, 5 mM EDTA, 1% Nonidet P-40, 0.5% sodium deoxycholate, 0.1% SDS, 1 µg/ml aprotinin, 1 µg/ml leupeptin and 1 mM phenylmethanesulfonyl fluoride, PMSF). Lysates were centrifuged at 15,000 x g for 10 min to remove nuclei and the protein content of supernatants was measured using a modified Coomassie blue assay (Pierce, Rockford, IL). Proteins were resolved at 125 V on 14% and 4-20% gels and electrophoretically transferred to 0.2 µm polyvinylidene fluoride (PVDF) membranes (Millipore, Bedford, MA) for 2 hours at 125 V. Membranes were blocked overnight in I-Block blocking buffer (Tropix, Bedford, MA). Blots were then probed for 1 hour with antibodies to p53 (clone PAb 1801), Hdm2 (clone SMP14), p21 (clone SX118) (Pharmingen, San Diego, CA), to Phospho-p53 (Ser15) (Transduction Laboratories, Lexington, KY), to Bax and XIAP (19).

The blots were developed with species-specific antisera, and visualized by alkaline phosphatase-based enhanced chemiluminescence (ECL; Amersham), according to the manufacturer's instructions. The x-ray films were scanned, acquired in Adobe Photoshop, and analyzed with NIH Image software.

### Cellular Assay for Caspase Activity

The method for the fluorimetric detection of caspases activity was previously described (4). Briefly, CLL cells lysed in caspase buffer. Lysates (10-20 µg of total protein) were mixed with HEB buffer and reactions were initiated by addition of 100 µM of the specific substrate. After 1 hour incubation at 37°C, caspase-3-like protease activity was measured with the substrate Ac-DEVD-AMC and caspase-9-like activity was measured using Ac-LEHD-AFC. Activity was measured by the release of 7-amino-4-trifluoromethyl-coumarin (AFC) or 7-amino-4-methyl-coumarin (AMC) monitoring fluorescence at excitation and emission wavelengths of 400 and 505 nm, and 380 and 460 nm respectively.

### Cytofluorimetric analysis of mitochondrial transmembrane potential ( $\Delta\psi_m$ ) by DiOC6 and cell membrane permeability by PI

CLL cells were treated with the indicated amount of the drugs at the indicated time points. Cells were then incubated for 10 min at 37°C in culture medium containing 40 nM 3,3'-dihexyloxycarbocyanine iodide (DiOC6, Molecular Probe, Eugene, OR) and 5 µg/ml propidium iodide (PI, Molecular Probe), followed by analysis within 30 minutes of fluorochrome in a Becton-Dickinson FACScalibur cytofluorometer. After suitable compensation, fluorescence was recorded at different wavelengths: DiOC6 at 525 nm (FL-1) and PI at 600 nm (FL-3).

### Immunohistochemistry

100 µl of the CLL cells at a concentration of 2x10<sup>6</sup>/ml treated for 24 hours with the indicated drugs were stained for the detection of the mitochondrial membrane potential with Mitotracker Orange (Molecular Probes, OR) for 30 min at 37°C. 2x10<sup>5</sup> cells were cytopspined at 300 g for 5 min on a slide. The cells were fixed 10 min in 4% Paraformaldehyde, washed in PBS and then incubated for 2 hours with the antibodies anti-p53 or anti-cytochrome c (clone 6H2.B4) (Pharmingen, San Diego, CA), at a concentration of 2-10 µg/ml in I-Block blocking buffer (Tropix, Bedford, MA) supplemented with 0.05 % Triton X-100. Alexa 488 (green) and Alexa 568 (red) species-specific secondary antibodies (Molecular Probes, OR) were used to visualize the proteins. The nuclear DNA was stained using DAPI. Coverslips were washed successively in PBS and deionized H<sub>2</sub>O for 5 min and mounted in Fluoromount (Fisher, CA). Images were obtained with a Zeiss Axioscope microscope.

### Fluorescent in situ Hybridization for p53 gene detection

DNA probes specific for the p53-locus on 17p13 (directly conjugated with SPECTRUM-Orange) were purchased from Vysis, Inc (Downers Grove, IL). Hybridization was performed as detailed in a previous report (20). Slides were analyzed

	Patience	p53	Phospho- p53	HDM2	P21	F-ara Toxicity
#1	TJK 0052	+	+	+	+	+
#2	<b>TJK0031</b>	-	-	-	-	-
#3	TJK 0024				+	+
#4	TJK 0018				+	+
#5	TJK 0016	+			+	+
#6	TJK 0008	(+)			+	+
#7	TJK 0009	+			+	+
#8	TJK0017	+			+	+
#9	TJK 0054					+
#10	TJK 0023	+	+	+	+	+
#11	<b>TJK0002</b>	+	(+)	-	-	-
#12	<b>TJK0035</b>	+	+	-	(+)	-
#13	TJK 0011	+	+	+	+	+
#14	TJK 0033	+	+	+	+	+
#15	<b>TJK0063</b>	+	(+)	-	-	-

**TABLE 1. Screening of 15 B-CLL patients for p53 status.**

15 B-CLL patients were tested for F-ara-A response and for p53 phosphorylation. The gene expression of p53-induced gene was also tested. The patients with a p53 mutated pathway are bold-highlighted.

## RESULTS

p53 has been postulated to play a major role in the pathogenesis of several tumors. In CLL the question of the involvement of p53 in response to therapeutic treatment is still unclear. Transfection of CLL is still a difficult method to perform and therefore we proceeded with the screening of 15 patients to characterize their p53 status and we correlated the response to the treatments (Table 1). What we observed in the activation of p53 after incubation the cells with the two deoxyadenosine analogs 2CdA and F-ara-A was the activation of p53 by phosphorylation, the expression of p53 induced genes as p21 and HDM2, which were correlated to the ability of the two drugs to induce apoptosis. Only 75% of the patients were responsive to F-ara-A treatment at 10  $\mu$ M for 24 hours, whereas all the patients were 2CdA sensitive. Viability was measured by dye exclusion. This inability of F-ara-A to induce cell death was correlated to a lack of ability to induce the p53 phosphorylation and expression of p53 dependent genes. This was completely reduced in patient TJK0031 or partially reduced in patients TJK0002, TJK0035 and TJK0063. Patient TJK0031 did not even present an inactivated form of p53, suggesting being a natural knock-out. In this study we selected a p53 positive patient TJK0052 responsive to the treatment and the p53 null patient to discriminate the involvement of p53 in the induction of apoptosis by 2CdA and F-ara-A. The patients were sequenced for mutations in p53 gene, where TJK0053 turned out to be p53 normal, and patient TJK0031 resulted by FISH analysis to be p53 homozygously deleted.

### Western blot analysis of p53 dependent genes

To determine the p53 status of the two selected patients we treated the CLL cells in a time course with the two nucleoside

analogues at a single concentration of 10  $\mu$ M. p53 positive patient displayed already after 8 hours incubations an increase of total p53, as well as phosphorylated p53. The p53 dependent genes p21 and HDM2 were also increased at the same time point. Only Bax, did not appear to get up-regulated. Interestingly XIAP, an anti-apoptotic molecule, was found to be concomitantly down-regulated. The p53 negative patient on the other side did not show any p53 band, no phosphorylation of p53 or any increase of the p53 dependent genes. Also XIAP was not reduced (Figure 1). Tubulin was used as a proof for loading.

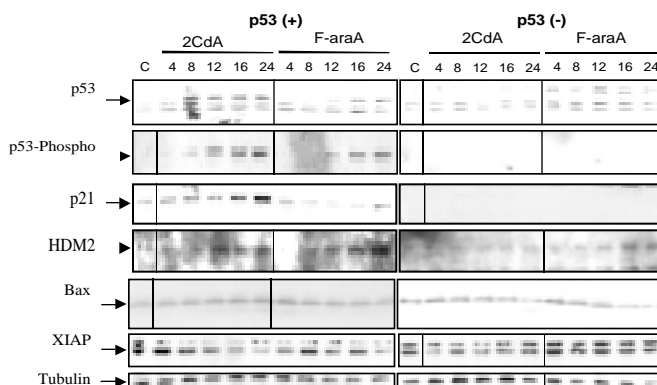


**Figure 1. Expression of p53 induced proteins CLL patients after treatment with 2CdA and F-ara-A.**

A p53 normal B-CLL patient ( p53(+)) and a p53 negative patient (p53(-)) were treated with 10 $\mu$ M of deoxynucleosides analogs 2CdA and F-ara-A in a time course. 5 x 10<sup>6</sup> cells were lysed in 100  $\mu$ l lysing buffer. The protein concentration was quantified by Coomassie blue assay. Cell extract (30  $\mu$ g per lane) were resolved by SDS-PAGE on 8-20 % gels and transferred on PVDF membranes. The indicated antibodies were visualized by enhanced chemiluminescence (ECL).

### Induction of apoptosis in CLL patients is different for 2CdA and F-ara-A depending on the p53 status

The cells tested in previous experiment were also tested for caspase-9 and -3 activation and for apoptosis analysis by flow cytometry. 2CdA was the only one drug able to induce cell death within 24 hours in p53 negative patient (Figure 2A). The strength of the effect was reduced compared to the p53 positive patient. F-ara-A instead induced apoptosis only in the p53 responding patient (Figure 2B) and this was correlated to the ability of F-ara-A to activate the caspases-9 and -3 only in the p53(+) patient after 12 hours, concomitantly to the increase of apoptosis (Figure 3A and 3B).

### Induction of apoptotic phenotype and release of cytochrome c by F-ara-A only in p53 positive patient

CLL cells of the two patients were probed with MT orange, cytochrome c and DaPi in immunofluorescence experiments after treatment with 2CdA and F-ara-A. Cytochrome c (green) colocalized with MT Orange (red) stain of mitochondria in

control cells. Treated p53(+) cells presented typical apoptotic phenotypes, displaying condensed nucleus (blue) and cytochrome c was released from the mitochondria, whereas MT orange was still detectable (Figure 4A). F-ara-A anyway was not able to induce any cytochrome c release or any apoptotic body in patient p53(-), cytochrome c and MT Orange colocalized in treated cells (Figure 4B). Only 2CdA was able to induce cytochrome c release and apoptotic phenotype in p53 null patient (data not shown).

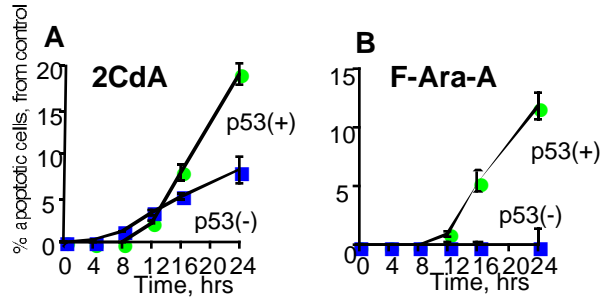


**Figure 2. Induction of apoptosis by 2CdA and F-ara-A.** B-CLL cells from the normal (●) and the null (■) p53 patient were treated with (2A) 2CdA, and (2B) F-Ara-A at 10 μM for the indicated time points. The cells were tested for mitochondria membrane potential by flow cytometry analysis of incorporation of DiOC<sub>6</sub>. % of the apoptotic cells to the control is represented in the diagrams.

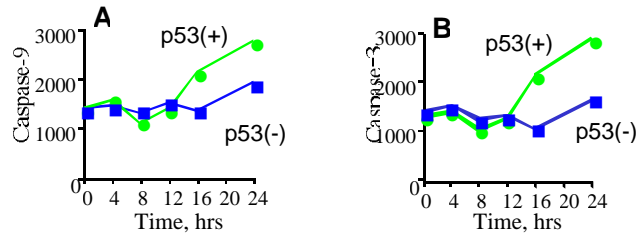


**Figure 3. F-ara-A induction of caspase-activity.** At the indicated time points, 5 x 10<sup>6</sup> F-ara-A treated B-CLL from the normal (●) and the null p53 patient (■) were washed with PBS and lysed in Caspase Buffer. (3A) Caspase-9 and (3B) caspase-3 activity of 10-20 μg of total protein was measured with specific substrates (100μM) after 1 h incubation at 37 °C. The cleavage of the fluorometric AMC/AFC was monitored fluorometrically at 400/380 nm excitation and 505/460 nm emission. Activity is represented in relative units to the control without treatment.

**Relocalization of p53 in cells undergoing apoptosis**

Stain of p53 with specific monoclonal antibody in whole cells showed ubiquitous localization of the protein in CLL. In cells undergoing apoptosis displaying condensed chromatin, caused by treatment with 2CdA or F-ara-A, p53 relocalized from the nucleus to the cytoplasm. Caspases-inhibitor z-VAD-fmk was not able to protect the nuclear export of p53 (Figure 5).

**Induction of cell death after longer exposition to the drug F-ara-A of p53 negative CLLs**

F-ara-A did not induce cytochrome c release and caspases activation in p53 negative patient, and did not induce the common pathway of apoptosis, but cells kept in culture for three days in the presence of the drug died anyway. Flow cytometry analysis showed an increase in the number of

apoptotic cells, from 39.7% in the control up to 55.1% for the treated cells. The caspases inhibitor IDUN did not protect

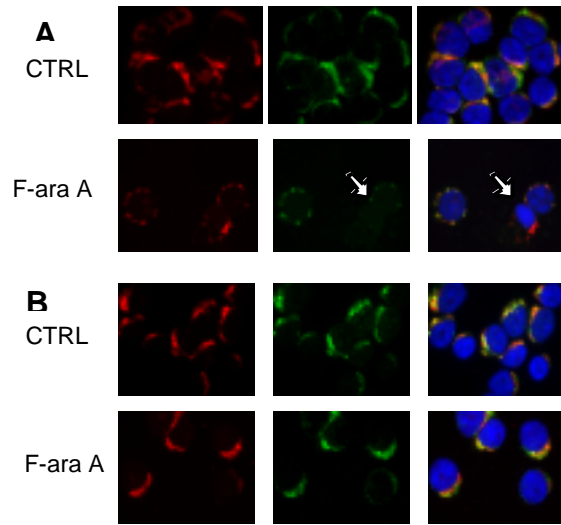


**Figure 4. Cytochrome c release in p53 positive patient after treatment with F-ara-A, but not in p53 negative patient.**

B-CLL cells were treated 24 hours with F-ara-A. (4A) p53 normal patient and (4B) p53 null-patient cells were incubated for 30 minutes with Mitotracker Orange at a final concentration 150 nm to stain mitochondria (red, left panels). 2 x 10<sup>4</sup> cells were then cytospun at 300 g for 5 minutes on a slide and then fixed for 10 minutes in 4 % paraformaldehyde. Cytochrome c primary antibody was incubated for 2 h, washed, and detected with the secondary Alexa 488-conjugated antibody (green, center panel). Nuclear DNA was stained using DAPI (blue, right panels in composite picture ). Micrographs (600x) (were obtained with a Zeiss Axioscope microscope.

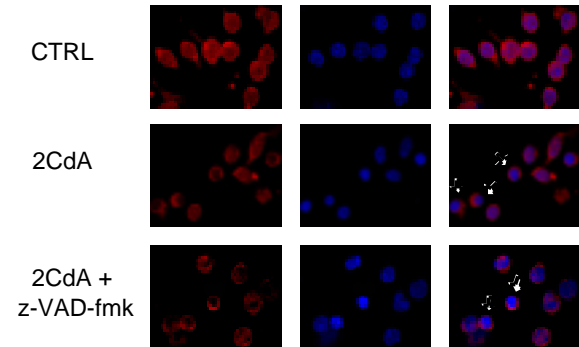


**Figure 5. Relocalization of p53 in cells presenting apoptotic phenotype.**

B-CLL cells were treated 24 hours with 2CdA in the presence or absence of caspases inhibitor z-VAD-fmk. 2 x 10<sup>4</sup> cells were then cytospun at 300 g for 5 minutes on a slide and then fixed for 10 minutes in 4 % paraformaldehyde. p53 primary antibody was incubated for 2 h, washed, and detected with the secondary Alexa 568-conjugated antibody (red, left panel). Nuclear DNA was stained using DAPI (blue, center panels). The right panels show the composite pictures of DAPI and p53 and the arrows indicate p53 relocalization from nuclei to cytoplasm in apoptotic phenotypic cells. Micrographs (600x) (were obtained with a Zeiss Axioscope microscope.



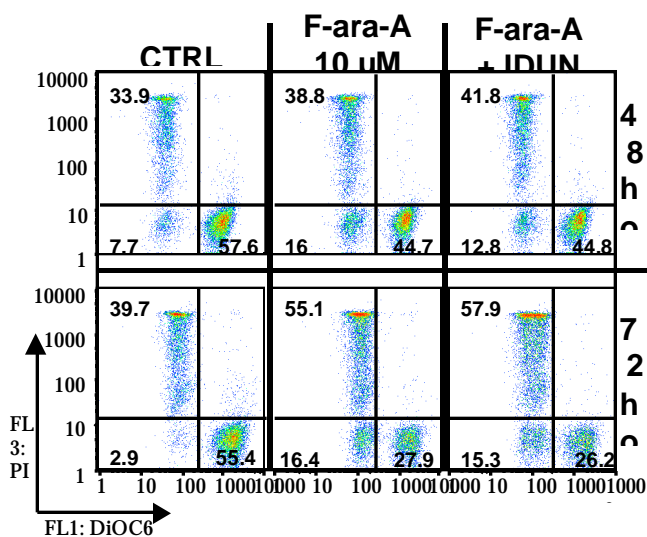


**Figure 6. Long-term cell death induced in p53 negative patient by F-ara-A.**

B-CLL cells from the p53 null-patient were treated for 48 and 72 hours with F-ara-A in the presence or absence of caspases-inhibitor IDUN 1965. Apoptotic cells were detected by flow cytometry by testing for mitochondria membrane potential by flow cytometry analysis of incorporation of DiOC<sub>6</sub>. The percentage of apoptotic cells and viable cells are represented in the diagrams.

## DISCUSSION

The ability of many antitumor agents to induce apoptosis is often dependent on DNA toxicity. As we previously demonstrated, deoxynucleoside analogs can induce DNA damage in non-dividing chronic lymphocytic leukemia cells (4, 7). In other systems DNA damage was correlated to p53 induced apoptosis (16, 21).

p53 is activated by phosphorylation following DNA damage, p53-dependent genes are up-regulated and cells undergo apoptosis (10, 11). In a previous publication we demonstrated how 2CdA and CaFdA, but not F-ara-A, can induce apoptosis in B-CLL also by damaging directly mitochondria (4). We concluded that F-ara-A kills B-CLL only through DNA damage. We used this concept to screen patients with different sensitivity toward 2CdA and F-ara-A, and we correlated such a response to the status of p53 activation. As we expected patients resistant to F-ara-A were also p53 pathway mutated. Only one patient was however completely resistant to a treatment with high concentration of F-ara-A in short time incubation (24 h) and the patient resulted to be p53 homozygously deleted. The other resistant patients, who presented a mutation in the p53 gene sequence analysis, displayed only a reduced toxicity for F-ara-A.

Our analyses were then focused on this p53-null patient (TJK 0031), compared to the p53 intact and F-ara-A responsive patient (TJK0052). The ability of 2CdA to induce apoptosis also in the p53 negative patient, confirmed our already published data that 2CdA is able to induce cytochrome c release early and efficiently, only by damaging directly mitochondria (4). On the other hand, it appears that F-ara-A

requires the p53-signaling pathway to induce apoptosis through the intrinsic pathway. Bax was postulated in other systems to mediate the p53 response leading to cytochrome c release (11, 22, 23). In our system, p53 was activated in the patient with intact p53, but Bax was not up-regulated. Anti-apoptotic protein XIAP (24) was down-regulated after the treatment of p53 positive patients as well as in p53 negative patients, suggesting XIAP to be downstream of caspases activation and cytochrome c release and not induced directly by p53. In fact, experiments carried out in presence of caspase-inhibitor z-VAD-fmk confirmed the down-regulation of XIAP due to caspase-activation. In our system probably another protein mediate the release of cytochrome c in the p53-signaling pathway. Our research is addressed to identify this molecule.

It has become clear from chemosensitivity testing of human cancer cell lines as a function of p53 status that there are important tissue specific differences in cancer cell sensitivity. For example, certain malignant hematopoietic cells are more sensitive to DNA-damaging agents than solid-tumor cell lines, regardless to p53 status. Also, p53 status does not always correlate with chemosensitivity. p53 is the most commonly mutated gene in human cancer, and it is clear that loss of p53 correlates with malignant tumor progression and drug resistance in vivo in many tumor types (16, 25). In spite of the recognition of the signaling protein inducing cytochrome c release, in B-CLL it appears that multidrug resistance for antitumor drugs is related to the status of p53 genes. This has high clinical relevance, because the use of a different treatment can be decided after a previous analysis of the status of p53.

We observed that F-ara-A can kill p53 negative B-CLL if incubated for a longer period of time. Caspases are also activated in this system (data not shown), but pretreatment with caspases inhibitors does not reduce the number of apoptotic cells. Accumulation of the analog can cause an imbalance in the nucleotides equilibrium in the cells, inducing poisoning or disrupting the metabolism of the cell and activation of the caspases. Caspase activity is however low and the concentration of caspase inhibitor used blocks completely their activity in a cell-free system, but does not protect entirely from caspase-9 activation in the cells (data not shown). Therefore the number of apoptotic cells is very similar. Increasing the concentration of the inhibitor was inducing toxicity by its own.

During our research we also interestingly observed an unusual localization of p53 protein in B-CLL cells. Cytosolic p53 in other cells is normally degraded in a proteasome-dependent pathway. B-CLL present however a high concentration of p53 in the cytosol. The lack of p53 degradation might play a role in the different sensitivity among B-CLL and normal PBL toward antitumoral agents.

p53 was also observed to be exported from the nucleus when apoptosis is occurring. When cells present the classical apoptotic phenotype with condensed chromatin, p53 relocalize into the cytosol. Caspases inhibitors can not prevent this event.

## REFERENCES

1. Beutler, E. Cladribine (2-chlorodeoxyadenosine) [see comments], *Lancet*. **340**: 952-6, 1992.
2. Carrera, C. J., Saven, A., and Piro, L. D. Purine metabolism of lymphocytes. Targets for chemotherapy drug development, *Hematol Oncol Clin North Am.* **8**: 357-81, 1994.
3. Begleiter, A., Mowat, M., Israels, L. G., and Johnston, J. B. Chlorambucil in chronic lymphocytic leukemia: mechanism of action, *Leuk Lymphoma.* **23**: 187-201, 1996.
4. Genini, D., Adachi, S., Chao, Q., Rose, D. W., Carrera, C. J., Cottam, H. B., Carson, D. A., and Leoni, L. M. Deoxyadenosine analogs induce programmed cell death in chronic lymphocytic leukemia cells by damaging the DNA and by affecting directly the mitochondria, *Blood. In review*; 2000.
5. Genini, D., Budihardjo, I., Plunkett, W., Wang, X., Carrera, C. J., Cottam, H. B., Carson, D. A., and Leoni, L. M. Nucleotide requirements for the in vitro activation of the apoptosis protein-activating factor-1-mediated caspase pathway, *Journal of Biological Chemistry.* **275**: 29-34, 2000.
6. Leoni, L. M., Chao, Q., Cottam, H. B., Genini, D., Rosenbach, M., Carrera, C. J., Budihardjo, I., Wang, X., and Carson, D. A. Induction of an apoptotic program in cell-free extracts by 2-chloro-2'-deoxyadenosine 5'-triphosphate and cytochrome c, *Proc Natl Acad Sci U S A.* **95**: 9567-71, 1998.
7. Carson, D. A., Wasson, D. B., Kaye, J., Ullman, B., Martin, D. W., Jr., Robins, R. K., and Montgomery, J. A. Deoxycytidine kinase-mediated toxicity of deoxyadenosine analogs toward malignant human lymphoblasts in vitro and toward murine L1210 leukemia in vivo, *Proc Natl Acad Sci U S A.* **77**: 6865-9, 1980.
8. Yuh, S. H., Tibudan, M., and Hentosh, P. Analysis of 2-chloro-2'-deoxyadenosine incorporation into cellular DNA by quantitative polymerase chain reaction, *Anal Biochem.* **262**: 1-8, 1998.
9. Xu, Y. and Baltimore, D. Dual roles of ATM in the cellular response to radiation and in cell growth control [see comments], *Genes Dev.* **10**: 2401-10, 1996.
10. Shieh, S. Y., Ikeda, M., Taya, Y., and Prives, C. DNA damage-induced phosphorylation of p53 alleviates inhibition by MDM2, *Cell.* **91**: 325-34, 1997.
11. Evan, G. and Littlewood, T. A matter of life and cell death, *Science.* **281**: 1317-22, 1998.
12. Freedman, D. A. and Levine, A. J. Nuclear export is required for degradation of endogenous p53 by MDM2 and human papillomavirus E6, *Mol Cell Biol.* **18**: 7288-93, 1998.
13. Soengas, M. S., Alarcon, R. M., Yoshida, H., Giaccia, A. J., Hakem, R., Mak, T. W., and Lowe, S. W. Apaf-1 and caspase-9 in p53-dependent apoptosis and tumor inhibition, *Science.* **284**: 156-9, 1999.
14. Pettitt, A. R., Sherrington, P. D., and Cawley, J. C. The effect of p53 dysfunction on purine analogue cytotoxicity in chronic lymphocytic leukaemia, *Br J Haematol.* **106**: 1049-51, 1999.
15. Morabito, F., Filangeri, M., Callea, I., Sculli, G., Callea, V., Fracchiolla, N. S., Neri, A., and Brugiattelli, M. Bcl-2 protein expression and p53 gene mutation in chronic lymphocytic leukemia: correlation with in vitro sensitivity to chlorambucil and purine analogs, *Haematologica.* **82**: 16-20, 1997.
16. Lowe, S. W., Ruley, H. E., Jacks, T., and Housman, D. E. p53-dependent apoptosis modulates the cytotoxicity of anticancer agents, *Cell.* **74**: 957-67, 1993.
17. Wu, J. C. and Fritz, L. C. Irreversible caspase inhibitors: tools for studying apoptosis, *Methods.* **17**: 320-8, 1999.
18. Kazimierczuk, Z., Cottam, H. B., Revankar, G. R., and Robins, R. K. Synthesis of 2'-Deoxytubercidin, 2'-Deoxyadenosine, and Related 2'-Deoxynucleosides via a Novel Direct Stereospecific Sodium Salt Glycosylation Procedure, *Journal of the American Chemical Society.* **106**: 6379-6382, 1984.
19. Tamm, I., Wang, Y., Sausville, E., Scudiero, D. A., Vigna, N., Oltersdorf, T., and Reed, J. C. IAP-family protein survivin inhibits caspase activity and apoptosis induced by Fas (CD95), Bax, caspases, and anticancer drugs, *Cancer Res.* **58**: 5315-20, 1998.
20. Drach, J., Angerler, J., Schuster, J., Rothermundt, C., Thalhammer, R., Haas, O. A., Jager, U., Fiegl, M., Geissler, K., Ludwig, H., and et al. Interphase fluorescence in situ hybridization identifies chromosomal abnormalities in plasma cells from patients with monoclonal gammopathy of undetermined significance, *Blood.* **86**: 3915-21, 1995.
21. Firestein, G. S., Echeverri, F., Yeo, M., Zvaifler, N. J., and Green, D. R. Somatic mutations in the p53 tumor suppressor gene in rheumatoid arthritis synovium, *Proc Natl Acad Sci U S A.* **94**: 10895-900, 1997.
22. Schuler, M., Bossy-Wetzell, E., Goldstein, J. C., Fitzgerald, P., and Green, D. R. p53 induces apoptosis by caspase activation through mitochondrial cytochrome c release, *J Biol Chem.* **275**: 7337-42, 2000.
23. Genini, D., Sheeter, D., Rought, S., Zauanders, J. J., Susin, S. A., Kroemer, G., Richman, D. D., Carson, D. A., Corbeil, J., and Leoni, L. M. HIV induces lymphocyte apoptosis by a p53-initiated, mitochondrial-mediated mechanism, *FASEB j*, Submitted.
24. Duckett, C. S., Nava, V. E., Gedrich, R. W., Clem, R. J., Van Dongen, J. L., Gilfillan, M. C., Shiels, H., Hardwick, J. M., and Thompson, C. B. A conserved family of cellular genes related to the baculovirus iap gene and encoding apoptosis inhibitors, *Embo J.* **15**: 2685-94, 1996.
25. Velculescu, V. E. and El-Deiry, W. S. Biological and clinical importance of the p53 tumor suppressor gene, *Clin Chem.* **42**: 858-68, 1996.

## Indanocine, a Microtubule-Binding Indanone and a Selective Inducer of Apoptosis in Multidrug-Resistant Cancer Cells

Lorenzo M. Leoni, Ernest Hamel, Davide Genini, Hsiencheng Shih, Carlos J. Carrera, Howard B. Cottam, Dennis A. Carson

**Background:** Certain antimetabolic drugs have antitumor activities that apparently result from interactions with nontubulin components involved in cell growth and/or apoptotic cell death. Indanocine is a synthetic indanone that has been identified by the National Cancer Institute's Developmental Therapeutics Program as having antiproliferative activity. In this study, we characterized the activity of this new antimetabolic drug toward malignant cells. **Methods:** We tested antiproliferative activity with an MTT [i.e., 3-(4,5-dimethylthiazol-2-yl)-2,5-diphenyl tetrazolium bromide] assay, mitochondrial damage and cell cycle perturbations with flow cytometry, caspase-3 activation with fluorometry, alterations of the cytoskeletal components with immunofluorescence, and antimicrotubule activity with a tubulin polymerization assay. **Results/Conclusions:** Indanocine is a cytostatic and cytotoxic indanone that blocks tubulin polymerization but, unlike other antimetabolic agents, induces apoptotic cell death in stationary-phase multidrug-resistant cancer cells at concentrations that do not impair the viability of normal nonproliferating cells. Of the seven multidrug-resistant cell lines tested, three (i.e., MCF-7/ADR, MES-SA/DX5, and HL-60/ADR) were more sensitive to growth inhibition by indanocine than were their corresponding parental cells. Confluent multidrug-resistant cells (MCF-7/ADR), but not drug-sensitive cancer cells (MCF-7) or normal peripheral blood lymphocytes, underwent apoptotic cell death 8–24 hours after exposure to indanocine, as measured by sequential changes in mitochondrial membrane potential, caspase activity, and DNA fragmentation. Indanocine interacts with tubulin at the colchicine-binding site, potently inhibits tubulin polymerization *in vitro*, and disrupts the mitotic apparatus in dividing cells. **Implications:** The sensitivity of stationary multidrug-resistant cancer cells to indanocine suggests that indanocine and related indanones be considered as lead compounds for the development of chemotherapeutic strategies for drug-resistant malignancies. [J Natl Cancer Inst 2000;92:217–24]

Antimetabolic drugs are a major group of antitumor agents, whose varied mechanisms of action have been only partly elucidated (1). Derivatives of natural products, such as the vinca alkaloids, colchicine, cryptophycin, the combretastatins, and related compounds (2,3), as well as several different synthetic heterocyclic compounds (4,5), inhibit tubulin polymerization and prevent microtubule assembly. The taxanes, on the other hand, prevent the depolymerization of tubulin, resulting in the

rearrangement of the microtubule cytoskeleton (6). Although some of the antimetabolic agents have broad-spectrum cancer chemotherapeutic activity, others, such as colchicine and nocodazole, have no selectivity toward malignant cells. In general, antimetabolic agents take advantage of kinetic abnormalities of cancer cells, such as their increased proliferation rate or loss of mitotic checkpoints. Many newer antineoplastic agents focus on biochemical abnormalities that differentiate malignant tumors from most normal tissues (7–9).

The multidrug-resistant phenotype, although not strictly specific for cancer cells, is an attractive target for anticancer drugs because it develops during chemotherapy with bulky hydrophobic antineoplastic agents, limiting their efficacy (10). Several mechanisms may contribute to intrinsic and acquired cross-resistance to multiple antineoplastic agents (clinical drug resistance). They include decreased drug accumulation due to overexpression of the P-glycoprotein drug efflux pump encoded by the *mdr1* gene (11,12), the multidrug resistance-associated protein (MRP) (13), and the p110 major vault glycoprotein (14). In addition, multidrug resistance has been linked to decreased expression of topoisomerase II $\alpha$  (15), to altered expression of drug-metabolizing enzymes and drug-conjugate export pumps (16,17), and to modification of the apoptotic machinery (18,19).

Various hydrophobic drugs with low toxicity for tumor cells can partially reverse multidrug resistance *in vitro* and *in vivo*. In contrast, cytotoxic compounds that preferentially target multidrug-resistant cells are not well described, but such agents should be very useful in the treatment of cancer. The National Cancer Institute's Developmental Therapeutics Program has identified indanocine, a newly synthesized indanone, as a compound with antiproliferative activity.

In this article, we investigate the action of indanocine on cultured multidrug-resistant cancer cells and their corresponding parental (wild-type) cells.

*Affiliations of authors:* L. M. Leoni, D. Genini, H. Shih, C. J. Carrera, H. B. Cottam, D. A. Carson, Department of Medicine and The Sam and Rose Stein Institute for Research on Aging, University of California San Diego, La Jolla; E. Hamel, Laboratory of Drug Discovery Research and Development, Developmental Therapeutics Program, Division of Cancer Treatment and Diagnosis, National Cancer Institute, National Cancer Institute-Frederick Cancer Research and Development Center, Frederick, MD.

*Correspondence to:* Lorenzo M. Leoni, Ph.D., Department of Medicine 0663, University of California San Diego, 9500 Gilman Dr., La Jolla, CA 92093 (e-mail: lleoni@ucsd.edu).

See "Notes" following "References."

© Oxford University Press

## MATERIALS AND METHODS

### Materials

Indanocine, NSC 698666 (Fig. 1, A), is one of a series of synthetic indanones with antiproliferative activity (Shih H, Deng L, Carrera CJ, Adachi S, Cottam HB, Carson DA: unpublished data). Solid indanocine is a white powder that is stable when stored dry at room temperature or when dissolved in dimethyl sulfoxide or in water containing cyclodextrins. Paclitaxel, vinblastine sulfate, and nocodazole were from Calbiochem (San Diego, CA). Electrophoretically homogeneous bovine brain tubulin was prepared as described previously (20). Media and tissue culture supplies were purchased from Irvine Scientific (Santa Ana, CA) and Fisher Scientific (San Diego, CA). All radiochemicals were from NEN-Dupont (Boston, MA). Unless otherwise indicated, all other reagents were obtained from Sigma Chemical Co. (St. Louis, MO).

### Cell Culture

Cell lines from the American Type Culture Collection (Manassas, VA), propagated according to the instructions of the supplier, were as follows: MES-SA

(human uterine sarcoma) and its multidrug-resistant variant MES-SA/DX5 raised against doxorubicin (21), monkey COS-1, and Hep-G2 (human hepatocellular carcinoma). KB-3-1 (human carcinoma) and KB-GRC-1 (a transfectoma expressing high levels of the MDR1-encoded 170-kd P-glycoprotein) were provided by Dr. Stephen Howell (University of California San Diego, La Jolla) and have been described previously (22). Dr. Michael J. Kelner (University of California San Diego) provided the following cell lines: MV522 (human metastatic lung carcinoma) and MV522/Q6 (a transfectoma expressing high levels of the MDR1 gene-encoded 170-kd P-glycoprotein); MCF-7/ADR, a human breast adenocarcinoma multidrug-resistant line selected against doxorubicin (expressing both gp170 and the embryonic glutathione transferase  $\pi$  isoform), and MCF-7/wt, the parental (wild-type) line; MDA-MB-231, a human breast adenocarcinoma line, and MDA3-1/gp170+, the doxorubicin-resistant daughter line expressing the 170-kd P-glycoprotein; and HL-60, a human acute promyelocytic leukemia line, and HL-60/ADR, the multidrug-resistant variant line selected against doxorubicin and expressing the MRP/gp180 protein. Dr. William T. Beck (Cancer Center, University of Illinois at Chicago) provided CEM, a human lymphoblastoid line, and CEM/VLB100, a multidrug-resistant line selected against vinblastine and expressing the 170-kd P-glycoprotein.

We incubated cells for 72 hours in 96-well plates with the test compounds and then measured cell proliferation by reduction of the yellow dye MTT [i.e., 3-(4,5-dimethylthiazol-2-yl)-2,5-diphenyl tetrazolium bromide] to a blue formazan product. The cleavage is performed by the "succinate-tetrazolium reductase" system, which belongs to the respiratory chain of the mitochondria and is active only in viable cells. Therefore, the amount of formazan dye formed is a direct indication of the number of metabolically active cells in the culture. The optical density of the blue formazan product was measured at 570 nm with a ThermoMax (Molecular Devices, Sunnyvale CA) and analyzed with the Vmax Program (BioMetallics, Princeton, NJ).

### Cell Cycle Analysis

Cells were harvested, fixed in ice-cold 70% ethanol, treated with ribonuclease A at 100  $\mu\text{g}/\text{mL}$ , and stained with propidium iodide at 50  $\mu\text{g}/\text{mL}$  for 1 hour at 37  $^{\circ}\text{C}$ . The DNA content of the cells was analyzed by flow cytometry (FACS-calibur; Becton Dickinson Immunocytometry Systems, San Jose, CA), and the cell cycle distribution was calculated with the ModFit LT 2.0 Program (Verity Software House, Topsham, ME).

### Caspase Analysis

Extracts were prepared by the suspension of  $5 \times 10^6$  cells in 100  $\mu\text{L}$  of a lysis buffer (i.e., 25 mM Tris-HCl [pH 7.5], 150 mM KCl, 5 mM EDTA, 1% Nonidet P-40, 0.5% sodium deoxycholate, and 0.1% sodium dodecyl sulfate), incubation on ice for 10 minutes, and then centrifugation at 14 000g for 5 minutes at 4  $^{\circ}\text{C}$ . The resulting supernatants were collected and frozen at  $-80^{\circ}\text{C}$  or used immediately. Lysates (20  $\mu\text{L}$  containing 5–10  $\mu\text{g}$  of total protein) were mixed with 30  $\mu\text{L}$  of assay buffer [50 mM piperazine-*N,N'*-bis(2-ethanesulfonic acid), 50 mM KCl, 5 mM ethylene glycol bis( $\beta$ -aminoethyl ether) *N,N,N',N'*-tetraacetic acid, 2 mM  $\text{MgCl}_2$ , 1 mM dithiothreitol, and 0.1 mM phenylmethylsulfonyl fluoride], containing 100  $\mu\text{M}$  of Z-DEVD-AFC (where DEVD is Asp-Glu-Val-Asp, Z is benzyloxycarbonyl, and AFC is 7-amino-4-trifluoromethyl coumarin). Caspase-3-like protease activity was measured at 37  $^{\circ}\text{C}$  with a spectrofluorometric plate reader (LS50B; The Perkin-Elmer Corp., Foster City, CA) in the kinetic mode with excitation and emission wavelengths of 400 nm and 505 nm, respectively. Activity was measured by the release of 7-amino-4-methyl coumarin (AMC) from the synthetic substrate Z-DEVD-AFC (Biomol, Plymouth Meeting, PA).

### Mitochondrial Analysis

Cells were treated with the indicated amount of drug and 10  $\mu\text{M}$  Ac-DEVD-fmk (*N*-acetyl-Asp-Glu-Val-Asp-fluoromethylketone; Enzyme System Products, Livermore, CA), the cell-permeable caspase-3/caspase-7-selective inhibitor. Cells were then incubated for 10 minutes at 37  $^{\circ}\text{C}$  in culture medium containing 40 nM 3,3'-dihexyloxycarbocyanine iodide (DiOC6; Molecular Probes, Inc., Eugene, OR), followed by immediate analysis in a FACScalibur cytofluorometer. Fluorescence at 525 nm was recorded.

### Immunofluorescence Assays

Hep-G2 (human hepatocellular carcinoma) cells were grown on glass coverslips in the presence or absence of drugs for 16 hours. Cells were fixed in

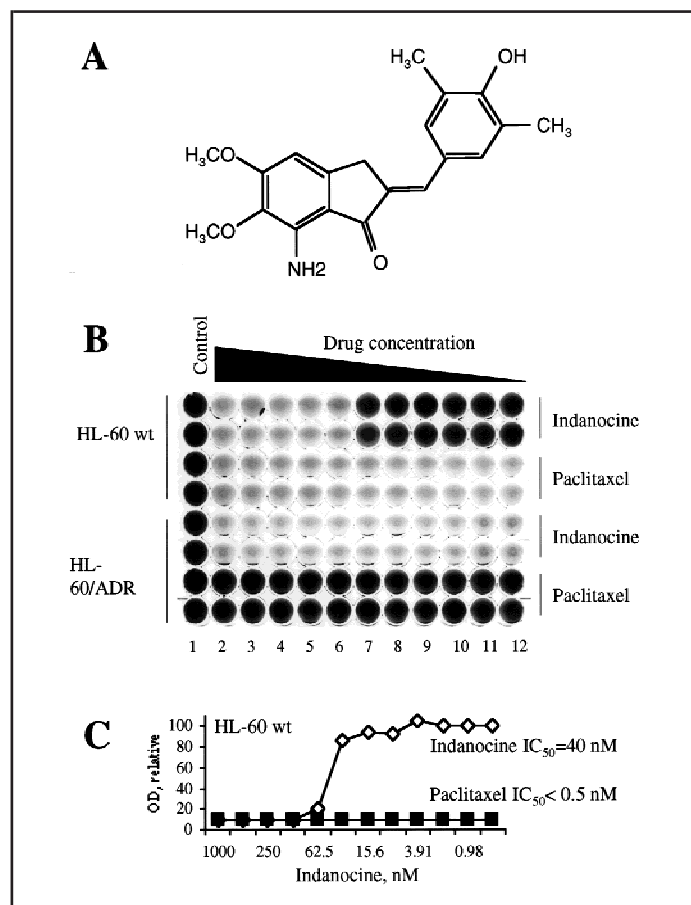


**Fig. 1.** A) Structure of indanocine. In panels B and C, HL-60 and HL-60/ADR cells display collateral sensitivity to indanocine; i.e., the multidrug-resistant cell line was substantially more sensitive to the growth-inhibitory effects of indanocine than the original parental cell line. B) Cytotoxic MTT [i.e., 3-(4,5-dimethylthiazol-2-yl)-2,5-diphenyl tetrazolium bromide] assay of HL-60 cells. Parental wild-type HL-60 and HL-60/ADR multidrug-resistant cells were plated at low density (<5000 cells per well), and indanocine and paclitaxel were added at 1:2 serial dilutions from column 2. Column 1 is the control without drugs. The initial concentrations were 1  $\mu\text{M}$  for indanocine and 10  $\mu\text{M}$  for paclitaxel, and the concentrations in column 12 were 1 nM and 10 nM, respectively. After 3 days, the MTT assay was used to quantitate viable cells. The picture of the plate was obtained by optically scanning the 96-well plate. Dark wells represent metabolically active cells, and clear wells represent metabolically inactive cells. C) Graphic representation of the scanned plate for parental wild-type HL-60 cells, with the calculated 50% inhibitory concentrations (IC<sub>50</sub>) shown (see Table 1).

paraformaldehyde, permeabilized in Triton X-100, and stained with an anti- $\beta$ -tubulin monoclonal antibody, followed by tetramethyl rhodamine B isothiocyanate-conjugated anti-mouse immunoglobulin G (IgG). To visualize filamentous actin filaments, we stained the cells with fluorescein isothiocyanate-conjugated phalloidin, as described previously (23). The type 1 nuclear mitotic apparatus protein was detected with monospecific human autoantibodies, as described previously by Andrade et al. (24). The secondary antibody was fluorescein isothiocyanate-labeled goat anti-human IgG (Tago, Burlingame, CA). Nuclei were stained with the DNA-binding dye 4',6-diamidino-2-phenylindole dihydrochloride (Molecular Probes, Inc.) according to the manufacturer's instructions.

## Tubulin Assays

Assessment of the inhibition of tubulin polymerization and the evaluation of the inhibition of [ $^3$ H]colchicine binding to tubulin were performed as described previously (25). In all experiments, tubulin without microtubule-associated proteins (20) was used. In brief, for inhibition of assembly, 10  $\mu$ M (1.0 mg/mL) tubulin was preincubated with various concentrations of drug (4% [vol/vol] dimethyl sulfoxide as drug solvent) and 0.8 M monosodium glutamate for 15 minutes at 30 °C. The reaction mixture was placed on ice, and guanosine 5'-triphosphate (0.4 mM) was added. Reaction mixtures were transferred to cuvettes at 0 °C in Gilford 250 spectrophotometers (Beckman-Gilford, Fullerton, CA), baselines were established, and the temperature was increased to 30 °C with electronic temperature controllers (over a period of about 60 seconds). The IC<sub>50</sub> value is the drug concentration required to inhibit 50% of the assembly, relative to an untreated control sample, after a 20-minute incubation. It should be noted that the bulk of polymer formed in the presence of glutamate consists of sheets of parallel protofilaments. The drug effects in this system are similar to those observed with a preparation containing tubulin and microtubule-associated proteins (i.e., microtubule proteins). The chief advantage of the glutamate system is that it unambiguously establishes tubulin as the drug target. For the colchicine-binding assay, reaction mixtures contained 1.0  $\mu$ M (0.1 mg/mL) tubulin and 5.0  $\mu$ M [ $^3$ H]colchicine and were incubated for 10 minutes at 37 °C before filtration through a stack of two DEAE-cellulose filters. At this time in reaction mixtures without inhibitor, binding is 40%–50% of maximum, so that the inhibition of the rate of colchicine binding to tubulin can be measured accurately.

## RESULTS

### Inhibition of Cell Growth

In an initial screen performed by the National Cancer Institute's Developmental Therapeutics Program, the mean 50% growth-inhibitory concentration (GI<sub>50</sub>) of indanocine was less than or equal to 20 nM. In 29 of 49 cell lines, including a doxorubicin-resistant breast cancer line, the GI<sub>50</sub> for indanocine was less than the lowest concentration tested (10 nM). Because the indanone is hydrophobic, its activity toward the multidrug-resistant cells was surprising. To confirm this result, we compared the effects of indanocine on the growth of the following pairs of parent and corresponding multidrug-resistant lines (Table 1): MCF-7 and MCF-7/ADR, MES-SA and MES-SA/DX5, MDA-MB-321 and MDA3-1/GP170+3-1, HL-60 and HL-60/ADR, CEM and CEM/VLB100, KB-3-1 and KB-GRC-1, and MV522 and MV522/Q6 cells. The multidrug-resistant cell lines have different multidrug resistance mechanisms, including alterations of gp170 (*mdr1* gene), gp180 (*MRP* gene), and the glutathione transferase  $\pi$  isoform. In several of the cell lines tested, the antiproliferative concentrations of indanocine were equivalent or lower in the multidrug-resistant cells than in the corresponding parent cells. Three of the cell lines tested (i.e., MCF-7, MES-SA, and HL-60) showed collateral sensitivity; i.e., the multidrug-resistant cell line was substantially more sensitive to the growth-inhibitory effects of indanocine than the parental cell line. An example of collateral sensitivity is shown in Fig. 1, where HL-60 and HL-60/ADR cells were plated in a 96-well plate and then treated for 3 days with decreasing (1:2 dilutions)

**Table 1.** Growth-inhibitory concentrations of indanocine and paclitaxel in seven multidrug-resistant cell lines\*

Cell line	GI <sub>50</sub> (indanocine), nM		GI <sub>50</sub> (paclitaxel), nM	
	Wild type	Multidrug resistant	Wild type	Multidrug resistant
MCF-7	20 ± 5	4 ± 1 <sup>†</sup>	50 ± 6	>10 000
MES-SA	85 ± 6	12 ± 3 <sup>†</sup>	<1	>1000
MDA-MB-321	10 ± 3	25 ± 2	50 ± 2	>1000
HL-60	40 ± 3	2 ± 0.2 <sup>†</sup>	<1	>1000
CEM	12 ± 2	20 ± 1	<1	606 ± 20
KB-3-1	7 ± 2	7 ± 3	7 ± 3	>1000
MV522	13 ± 3	8 ± 2	15 ± 4	358 ± 58

\*The cells were treated with various concentrations of indanocine or paclitaxel for 72 hours. Cell proliferation was assessed by the MTT [i.e., 3-(4,5-dimethylthiazol-2-yl)-2,5-diphenyl tetrazolium bromide] assay. The results represent the 50% growth-inhibitory concentrations (GI<sub>50</sub>) (mean ± standard deviation; n > 5). The human breast adenocarcinoma MCF-7/ADR cell line was selected against doxorubicin and expresses both gp170 and the embryonic glutathione transferase  $\pi$  isoform. The human uterine sarcoma line MES-SA/DX5 line was selected against doxorubicin (21). The doxorubicin-resistant human breast adenocarcinoma cell line MDA3-1/gp170+ expresses the 170-kd P-glycoprotein. The human acute promyelocytic leukemia line HL-60/ADR was selected against doxorubicin and expresses the *MRP/gp180* protein. The human lymphoblastoid CEM/VLB100 line was selected against vinblastine and expresses the 170-kd P-glycoprotein. The transfectoma KB-GRC-1 expresses high levels of the *MDR1*-encoded 170-kd P-glycoprotein (22). The metastatic human lung transfectoma MV522/Q6 expresses high levels of the *MDR1*-encoded 170-kd P-glycoprotein.

<sup>†</sup>P < .001 versus wild-type value by Wilcoxon signed rank test.

concentrations of indanocine (from 1  $\mu$ M) or paclitaxel (from 10  $\mu$ M). The MTT assay was then performed at day 3. To prove that P-glycoprotein expression did not confer resistance to the indanone, we compared its effects on two carcinoma cell lines, KB-3-1 and MV522, and their corresponding transfectoma clones that overexpressed P-glycoprotein (the *mdr1* gene product), KB-GRC-1 and MV522/Q6 (22). These transfectomas were resistant to paclitaxel, as expected, but retained complete sensitivity to indanocine (Table 1).

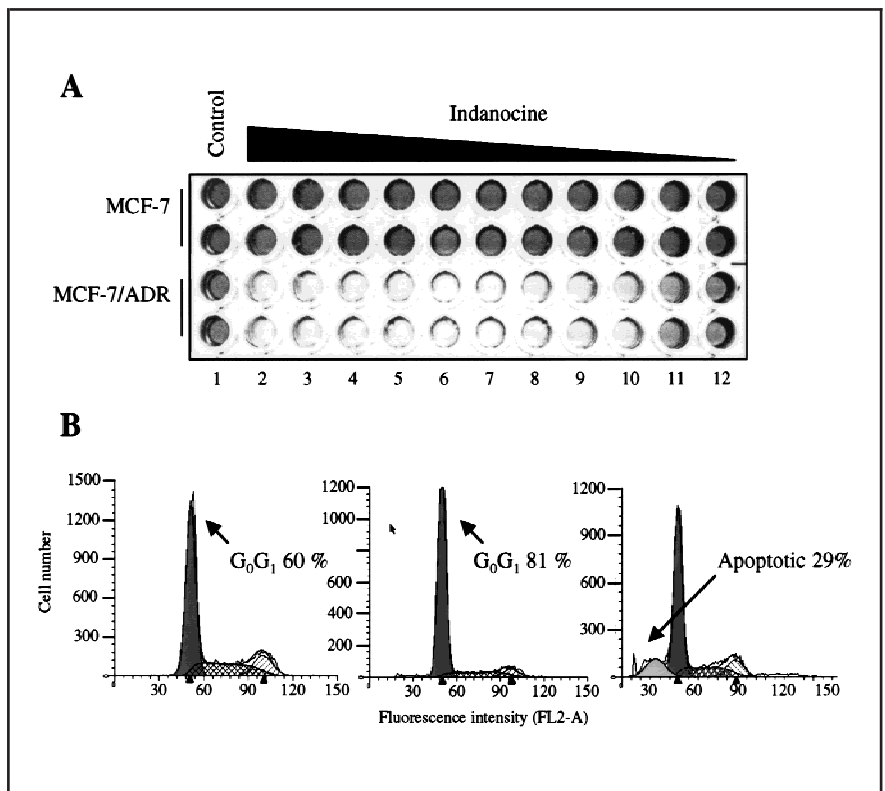
### Effect of Indanocine on Stationary-Phase Cells

The results obtained with the actively growing parent and multidrug-resistant cell lines led us to test indanocine in stationary-phase cell lines. As determined by flow cytometry after propidium iodide staining, up to 81% of stationary MCF-7/ADR cells (1 week in confluent culture) were in the G<sub>1</sub> phase of the cell cycle (Fig. 2, B; middle panel). Remarkably, indanocine treatment of stationary-phase multidrug-resistant cells, but not parental cells, resulted in cell death (IC<sub>50</sub> = 32 nM) (Fig. 2, A). The cytotoxic effect of indanocine in noncycling MCF-7/ADR cells was confirmed by the detection of an apoptotic sub-G<sub>0</sub>/G<sub>1</sub> population by flow cytometry and by the activation of caspase-3 (Fig. 2, B; left panel). Parental (wild-type) MCF-7 cells were similarly growth arrested but did not show apoptotic features (data not shown). In addition, normal peripheral blood lymphocytes exposed to 1000-fold higher concentrations of indanocine for 72 hours showed no loss of viability (data not shown).

### Apoptosis

The study described above demonstrated that stationary MCF-7/ADR cells, but not wild-type MCF-7 cells, were sensitive to treatment with indanocine. To test this observation in

**Fig. 2.** Effect of indanocine on resting multidrug-resistant cells. **A)** Toxicity of indanocine on resting MCF-7 cells. Parental wild-type MCF-7 and MCF-7/ADR multidrug-resistant cells were maintained in a confluent state for 7 days by daily replacement of the medium. Indanocine was then added at 10  $\mu\text{M}$  in wells in **column 2** and serially diluted 1 : 2 in each successive column (reaching 10 nM in **column 12**). **Column 1** is the control, without indanocine. After 3 days, the MTT [i.e., 3-(4,5-dimethylthiazol-2-yl)-2,5-diphenyl tetrazolium bromide] assay was used to quantitate viable cells. **B)** DNA content and caspase activity of indanocine-treated cells. MCF-7/ADR multidrug-resistant cells were harvested, permeabilized, and stained with propidium iodide. The DNA content of cells was established by flow cytometry. **Solid peak** = cells in the  $G_0/G_1$  phase; **cross-hatched peak** = cells in the S phase; **hatched peak** = cells in the  $G_2/M$  phase; **shaded peak** (present only in the **right panel**) = hypodiploid, apoptotic cells, as modeled with the ModFit Program. At the **left** are normally proliferating cells, in the **middle** are confluent cells (7 days), and at the **right** are indanocine-treated, growth-arrested confluent MCF-7/ADR cells. The percentage of cells that are in  $G_0/G_1$  phase or that are apoptotic is indicated. The relative caspase activity is the fluorometric measurement of the caspase-3-like activity normalized to the control cells (**left**). For normally proliferating MCF-7/ADR cells, the relative caspase activity is 100; for 7-day confluent MCF-7/ADR cells, it is 100; for growth-arrested, confluent MCF-7/ADR cells treated with indanocine, it is 450.



another cell line pair that displayed collateral sensitivity to indanocine in the multidrug-resistant derivative line, we selected HL-60 and HL-60/ADR cells because of the exquisite sensitivity of HL-60/ADR cells to indanocine. In the experiment shown in Fig. 3, we tested the ability of indanocine to activate caspase-3 in parental and multidrug-resistant HL-60 cells. Caspase-3, considered an “executioner” caspase, is implicated in the last and irreversible phase of the apoptotic caspase pathway and is activated by upstream “initiator” caspases, such as caspase-8 and caspase-9 [reviewed in (26)]. Caspase activity was measured by use of the fluorogenic caspase-3-specific substrate DEVD-AMC. HL-60/ADR cells incubated with 10 nM indanocine showed a time-dependent increase in caspase-3 activity compared with untreated cells, reaching a maximum at 24 hours. In contrast, wild-type HL-60 cells showed only a slight increase in caspase-3 activity, about 25% of that obtained in the multidrug-resistant cells (Fig. 3, A).

To determine the effect of indanocine treatment on the mitochondrial transmembrane potential of multidrug-resistant and wild-type cells, we used the fluorochrome DiOC6 (Fig. 3, B). In apoptosis induced by various stimuli, a decrease in the mitochondrial transmembrane potential has been shown to precede nuclear DNA fragmentation (27). The flow cytometry results showed a visible reduction in DiOC6 fluorescence for HL-60/ADR cells incubated with indanocine for 8 hours, indicating that the mitochondrial transmembrane potential in these cells was reduced. After 16 hours, the percentage of cells with reduced DiOC6 fluorescence had reached 44%. HL-60 wild-type cells incubated with the same amount of indanocine did not display the same strong reduction in DiOC6 fluorescence.

### Effect on Tubulin Polymerization

Indanocine did not change the flow cytometry profile of stationary-phase cells stained for DNA, other than to cause the

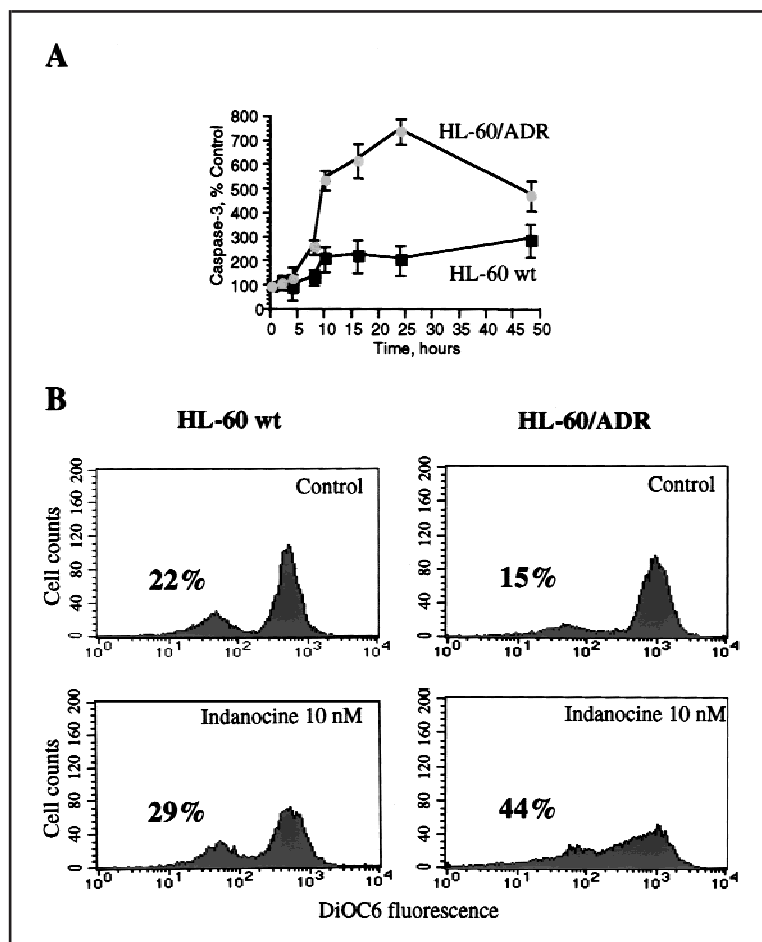
appearance of hypodiploid apoptotic cells in multidrug-resistant cultures (Fig. 2). However, concentrations of the drug that inhibited cell proliferation caused a rapid increase in the number of cells in  $G_2/M$  phases in growing cultures (data not presented).

Antimitotic drugs usually interfere with cellular microtubules by interacting with tubulin (3). Using glutamate-induced assembly of purified tubulin (containing no microtubule-associated proteins) as our assay, we found (Fig. 4, A) that indanocine inhibited tubulin assembly in a manner comparable to that of nocodazole rather than inducing polymerization as would paclitaxel. This observation led us to perform a quantitative analysis (Fig. 4, B), in which we found that indanocine was nearly as potent as combretastatin A-4 (a gift of Dr. G. R. Pettit, Arizona State University, Tempe, AZ) as an inhibitor of tubulin assembly. We measured the extent of tubulin assembly after a 20-minute incubation at 30 °C and determined that the  $IC_{50}$  of combretastatin A-4 was  $1.20 \pm 0.03 \mu\text{M}$  (mean  $\pm$  standard deviation;  $n = 4$ ) and that the  $IC_{50}$  of indanocine was  $1.7 \pm 0.1 \mu\text{M}$  ( $n = 3$ ). Both compounds practically eliminated the binding of 5  $\mu\text{M}$  [ $^3\text{H}$ ]colchicine to 1  $\mu\text{M}$  tubulin when present at 5  $\mu\text{M}$ —combretastatin A-4 inhibited  $98\% \pm 4\%$  of colchicine binding ( $n = 4$ ), and indanocine inhibited  $95\% \pm 2\%$  of colchicine binding ( $n = 4$ ). The effects of various concentrations of the two drugs on colchicine binding are shown in Fig. 4, C. Neither agent inhibited the binding of [ $^3\text{H}$ ]vinblastine to tubulin (single experiment).

### Cytoskeletal Effects of Indanocine

COS-1 and Hep-G2 cells were grown on glass coverslips and treated with various concentrations of indanocine, nocodazole, or vinblastine sulfate. The microtubule network was then visualized by indirect immunofluorescence with an anti- $\beta$ -tubulin antibody, and the microfilament network was stained with fluorescein isothiocyanate-coupled phalloidin. COS-1 and Hep-G2

**Fig. 3.** Indanocine induces apoptosis in multidrug-resistant cells. **A)** Activation of caspase-3 by indanocine. HL-60 wild-type (wt) and multidrug-resistant (ADR) cells were treated with 10 nM indanocine; at the indicated times, caspase-3-like activity was measured with the specific fluorogenic substrate DEVD-AMC (Asp-Glu-Val-Asp coupled to 7-amino-4-methyl coumarin). The results are expressed as the means  $\pm$  standard deviation (**error bars**) and are representative of up to four experiments. **B)** Reduction of mitochondrial transmembrane potential by indanocine. HL-60 cells were treated with and without indanocine at 10 nM. After 16 hours of incubation, cells were incubated with 40 nM 3,3'-dihexyloxycarbocyanine iodide (DiOC6), followed immediately by flow cytometry in a FACScalibur. The *x-axis* represents the DiOC6 fluorescence. The *y-axis* represents the number of cells. The percentage of low-DiOC6 fluorescence-gated cells is indicated.



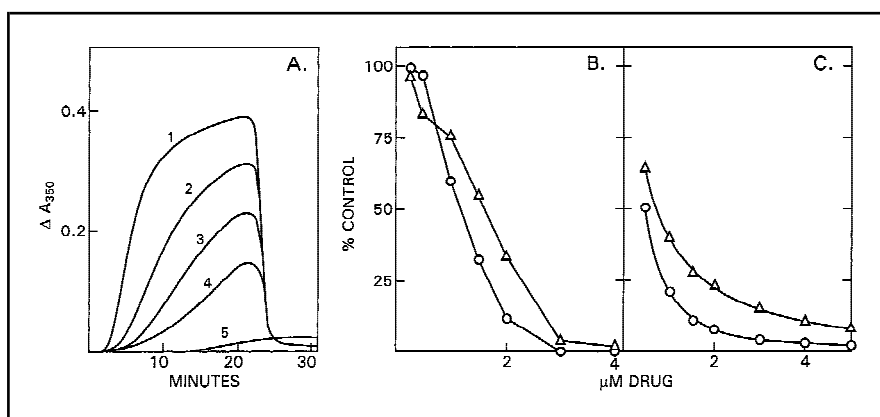
cells were used for these studies because of their clearly defined microtubule and microfilament networks, respectively. Untreated cells had extensive microtubule systems with perinuclear organizing centers (Fig. 5, a and b) and had microfilament bundles and stress fibers that were predominantly aligned with the major axis of the cell (Fig. 6, a and b).

Treatment of COS-1 cells with 0.5 or 5  $\mu\text{M}$  indanocine for 1 hour depleted the cells of microtubules, resulting in diffuse cytoplasmic staining with anti- $\beta$ -tubulin antibody (Fig. 5, c and d).

Treatment with 0.55  $\mu\text{M}$  (0.5  $\mu\text{g}/\text{mL}$ ) vinblastine sulfate (Fig. 5, f) for 1 hour had a similar effect. Modifications induced by 3.3  $\mu\text{M}$  (1  $\mu\text{g}/\text{mL}$ ) nocodazole (Fig. 5, e) for 1 hour were less pronounced, and some of the perinuclear organizing centers were still visible.

Indanocine-treated Hep-G2 cells had a rounded shape, and the microfilament cytoskeleton in these cells was disorganized, characteristic of treatment with a depolymerizing agent (Fig. 6, c). After a 1-hour incubation in 0.5  $\mu\text{M}$  indanocine, some cells

**Fig. 4.** Effect of indanocine on tubulin polymerization and binding of [ $^3\text{H}$ ]colchicine to tubulin. Absorbance was measured at 350 nm ( $A_{350}$ ). Inhibition of tubulin polymerization (**A** and **B**) and inhibition of [ $^3\text{H}$ ]colchicine binding to tubulin (**C**) by indanocine and by combretastatin A-4. **Panel A:** For the tubulin polymerization assay, tubulin (10  $\mu\text{M}$ ) was incubated with indanocine at the following concentrations: 0 for **curve 1**, 1.0  $\mu\text{M}$  for **curve 2**, 1.5  $\mu\text{M}$  for **curve 3**, 2.0  $\mu\text{M}$  for **curve 4**, and 3.0  $\mu\text{M}$  for **curve 5**. At 0 time, the temperature controller was set at 30  $^{\circ}\text{C}$  for 20 minutes to measure polymerization; at 20 minutes, the temperature controller was set at 0  $^{\circ}\text{C}$  to measure the amount of cold-reversible tubulin polymer formation. **Panels B** and **C:** Concentrations of indanocine ( $\Delta$ ) and combretastatin A-4 ( $\circ$ ) were as indicated. **Panel B:** Values obtained for the inhibition of tubulin polymerization in all experiments were averaged. For 1.0, 1.5, and 2.0  $\mu\text{M}$  drug, there were four values for combretastatin A-4 and five for indanocine. There were fewer experimental values for the other concentrations. The mean control  $A_{350}$  value in these experiments was 0.382. **Panel C:** Indanocine inhibition of [ $^3\text{H}$ ]colchicine binding to tubulin. In this assay, indanocine was added at various



concentrations to a reaction mixture containing purified tubulin and [ $^3\text{H}$ ]colchicine and incubated for 10 minutes at 37  $^{\circ}\text{C}$ . The amount of [ $^3\text{H}$ ]colchicine bound to tubulin was then measured after filtration on DEAE-cellulose. The experiment shown in panel C was performed once with duplicate samples for each data point.

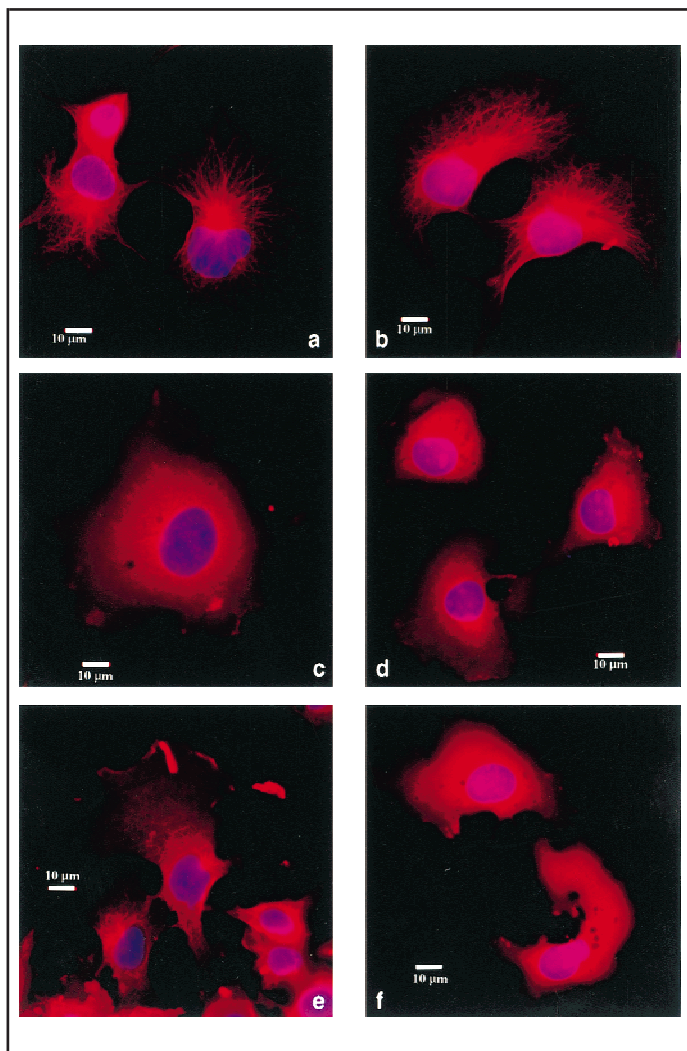


**Fig. 5.** Effect of indanocine on the microtubular network. COS-1 cells were incubated for 2 hours with dimethyl sulfoxide (a) or ethanol (b), 5  $\mu$ M and 500 nM indanocine (c and d, respectively), 3.3  $\mu$ M (1  $\mu$ g/mL) nocodazole (e), or 0.55  $\mu$ M (0.5  $\mu$ g/mL) vinblastine sulfate (f). The cells were fixed, microtubules were labeled (red) with an anti- $\beta$ -tubulin antibody, and nuclei were stained (blue) with 4',6-diamidino-2-phenylindole dihydrochloride.

had a characteristic rounded shape, but other cells had normal microfilament bundles (Fig. 6, d). A similar effect was observed after exposure to nocodazole (Fig. 6, e) or vinblastine sulfate (Fig. 6, f). This is probably an indication that the microfilament breakdown observed at 5  $\mu$ M indanocine is not a direct effect but rather is a consequence of the rapid and potent disruption of the microtubule network.

After treatment of Hep-G2 cells with 100 nM indanocine, the subcellular localization of the mitotic apparatus (as shown by human autoantibodies against the type 1 nuclear mitotic apparatus protein) was determined by immunofluorescence. In control cells undergoing mitosis, the type 1 nuclear mitotic apparatus protein was localized at the poles of the mitotic spindle (Fig. 7, a). In cells exposed to 100 nM indanocine and arrested in the M phase, type 1 nuclear mitotic apparatus protein was distributed in spots scattered over the nucleus (Fig. 7, b). A similar effect was observed with 3.3  $\mu$ M nocodazole (Fig. 7, c). Paclitaxel treatment did not interfere with the subcellular distribution of the type 1 nuclear mitotic apparatus protein, although it affected the formation of a functional mitotic spindle (Fig. 7, d).

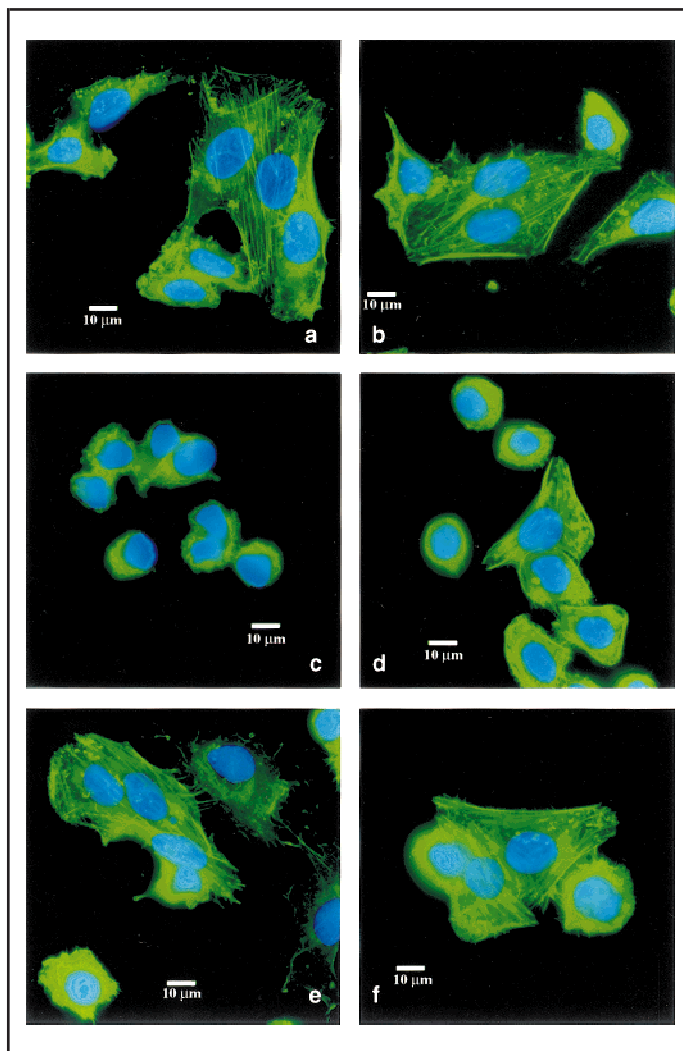


**Fig. 6.** Effect of indanocine on the microfilament network. Hep-G2 cells were incubated for 2 hours with dimethyl sulfoxide (a) or ethanol (b), 5  $\mu$ M and 500 nM indanocine (c and d, respectively), 3.3  $\mu$ M (1  $\mu$ g/mL) nocodazole (e), and 0.55  $\mu$ M (0.5  $\mu$ g/mL) vinblastine sulfate (f). Cells were fixed, microfilaments were stained with fluorescein isothiocyanate-coupled phalloidin (green), and nuclei were stained with 4',6-diamidino-2-phenylindole dihydrochloride (blue).

## DISCUSSION

Indanocine is a derivative of indanone with antiproliferative activity (Shih H, Deng L, Carrera CJ, Adachi S, Cottam HB, Carson DA: unpublished data). An initial screen of malignant cell lines performed by the National Cancer Institute's Developmental Therapeutics Program and the COMPARE Program (28) suggested that these compounds had tubulin-binding properties. In this screening, the indanones, including indanocine, retained activity toward multidrug-resistant breast cancer cells. Indanocine interacts with tubulin at the colchicine-binding site, and it inhibits tubulin polymerization with an  $IC_{50}$  value equivalent to values obtained with podophyllotoxin and combretastatin A-4 (29). Consistent with these biochemical effects, in intact cells, indanocine disrupts intracellular microtubules including those of the mitotic spindle and leads to redistribution of the components of the nuclear mitotic apparatus. The discrepancy between the micromolar concentration of drug required for *in vitro* inhibition of tubulin polymerization and the nanomolar concentrations of drug that blocked cell proliferation has been



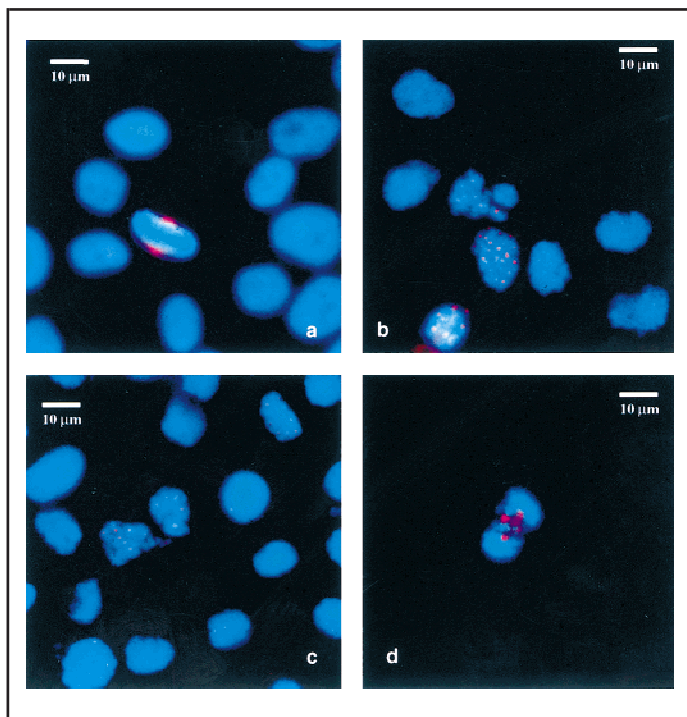


**Fig. 7.** Effect of indanocine on type 1 nuclear mitotic apparatus protein. Hep-G2 cells were incubated for 16 hours with dimethyl sulfoxide (a), 0.1  $\mu\text{M}$  indanocine (b), 3.3  $\mu\text{M}$  (1  $\mu\text{g}/\text{mL}$ ) nocodazole (c), or 0.1  $\mu\text{M}$  paclitaxel (d). Cells were fixed and labeled with monospecific human autoantibodies to type 1 nuclear mitotic apparatus protein.

observed with other antitubulin agents (5,25,29). This discrepancy may indicate that indanocine interacts with other nontubulin cellular components to produce a cytotoxic response. This hypothesis is supported by the ability of short-term treatment with indanocine to trigger apoptosis in stationary multidrug-resistant cancer cells (whose survival should not depend on DNA synthesis or an intact mitotic apparatus) but not in control cells.

Modification of the apoptotic machinery has been proposed as an explanation for the *de novo* and acquired cross-resistance to multiple antineoplastic agents. It has been shown that the Bcl-2 protein may protect cancer cells from drug-induced apoptotic cell death (18,30,31). Microtubule-disrupting drugs, such as vincristine, vinblastine, and colchicine, and microtubule-stabilizing drugs, such as paclitaxel and docetaxel, induce growth arrest, which is followed by phosphorylation and inactivation of Bcl-2, which eventually leads to apoptotic cell death in the  $G_2/M$  phase of the cell cycle (32–34). In contrast, cells in the stationary phase are generally resistant to many of these agents, and phosphorylation of Bcl-2 in the  $G_0/G_1$  phase is generally not observed. This property limits the utility of tubulin-binding drugs for the treatment of malignant tumors containing only a few proliferating cells (i.e., tumors with a low S-phase fraction).

As with other microtubule-damaging drugs, indanocine arrested the growth of multidrug-sensitive cancer cells at the  $G_2/M$  boundary and induced apoptotic cell death. The nanomolar concentrations of indanocine that induced apoptosis in multidrug-resistant cells did not kill wild-type  $G_1$ -phase cancer cells or quiescent normal peripheral blood lymphocytes. Nanomolar concentrations of indanocine forced stationary, multidrug-

resistant cells into the apoptotic program. That these cells were arrested in the  $G_0/G_1$  phase of the cell cycle was confirmed by cytofluorometric analysis. Apoptosis, in these cells, was confirmed by the appearance of a subdiploid-DNA flow-cytometry peak and by caspase-3 activation. Compared with their respective parental lines, five multidrug-resistant cell lines displayed higher or indistinguishable sensitivity to indanocine toxicity.

The cell lines hypersensitive to indanocine have modified various systems for multidrug resistance. MES-SA/DX5 cells overexpress P-glycoprotein, and MCF-7/ADR cells overexpress P-glycoprotein and also have an embryonic  $\pi$  isoform of glutathione transferase (35). HL-60/ADR cells express the MRP/gp180 protein. The other two cell lines that we examined, with unaltered sensitivity to indanocine, only express P-glycoprotein.

The fact that sensitivity to indanocine was retained by all of the multidrug-resistant cells tested, including both KB-3-1 and MV522 transfectomas that overexpress the P-glycoprotein, suggests that this agent acts independently of the P-glycoprotein hydrophobic multidrug transporter and/or that the cytoskeletal disorganization induced by the indanone interfered with P-glycoprotein functions. In other experiments, indanocine did not alter the rate of rhodamine efflux from loaded cells (data not shown). Thus, it seems probable that the uptake and regulation of indanocine do not depend on or directly influence the P-glycoprotein multidrug transporter.

Several different microtubule-disrupting agents have been developed that do not depend on the 170-kd P-glycoprotein and that display antiproliferative activity against multidrug-resistant cancer cells (23,36). It should be of interest to determine whether any of these agents, like indanocine, are cytotoxic to noncycling *mdr1*-expressing cells. Such comparative studies could answer the question whether the mechanism of action of indanocine is related only to inhibition of microtubule function. If indanocine-induced cell death involves another intracellular target, then other microtubule-disrupting agents with antiproliferative activity toward multidrug-resistant cells should not be able to induce apoptosis in the  $G_0/G_1$  phase.

The observation that indanocine kills noncycling, multidrug-resistant cells has practical implications. The low percentage of cycling cells in many human solid tumors limits the potential of antimetabolic drugs. The combination of a drug that is selectively cytotoxic to nondividing, multidrug-resistant cells and an antineoplastic agent that kills tumors with abnormalities of cell cycle checkpoints could represent an exceptionally effective approach to eradicating malignant cells while sparing most normal tissues. Thus, we suggest that indanocine and related indanones be considered lead compounds for the development of chemotherapeutic strategies for drug-resistant malignancies.

## REFERENCES

- (1) Rowinsky EK, Donehower RC. The clinical pharmacology and use of antimicrotubule agents in cancer chemotherapeutics. *Pharmacol Therap* 1991;52:35–84.
- (2) Sinha S, Jain S. Natural products as anticancer agents. *Prog Drug Res* 1994;42:53–132.
- (3) Hamel E. Antimitotic natural products and their interactions with tubulin. *Med Res Rev* 1996;16:207–31.
- (4) Cushman M, He HM, Lin CM, Hamel E. Synthesis and evaluation of a series of benzyraniline hydrochlorides as potential cytotoxic and antimitotic agents acting by inhibition of tubulin polymerization. *J Med Chem* 1993; 36:2817–21.
- (5) Xia Y, Yang ZY, Xia P, Bastow KF, Tachibana Y, Kuo SC, et al. Anti-

- tumor agents. 181. Synthesis and biological evaluation of 6,7,2',3',4'-substituted-1,2,3,4-tetrahydro-2-phenyl-4-quinolones as a new class of antimetabolic antitumor agents. *J Med Chem* 1998;41:1155-62.
- (6) Adams JD, Flora KP, Goldspiel BR, Wilson JW, Arbuck SG, Finley R. Taxol: a history of pharmaceutical development and current pharmaceutical concerns. *J Natl Cancer Inst Monogr* 1993;21:141-7.
- (7) Jordan VC. Tamoxifen treatment for breast cancer: concept to gold standard. *Oncology (Huntingt)* 1997;11:7-13.
- (8) Manges R, Corral T, Kohl NE, Symmans WF, Lu S, Malumbres M, et al. Antitumor effect of a farnesyl protein transferase inhibitor in mammary and lymphoid tumors overexpressing N-ras in transgenic mice. *Cancer Res* 1998;58:1253-9.
- (9) Arguello F, Alexander M, Sterry JA, Tudor G, Smith EM, Kalavar NT, et al. Flavopiridol induces apoptosis of normal lymphoid cells, causes immunosuppression, and has potent antitumor activity *in vivo* against human leukemia and lymphoma xenografts. *Blood* 1998;91:2482-90.
- (10) Ling V. Multidrug resistance: molecular mechanisms and clinical relevance. *Cancer Chemother Pharmacol* 1997;40 Suppl:S3-8.
- (11) Bosch I, Croop J. P-glycoprotein multidrug resistance and cancer. *Biochim Biophys Acta* 1996;1288:F37-54.
- (12) Higgins CF. The multidrug resistance P-glycoprotein. *Curr Opin Cell Biol* 1993;5:684-7.
- (13) Loe DW, Deeley RG, Cole SP. Biology of the multidrug resistance-associated protein, MRP. *Eur J Cancer* 1996;32A:945-57.
- (14) Izquierdo MA, Scheffer GL, Flens MJ, Schroeijs AB, van der Valk P, Scheper RJ. Major vault protein LRP-related multidrug resistance. *Eur J Cancer* 1996;32A:979-84.
- (15) Wessel I, Jensen PB, Falck J, Mirski SE, Cole SP, Sehested M. Loss of amino acids 1490Lys-Ser-Lys1492 in the COOH-terminal region of topoisomerase IIalpha in human small cell lung cancer cells selected for resistance to etoposide results in an extranuclear enzyme localization. *Cancer Res* 1997;57:4451-4.
- (16) Kawasaki H, Carrera CJ, Piro LD, Saven A, Kipps TJ, Carson DA. Relationship of deoxycytidine kinase and cytoplasmic 5'-nucleotidase to the chemotherapeutic efficacy of 2-chlorodeoxyadenosine. *Blood* 1993;81:597-601.
- (17) Goker E, Waltham M, Kheradpour A, Trippett T, Mazumdar M, Elisseyeff Y, et al. Amplification of the dihydrofolate reductase gene is a mechanism of acquired resistance to methotrexate in patients with acute lymphoblastic leukemia and is correlated with p53 gene mutations. *Blood* 1995;86:677-84.
- (18) Strasser A, Huang DC, Vaux DL. The role of the bcl-2/ced-9 gene family in cancer and general implications of defects in cell death control for tumorigenesis and resistance to chemotherapy. *Biochim Biophys Acta* 1997;1333:F151-78.
- (19) Hickman JA. Apoptosis and chemotherapy resistance. *Eur J Cancer* 1996;32A:921-6.
- (20) Hamel E, Lin CM. Separation of active tubulin and microtubule-associated proteins by ultracentrifugation and isolation of a component causing the formation of microtubule bundles. *Biochemistry* 1984;23:4173-84.
- (21) Chen G, Duran GE, Steger KA, Lacayo NJ, Jaffrezou JP, Dumontet C, et al. Multidrug-resistant human sarcoma cells with a mutant P-glycoprotein, altered phenotype, and resistance to cyclosporins. *J Biol Chem* 1997;272:5974-82.
- (22) Shalinsky DR, Andreeff M, Howell SB. Modulation of drug sensitivity by dipyrindamole in multidrug resistant tumor cells *in vitro*. *Cancer Res* 1990;50:7537-43.
- (23) Smith CD, Zhang X, Mooberry SL, Patterson GM, Moore RE. Cryptophycin: a new antimicrotubule agent active against drug-resistant cells. *Cancer Res* 1994;54:3779-84.
- (24) Andrade LE, Chan EK, Peebles CL, Tan EM. Two major autoantigen-antibody systems of the mitotic spindle apparatus. *Arthritis Rheum* 1996;39:1643-53.
- (25) Verdier-Pinard P, Lai JY, Yoo HD, Yu J, Marquez B, Nagle DG, et al. Structure-activity analysis of the interaction of curacin A, the potent colchicine site antimetabolic agent, with tubulin and effects of analogs on the growth of MCF-7 breast cancer cells. *Mol Pharmacol* 1998;53:62-76.
- (26) Salvesen GS, Dixit VM. Caspases: intracellular signaling by proteolysis. *Cell* 1997;91:443-6.
- (27) Castedo M, Hirsch T, Susin SA, Zamzami N, Marchetti P, Macho A, et al. Sequential acquisition of mitochondrial and plasma membrane alterations during early lymphocyte apoptosis. *J Immunol* 1996;157:512-21.
- (28) Paull KD, Lin CM, Malspeis L, Hamel E. Identification of novel antimetabolic agents acting at the tubulin level by computer-assisted evaluation of differential cytotoxicity data. *Cancer Res* 1992;52:3892-900.
- (29) Chen K, Kuo SC, Hsieh MC, Mauger A, Lin CM, Hamel E, et al. Antitumor agents. 178. Synthesis and biological evaluation of substituted 2-aryl-1,8-naphthyridin-4(1H)-ones as antitumor agents that inhibit tubulin polymerization. *J Med Chem* 1997;40:3049-56.
- (30) Ringborg U, Platz A. Chemotherapy resistance mechanisms. *Acta Oncol* 1996;35 Suppl 5:76-80.
- (31) Reed JC, Miyashita T, Takayama S, Wang HG, Sato T, Krajewski S, et al. BCL-2 family proteins: regulators of cell death involved in the pathogenesis of cancer and resistance to therapy. *J Cell Biochem* 1996;60:23-32.
- (32) Haldar S, Chintapalli J, Croce CM. Taxol induces bcl-2 phosphorylation and death of prostate cancer cells. *Cancer Res* 1996;56:1253-5.
- (33) Srivastava RK, Srivastava AR, Korsmeyer SJ, Nesterova M, Cho-Chung YS, Longo DL. Involvement of microtubules in the regulation of Bcl2 phosphorylation and apoptosis through cyclic AMP-dependent protein kinase. *Mol Cell Biol* 1998;18:3509-17.
- (34) Blagosklonny MV, Giannakakou P, el-Deiry WS, Kingston DG, Higgs PI, Neckers L, et al. Raf-1/bcl-2 phosphorylation: a step from microtubule damage to cell death. *Cancer Res* 1997;57:130-5.
- (35) Moscow JA, Townsend AJ, Goldsmith ME, Whang-Peng J, Vickers PJ, Poisson R, et al. Isolation of the human anionic glutathione S-transferase cDNA and the relation of its gene expression to estrogen-receptor content in primary breast cancer. *Proc Natl Acad Sci U S A* 1988;85:6518-22.
- (36) Bollag DM, McQueney PA, Zhu J, Hensens O, Koupal L, Liesch J, et al. Epothilones, a new class of microtubule-stabilizing agents with a taxol-like mechanism of action. *Cancer Res* 1995;55:2325-33.

## NOTES

Supported in part by a grant from the Swiss National Science Foundation; by Public Health Service grants GM23200 (National Institute of General Medical Sciences) and CA78040-01 (National Cancer Institute), National Institutes of Health, Department of Health and Human Services; and by a grant from the Novartis corporation.

Manuscript received June 29, 1999; revised November 4, 1999; accepted November 18, 1999.

## Selective Induction of Apoptosis in Chronic Lymphocytic Leukemia by Indanocine, a Potent Anti-Mitotic Drug.

Davide Genini, Rommel Tawatao, Dennis Sheeter, Helen Hua, Dennis A. Carson, Lorenzo M. Leoni\*

Department of Medicine and The Sam and Rose Stein Institute for Research on Aging, University of California San Diego, 9500 Gilman Drive, La Jolla, California 92093-0663.

Lorenzo M. Leoni, Department of Medicine, University of California San Diego, 9500 Gilman Drive, La Jolla CA 92093-0663, tel: (858) 534-5442, fax: (858) 534-5399, e-mail: [lleoni@ucsd.edu](mailto:lleoni@ucsd.edu)

This work was supported in part by grant GM23200 from the National Institutes of Health.

Key words: Bcl-2, phosphorylation, microtubules, caspases, mitochondria

### ABSTRACT

**Despite their slow proliferative rate, chronic lymphocytic leukemia cells (CLL) are hypersensitive to the toxicity of some microtubule-binding antimitotic agents. The biochemical basis for the hypersensitivity is unknown, and has been difficult to exploit clinically. Indanocine is a recently described tubulin-binding agent that induces apoptosis in some stationary phase, multidrug resistant cancer cell lines. We report here that indanocine is also cytotoxic to CLL cells, but not to normal peripheral blood lymphocytes. Within two hours of CLL cell exposure to indanocine, Bcl-2 phosphorylation and dimerization increased, followed quickly by a reduction in cytosolic Bax, the cytochrome c release from mitochondria to the cytosol, and caspase activation. Concomitantly to Bcl-2 phosphorylation, activation of the JNK pathway was observed. Indanocine did not induce detectable DNA strand break formation, or p53 phosphorylation at Ser15, but stimulated a variety of p53-inducible genes. The increased expression of Fas ligand, and Apo2/TRAIL ligand, was a later event occurring 12-24 hours after indanocine treatment. Collectively, these results suggest that indanocine-induced microtubule disruption in CLL activates an internal apoptosis program, independent of both DNA damage and cell cycle arrest.**

### INTRODUCTION

Chronic lymphocytic leukemia (CLL) is the most common leukemia in the U.S and occurs nearly exclusively in the senior population. It is characterized by the clonal proliferation and accumulation of neoplastic B lymphocytes in the blood, bone marrow, lymph nodes, and spleen. The incidence rate of this disease appears to be on the rise in association with the aging of the American population (1). Despite recent advances in our understanding of CLL and leukemogenesis in general, we still do not know the underlying genetic and biochemical basis for this disease. Also, there is no established cure.

It was discovered several years ago that CLL cells displayed *in vitro* hypersensitivity to colchicine toxicity (2). A

two-hour exposure of CLL cells to colchicine caused ultrastructural changes in mitochondria, followed by apoptosis (3). The exact biochemical basis for colchicine-induced apoptosis could not be elucidated with the knowledge available at that time. Moreover, the systemic toxicity of most microtubule-binding drugs has hampered their routine use for the treatment of CLL and other lymphoproliferative diseases, except in refractory cases.

Since these early reports, the understanding of the molecular events that lead to drug-induced apoptosis has rapidly evolved. Two main pathways are known to activate programmed cell death; an extrinsic death receptor-activated pathway and an intrinsic mitochondrial-mediated pathway (4). Both pathways lead to the activation of effector enzymes collectively known as caspases (5, 6). The extrinsic Fas pathway is important in the regulation of lymphocyte homeostasis (7). The cytoplasmic domain of Fas receptor has no intrinsic activity, but contains a death domain for protein interactions that recruit procaspase-8 to initiate the apoptotic cascade (8, 9). Several other cell death induction proteins that interact with Fas receptors have been identified and alternative pathways have been described for the Fas signaling pathway (10, 11).

The intrinsic apoptotic pathway often involves changes in the mitochondria (4). Damage to the mitochondrial membrane fosters the release from the intermembrane space into the cytosol of apoptotic effector proteins, including cytochrome c (4, 12), apoptosis-inducing factors (AIFs) (13), and procaspases-2 and 9 (14). Procaspase-9 reacts with the cytosolic apoptotic protease activating factor-1 (APAF-1), and in the presence of dATP and cytochrome c oligomerizes to form an active complex called the apoptosome (15, 16). The apoptosome then induces the cleavage of procaspase-3. The intrinsic apoptosis pathway is regulated by pro-apoptotic and anti-apoptotic proteins of the BCL-2 family, which control the integrity of mitochondrial membranes, inducing or preventing cytochrome c release (17, 18). The ratio of anti-apoptotic BCL-2 to pro-apoptotic BAX has been proposed to be a key regulator of apoptosis in lymphocytes (19).

We recently reported the synthesis and characterization of indanocine, a tubulin-binding drug that potently inhibited cell proliferation (20). Unlike other bulky hydrophobic tubulin-binding drugs, indanocine was not a substrate for the

multidrug resistant transporter systems. Moreover, indanocine displayed a unique ability to kill multidrug resistant cancer cells in stationary phase. Considering that CLL cells have a very low rate of proliferation, and have been reported to display colchicine hypersensitivity, we investigated the potential cytotoxic activity of indanocine in CLL cells, and studied its mechanism of action in light of recent findings in the field of apoptosis.

## MATERIAL AND METHODS

### Patients, cell isolation and viability assays

Written informed consent was obtained to procure peripheral blood from all patients with normal healthy volunteers. Patients had to have B-CLL according to National Cancer Institute (NCI) criteria of any Rai stage. Heparinized peripheral blood samples from patients with CLL containing at least 90 % malignant cells, were fractionated by Ficoll/Hypaque sedimentation. Non adherent mononuclear cells were resuspended in complete medium (RPMI-1640 supplemented with 10% fetal bovine serum) at a density of 1 to 2 x 10<sup>6</sup> per ml. Cells were incubated at 37°C in an atmosphere of 5% CO<sub>2</sub> with the indicated drugs. In some experiments frozen cells were used. At the indicated times, viability assays were performed by erythrosin B dye exclusion.

### Subcellular fractionation and Immunoblotting

For total cell lysates, washed B-CLL cells were lysed in Lysis buffer (25 mM Tris, pH 7.4, 150 mM KCl, 5 mM EDTA, 1% Nonidet P-40, 0.5% sodium deoxycholate, 0.1% SDS, 1 µg/ml aprotinin, 1 µg/ml leupeptin, 1 mM phenylmethanesulfonyl fluoride, 1 mM sodium orthovanadate, 1 mM sodium fluoride). Lysates were centrifuged at 15,000 x g for 10 min to remove nuclei and the protein content of supernatants was measured using a modified Coomassie blue assay (Pierce, Rockford, IL). For the isolation of the cytosolic and membrane-bound proteins, cells were washed with PBS, and incubated for 10 minutes on ice with frequent vortexing in Hypotonic Extraction Buffer (HEB; containing 50 mM PIPES/50 mM KCl/5 mM EGTA/2 mM MgCl<sub>2</sub>/1 mM DTT/0.1 phenylmethanesulfonyl fluoride) freshly supplemented with 0.05% digitonin (Sigma, St. Louis). The cells were then centrifuged at 15,000 x g for 10 min at 4°C, the pellet containing the nuclei and membranes was resuspended in Lysis buffer. The supernatant represented the cytosolic proteins. The concentration of digitonin (0.05%) used to optimally recover the of cytosolic proteins but not to damage the mitochondrial membranes was obtained by titration, followed by immunoblotting of mitochondrial proteins residing on the mitochondrial intermembrane compartment. The extracted proteins were resolved at 125 V on 14% and 4-20% Tris-gly pre-cast gels (Novex, San Diego) and electrophoretically transferred to 0.2 µm polyvinylidene fluoride (PVDF) membranes (Millipore, Bedford, MA) for 2 hours at 125 V. Membranes were blocked overnight in I-Block blocking buffer (Tropix, Bedford, MA). Blots were probed with polyclonal antibodies anti-Mcl-1, anti-Bcl-2, monoclonal anti-Bag-1 (all developed in J. Reed's lab), monoclonal anti-XIAP (Transduction Laboratories Inc.), monoclonal anti-PARP (gift of N.A. Berger), or monoclonal anti-PPAR- (Santa Cruz

Laboratories, California) antibody, followed by a secondary antibody consisting of horseradish peroxidase (HRP)-conjugated goat anti-rabbit (Mcl-1) or anti-mouse (PPAR-) IgG. Detection was performed by an enhanced chemiluminescence (ECL, Amersham) method, followed by colorimetric detection, using SG substrate. The X-ray films were scanned, acquired in Adobe Systems Photoshop and analyzed with NIH Image Software.

### Cellular Assay for Caspase Activity

At the indicated time point, CLL cells were washed twice with PBS, the pellet was resuspended in caspase buffer (50 mM Hepes, pH 7.4, 100 mM NaCl, 1 mM EDTA, 0.1% Chaps, and 5 mM dithiothreitol) for 10 min at 4 °C. Lysates were then stored at -80 °C. The caspase enzymatic assays were carried out in 96 well plates, lysates (10-20 µg of total protein) were mixed with 50 µl of HEB buffer (PIPES 50 mM, KCl 20 mM, EGTA 5 mM, MgCl<sub>2</sub> 2 mM, and DTT 1 mM, pH 7), and reactions were initiated by addition of 100 µM of the specific substrate. After 1 hour incubation at 37°C, caspase-3-like protease activity was measured with the substrate Ac-DEVD-AMC and caspase-9-like activity was measured using Ac-LEHD-AFC. Activity was measured by the release of 7-amino-4-trifluoromethyl-coumarin (AFC) or 7-amino-4-methyl-coumarin (AMC) monitoring fluorescence at excitation and emission wavelengths of 400 and 505 nm, and 380 and 460 nm respectively.

### Cytofluorimetric analysis of mitochondrial transmembrane potential ( $\Delta\Psi$ m) by DiOC6, cell membrane permeability by PI, Fas Ligand and Apo2L/TRAIL surface expression

CLL cells were treated with the indicated amount of the drugs and/or with 50 µM of the cell-permeable caspase inhibitors Z-VAD-fmk (Z-Val-Ala-Asp(Ome)-CH<sub>2</sub>F, Biomol, Plymouth Meeting, PA). Cells were then incubated for 10 min at 37°C in culture medium containing 40 nM 3,3' dihexyloxacarbocyanine iodide (DiOC6, Molecular Probe, Eugene, OR) and 5 µg/ml propidium iodide (PI, Molecular Probe), followed by analysis within 30 minutes of fluorochrome in a Becton-Dickinson FACScalibur cytofluorometer. After suitable compensation, fluorescence was recorded at different wavelengths: DiOC6 at 525 nm (FL-1) and PI at 600 nm (FL-3). For the detection of surface FasL and Apo2L/TRAIL, cells (1 x 10<sup>6</sup>) were washed in PBS, and resuspended in 50 µl PBS containing 3% FBS with 1 µg monoclonal antibody to Fas Ligand FITC labeled (Clone H11, Apotech, Switzerland) or 1 µg of the FITC-labeled recombinant fusion protein TRAIL-R2:Fc (Apotech, Switzerland). Cells were incubated 30 min on ice, washed in PBS and analyzed by flow cytometry.

### Gene expression analysis

Using the Perkin-Elmer ABI Prism 7700 and Sequence Detection System software, the level of mRNA for human p53, HDM2, DAXX, BAX, p21 and GADD45 were quantified. Total RNA was isolated using the TRIzol Method (Gibco-BRL) and treated with deoxyribonuclease (Boehringer-Mannheim) to remove any contaminating genomic DNA. A control without RT was used to control for the efficiency of this process. 10 µg of total RNA were used to generate cDNA using a T7-poly dT

oligodeoxynucleotide primer (ggc cag tga att gta ata cga ctg act ata ggg agg cgg-T24) following the protocol for SuperScript II (Gibco-BRL). 50 ng of cDNA were used in triplicate and amplified with the TaqMan Master Mix supplied by Perkin-Elmer. Amplification efficiencies were validated and normalized against GAPDH and fold increases were calculated using either the Comparative CT Method for quantitation or by generating a standard curve (Ref: ABI Prism 7700 SDS User Bulletin #2 P/N 4303859 Rev. A (<http://www2.perkinelmer.com/ab/techsupp/7700.html>)).

#### Sequences for primers and probes:

Taqman probes (T) are labeled with 5' FAM and 3' TAMRA, forward (F) and reverse (R) primers are unlabeled (IDT, Coralville, IA). DNA oligo sequences are written 5' to 3' as follows:

**P53:** F-gcgtgagcgccttcgagat; R-cagcctgggcatccttga; T-cgagagctgaatgaggccttgaa

**MDM2:** F-ctacagggagcgcctcgaat; R-tgaatcctgatccaaccaatca; T-cggatcttgatgctggtgtaaggaacattc;

**BAX alpha:** F-ctgatcagaaccatcatgggc; R-gaggccgtcccaaccac; T-tccgggagcggctgttggg;

**P21:** F-ctggagactctcagggtcgaa; R-cggcgtttgagtgtagaa; T-acggcggcagaccagcatgac;

**GADD45:** F-tctgcagatccacttcaccct; R-gctgacgcgaggatgtt; T-tccaggcgtttgctgagagaac;

Patient	IC50	FasL	Apo2/TRAIL
B-CLL	850±60	Up	Not tested
B-CLL	1100±100	Up	Up
B-CLL	5600±110	Up	Up
B-CLL	6700±80	Up	Up
B-CLL	3600±50	Not Tested	Not Tested
B-CLL	2500±70	Not Tested	Not Tested
B-CLL	8000±120	Up	Up
PBL	>50,000	Unchanged	Unchanged
PBL	>50,000	Not tested	Not tested

**Table 1** Cytotoxicity of indanocine was tested in chronic lymphocytic leukemia (B-CLL) cells and normal peripheral blood cells (PBL).

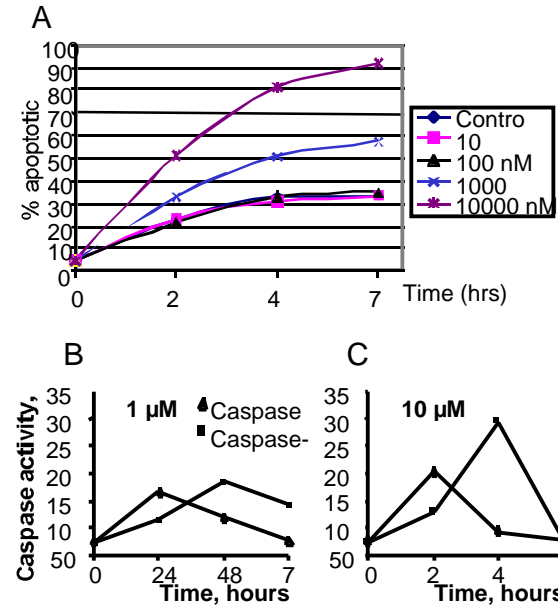
Cell count and viability were assessed by dye-exclusion and MTT assay in cells after 3 days continuous exposure to decreasing concentrations of the drug, starting at 50µM. The level of surface Fas-ligand and Apo2/Trail was measured by flow cytometry using a monoclonal antibody against Fas-ligand (clone H11, Apotech, Switzerland) and using a recombinant chimeric protein TRAIL-R2:Fc (Apotech, Switzerland), respectively.

## RESULTS

### Indanocine Selectivity Towards CLL

As assessed by cell survival after three days incubation, the median concentration of indanocine that killed 50% of CLL cells was approximately 3.6 µM (range 0.85-8 µM, n=7), whereas normal PBL were impervious to 50 µM indanocine (<10% cell death, Table 1). Drug toxicity was both dose and time dependent, with longer exposures producing more killing (Figure 1A). Cell death occurred by the internal apoptosis pathway, with caspase 3 activation preceding the activation of

caspase 8 (Figure 1B and 1C). Blockade of caspase activity with a pan-specific peptidic inhibitor of these proteases (1-Me,3-Me-indole-2)CO-V-D-fmk, (Idun-1965, IDUN Pharmaceuticals, La Jolla) (21) protected B-CLL cells from indanocine toxicity, consistent with an apoptotic mechanism of cell death (data not shown).



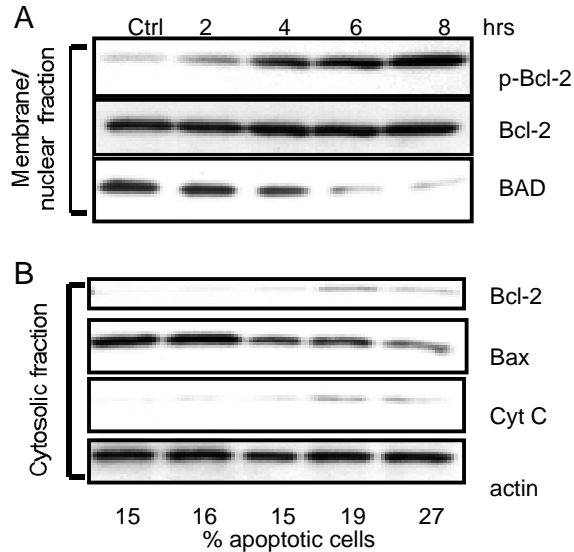
**Figure 1. Indanocine Selective Cytotoxicity to B-CLL Cells.**

Figure 1A. B-CLL cells were incubated in presence of the indicated concentration of indanocine. At the indicated time course, apoptosis was assessed by flow cytometry using a double staining DiOC<sub>6</sub>/propidium iodide (PI). Briefly, B-CLL were exposed for 10 min in culture medium at 37°C to 40 nM DiOC<sub>6</sub> and 5 µg/ml PI. The cells were then rapidly analyzed using a Becton Dickinson FACS-Calibur. The subset of apoptotic cells was defined as displaying low-DiOC<sub>6</sub> (FL-1) and low PI fluorescence (FL-3), after suitable compensation. B-CLL cells were incubated with 1 µM (left panel, Figure 1B) and 10 µM (right panel, Figure 1C) of indanocine. At the indicated times, 2x10<sup>6</sup> cells were washed once in ice-cold PBS and resuspended in 50 µl Caspase Buffer. The enzymatic caspase-3-like (▲) and caspase-8-like (■) activities were measured using the fluorometric substrates Ac-DEVD-AMC and Z-IETD-AFC, respectively.

### Indanocine Increases Bcl-2 Phosphorylation and Alters the Subcellular Localization of Apoptotic Proteins.

In order to analyze the molecular events induced by indanocine in B-CLL cells, the treated cells were fractionated into cytosolic and membrane/nuclear fractions by hypotonic buffer extraction in presence of 0.05% digitonin. The earliest pro-apoptotic change observed in indanocine treated CLL cells was Bcl-2 phosphorylation, which was detectable at 2 hours, and increased thereafter (Figure 2A, top). The total amount of membrane-bound Bcl-2 did not change during the same treatments (Figure 2A, middle), the cytosolic pool showed a slight increase at 6 and 8 hours post-treatment (Figure 2B, top). In parallel to Bcl-2 phosphorylation, the membrane-associated Bad was greatly reduced (Figure 2A, bottom), the cytosolic Bax decreased, and cytochrome c was released into the soluble cytosolic fraction. The observed events are consistent with a model in which Bcl-2 phosphorylation induces its dissociation from Bax, which

becomes free to insert into mitochondrial membranes, thus allowing cytochrome c release into the cytosol. The % of apoptotic cells measured in the same cells by flow cytometry using the DiOC6 staining, reported at the bottom of the gels, shows that the induction of apoptosis is concomitant with the cytochrome c release.



**Figure 2. Indanocine Increases Bcl-2 Phosphorylation and Alters the Subcellular Localization of Apoptotic Proteins.**

B-CLL cells were treated with 10  $\mu$ M indanocine. At the indicated time-points cells were incubated with an hypotonic extraction buffer containing 0.05% digitonin. The membrane/nuclear (Figure 2A) and cytosolic-enriched (Figure 2B) fractions were loaded on a 4-20% Tris-gly SDS-PAGE gel, and blotted on a PVDF membrane. Antibodies against phosphorylated Bcl-2 (Upstate Biotechnology), against Bcl-2, cytochrome c (Santa Cruz Biotechnology), and Bad (New England Biolabs) were used to quantify the apoptotic components. The total amount of protein was analyzed by using an anti-actin antibody. The percent of apoptotic cells (indicated at the bottom of figure 2B) was measured by flow cytometry using a double labeling with DiOC6 and propidium iodide (PI). The subset of apoptotic cells was defined as displaying low-DiOC6 and low PI fluorescence. The results obtained are representative of 3 different B-CLL patients.

#### Indanocine Activates the c-Jun Kinase Pathway.

In order to determine the Bcl-2-phosphorylating enzymatic cascade activated by indanocine on the quiescent B-CLL cells, a variety of candidates were tested. Several phospho-specific antibodies against ERK 1 and 2, and p38 kinase obtained from a variety of vendors (NEB, Promega, Santa Cruz Biotechnology) showed negative results (data not shown), indicating that these two pathways are probably not involved in the indanocine-induced cytoskeletal stress pathway. On the contrary, indanocine induced a rapid and strong phosphorylation of the transcription factors c-Jun and ATF-2 (Figure 3, first and second panel), as well as JNK-1 and -2 (Figure 3, third panel), suggesting the activation of the ASK/JNK pathway, as previously reported in proliferating cells (22). The phosphorylation of ATF-2, c-Jun, and JNKs is concomitant to the Bcl-2 phosphorylation, starting at 4 hours and peaking at 8 hours. Finally, the % of apoptotic cells increases significantly after 8 hours, following the activation of

the stress signaling pathway, and confirming the results shown in figure 2 obtained in cells from a different CLL patient.

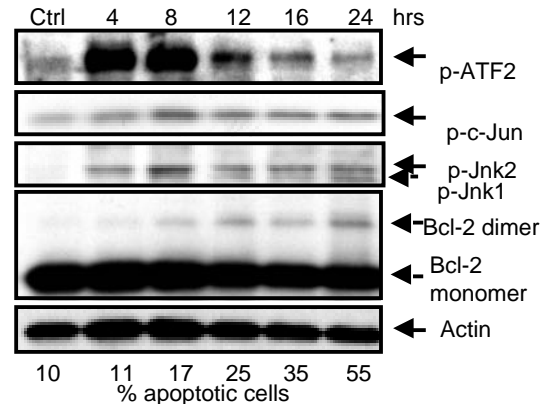


**Figure 3. Activation of stress-signaling pathway by indanocine in B-CLL.**

B-CLL cells were treated with 10  $\mu$ M indanocine, at the indicated time-points total cell lysates were obtained as described in the Material and Methods. The lysates were loaded on a 4-20% Tris-gly SDS-PAGE gel, and blotted on a PVDF membrane. Phospho-specific antibodies from New England Biolabs were used to analyze the activation of the transcription factors ATF-2 and c-Jun, of the c-Jun Kinases-1 and -2. A monoclonal antibody was used to look at the level of Bcl-2 and at the appearance of the Bcl-2 dimers. The total amount of protein was analyzed by using an anti-actin antibody. The results obtained are representative of 3 different B-CLL patients.

#### Indanocine Activates the p53 Pathway Without DNA Damage.

In order to verify if the induction of apoptosis by indanocine was also mediated by a transcriptional activation of the pro-apoptotic p53 pathway, we investigated the DNA damage activity of indanocine and the expression levels of both mRNA and protein of p53-inducible genes. As measured by a sensitive alkaline DNA unwinding assay that could detect damage inflicted by 1Gy, or with the single cell-based comet assay, 20  $\mu$ M indanocine did not induce DNA strand break in CLL cells (data not shown). Immunoblotting analysis confirmed the lack of direct DNA damage by indanocine. No detectable phosphorylation of p53 at the serine 15 residue was observed in indanocine-treated CLL cells from several patients (Figure 4, top panels). As a positive control, incubation of CLL cells with the DNA-damaging nucleoside analog fludarabine (F-AraA) for 24 hours showed a strong band, indicating Ser15 p53 phosphorylation. An antibody recognizing p53 phosphorylated at residue Ser392 was also tested, but no increase was observed with both fludarabine and indanocine. Interestingly, quantitative mRNA analysis (RQ-PCR, TaqMan analysis) of indanocine treated cells showed up-regulation of the p53 inducible genes p21, Bax, HDM2, and p53, suggesting the activation of a functional p53 pathway. The analysis of the protein expression levels of the same p53-inducible genes confirmed the RQ-PCR results showing induction of p21, Bax, p53, and HDM2 after treatment with indanocine at 1 and 10  $\mu$ M at 8 or 24 hours. However, these changes were first apparent at 8 hours, after the hyperphosphorylation of Bcl-2. Moreover, a CLL cell clone

that failed to express detectable p53 in immunoblots still underwent Bcl-2 phosphorylation and apoptosis after incubation with indanocine (results not shown).

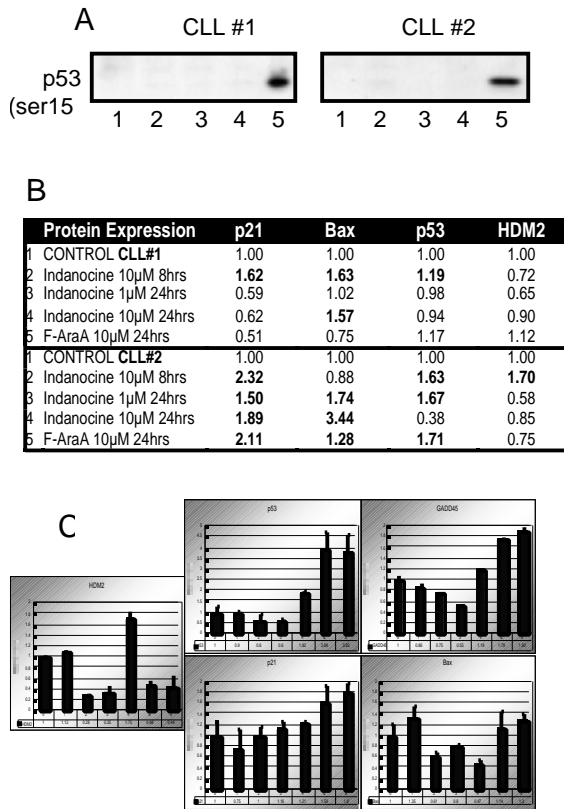


**Figure 4. Indanocine activates p53-inducible genes.** B-CLL cells from two different patients (CLL#1 and CLL#2) were incubated in presence of DMSO (lane 1), indanocine at 10 µM (lanes 2 and 4) and 1 µM (lane 3), or the DNA-damaging nucleoside fludarabine (lane 5), for 24 hours (lanes 1, 3, 4, 5) or 8 hours (lane 2). At the indicated time-points, cells were lysed and the (Ser15)-phosphorylated p53 level was measured by immunoblotting (Fig. 4A). The expression of the p53-inducible proteins p21, Bax, HDM2, the total level of p53 were measured by immunoblotting using specific antibodies. The table (Fig. 4B) represents the expression levels quantified by scanning the autoradiography films. The relative expression levels were calculated after analysis of the total amount of protein per lane obtained by immunoblotting with anti-actin antibody. In bold are the conditions that showed up-regulation of the protein expression from the controls. Total RNA was isolated from patient CLL#2 and the mRNA levels of the p53-inducible genes (p21, Bax, GADD45, HDM2, and p53) were quantified by RQ-PCR (TaqMan) using specific primers (Fig 4C). Amplification efficiencies were validated and normalized against GAPDH, and the results are expressed as fold increase over the control (first column, normalized to 1). The results are representative of two independent experiments.

**Indanocine Induces a Late Induction of the Surface Expression of the Death Ligands FasL and Apo2L/TRAIL.**

Phosphorylated c-Jun and ATF-2 can cooperate to increase the transcription of stress-activated genes, that may include the ligands for the death receptors Fas and Apo2/TRAIL. In addition, these two ligands can be induced by p53 transcriptional activation (23, 24). Fluorometric analysis

indeed showed that Fas ligand and Apo2/TRAIL ligand expression increased 24 hours after indanocine treatment of B-CLL cells (Figure 6). However, these events also occurred subsequent to Bcl-2 phosphorylation and initial caspase-3 activation. The up-regulation of both FasL and Apo2/TRAIL appears to be concomitant with the observed enzymatic activation of caspase-8 (Figure 1), and may be responsible for the killing of the cells that did not respond to the early apoptotic induction.

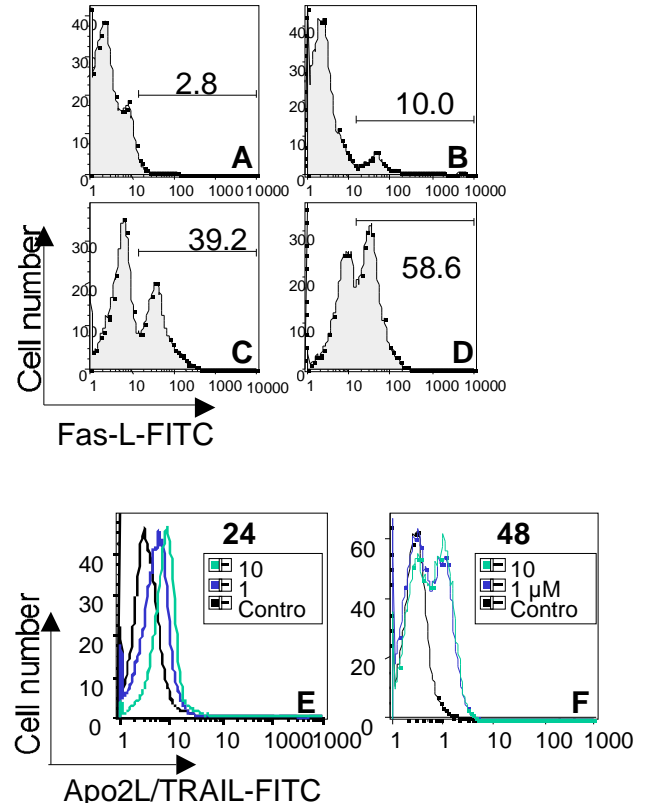


**Figure 5. Surface expression of Fas-ligand and Apo2L/TRAIL in indanocine-treated B-CLL cells.** A: Control antibody, B: Unstimulated B-CLL, C: B-CLL+Indanocine-P 10 µM for 24 hrs, D: Indanocine-P 10 µM 48 hrs. Figure 5B. B-CLL cells isolated by Ficoll gradient were cultured in RPMI-1640 supplemented with 10% FBS. B-CLL were exposed to the indicated concentrations of indanocine. At the selected time point, B-CLL (1x10<sup>6</sup>) were washed in PBS and resuspended in 50 µl FACS medium (culture medium with 0.03% sodium azide) containing 1 µg/ml of the FITC-labeled recombinant fusion protein TRAIL-R2:Fc (Apotech, Switzerland). Cells were incubated 30 min at 4°C, washed with FACS buffer and analyzed using a Becton Dickinson FACS-Calibur.

**DISCUSSION**

The progress of chemotherapy in CLL depends upon the elucidation of biochemical differences between the malignant B cells and normal cells. In general, drugs that inhibit tubulin polymerization selectively arrest proliferating cells in the G2/M phase of the cell cycle, and spare cells in G1. At first analysis, it is paradoxical that indanocine, a tubulin binding agent, should induce apoptosis in CLL cells, that have a very slow turnover rate. Moreover, the malignant CLL cells are many-

fold more sensitive to indanocine toxicity than are normal peripheral blood lymphocytes (PBL).

However, there is reason to suspect that the cytoskeletal network may be regulated much differently in CLL cells than in PBL. Unlike resting peripheral blood lymphocytes, CLL cells spontaneously migrate under stromal cell monolayers, display random chemokinesis, and express high levels of the chemokine receptor CXCR3 and CXCR4 (25, 26). The continuous movement of CLL cells would be expected to require dynamic reorganization of the cytoskeleton. Similarly, in cultured cells, cytoskeletal remodeling is a critical event at the G2/M boundary. Thus, the shared sensitivity to tubulin-binding agents of migrating CLL cells, and proliferating cells at the G2/M check point, may reflect a shared dependence of cell survival on cytoskeletal integrity.

Exactly how inhibition of tubulin polymerization in CLL cells triggers apoptosis is still not clear. Our data indicate that neither DNA-dependent p53 activation, nor signaling through the cell death receptors Fas and Apo2/TRAIL, are primary events in indanocine-induced apoptosis. The results rather point to a more proximal connection between the microtubule network, mitochondria, and proteins of the BCL-2 family. Recently, a BH3-only Bcl-2 family member called Bim, normally associated to the microtubular network, has been shown to translocate to the mitochondria, bind Bcl-2 and neutralize its anti-apoptotic activity upon pro-apoptotic stimulation (27).

In lymphocytes, the Bcl-2/Bax ratio has been proposed to be a central regulator of the intrinsic apoptotic program (28, 29). The overexpression of the pro-apoptotic Bcl-2 family member Bax sensitizes cells to death signals and is sufficient to induce cytochrome c release and apoptosis (30). By forming heterodimers with Bax, Bcl-2 can antagonize this effect. Anticancer microtubule-binding agents have been shown to induce phosphorylation of Bcl-2 and to diminish its anti-apoptotic activity (31). The mechanism of action may be that Bcl-2 phosphorylation reduces its heterodimerization with Bax, releasing the pro-apoptotic Bax protein for insertion into mitochondrial membranes. Recently, mutation of the Bcl-2 phosphorylation sites to non-phosphorylatable residues has been shown to enhance its anti-apoptotic activity (22). A variety of different kinases have been reported to regulate the drug-induced BCL-2 phosphorylation in malignant cell lines, including Raf-1, PKA, and ASK/Jun N-terminal kinase 1 (reviewed in (32)).

BAD is a pro-apoptotic molecule that lacks the hydrophobic c-terminal sequence typical of membrane-based BCL-2 family members, but can bind to, sequester, and inactivate BCL-2 and BCL-XL (28). Serine phosphorylation of BAD in response to cell survival factors renders it incapable of forming such inactivating heterodimers (33). BAD phosphorylation is controlled by several different kinases, including phosphatidylinositol-3 kinase (PI3-kinase), AKT, Raf p21 activated kinase (PAK1), ERKs, and RSK (see (34)).

Treatment of CLL cells with cytotoxic concentrations of indanocine for as little as 2-4 hours induced BCL-2 hyperphosphorylation, BAD relocalization to the cytosolic compartment, and increased membrane-bound BAX. These early events preceded p53 activation or FasL expression. They were followed by the release of cytochrome c, and the enzymatic activation of procaspases-9 and -3, prior to

procaspase-8. These data suggest that CLL cells, in common with some proliferating malignant cells may have a distinct cytoskeletal damage response pathway that is distinct from both the DNA-damage and death-receptor response pathways (35).

Because it is difficult to manipulate genetically CLL cells by transfection, we could not discriminate the precise enzymes responsible for BCL-2 phosphorylation and BAD dephosphorylation, although indanocine did activate the JNK pathway, as demonstrated by the early phosphorylation of JNK-1 and -2, and of the two downstream transcription factors ATF-2 and c-Jun. It also is possible that disorganization of the cytoskeleton interfered with coordinated BAD phosphorylation, and disturbed the cellular distribution of mitochondria. Future experiments will need to discriminate the subcellular localization of microtubules, protein kinases, BCL-2 family members and mitochondria in CLL cells, compared to normal lymphocytes, before and after indanocine treatment.

Two factors that have impeded the use of microtubule binding drugs for the treatment of CLL are toxicity to normal cells, and the expression in CLL of a multidrug resistant (MDR) phenotype (36). However, in vivo preclinical studies have shown that parental indanocine is remarkably nontoxic to mice (unpublished data). Moreover, malignant cells resistant to vinca alkaloids and paclitaxel retain sensitivity to indanocine toxicity (20). Taken together, these results suggest that indanocine is a useful agent to dissect the cytoskeletal damage response pathway in CLL, and may have potential value for the treatment of refractory disease.

## REFERENCES

1. Call, T. G., Phyllyk, R. L., Noel, P., Habermann, T. M., Beard, C. M., O'Fallon, W. M., and Kurland, L. T. Incidence of chronic lymphocytic leukemia in Olmsted County, Minnesota, 1935 through 1989, with emphasis on changes in initial stage at diagnosis, *Mayo Clin Proc.* 69: 323-8, 1994.
2. Schrek, R. Letter: Sensitivity to colchicine as a test for leukemic lymphocytes, *New England Journal of Medicine.* 293: 151, 1975.
3. Allen, T. D., Scarffe, J. H., and Crowther, D. Ultrastructural aspects of colchicine ultrasensitivity in CLL lymphocytes, *Blood Cells.* 7: 147-60, 1981.
4. Green, D. R. and Reed, J. C. Mitochondria and apoptosis, *Science.* 281: 1309-12, 1998.
5. Martin, S. J. and Green, D. R. Protease activation during apoptosis: death by a thousand cuts?, *Cell.* 82: 349-52, 1995.
6. Miura, M., Zhu, H., Rotello, R., Hartweg, E. A., and Yuan, J. Induction of apoptosis in fibroblasts by IL-1 beta-converting enzyme, a mammalian homolog of the *C. elegans* cell death gene *ced-3*, *Cell.* 75: 653-60, 1993.
7. Nagata, S. Apoptosis by death factor, *Cell.* 88: 355-65, 1997.
8. Boldin, M. P., Varfolomeev, E. E., Pancer, Z., Mett, I. L., Camonis, J. H., and Wallach, D. A novel protein that interacts with the death domain of Fas/APO1 contains a sequence motif related to the death domain, *J Biol Chem.* 270: 7795-8, 1995.
9. Chinnaiyan, A. M., O'Rourke, K., Tewari, M., and Dixit, V. M. FADD, a novel death domain-containing protein, interacts with the death domain of Fas and initiates apoptosis, *Cell.* 81: 505-12, 1995.



10. Stanger, B. Z., Leder, P., Lee, T. H., Kim, E., and Seed, B. RIP: a novel protein containing a death domain that interacts with Fas/APO-1 (CD95) in yeast and causes cell death, *Cell*. *81*: 513-23, 1995.
11. Yang, X., Khosravi-Far, R., Chang, H. Y., and Baltimore, D. Daxx, a novel Fas-binding protein that activates JNK and apoptosis, *Cell*. *89*: 1067-76, 1997.
12. Bossy-Wetzel, E., Newmeyer, D. D., and Green, D. R. Mitochondrial cytochrome c release in apoptosis occurs upstream of DEVD- specific caspase activation and independently of mitochondrial transmembrane depolarization, *Embo J*. *17*: 37-49, 1998.
13. Susin, S. A., Lorenzo, H. K., Zamzami, N., Marzo, I., Snow, B. E., Brothers, G. M., Mangion, J., Jacotot, E., Costantini, P., Loeffler, M., Larochette, N., Goodlett, D. R., Aebersold, R., Siderovski, D. P., Penninger, J. M., and Kroemer, G. Molecular characterization of mitochondrial apoptosis-inducing factor [see comments], *Nature*. *397*: 441-6, 1999.
14. Susin, S. A., Lorenzo, H. K., Zamzami, N., Marzo, I., Brenner, C., Larochette, N., Prevost, M. C., Alzari, P. M., and Kroemer, G. Mitochondrial release of caspase-2 and -9 during the apoptotic process, *J Exp Med*. *189*: 381-94, 1999.
15. Liu, X., Kim, C. N., Yang, J., Jemmerson, R., and Wang, X. Induction of apoptotic program in cell-free extracts: requirement for dATP and cytochrome c, *Cell*. *86*: 147-57, 1996.
16. Zou, H., Henzel, W. J., Liu, X., Lutschg, A., and Wang, X. Apaf-1, a human protein homologous to *C. elegans* CED-4, participates in cytochrome c-dependent activation of caspase-3 [see comments], *Cell*. *90*: 405-13, 1997.
17. Kluck, R. M., Bossy-Wetzel, E., Green, D. R., and Newmeyer, D. D. The release of cytochrome c from mitochondria: a primary site for Bcl-2 regulation of apoptosis [see comments], *Science*. *275*: 1132-6, 1997.
18. Yang, J., Liu, X., Bhalla, K., Kim, C. N., Ibrado, A. M., Cai, J., Peng, T. I., Jones, D. P., and Wang, X. Prevention of apoptosis by Bcl-2: release of cytochrome c from mitochondria blocked [see comments], *Science*. *275*: 1129-32, 1997.
19. Reed, J. C. Bcl-2 family proteins, *Oncogene*. *17*: 3225-36, 1998.
20. Leoni, L. M., Hamel, E., Genini, D., Shih, H., Carrera, C. J., Cottam, H. B., and Carson, D. A. Indanocene, a microtubule-binding indanone and a selective inducer of apoptosis in multidrug-resistant cancer cells [see comments], *Journal of the National Cancer Institute*. *92*: 217-24, 2000.
21. Wu, J. C. and Fritz, L. C. Irreversible caspase inhibitors: tools for studying apoptosis, *Methods*. *17*: 320-8, 1999.
22. Yamamoto, K., Ichijo, H., and Korsmeyer, S. J. BCL-2 is phosphorylated and inactivated by an ASK1/Jun N-terminal protein kinase pathway normally activated at G(2)/M, *Molecular and Cellular Biology*. *19*: 8469-78, 1999.
23. Kastan, M. On the TRAIL from p53 to apoptosis? [news], *Nature Genetics*. *17*: 130-1, 1997.
24. Müller, M., Strand, S., Hug, H., Heinemann, E. M., Walczak, H., Hofmann, W. J., Stremmel, W., Krammer, P. H., and Galle, P. R. Drug-induced apoptosis in hepatoma cells is mediated by the CD95 (APO-1/Fas) receptor/ligand system and involves activation of wild-type p53, *Journal of Clinical Investigation*. *99*: 403-13, 1997.
25. Burger, J. A., Burger, M., and Kipps, T. J. Chronic lymphocytic leukemia B cells express functional CXCR4 chemokine receptors that mediate spontaneous migration beneath bone marrow stromal cells, *Blood*. *94*: 3658-67, 1999.
26. Trentin, L., Agostini, C., Facco, M., Piazza, F., Perin, A., Siviero, M., Gurrieri, C., Galvan, S., Adami, F., Zambello, R., and Semenzato, G. The chemokine receptor CXCR3 is expressed on malignant B cells and mediates chemotaxis, *Journal of Clinical Investigation*. *104*: 115-21, 1999.
27. Puthalakath, H., Huang, D. C., O'Reilly, L. A., King, S. M., and Strasser, A. The proapoptotic activity of the Bcl-2 family member Bim is regulated by interaction with the dynein motor complex, *Molecular Cell*. *3*: 287-96, 1999.
28. Chao, D. T. and Korsmeyer, S. J. BCL-2 family: regulators of cell death, *Annual Review of Immunology*. *16*: 395-419, 1998.
29. Thomas, A., El Roubi, S., Reed, J. C., Krajewski, S., Silber, R., Potmesil, M., and Newcomb, E. W. Drug-induced apoptosis in B-cell chronic lymphocytic leukemia: relationship between p53 gene mutation and bcl-2/bax proteins in drug resistance, *Oncogene*. *12*: 1055-62, 1996.
30. Jürgensmeier, J. M., Xie, Z., Deveraux, Q., Ellerby, L., Bredesen, D., and Reed, J. C. Bax directly induces release of cytochrome c from isolated mitochondria, *Proceedings of the National Academy of Sciences of the United States of America*. *95*: 4997-5002, 1998.
31. Haldar, S., Basu, A., and Croce, C. M. Bcl2 is the guardian of microtubule integrity, *Cancer Research*. *57*: 229-33, 1997.
32. Wang, L. G., Liu, X. M., Kreis, W., and Budman, D. R. The effect of antimicrotubule agents on signal transduction pathways of apoptosis: a review, *Cancer Chemotherapy and Pharmacology*. *44*: 355-61, 1999.
33. Zha, J., Harada, H., Yang, E., Jockel, J., and Korsmeyer, S. J. Serine phosphorylation of death agonist BAD in response to survival factor results in binding to 14-3-3 not BCL-X(L) [see comments], *Cell*. *87*: 619-28, 1996.
34. Downward, J. How BAD phosphorylation is good for survival [news], *Nature Cell Biology*. *1*: E33-5, 1999.
35. Srivastava, R. K., Mi, Q. S., Hardwick, J. M., and Longo, D. L. Deletion of the loop region of Bcl-2 completely blocks paclitaxel-induced apoptosis, *Proceedings of the National Academy of Sciences of the United States of America*. *96*: 3775-80, 1999.
36. Friedenberg, W. R., Spencer, S. K., Musser, C., Hogan, T. F., Rodvold, K. A., Rushing, D. A., Mazza, J. J., Tewksbury, D. A., and Marx, J. J. Multi-drug resistance in chronic lymphocytic leukemia, *Leukemia and Lymphoma*. *34*: 171-8, 1999.



## Establishment and Characterization of a New Indanocine-Resistant Cell Line CEM-178

Davide Genini<sup>1</sup>, Xuequn H. Hua<sup>1</sup>, Rommel I. Tawato<sup>1</sup>, Maria Dell'Aquila<sup>2</sup>, Dennis A. Carson<sup>1</sup>, Lorenzo M. Leoni<sup>1</sup>

<sup>1</sup>Department of Medicine and The Sam and Rose Stein Institute for Research on Aging, University of California at San Diego, <sup>2</sup>Department of Biology, Center for Molecular Genetics, University of California, San Diego, 9500 Gilman Drive, La Jolla, CA 92093, USA.

Correspondence should be addressed to L.M.L.:

Leoni M. Lorenzo, Dept. Medicine, UCSD-0663, Stein Clinical Res. 126D, 9500 Gilman Drive, LA JOLLA, CA-92093, USA. Tel: 858-534-5442, Fax: 858-534-5399, e-mail: [lleoni@ucsd.edu](mailto:lleoni@ucsd.edu)

### ABSTRACT

Indanocine is a very potent tubulin-binding drug that is active against multidrug resistant cancer cells. In order to gain informations on its mechanism of action, an indanocine-resistant cell line (CEM-178) was derived from the human T lymphoblastoid CCRF-CEM cell line by exposing the cells to gradually increasing concentrations of indanocine. The stable indanocine-resistant clone was found to be cross-resistant to vinblastine and colchicine, but not to paclitaxel or staurosporin. In the CEM-178 cells, indanocine failed to intracellularly depolymerize paclitaxel-polymerized tubulin. Immunofluorescence analysis demonstrated the CEM-178 altered tubulin subcellular localization. Fusion experiments with an ouabain-resistant, hypoxanthine phosphoribosyltransferase (HPRT)-deficient indanocine-sensitive CEM cell line suggested that the indanocine resistance could be due to a homozygous codominant mutation. These results indicate that tubulin binding is the main mechanism of action of indanocine and also suggest that cytoskeletal alterations induced by indanocine are probably responsible for its anti-cancer activity.

### INTRODUCTION

Treatment of human malignancies with antitumoral agents often results in acquired resistance, which represent a great limitation to curative chemotherapy.

Multidrug resistance (MDR) is cell resistance to numerous substances characterized by different mechanisms of action. Decreased accumulation in the cells is the first step in MDR. Decrease drug influx can result from mutation in the structure

of the membrane lipid bilayer (1). Drug efflux is considered to be the main mechanism of decreased accumulation, which is mediated by the activity of transporter proteins, such as P-glycoprotein, transporter of the Multidrug Resistance-associated Protein (MRP) family, functioning as an ATP-dependent pump of abroad substrate specificity.

MDR can also result from detoxification of the drug in the cell. Modification of the compound by conjugation with glutathion for example, can weaken its cytotoxicity. MDR can be mediated by alteration of the drug targets or by enhancement of the target repair. Sometimes alteration of

genes that mediate apoptosis increase the resistance of the cell to the drug (2).

Indanocine is a microtubule-depolymerizing agent with antiproliferative activity. Indanocine displayed toxicity toward multidrug-resistant breast cancer cells. It interacts with tubuline at the colchicine-binding site. Indanocine is also thought to interact with non-tubulin cellular components to produce a cytotoxic response (3).

We established an indanocine-resistant cell line derived from human T lymphoblastoid CEM [CRL-119], by culturing the cells under permanent treatment with indanocine for months. The cells present cross-reactivity to other microtubule-depolymerizing agents.

### MATERIALS and METHODS

#### Drugs and Chemicals

Indanocine, NSC 698666, is a microtubule-binding indanone with antiproliferative activity (3). Paclitaxel, vinblastine sulfate, colchicine, staurosporine and mitomycin were from Calbiochem (San Diego, CA). Ethyl metanesulfonate (EMS) was from Sigma (St. Louis, MO). Cladribine (2CdA) was synthesized by published procedure (4).

#### Cells and Selection of Cell mutant

Human T lymphoblastoid CCRF CEM cell line [CRL-119] from the American Type Culture Collection (Manassas, VA), propagated according to the instructions of the supplier, were provided from Dr. William T. Beck (Cancer Center, University of Illinois at Chicago).

$5 \times 10^6$  CEM cells were cultured for 18 hours in presence 1 mg/ml of alkylating agent EMS. After removal of EMS by washing with medium, the cells were cultured for two days in normal RPMI medium supplemented with 10% FBS. The cells were then cultured under continuous selection in presence of Indanocine at 10  $\mu$ M. The concentration of indanocine was raised in a way that 10% of the cells were still viable. After more than a year of continuous selection of increased concentration of indanocine, the cells were able to grow in 300 nM indanocine. Cells were then cultured in drug-free medium.

#### Toxicity test

We incubated the cells for 72 hours in 96-well plates with the test compounds and then measured cell proliferation by reduction of the yellow dye MTT [3-(4,5-dimethylthiazol-2-yl)-

2,5-diphenyl tetrazolium bromide] to a blue formazan product. The cleavage is performed by the "succinate-tetrazolium reductase" system, which belongs to the respiratory chain of the mitochondria and is active only in viable cells. Therefore, the amount of formazan dye formed is a direct indication of the number of metabolically active cells in the culture. The optical density of the blue formazan product was measured at 570 nm with a ThermoMax (Molecular Devices, Sunnyvale CA) and analyzed with Vmax program.

#### Pretreatment of Cells in Preparation for Mitotic Analysis

Eleven hours after infection, 5 µg/ml ethidium bromide was added to the cells for 20 min to prevent overcondensation of chromosomes. Fresh media containing 0.1 µg/ml demecolcine was added for an additional 20 min to block microtubule polymerization, and then cells were trypsinized and collected for mitotic analysis. Cells were swollen in a hypotonic buffer containing 75 mM KCl and 10 mM EDTA (to prevent nuclease activity) for 20 min at room temperature. They were then pelleted, fixed using a series of incubations in 3:1 MeOH/acetic acid, and metaphase spreads were prepared and G-banded by standard cytogenetic methods. One hundred metaphase cells per sample were analyzed, unless otherwise noted.

#### Caspase Assay

2 × 10<sup>6</sup> cells per point were treated with increasing concentration of indanocine for 16 hours and staurosporine for 4 hours. The cells were washed twice with PBS, the pellet was resuspended in 120 µl caspase buffer (50 mM Hepes, pH 7.4, 100 mM NaCl, 1 mM EDTA, 0.1% Chaps, and 5 mM dithiothreitol) for 10 min at 4 °C. The caspase enzymatic assays were carried out in 96 well plates. Lysates (10-20 µg of total protein) were mixed with 50 µl of HEB buffer (PIPES 50 mM, KCl 20 mM, EGTA 5 mM, MgCl<sub>2</sub> 2 mM, and DTT 1 mM, pH 7), and reactions were initiated by addition of 100 µM of the specific substrate. After 1 hour incubation at 37°C, caspase-3-like protease activity was measured with the substrate Ac-DEVD-AMC and caspase-9-like activity was measured using Ac-LEHD-AFC. Activity was measured by the release of 7-amino-4-trifluoromethyl-coumarin (AFC) or 7-amino-4-methyl-coumarin (AMC), monitoring fluorescence at excitation and emission wavelengths of 400 and 505 nm, and 380 and 460 nm respectively. The results were normalized according to the protein concentration measured using a modified Coomassie blue assay (Pierce, Rockford, IL).

#### Tubulin Polymerization-Depolymerization Experiment

Indanocine-induced tubulin depolymerization was measured by immunoblotting. 2×10<sup>5</sup> CEM wt and CEM-178 were treated for 4 hours with 5 µM of paclitaxel to allow tubulin polymerization and then depolymerized by treating the cells with 10 µM indanocine for 1 hours. Cytosolic fraction was harvested by digitonin-extraction in 50 µl digitonin buffer (50 mM Hepes, pH 7.4, 100 mM NaCl, 1 mM EDTA, 5 mM dithiothreitol, 1 mM sodium orthovanadate, 10 µM β-Glycerophosphate 1 mM sodium fluoride and protease inhibitor cocktail tablets (Boehringer Mannheim, Germany), and 0.1% digitonin). Membrane-fraction was lysed in 50 µM lysing buffer (25 mM Tris, pH 7.4, 150 mM KCl, 5 mM EDTA, 1% Nonidet P-40, 0.5% sodium deoxycholate, 0.1% SDS, 1 µg/ml aprotinin, 1 µg/ml leupeptin, 1 mM phenylmethanesulfonyl fluoride, 1 mM sodium orthovanadate, 1 mM sodium fluoride).

Lysates were normalized for total protein content using a modified Coomassie blue assay (Pierce, Rockford, IL). Proteins (25 µg per lane) were resolved at 125 V on pre-cast 4-20 and 14% Tris-glycine polyacrylamide gels (Novex, San Diego, CA) and transferred to 0.2 µm polyvinylidene fluoride (PVDF) membranes (Millipore, Bedford, MA) for 2 hrs at 125 V. Membranes were blocked overnight in I-Block blocking buffer (Tropix, Bedford, MA). Blots were then probed for 1 hr or overnight with specific antibodies to α-tubulin (Santa Cruz, CA). The blots were developed with species-specific antisera and visualized by peroxidase-based enhanced chemiluminescence (ECL, Amersham), according to the manufacturer's instructions.

#### Immunofluorescence

2×10<sup>4</sup> cells from the tubulin experiment were pelleted at 300 g for 5 min on a slide. The cells were fixed for 15 min in 0.7% glutaraldehyde and then in 0.5% of SDS, washed in PBS and then incubated for 1 hours with the monoclonal antibodies specific for tubulin α (sc-8035, Santa Cruz Biotech, Santa Cruz, CA) at a concentration of 2 µg/ml in I-Block blocking buffer (Tropix, Bedford, MA). FITC-labeled phalloidin (Molecular Probes, Eugene, OR) was used to stain actin filaments. Alexa 568 (red) served as species-specific secondary antibodies. The nuclear DNA was stained using DAPI. Coverslips were washed successively in PBS and deionized H<sub>2</sub>O for 5 min and mounted in Fluoromount (Fisher, CA). Images were obtained with a Zeiss Axio microscope.

#### Fusion Experiments

A CEM mutant ouabain-resistant and hypoxanthine phosphoribosyltransferase (HPRT)-negative cell line was selected as previously described (5). 40 × 10<sup>6</sup> of the ouabain-resistant CEM mutants and of the resistant clones CEM-178 were mixed in a ratio 1:1 in serum-free RPMI media. Cells were pelleted and incubated 2 minutes at 37°C. First, 1 ml 50 % Polyethylene Glycol 1500 (PEG 1500, Boehringer Mannheim, Germany) and then 1 ml serum-free RPMI were drop-wise added to the cells at 37°C over 1 minute. 7 additional ml of serum-free RPMI were slowly added to the cells. Cells were then centrifuged and resuspended at a concentration of 2.5 × 10<sup>6</sup> cells/ml in RPMI supplemented with

TREATMENT S	GI <sub>50</sub> Wild Type CEM (nM)	GI <sub>50</sub> Resistant CEM (nM)	Fold Increase
Indanocine	3.0 ± 0.2	350 ± 20	116 ×
Colchicine	2.0 ± 0.1	62.5 ± 4	31 ×
Paclitaxel	0.5 ± 0.04	0.5 ± 0.03	1 ×
Vinblastine	0.1 ± 0.01	4.0 ± 0.3	40 ×
Staurosporine	10 ± 0.8	10 ± 1	1 ×
Mitomycine	100 ± 9	100 ± 7	1 ×
2CdA	50 ± 0.3	50 ± 0.5	1 ×

**Table 1 Anti-cancer drugs cross-resistance.**

CEM wild type and resistant CEM 178 were treated with the indicated drugs for 27 hours. Cell proliferation was assessed by the MTT [i.e., 3-(4,5-dimethylthiazol-2-yl)-2,5-diphenyl tetrazolium bromide] assay. The table represent the IC<sub>50</sub> values for the indicated drugs and the fold increase for the resistant clone compared to wild type CEM. The results represent the 50% growth-inhibitory concentrations (GI<sub>50</sub>) (mean ± standard deviation).

10 % FBS. 50  $\mu$ l of cells were plated in a 96-well plate and the next day 50  $\mu$ l of HAT media (Sigma), for HPRT-selection, containing 1 $\mu$ M ouabain (Calbiochem) was added to the cells for double selection. When cells started to grow the medium was changed with HT medium (Sigma) containing 1 $\mu$ M Ouabain for one week. Then cells were cultured in normal RPMI containing 10% FBS.

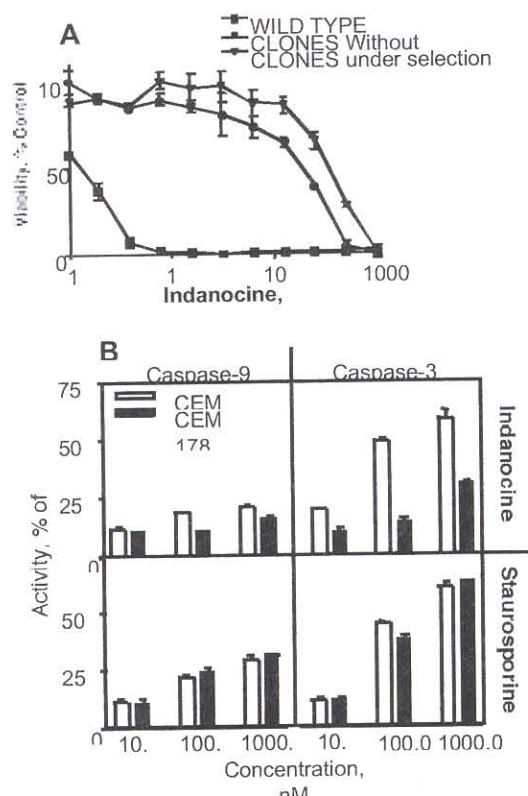


**Figure 1 Toxicity of indanocine.** (A) CEM wild type (■), indanocine-resistant CEM-178 out of selection (●) and CEM-178 under selection of indanocine (▼) were treated with increasing concentration of indanocine for 3 days. Cytotoxic MTT assay was used to quantitate viable cells. Data represent the percentage of the control cells without treatment. (B) CEM wt and CEM-178 were probed for caspase activity after treatment with increasing concentration of indanocine for 4 hours and staurosporine for 16 hours. Cells were lysed in caspase buffer and caspase activity of 10-20  $\mu$ g of total protein was measured with specific substrates for caspase-9 (● for wild type and ○ for CEM-178), and 9 (■ for wild type and □ for CEM-178) after 1 hour incubation at 37 °C. The cleavage of the fluorimetric AMC/AFC was monitored fluorimetrically at 400/380 nm excitation and 505/460 nm emission. Activity is represented in relative units to the control without treatment.

## RESULTS

### Establishment of the resistant cell-line.

To establish a resistant cell line to indanocine, we started from several cell lines. MCF-7, MDA, Jurkat, and HL-60 were treated with the alkylating agent EMS and then kept under

selection with indanocine, but no one of these cell lines developed a resistant phenotype. Only the T lymphoblastoid cell line CEM was able to develop resistance in a stepwise selection over a period of time of one year. The cells retained resistance also after removing indanocine from the medium for a long period of time. The stable Indanocine-resistant cell line called CEM-178 possessed the same amount of DNA compared to the wild type. Morphological analysis did not show any difference. Only the doubling time was slightly reduced in the resistant clones. Doubling time for wild type was 18 hours compared to resistant clone with 24 hours. Karyotype analysis revealed several deletions in both cell lines, but no major difference between the wild type and the resistant CEM-178.

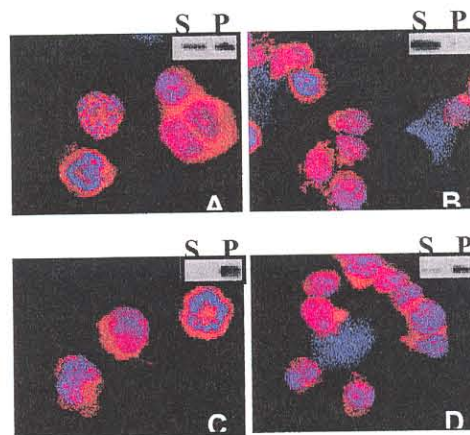


**Figure 2 Tubulin depolymerization assays.**

CEM wild type and CEM-178 were treated with 5  $\mu$ M paclitaxel for 4 hour to induce tubulin polymerization. Tubulin-depolymerization was induced by 1 hour treatment with 10  $\mu$ M indanocine. Cells were cytopinned and stained for  $\alpha$ -tubulin with a monoclonal antibody and with Alexa 488 conjugated secondary antibody (Red). DNA was visualized with DAPI (Blue). Paclitaxel-treated wild type CEM (A) and CEM-178 (C) and indanocine-induced depolymerization of wild type CEM (B) and CEM-178 (D) were also lysed for immunoblot-detection of tubulin in dissolved form present in cytosolic fraction (S) and polymerized form (P).

### Multidrug-resistance Phenotype.

The drug resistance phenotype of CEM-178 is shown in Table 1 and Figure 1. IC<sub>50</sub> of wild type, CEM-178 under selection and CEM-178 out of selection were determined for several drugs. Resistance was similar for the clones under and out of selection (Figure 1A). The level of resistance for indanocine was increased of 116-fold. Cross-resistance was also observed for colchicine (31-fold) and Vinblastine (40-fold), whereas no cross-resistance was observed for the microtubule-polymerizing agent paclitaxel and for the drugs staurosporine, mitomycin and 2CdA (Table 1). Caspase activation was measured in cells treated with increasing concentration of indanocine and staurosporine. No difference was observed when the cells were treated with staurosporine, but caspase activity was different in cells treated with indanocine (Figure 1B).

Analysis of expression of MDR proteins showed that the amount expressed by CEM-178 is comparable to CEM wild type (data not shown).

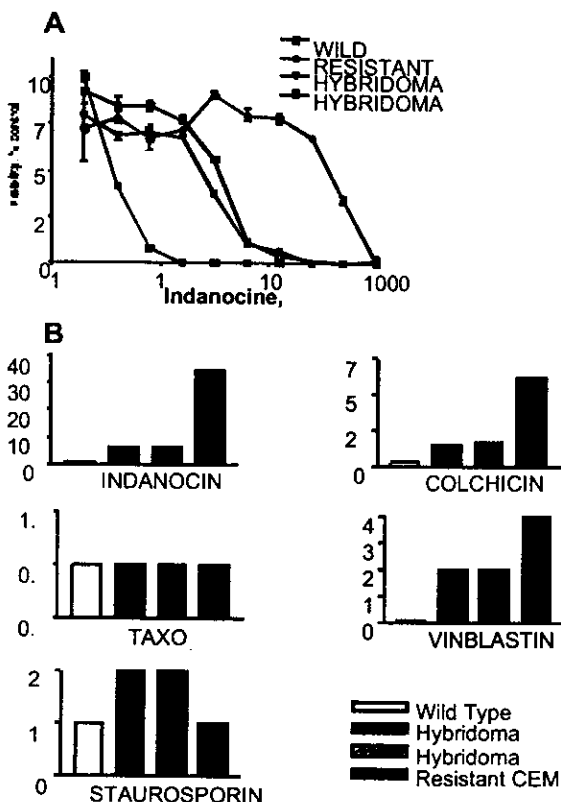


**Figure 3** Indanocine-toxicity in hybridoma cell line and cross-resistance.

(A) Wild type CEM (■), resistant CEM-178 (●) and 2 different hybridomas (▼,□) resulting from the fusion of wild type and resistant CEM were probed for indanocine toxicity. (B) Cross-resistance for colchicine, paclitaxol, vinblastine, and staurosporine was tested.

#### Tubulin-depolymerization assay.

Tubulin in CEM cells is mostly depolymerized (data not shown). To detect the effect of depolymerization by indanocine, we first induced polymerization of the microtubule by treating the cells with paclitaxel at a concentration of 5 μM for 4 hours. Tubulin was then depolymerized by treatment with 10 μM indanocine for 1 hour. Immunoblot analysis of cytosolic dissolved tubulin and polymerized tubulin pelleted with the membranes showed complete depolymerization of tubulin for CEM wild type (Figure 2B), whereas 10 μM of indanocine were not able to induce depolymerization of tubulin and the band was only present in the membrane extract (Figure 2D). Immunohistochemistry analysis also showed the same trend. Wild type and CEM-178 display similar structure of tubulin after treatment with paclitaxel (Figure 2, Panel A (wt) and C (178)). Depolymerization by indanocine induces a morphological change only in the wild type CEM cells (Panel B), where tubulin dissolves, whereas in the CEM-178 no alteration is observed (Panel D).

#### Establishment of Hybridomas.

Hybridomas were produced to determine if the indanocine-resistance and the cross-resistance were dominant or recessive phenotype. Toxicity of indanocine was tested for wild type CEM, CEM-178 and two hybridomas (Figure 4A). Hybridomas were more resistant than wild type of about 30-fold, but less resistant than CEM-178. Resistance-phenotype appears to be a codominant homozygous mutation. Cross-resistance was also maintained in the hybridomas (Figure 4B), where both vinblastine and colchicine IC<sub>50</sub> was higher than in the wild type CEM. Paclitaxel sensitivity did not change, whereas staurosporine-sensitivity was increased in the hybridomas compared to both wild type and CEM-178.

#### DISCUSSION

Development of resistance to anti-cancer drugs is one of the major problems for a successful chemotherapy (6, 7). The newly synthesized microtubule-disrupting agent indanocine appeared to open new doors in the treatment of multidrug-resistant tumors (3). We previously demonstrated that indanocine has higher toxicity for MDR cell lines compared to the wild types. During the early selection of an indanocine-resistant cell line, most of the cell lines were so sensitive to the drug that no resistant clone survived (3).

The T lymphoblastoid cell line CEM was the only one that successfully allowed the generation of resistant clones. The resulting CEM-178 cells did not display any major difference in volume, doubling time, or karyotype compared to the wild type. Susceptibility to apoptosis induced by some anti-cancer drugs was also similar between the CEM wild type and CEM-178, suggesting intact apoptotic machinery. We also established that CEM-178 cells did not express higher amount of the MDR-1 proteins (P-glycoprotein). We can't exclude that the mechanism of resistance to indanocine of the CEM-178 may be due to reduced intracellular accumulation, but all the data we accumulated point toward a difference at the tubulin-binding level. In fact, results of the tubulin subcellular localization experiments and the immunofluorescence images suggest that indanocine-induced depolymerization of tubulin may be reduced in the resistant clone. The cross-resistance results also suggest that tubulin plays a central role in resistance, since vinblastine (8) and colchicine (9), both microtubule-depolymerizing agents had reduced toxicity on CEM-178 compared to wild type. Paclitaxel, which binds tubulin to a different binding site and promotes tubulin polymerization (8), instead of depolymerization, did not display cross-resistance. The lack of paclitaxel cross-resistance suggests that the eventual tubulin mutation(s) will be limited to the vinca or colchicine binding-site. Preliminary data of depolymerization of tubulin in a cell-free system from lysates of CEM wild type and CEM-178 showed depolymerization of paclitaxel-induced polymerized tubulin only in the CEM wild type, implying a mutation in the tubulin structure. Further experiments will be carried-out to define the molecular differences between the CEM wild type and the resistant clone CEM-178. This cell line will be used for further investigation in the mechanism of action of indanocine.

The results obtained with generation of the hybridomas from the fusion of the CEM-178 and the indanocine-sensitive ouabain-resistant, HPRT-sensitive CEM suggest that the

resistance is not due to an episomal amplification of a detoxifying gene. It seems more likely that the resistance is due to homozygous mutation, in fact, all the hybridomas obtained showed an intermediate sensitivity to indanocine.

#### REFERENCES

1. Simon, S. M., and M. Schindler. Cell biological mechanisms of multidrug resistance in tumors. *Proc Natl Acad Sci U S A* 91(9):3497-504 (1994).
2. Stavrovskaya, A. A. Cellular mechanisms of multidrug resistance of tumor cells. *Biochemistry* 65(1):95-106 (2000).
3. Leoni, L. M., E. Hamel, D. Genini, H. Shih, C. J. Carrera, H. B. Cottam, and D. A. Carson. Indanocine, a microtubule-binding indanone and a selective inducer of apoptosis in multidrug-resistant cancer cells [see comments]. *Journal of the National Cancer Institute* 92(3):217-24 (2000).
4. Kazimierczuk, Z., H. B. Cottam, G. R. Revankar, and R. K. Robins. Synthesis of 2'-Deoxytubercidin, 2'-Deoxyadenosine, and Related 2'-Deoxynucleosides via a Novel Direct Stereospecific Sodium Salt Glycosylation Procedure. *Journal of the American Chemical Society* 106(21):6379-6382 (1984).
5. Lakow, E., C. D. Tsoukas, J. H. Vaughan, A. Altman, and D. A. Carson. Human T cell hybridomas specific for Epstein Barr virus-infected B lymphocytes. *J Immunol* 130(1):169-72 (1983).
6. Gottesman, M. M. How cancer cells evade chemotherapy: sixteenth Richard and Hinda Rosenthal Foundation Award Lecture. *Cancer Res* 53(4):747-54 (1993).
7. Ling, V. Charles F. Kettering Prize. P-glycoprotein and resistance to anticancer drugs. *Cancer* 69(10):2603-9 (1992).
8. Kumar, N. Taxol-induced polymerization of purified tubulin. Mechanism of action. *J Biol Chem* 256(20):10435-41 (1981).
9. Patzelt, C., A. Singh, Y. L. Marchand, L. Orci, and B. Jeanrenaud. Colchicine-binding protein of the liver. Its characterization and relation to microtubules. *J Cell Biol* 66(3):609-20 (1975).





## Mechanisms of Lymphocyte Depletion after Treatment of B-Chronic Lymphocytic Leukemia with Etodolac, a Nonsteroidal Anti-inflammatory Agent

Souichi Adachi<sup>1</sup>, John Welch<sup>1</sup>, Shinichi Kitada<sup>2</sup>, Ngan K. Pham-Mitchell<sup>1</sup>, Rommel I. Tawatao<sup>1</sup>, Davide Genini<sup>1</sup>, Howard B. Cottam<sup>1</sup>, Carlos J. Carrera<sup>1</sup>, Roberta A. Gottlieb<sup>3</sup>, John C. Reed<sup>2</sup>, Christopher K. Glass<sup>1</sup>, Diane G. Amox<sup>1</sup>, Dennis A. Carson<sup>1</sup> and Lorenzo M. Leoni<sup>1</sup>

<sup>1</sup>Department of Medicine and The Sam and Rose Stein Institute for Research on Aging, University of California at San Diego, <sup>2</sup>The Burnham Institute, Cancer Research Center and <sup>3</sup>Department of Molecular and Experimental Medicine, The Scripps Research Institute.

Correspondence should be addressed to L.M.L.; Leoni M. Lorenzo, Dept. Medicine, UCSD-0663, Stein Clinical Res. 126D, 9500 Gilman Drive, LA JOLLA, CA-92093, USA. Tel: 858-534-5442, Fax: 858-534-5399, email: [leoni@ucsd.edu](mailto:leoni@ucsd.edu)

This work was supported in part by grants GM23200, CA81534, AR07567, RR00833 and RR00827 from the National Institutes of Health, and grant number DAMD17-99-1-9100 from the U.S. Army Medical Research and Material Command.

Key words: Apoptosis, chemotherapy, peroxisome proliferator-activated receptor, mitochondria, chemotaxis.

### ABSTRACT

**Nonsteroidal anti-inflammatory drugs (NSAIDs) recently have attracted attention as chemopreventive and chemotherapeutic agents for malignant diseases. However, their mechanisms of action, and spectrum of activity, are poorly understood. We show here that etodolac, a chiral NSAID that is taken as a racemic mixture, increased apoptosis in B-chronic lymphocytic leukemia cells (B-CLL), at concentrations that did not kill normal B or T-lymphocytes. Incubation of B-CLL cells with etodolac caused rapid down-regulation of the anti-apoptotic protein Mcl-1, reduced the mitochondrial transmembrane potential, and inhibited mitochondrial respiration. These effects preceded the appearance of an apoptotic phenotype. Both the etodolac enantiomers also activated the peroxisome proliferator-activated receptor- $\alpha$ , which was expressed in B-CLL cells at approximately 10-fold higher levels than in normal lymphocytes. CXCR3-dependent chemotaxis of B-CLL cells was also activated by etodolac. Challenge of B-CLL patients with low dose etodolac (800 mg/day) reduced the subsequent *ex vivo* survival of the leukemic cells. The same doses of etodolac given for 30 days caused a significant fall in circulating leukemic cells in 5 of 6 patients treated. These results demonstrate that etodolac has diverse metabolic effects on B-CLL cells that could contribute to their elimination or redistribution *in vivo*. The R-enantiomer of etodolac may represent a useful adjunctive agent for the control of B-CLL progression.**

### INTRODUCTION

Recently, interest has arisen in the anti-cancer activity of certain nonsteroidal anti-inflammatory agents (NSAIDs).

NSAIDs induce apoptosis in several cell types, including myelocytic and lymphocytic leukemia cells, embryonic fibroblasts, and colonic epithelial cells, at concentrations that are nontoxic to many adult tissues (1-4). The mechanism of death is apoptosis, since broad-spectrum caspase inhibitors block cell killing by NSAIDs, but the molecular details of NSAID-induced apoptosis are not understood.

The *in vitro* toxicity of NSAIDs does not correlate with their ability to inhibit cyclooxygenase 1 and 2 (COX-1,2) (5). These planar hydrophobic compounds are known to insert into membranes and to interfere with multiple signaling pathways. NSAIDs can uncouple oxidative phosphorylation, and cause the release of adenosine into the extracellular space (6). Sodium salicylate causes swelling and impairs respiration in isolated mitochondria (7, 8). Various NSAIDs at high concentrations (100  $\mu$ M and above) can bind and activate the nuclear hormone receptor, peroxisome proliferator activated receptor- $\alpha$  (PPAR- $\alpha$ ) (9). In cells with high levels of PPAR- $\alpha$ , maximal activation of the receptor can induce apoptosis (10).

Etodolac is a chiral NSAID developed in the 1970s, and is available in several countries for the treatment of arthritis and the alleviation of pain (11). Etodolac is sold as a racemic mixture, but only the S-enantiomer has been reported to have potent COX inhibitory activity (12). The pharmacology of etodolac differs from that of other NSAIDs in two aspects. First, the two enantiomers are not readily interconvertible, second, "inactive" R-enantiomer is metabolized much more slowly than the S-enantiomer (11), and consequently accumulates to 10-fold higher concentrations than the S-enantiomer in plasma (11).

Recently, Nardella and colleagues described a patient with B-CLL, who fortuitously responded to etodolac therapy with a drop in circulating lymphocytes (13). Treatment of the patient with seven other NSAIDs did not induce lymphopenia. In this study, therefore, we have investigated the *in vitro* and *in vivo* activity of etodolac in B-CLL, and its mechanism of action. The results demonstrate that both etodolac enantiomers can reduce survival and stimulate chemotaxis of B-CLL cells *in vitro*, and that even low dose etodolac can deplete circulating B-CLL cells in B-CLL patients.

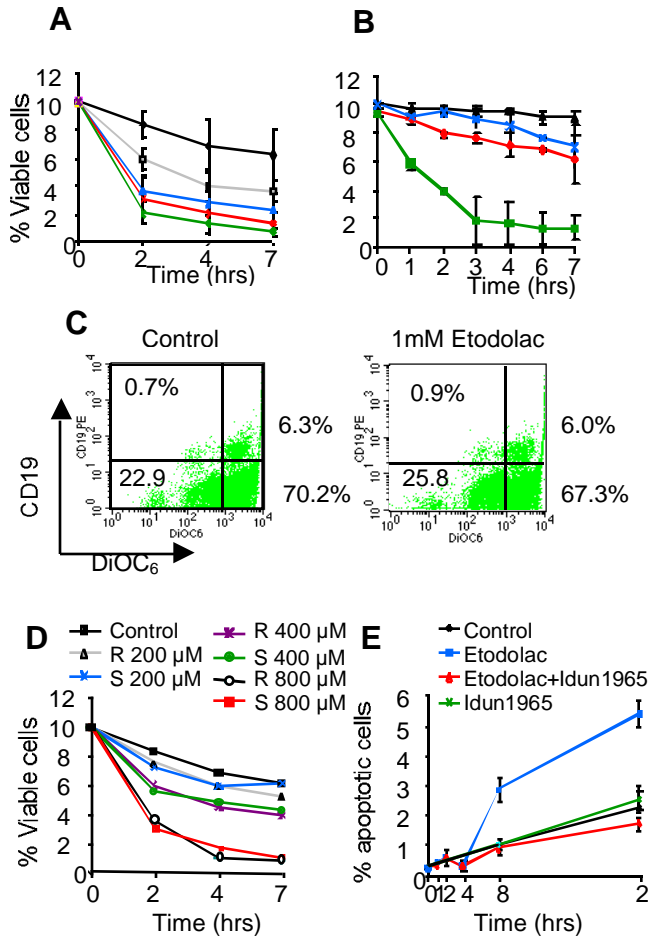


Figure 1. Cytotoxic effect of etodolac on B-CLL cells and normal lymphocytes.

(1A) Dose-response and time-course of the cytotoxic effect of racemic etodolac on B-CLL cells. Cells were incubated for the indicated times with various concentrations of racemic etodolac. The results show the mean % viability  $\pm$  SD (n = 4). (1B) Comparison of the time-course of the cytotoxic effect of racemic etodolac on B-CLL cells and normal lymphocytes. Cells from 4 patients (B-CLL) or 4 normal donors (normal lymphocytes) were incubated for the indicated times with or without 500  $\mu$ M racemic etodolac (mean $\pm$ SE). (1C) Etodolac does not induce apoptosis in normal B CD19+ lymphocytes. Lymphocytes from normal donors were cultured *in vitro* 24 hours with or without 1000  $\mu$ M racemic etodolac, which killed >80% of B-CLL. The x-axis shows DiOC6 (FL-1) fluorescence and the y-axis shows CD19-PE (FL-2) fluorescence. Cells in the upper-left quadrant are apoptotic B lymphocytes (CD19-positive low  $\Delta\Psi$ m). Cells in the lower left quadrant are apoptotic non-B cells (CD19-negative low  $\Delta\Psi$ m). The upper right quadrant (CD19-positive high  $\Delta\Psi$ m cells) shows viable B cells, and the lower-right quadrant (CD19-negative high  $\Delta\Psi$ m) shows viable non-B cells. (1D) Dose-response and time-course of the cytotoxic effect of purified R-etodolac and S-etodolac on B-CLL cells. Cells from 4 patients were incubated for the indicated times with various concentrations of R- and S-etodolac. (1E) Inhibition of etodolac-induced apoptosis in B-CLL by the pan-specific caspase inhibitor IDUN-1965 (16).

**RESULTS**

**Etodolac is more toxic to B-CLL than to normal B and T lymphocytes.**

Compared to normal peripheral blood lymphocytes (PBL), B-CLL have reduced spontaneous survival *in vitro* (Figure 1 and (14)). As little as 200  $\mu$ M etodolac accelerated the rate of B-CLL cell death (Figure 1A). Among 15 patients samples

tested, 12 were found to be sensitive ( $IC_{50}$ <500  $\mu$ M at 72 hours) and 3 were resistant ( $IC_{50}$ >1 mM). In contrast, all the tested normal PBL samples (n=4) were etodolac resistant ( $IC_{50}$ >1 mM, Figure 1B). The etodolac sensitivity of normal B lymphocytes was assessed by double-labeling with fluorescent antibody to a B cell marker (CD19) and a mitochondria-specific dye (DiOC<sub>6</sub>), which measures mitochondrial transmembrane potential ( $\Delta\Psi$ m) (15). Culture of normal PBL with 1 mM etodolac for 24 hours did not affect the  $\Delta\Psi$ m of CD19-positive cells (Figure 1C), whereas an equivalent exposure of B-CLL to the drug induced a dramatic reduction of the  $\Delta\Psi$ m followed by cell death (Figure 2A). Blockade of caspase activity with a pan-specific peptidic inhibitor of these proteases (1-Me,3-Me-indole-2)CO-V-D-fmk, (Idun-1965, IDUN Pharmaceuticals, La Jolla) (16) protected B-CLL cells from etodolac toxicity, consistent with an apoptotic mechanism of cell death. An apoptotic demise of etodolac-treated cells was also supported proteolytic processing of caspase-9, caspase-3, and poly(ADP-ribose) polymerase (detected by immunoblotting), and by flow-cytometric detection of hypodiploid DNA (data not shown). Purified R-etodolac and S-etodolac enantiomers were equivalently toxic to the B-CLL cells (Figure 1D).

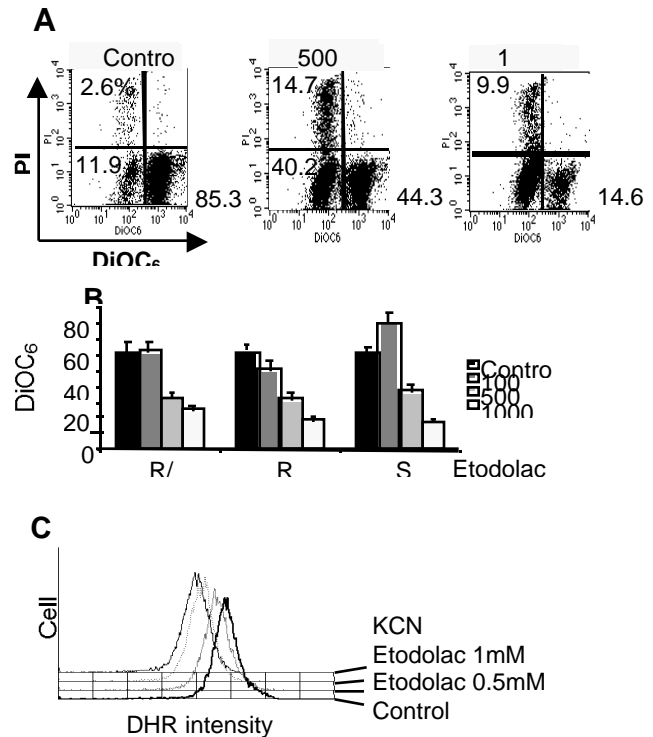


Figure 2. Flow cytometric analysis of B-CLL cells after *in vitro* culture of racemic etodolac.

(2A) Effect of racemic etodolac on mitochondrial membrane potential and apoptosis. B-CLL cells were incubated for 12 hours with the indicated concentrations of etodolac. Cell membrane permeability and  $\Delta\Psi$ m were assayed by incubating the unfixed cells for 10 min at 37°C in presence of 5  $\mu$ g/ml propidium iodide (PI) and 40 nM DiOC<sub>6</sub>. The x-axis is DiOC<sub>6</sub> (FL-1) fluorescence, and the y-axis is PI (FL-3) fluorescence. Numbers refer to the percentage of cells in the upper-left quadrant (dead cells), lower-right quadrant (low  $\Delta\Psi$ m cells, apoptotic cells), and the lower-right quadrant (normal cells). (2B) Effect of the purified R- and S-enantiomers of etodolac on mitochondrial membrane potential. (2C) Effect of racemic etodolac on the oxidation of dihydrorhodamine (DHR). B-CLL cells were incubated for 3 hours with indicated concentrations of etodolac. Oxidation of DHR was assessed by fluorescence intensity at 525 nm. DHR fluorescence in the presence of KCN (10  $\mu$ M) indicated non-mitochondrial respiration (background).

### Etodolac reduces mitochondrial transmembrane potential in whole cells and isolated mitochondria, and inhibits mitochondrial respiration.

A reduction in mitochondrial transmembrane potential ( $\Delta\psi$ ) is an early event in apoptosis induced by internal stimuli and has been shown to correlate with loss of viability and onset of apoptosis in B-CLL cells treated with nucleoside analogs (15). Even short-term treatment (12 hours) of B-CLL cells with etodolac reduced the  $\Delta\psi$ , as measured by DiOC<sub>6</sub> fluorescence (Figure 2A). To determine if etodolac had a direct effect on mitochondria, the organelles were purified from B-CLL cells by a gentle nitrogen cavitation method (17), and were incubated for 10 min at 37°C with different concentrations of etodolac. Both the R- and S-enantiomers of etodolac reduced the  $\Delta\psi$  of purified mitochondria in a dose-dependent manner (Figure 2B).

The flow-cytometric measurement of dihydrorhodamine (DHR) oxidation in lymphocytes has been shown to correlate with the respiration of mitochondria, as assessed with an oxygen electrode (18). The oxidation of DHR depends upon the availability of substrate (succinate + ADP) and is inhibited by the addition of KCN. B-CLL cells incubated with etodolac for 3 hours displayed a dose-dependent decrease in DHR oxidation (Figure 2C). Taken together, the data with intact B-CLL cells and their isolated mitochondria suggest that inhibition of mitochondrial respiration is an early event in apoptosis induced by etodolac.

### Rapid down-regulation of Mcl-1 correlates with B-CLL sensitivity to etodolac.

The balance in the levels of pro-apoptotic and anti-apoptotic members of the Bcl-2 family is an important regulator of apoptosis in lymphocytes. Levels of the anti-apoptotic protein Mcl-1 have been shown to correlate with sensitivity of B-CLL to chemotherapy (19). Therefore, we examined the time-dependent effects of etodolac on the expression in CLL of the Bcl-2 family proteins Mcl-1 and Bcl-2. Expression of the caspase inhibitory protein XIAP, the Bcl-2 binding protein BAG-1, the caspase substrate poly(adenosine 5'-diphosphate)-ribose polymerase (PARP) were also examined (Figure 3D). The levels of Mcl-1, but not Bcl-2, XIAP, or BAG-1 fell in B-CLL cells by 2 hours after etodolac incubation. Mcl-1 levels did not decline in etodolac-resistant B-CLL cells or in normal PBL (Figure 3A), suggesting that Mcl-1 down-regulation correlates with cellular sensitivity to etodolac. Pretreatment of etodolac-sensitive B-CLL cells for 30 min with the proteasome inhibitors, MG-132 (Figure 3B) or lactacystin (data not shown), prevented the drop in Mcl-1 protein levels. The etodolac-induced Mcl-1 downregulation was quantified (Figure 3C), and found to be dose-dependent, reaching a maximum (50%) at 500  $\mu$ M. Subsequent to Mcl-1 degradation, etodolac exposure induced activation of caspase-3, measured using the fluorometric substrate DEVD-AFC (data not shown), and by the cleavage of PARP into an 86-kD proteolytic fragment (Figure 3D). Inhibition of the caspases activity prevented the reduction of XIAP and BAG-1 protein levels, suggesting that caspase activation was associated with the degradation of XIAP and BAG-1 (data not shown).

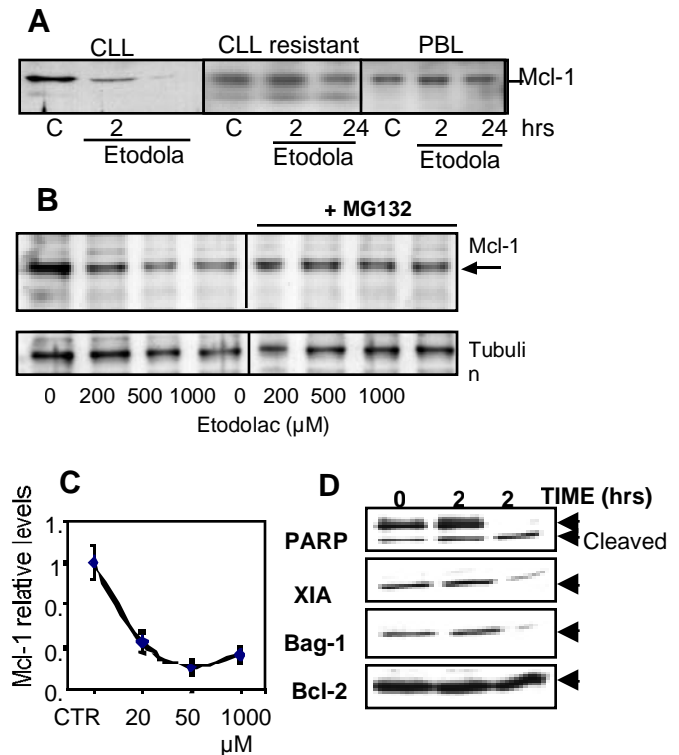


**Figure 3. Effect of etodolac on the apoptosis-regulating proteins.**

(3A) Etodolac induced declines in Mcl-1 protein levels in B-CLL cells *in vitro*. Representative immunoblot data are presented for B-CLL cells that exhibited *in vitro* sensitivity ( $IC_{50} < 500 \mu$ M at 72 hours, left panel) or resistance ( $IC_{50} > 1 \text{ mM}$ , middle panel), and for normal peripheral blood lymphocytes (PBL, right panel). B-CLL cells and PBL were cultured *in vitro* for 2 or 24 hours with 1 mM racemic etodolac. Detergent lysates from B-CLL cells and normal lymphocytes were normalized for total protein content (20  $\mu$ g per lane) and analyzed by SDS-PAGE/immunoblot assay (4-20% gels). (3B) Etodolac-induced Mcl-1 down-regulation is dose dependent and inhibited by proteasome inhibitors. B-CLL cells were incubated for 2 hours with increasing concentrations of racemic etodolac (left panel), or pre-incubated for 1 hour with 5  $\mu$ M of the peptidic proteasome inhibitor MG132, and then exposed to etodolac (right panel). Cells were lysed, and the Mcl-1 (top panel) and tubulin levels were analyzed by immunoblotting. (3C) Quantification of the Mcl-1 downregulation. The relative Mcl-1 level was quantified by densitometry, performed after immunoblotting of B-CLL cells treated with racemic etodolac for 2 hours. The Mcl-1 relative level was normalized based on the control lane, and based on the intensity of the control tubulin band. The data are expressed as the mean of 4 independent experiments, using cells from B-CLL 4 patients  $\pm$  standard deviation. (3D) Expression of apoptotic regulatory molecules in etodolac-treated B-CLL cells. B-CLL cells treated for 2 and 24 hours with 1 mM racemic etodolac were lysed, and expression of PARP, XIAP, Bag-1, and Bcl-2 was analysed by immunoblotting. Note that, while Mcl-1 levels fell after 2 hours in the sensitive B-CLL prior to apoptosis (3A), Bag-1 and XIAP levels fell only after 24 hours, when PARP cleavage already was complete.

### Etodolac enantiomers activate PPAR- $\gamma$

Indomethacin and various other NSAIDs have been shown to bind and activate the nuclear receptor PPAR- $\gamma$  (9). To determine if etodolac also could activate PPAR- $\gamma$ , RAW 267.4 macrophages were incubated with various concentrations of etodolac (racemic, S-, and R-enantiomers). As assessed by stimulation of PPAR- $\gamma$ -dependent reporter gene, as little as 10  $\mu$ M etodolac (racemic, S-, and R-etodolac) activated PPAR- $\gamma$ -dependent transcription (Figure 4 A).

Immunoblotting experiments showed that PPAR- $\gamma$  protein levels were about 10-fold higher in B-CLL than in normal PBL (Figure 4B). The combination of ligand activation of PPAR- $\gamma$ , together with protein kinase C activation by a phorbol ester, has been reported to induce the scavenger receptor CD36 in macrophages (20). Using CD36 as an indicator, 200  $\mu$ M racemic etodolac and 20  $\mu$ M of the high affinity PPAR-activator troglitazone, displayed equivalent potency (Figure 4C). Collectively, these results suggest that both the R and S enantiomers of etodolac are PPAR- $\gamma$  activators, and that PPAR- $\gamma$  is highly expressed in B-CLL.

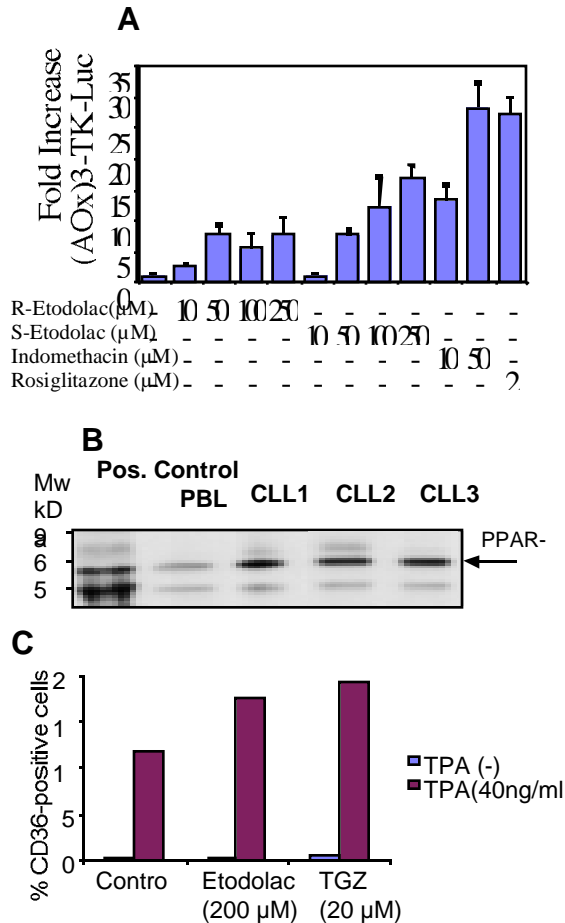


**Figure 4. Activation of PPAR- $\gamma$**   
**(4A)** Activation of a PPAR- $\gamma$  reporter construct (AOx)<sub>3</sub>-TK-Luc by etodolac, indomethacin, and rosiglitazone in RAW 267.4 mouse macrophages. Cells were transfected at a density of 3 x 10<sup>5</sup> cells/ml in six well plates using Lipofectamine, the PPAR- $\gamma$  expression vector pCMX-PPAR (0.1 mg), and the PPAR- $\gamma$  reporter construct (AOx)<sub>3</sub>-TK-Luc (1 mg). Cells were treated for 24 hours in 0.5% DME with the indicated compounds, harvested and assayed for luciferase activity. Results were expressed as the mean  $\pm$  SD of three determinations. **(4B)** Expression of PPAR- $\gamma$  protein in cell lysates from B-CLL cells and normal PBL. The results shown are representative of 16 B-CLL samples, and 5 normal PBL. **(4C)** Enhancement of TPA induced expression the CD36 scavenger receptor in THP-1 cells by etodolac and troglitazone (TGZ).

Patient	ViabilityBefore	ViabilityAfter	% Increased cell death
#1	90 $\pm$ 8	78 $\pm$ 5	13
#2	47 $\pm$ 5	20 $\pm$ 3	57
#3	75 $\pm$ 6	31 $\pm$ 5	69
#4	96 $\pm$ 11	96 $\pm$ 9	0
#5	50 $\pm$ 6	33 $\pm$ 4	34
#6	68 $\pm$ 4	40 $\pm$ 6	41

Table 1. Etodolac therapy enhances the spontaneous apoptosis of isolated B-CLL cells. Isolated B-CLL cells before and after etodolac treatment (400 mg bid) were cultured in RPMI-1640 with 20% autologous plasma, collected either before or after therapy. After 72 hour of incubation, viability assays were performed by erythrosin B staining. Numbers indicate the % of viable cells. Note that B-CLL cells die spontaneously over time and that etodolac increased the cell death in 5 out of 6 patients. The 5 patients that responded to etodolac were enrolled in the clinical trial, see figure 5.

**Etodolac induces a reduction of lymphocyte counts in B-CLL patients.**

To determine if etodolac could reduce B-CLL survival in vivo, six B-CLL patients were enrolled in a first step challenge assay for etodolac sensitivity. Each patient received one 400 mg etodolac tablet, and a second tablet 12 hours later. B-CLL cells were isolated just before the first tablet, and 12 hours after the second. B-CLL cells recovered from patients were then cultured with 20% autologous plasma and apoptosis rates were measured, either before or after etodolac treatment. In 5 out of 6 patients, cells isolated after *in vivo* etodolac challenge displayed more *ex vivo* spontaneous apoptosis than cells obtained just before etodolac therapy (Table 1). The five etodolac-sensitive patients were then enrolled in a second-step clinical trial in which they took etodolac for one month (400mg bid). After etodolac treatment, blood lymphocytes counts of all of 5 patients had decreased by 10-60% (Figure 5). When etodolac treatment was interrupted, B-CLL counts rebounded to pre-treatment levels. Two of the patients subsequently were retreated, and the circulating lymphocyte counts dropped again by almost 50% over one month (results not shown).

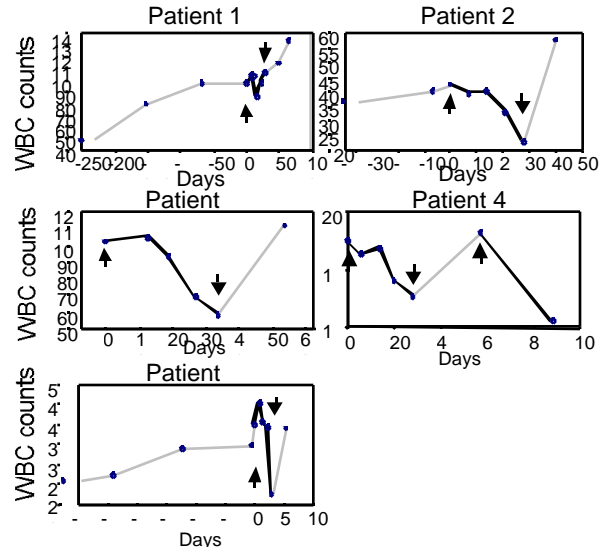


**Figure 5. Etodolac leads to a reduction of the blood lymphocyte counts in B-CLL patients.**

The white blood cell counts (WBC, cellsx10<sup>3</sup>/ $\mu$ l, y-axis) of B-CLL patients were measured before, during, and after the etodolac treatment (400mg bid). The x-axis represents the time of the WBC cell count, the beginning of etodolac therapy is labeled 0 (upward arrow) and the end of the 1-month treatment is indicated with a downward arrow. The results

obtained in the 5 patients enrolled in the clinical trial are represented. Patient 4 was treated twice with etodolac, and is now under continuous therapy.

### Etodolac effect on lymphocyte mobility

The reversible reduction in lymphocyte counts observed in B-CLL patients treated with etodolac prompted us to assess the drug's effects on chemotaxis. B-CLL were pre-incubated in the presence of various concentrations of etodolac for 16 hours, prior to loading in the upper part of a modified Boyden chamber with pore size of 3  $\mu\text{m}$ . The lower reservoir contained either medium alone, or the CXCR3-binding chemokine IFN-inducible protein 10 (IP-10, 200 ng/ml). After 2 hours of incubation, the cells that traveled through the polycarbonate membrane were enumerated by flow cytometry. We used IP-10 because B-CLL cells express high levels of the CXCR3 chemokine receptor and are attracted by IP-10 (21). In all B-CLL patients tested (n=4), etodolac increased the chemotactic response of B-CLL cells to IP-10 (Figure 6A). Enhanced chemotaxis was observed in B-CLL cells incubated with 50  $\mu\text{M}$  etodolac, well below the plasma concentration expected in patients receiving 800 mg/day of the drug. At concentrations of 500  $\mu\text{M}$  and above, chemotaxis decreased, due to a loss of cell viability. Not only the racemic (R/S) mixture of etodolac, but also the purified R and S enantiomers, enhanced B-CLL chemotaxis. Stimulation of chemotaxis was not due to increased expression of the CXCR receptor, as assessed by antibody staining (data not shown).

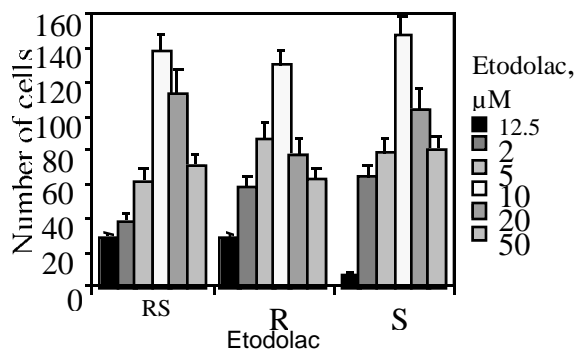


**Figure 6. Etodolac effect on B-CLL lymphocyte mobility**

B-CLL lymphocytes from B-CLL patients were incubated in presence of the indicated concentrations of etodolac (racemic R/S, purified R, and S enantiomers) for 16 hours in RPMI-1640 medium supplemented with 10% FBS. A total of  $5 \times 10^5$  B-CLL cells (100  $\mu\text{l}$ ) were then added to the upper chamber of the 24-well chemotaxis chamber. The lower chamber was filled with 600  $\mu\text{l}$  of culture medium containing 100 ng/ml of the human CXCR3-dependent chemokine IP-10. After two hours incubation at 37°C, the numbers of cells that migrated into the lower chamber were enumerated by cytometry after gating the B-CLL lymphocytes. Results are expressed as number of B-CLL cells in lower chamber  $\pm$  SD from triplicate wells. The results are representative of separate experiments using cells isolated from four different B-CLL donors.

## DISCUSSION

Treatment with racemic etodolac, an NSAID used for control of pain and inflammation, reduced circulating B-CLL cells in 5 out of 6 patients. The B-CLL cells recovered from patients as early as one day after institution of etodolac therapy had reduced survival *in vitro*, indicative of a metabolic derangement. Analyses of etodolac effects on purified CLL cells showed that the drug impaired mitochondrial respiration, induced rapid degradation of the anti-apoptotic protein Mcl-1, activated the peroxisome proliferator activated receptor – (PPAR-), and stimulated CXCR3-dependent chemotaxis. The purified R-enantiomer of etodolac, which has been reported to

be a poor COX inhibitor, displayed all the *in vitro* biochemical effects toward B-CLL cells of the racemic mixture.

Results obtained with isolated mitochondria from CLL cells confirmed that etodolac interfered with substrate oxidation and reduced the transmembrane potential. Mitochondria play a key role in the events leading to caspase activation in cells undergoing apoptosis because of DNA damage or disturbed metabolism (22, 23). Alteration of the mitochondrial transmembrane potential and release of pro-apoptotic proteins, such as cytochrome c and apoptosis-inducing factor (AIF), from the intermembrane space into the cytosol, leads to the activation of caspases and endonucleases and to the eventual appearance of an apoptotic phenotype.

Bcl-2 family members regulate the release of pro-apoptotic proteins. Mcl-1 is an anti-apoptotic member of the bcl-2 family, which is highly expressed in B-CLL and found in mitochondria and light membrane fractions (24). Elevated levels of Mcl-1 correlate significantly with failure to achieve complete remission in B-CLL after single agent therapy, suggesting that Mcl-1 is a natural regulator of apoptosis in these leukemic cells. (19). Thus, it is notable that, as early as two hours after incubation with etodolac, Mcl-1 expression fell in B-CLL cells. Both R- and S-etodolac induced Mcl-1 degradation at equivalent concentrations, suggesting this event is not due to COX2 inhibition. Etodolac could either reduce the rate of Mcl-1 synthesis through effects on Mcl-1 gene transcription, or it could accelerate the rate of Mcl-1 protein turnover. In this regard, Mcl-1 is one of the few Bcl-2 family proteins which has PEST motifs associated with rapid degradation (data not shown). Pre-incubation of the cells with Idun-1965, a broad-spectrum caspase inhibitor, did not prevent etodolac-induced Mcl-1 down-regulation, indicating that this event is not a mere concomitant of apoptosis. Furthermore, etodolac incubation did not alter the expression levels of Bcl-2, Bax, and Bcl-X<sub>L</sub>. The mechanism by which etodolac induces a rapid decline in Mcl-1 protein levels remains to be elucidated. Regardless of the mechanism, the down-regulation of Mcl-1 would be expected to render B-CLL cells more susceptible to apoptosis.

Various NSAIDs at relatively high concentrations (100  $\mu\text{M}$  and above) can bind and activate the nuclear hormone receptor PPAR- (9). Both R and S etodolac at concentrations of 10-100  $\mu\text{M}$  stimulated a PPAR- reporter gene, and increased expression of the PPAR- dependent scavenger receptor CD36. Activated PPAR- dimerizes with RXR receptors, and also binds co-activator molecules, such as the cyclic AMP response element binding protein co-activator protein (CBP) (25), and ARA70, a co-activator of the androgen receptor that is overexpressed in hormone resistant prostate cancer (26). PPAR- regulates adipocyte differentiation, and insulin sensitivity, and is the target for the thiazolidine-diones used to treat type II diabetes. However, the ligand binding-site on PPAR- is capacious, and potentially can accommodate different ligands that might exert distinctive metabolic effects (25). In some cells with high levels of PPAR-, maximal activation of the receptor can induce apoptosis (10). The mechanism of PPAR- mediated apoptosis is unclear, and it may be due to sequestration of CBP and other transcriptional co-activators with subsequent squelching of the production of labile survival factors. The fact that quiescent B-CLL cells expressed very high levels of PPAR- suggests that maximal activation of the receptor could deplete co-activator molecules. PPAR- activation alone probably was not sufficient to induce B-CLL apoptosis, since

the high affinity PPAR- activator troglitazone was nontoxic at concentrations 100  $\mu$ M (results not shown), which are sufficient for receptor stimulation. However, the sequestration of general transcription factors by ligand-bound PPAR- could enhance the sensitization of B-CLL cells to the other apoptosis-inducing effects of etodolac.

Peak plasma concentrations ( $C_{max}$ ) of etodolac are attained within 1 to 2 hours, and range from 33 to 77  $\mu$ M after a single 200 mg dose (27). Thus, 800 mg potentially could achieve a plasma concentration of 200  $\mu$ M, which was sufficient to reduce B-CLL survival *in vitro*. In an indolent disease such as B-CLL, circulating leukocyte counts depend upon a delicate balance between the relative rates of cell generation, death, and distribution. Even a minor uncompensated decrease in B-CLL life span will eventually produce a fall in circulating cells.

The B-CLL patients on etodolac therapy did not have clinically obvious changes in lymphadenopathy. To determine if etodolac could alter the distribution of B-CLL between the blood and lymphoid organs, the effects of the drug on CXCR3-dependent chemotaxis were tested. Both the R- and S-enantiomers of etodolac stimulated chemotaxis at concentrations (50  $\mu$ M) readily achievable in plasma. It is possible the B-CLL cells exposed to etodolac therefore may be sequestered within lymphoid organs, where chemokine concentrations are likely to be higher than in the plasma (28). Even if the early clearance of B-CLL cells from the circulation resulted mainly from a change in cell distribution, the impaired survival observed after *in vivo* treatment should be reflected eventually by reductions in tumor burden.

Our data indicate that B-CLL cells undergo more rapid apoptosis at higher concentrations of etodolac than are conventionally used for the treatment of pain and inflammation. The dose-limiting side-effects of NSAIDs, such as gastric ulcer and kidney dysfunction, are associated with inhibition of COX-1 (29, 30). Insofar as (i) the R-enantiomer of etodolac induces apoptosis, and stimulates chemokines in B-CLL, (ii) plasma levels of the R-enantiomer are 10-fold higher than those of the S-enantiomer, and (iii) other NSAIDs do not induce B-CLL cell depletion, it is likely that R-etodolac is the principal active agent. Because R-etodolac has much less COX-inhibitory activity than S-etodolac, patients should tolerate higher dosages of the former agent. Thus, treatment of B-CLL patients with the isolated R-etodolac should allow one to attain plasma concentrations within the *in vitro* cytotoxic range with fewer side-effects. Thus, efforts should be made to produce pure R-etodolac in the goal to increase the anti-leukemic activity of this compound, in hope that it may become a new drug for the treatment of B-CLL.

## METHODS

### Patients, cell isolation and viability assays

Written informed consent was obtained to procure peripheral blood from all patients and with normal healthy volunteers. Patients had to have B-CLL according to National Cancer Institute (NCI) criteria of any Rai stage. Criteria for requiring therapy were as follows: disease-related symptoms, anemia and/or thrombocytopenia, bulky lymphadenopathy, and/or clinically relevant splenomegaly. Mononuclear cells were isolated by gradient centrifugation through Ficoll-Paque. Cells were cultured at  $2 \times 10^6$  per mL in RPMI 1640 with 20% autologous plasma and antibiotics in 96-well plates without or with various concentrations of etodolac (racemic, S-etodolac,

R-etodolac). At the indicated times, viability assays were performed by erythrosin B dye exclusion.

### Separation of etodolac enantiomers

Etodolac isomers were separated by fractional crystallization by a modification of the procedure of Becker-Scharfenkamp and Blaschke (31). Briefly, pharmaceutical grade tablets of racemic etodolac (6x400 mg) were crushed in a mortar and pestle and extracted with hot ethyl acetate (2x50 mL) and filtered. Evaporation of the filtrate gave 1.52 g of white powder (68% recovery). This material was dissolved in 2-propanol (10mL) and S- or R-phenylethylamine was added. The clear solution was allowed to stand at 4°C for several days. The resulting colorless needles were collected and recrystallized from 2-propanol two times. The salt product was decomposed by adding to ice cold 10% sulfuric acid and extracting with ethyl acetate. After evaporation, the syrupy residue of R- or S-etodolac was crystallized from methanol-water. The enantiomeric purity of each product was at least 97% as assayed by HPLC on a chiral column (AGP, ChromTech, Sweden).

### Mitochondrial function assays

Viability and mitochondrial transmembrane potential ( $\psi_m$ ) were concomitantly analyzed by 3,3' dihexyloxycarbocyanine iodide (DiOC<sub>6</sub>) and propidium iodide (PI) staining as described (15). Briefly, after etodolac treatment, B-CLL cells were incubated for 10 min at 37°C in culture medium containing 40 nM of DiOC<sub>6</sub> and 5  $\mu$ g/ml PI.

Mitochondrial respiration in intact cells was assessed by dihydrorhodamine 123 oxidation (DHR) (Molecular Probes, Eugene, Oregon), as described (18). B-CLL cells were centrifuged at 200g for 10 min, resuspended in fresh respiration buffer (250mM sucrose, 1g/L bovine serum albumin, 10mM MgCl<sub>2</sub>, 10mM K/Hepes, 5mMKH<sub>2</sub>PO<sub>4</sub> [pH 7.4]) and cultured for 10 min at 37°C with 0.04% digitonin, 10 mM ADP, and 5mM succinate. Cells were then incubated for 5 min in 0.1  $\mu$ M DHR in respiration buffer. Cells were analyzed within 30 min in a Becton Dickinson FACScalibur cytofluorometer. After suitable compensation, fluorescence was recorded at 525 nm (FL-1) for DiOC<sub>6</sub> and DHR at 525 nm (FI-1), at 600 nm (FL-3) for PI.

Mitochondria were isolated from B-CLL cells by nitrogen cavitation as described (18). The B-CLL cells were washed in ice-cold Dulbecco's phosphate-buffered saline for disruption by N<sub>2</sub>. All subsequent steps were carried out on ice or at 4 °C. The cells were washed with MA buffer (100 mM sucrose, 1 mM EGTA, 20 mM MOPS (pH 7.4), bovine serum albumin 1 g/liter) then resuspended at  $2 \times 10^8$  cells/ml in MB buffer (MA buffer plus 10 mM triethanolamine, 5% Percoll, and an antiproteinase mixture consisting of aprotinin, pepstatin A, and leupeptin, each at 10  $\mu$ M, and 1 mM phenylmethylsulfonyl fluoride). The cells were then disrupted by N<sub>2</sub> cavitation using a cavitation bomb (Parr Instrument Company, Moline, IL). Lysates were centrifuged twice at 2500 g for 5 min to remove nuclei and unbroken cells then at 25,000 g for 30 min to isolate mitochondria. The mitochondria were suspended in MC buffer (identical to MA buffer except that the sucrose concentration was 300 mM and an antiprotease mixture was included that consisted of aprotinin, pepstatin A, and leupeptin, each at 10  $\mu$ M) and incubated for 10 min at 37°C with the indicated concentrations of etodolac. Isolated mitochondria were incubated for 10 min at 37°C with 100 nM DiOC<sub>6</sub> and their  $\psi_m$  was measured by flow cytometry at 525 nm (FL-1) and by gating on mitochondria size (FSC/SSC).

### Protein expression assays

Washed B-CLL cells were lysed in Lysis buffer (25 mM Tris, pH 7.4, 150 mM KCl, 5 mM EDTA, 1% Nonidet P-40, 0.5% sodium deoxycholate, 0.1% SDS, 1 µg/ml aprotinin, 1 µg/ml leupeptin, 1 mM phenylmethanesulfonyl fluoride, 1 mM sodium orthovanadate, 1 mM sodium fluoride). Lysates were centrifuged at 15,000 x g for 10 min to remove nuclei and the protein content of supernatants was measured using a modified Coomassie blue assay (Pierce, Rockford, IL). Proteins were resolved at 125 V on 14% and 4-20% Tris-glycine pre-cast gels (Novex, San Diego) and electrophoretically transferred to 0.2 µm polyvinylidene fluoride (PVDF) membranes (Millipore, Bedford, MA) for 2 hours at 125 V. Membranes were blocked overnight in I-Block blocking buffer (Tropix, Bedford, MA). Blots were probed with polyclonal antibodies anti-Mcl-1, anti-Bcl-2, monoclonal anti-Bag-1 (all developed in J. Reed's lab), monoclonal anti-XIAP (Transduction Laboratories Inc.), monoclonal anti-PARP (gift of N.A. Berger), or monoclonal anti-PPAR (Santa Cruz Laboratories, California) antibody, followed by secondary antibody consisted of horseradish peroxidase (HRP)-conjugated goat anti-rabbit (Mcl-1) or anti-mouse (PPAR-) IgG. Detection was performed by an enhanced chemiluminescence (ECL, Amersham) method, followed by colorimetric detection, using SG substrate. The X-ray films were scanned, acquired in Adobe Systems Photoshop and analyzed with NIH Image Software.

### PPAR-γ assays

The mouse macrophage RAW264.7 cells (ATCC) were grown in DME with 1 gm/L glucose and L-glutamine and the addition of 10% fetal bovine serum (Gemini Bio-Products), non-essential amino acids 100 mM (GibcoBRL) and penicillin-streptomycin 100U/ml (Cellgro). Cells were transfected at a density of  $3 \times 10^5$  cells/ml in six well plates using Lipofectamine, the PPAR- expression vector pCMX-PPAR- (0.1 mg), and the PPAR- reporter construct (AOx)<sub>3</sub>-TK-Luc (1

mg) as previously described (32). Cells were treated for 24 hours in 0.5% DME with the indicated compounds, harvested and assayed for luciferase activity. Results were expressed as the mean ± SD of three determinations. Activation of PPAR- was also functionally assayed as previously described (20). Briefly, human monocytic THP-1 cells (ATCC) were grown in RPMI-1640 with 10% FBS and antibiotics, treated for 5 days with 200 µM etodolac (racemic) and 20 µM troglitazone as indicated, or for 48 hr with 40 ng/ml phorbol ester (TPA). Cells were analyzed by flow cytometry using unconjugated anti-CD36 and FITC-conjugated anti-IgG. A population of 10000 viable cells was analyzed for each treatment. Data are presented as the difference in mean fluorescence between anti-CD36 antibody and control isotype-matched antibody.

### Migration/chemotaxis assay

Cell migration was measured in a 24-well modified Boyden chamber (Transwell, Corning-Costar, NY). The recombinant human IP-10 chemokine (R&D Systems, McKinley Place, NE) was diluted in RPMI-1640 medium at 200 ng/ml, and used to evaluate the chemotactic properties of lymphocytes from B-CLL patients. Polycarbonate membranes with pore size of 3 µm were used. A total of 600 µL of chemokines or control medium was added to the bottom wells, and 100 µL of  $2$  to  $5.0 \times 10^6$  cells/ml cells resuspended in RPMI-1640 were added to the top wells. The chamber was incubated at 37°C with 5% CO<sub>2</sub> for 2 hours. The membranes were then removed, and the cells present on the bottom well were quantified by flow cytometry. For cell quantification, a fixed acquisition time of 30 seconds was used per sample, and beads were run during each experiment to ensure a reproducible acquisition. All assays were performed in triplicate.

### ACKNOWLEDGMENTS

We thank Drs. Alberto Bessudo for referring patients and Nancy Noon for preparing the manuscript.

### REFERENCES

1. Bellosillo, B., M. Piqué, M. Barragán, E. Castaño, N. Villamor, D. Colomer, E. Montserrat, G. Pons, and J. Gil. 1998. Aspirin and salicylate induce apoptosis and activation of caspases in B-cell chronic lymphocytic leukemia cells. *Blood* 92, no. 4:1406-14.
2. Klampfer, L., J. Cammenga, H.G. Wisniewski, and S.D. Nimer. 1999. Sodium salicylate activates caspases and induces apoptosis of myeloid leukemia cell lines. *Blood* 93, no. 7:2386-94.
3. Shiff, S.J., L. Qiao, L.L. Tsai, and B. Rigas. 1995. Sulindac sulfide, an aspirin-like compound, inhibits proliferation, causes cell cycle quiescence, and induces apoptosis in HT-29 colon adenocarcinoma cells. *J Clin Invest* 96, no. 1:491-503.
4. Zhang, X., S.G. Morham, R. Langenbach, and D.A. Young. 1999. Malignant transformation and antineoplastic actions of nonsteroidal antiinflammatory drugs (NSAIDs) on

cyclooxygenase-null embryo fibroblasts [see comments]. *J Exp Med* 190, no. 4:451-59.

5. Shiff, S.J., and B. Rigas. 1999. The role of cyclooxygenase inhibition in the antineoplastic effects of nonsteroidal antiinflammatory drugs (NSAIDs) [comment]. *J Exp Med* 190, no. 4:445-50.

6. Cronstein, B.N., M.C. Montesinos, and G. Weissmann. 1999. Salicylates and sulfasalazine, but not glucocorticoids, inhibit leukocyte accumulation by an adenosine-dependent mechanism that is independent of inhibition of prostaglandin synthesis and p105 of NFκB. *Proceedings of the National Academy of Sciences of the United States of America* 96, no. 11:6377-81.

7. Martens, M.E., C.H. Chang, and C.P. Lee. 1986. Reye's syndrome: mitochondrial swelling and Ca<sup>2+</sup> release induced by Reye's plasma, allantoin, and salicylate. *Arch Biochem Biophys* 244, no. 2:773-86.

8. Tomoda, T., K. Takeda, T. Kurashige, H. Enzan, and M. Miyahara. 1994. Acetylsalicylate (ASA)-induced mitochondrial dysfunction and its potentiation by Ca<sup>2+</sup>. *Liver* 14, no. 2:103-8.

9. Lehmann, J.M., J.M. Lenhard, B.B. Oliver, G.M. Ringold, and S.A. Kliewer. 1997. Peroxisome proliferator-activated

- receptors alpha and gamma are activated by indomethacin and other non-steroidal anti-inflammatory drugs. *J Biol Chem* 272, no. 6:3406-10.
- 10.Chinetti, G., S. Griglio, M. Antonucci, I.P. Torra, P. Delerive, Z. Majd, J.C. Fruchart, J. Chapman, J. Najib, and B. Staels. 1998. Activation of proliferator-activated receptors alpha and gamma induces apoptosis of human monocyte-derived macrophages. *J Biol Chem* 273, no. 40:25573-80.
- 11.Brocks, D.R., and F. Jamali. 1994. Etodolac clinical pharmacokinetics. *Clin Pharmacokinet* 26, no. 4:259-74.
- 12.Demerson, C.A., L.G. Humber, N.A. Abraham, G. Schilling, R.R. Martel, and C. Pace-Asciak. 1983. Resolution of etodolac and antiinflammatory and prostaglandin synthetase inhibiting properties of the enantiomers. *J Med Chem* 26, no. 12:1778-80.
- 13.Nardella, F.A., and J.A. LeFevre. 1999. Enhanced clearance of leukemic lymphocytes in B cell chronic lymphocytic leukemia (CLL) with etodolac. *Arthritis & Rheumatism* 42, no. 9 SUPPL.:S56.
- 14.Collins, R.J., L.A. Verschuer, B.V. Harmon, R.L. Prentice, J.H. Pope, and J.F. Kerr. 1989. Spontaneous programmed death (apoptosis) of B-chronic lymphocytic leukaemia cells following their culture in vitro. *Br J Haematol* 71, no. 3:343-50.
- 15.Leoni, L.M., Q. Chao, H.B. Cottam, D. Genini, M. Rosenbach, C.J. Carrera, I. Budihardjo, X. Wang, and D.A. Carson. 1998. Induction of an apoptotic program in cell-free extracts by 2-chloro-2'-deoxyadenosine 5'-triphosphate and cytochrome c. *Proc Natl Acad Sci USA* 95, no. 16:9567-71.
- 16.Wu, J.C., and L.C. Fritz. 1999. Irreversible caspase inhibitors: tools for studying apoptosis. *Methods* 17, no. 4:320-8.
- 17.Adachi, S., A.R. Cross, B.M. Babior, and R.A. Gottlieb. 1997. Bcl-2 and the outer mitochondrial membrane in the inactivation of cytochrome c during Fas-mediated apoptosis. *J Biol Chem* 272, no. 35:21878-82.
- 18.Gottlieb, R., and S. Adachi. Nitrogen cavitation for cell disruption to obtain mitochondria from cultured cells. *Methods Enzymol* In Press.
- 19.Kitada, S., J. Andersen, S. Akar, J.M. Zapata, S. Takayama, S. Krajewski, H.G. Wang, X. Zhang, F. Bullrich, C.M. Croce, K. Rai, J. Hines, and J.C. Reed. 1998. Expression of apoptosis-regulating proteins in chronic lymphocytic leukemia: correlations with In vitro and In vivo chemoresponses. *Blood* 91, no. 9:3379-89.
- 20.Tontonoz, P., L. Nagy, J.G. Alvarez, V.A. Thomazy, and R.M. Evans. 1998. PPARgamma promotes monocyte/macrophage differentiation and uptake of oxidized LDL. *Cell* 93, no. 2:241-52.
- 21.Trentin, L., C. Agostini, M. Facco, F. Piazza, A. Perin, M. Siviero, C. Gurrieri, S. Galvan, F. Adami, R. Zambello, and G. Semenzato. 1999. The chemokine receptor CXCR3 is expressed on malignant B cells and mediates chemotaxis. *J Clin Invest* 104, no. 1:115-21.
- 22.Green, D.R., and J.C. Reed. 1998. Mitochondria and apoptosis. *Science* 281, no. 5381:1309-12.
- 23.Kroemer, G., N. Zamzami, and S.A. Susin. 1997. Mitochondrial control of apoptosis. *Immunol Today* 18, no. 1:44-51.
- 24.Wang, X., and G.P. Studzinski. 1997. Antiapoptotic action of 1,25-dihydroxyvitamin D3 is associated with increased mitochondrial MCL-1 and RAF-1 proteins and reduced release of cytochrome c. *Exp Cell Res* 235, no. 1:210-7.
- 25.Gelman, L., G. Zhou, L. Fajas, E. Raspé, J.C. Fruchart, and J. Auwerx. 1999. p300 interacts with the N- and C-terminal part of PPARgamma2 in a ligand-independent and -dependent manner, respectively. *J Biol Chem* 274, no. 12:7681-8.
- 26.Heinlein, C.A., H.J. Ting, S. Yeh, and C. Chang. 1999. Identification of ARA70 as a ligand-enhanced coactivator for the peroxisome proliferator-activated receptor gamma. *J Biol Chem* 274, no. 23:16147-52.
- 27.Ferdinandi, E.S., S.N. Sehgal, C.A. Demerson, J. Dubuc, J. Zilber, D. Dvornik, and M.N. Cayen. 1986. Disposition and biotransformation of 14C-etodolac in man. *Xenobiotica* 16, no. 2:153-66.
- 28.Baggiolini, M. 1998. Chemokines and leukocyte traffic. *Nature* 392, no. 6676:565-8.
- 29.Vane, J.R., Y.S. Bakhle, and R.M. Botting. 1998. Cyclooxygenases 1 and 2. *Annu Rev Pharmacol* 38, no. 1:97-120.
- 30.Warner, T.D., F. Giuliano, I. Vojnovic, A. Bukasa, J.A. Mitchell, and J.R. Vane. 1999. Nonsteroid drug selectivities for cyclo-oxygenase-1 rather than cyclo-oxygenase-2 are associated with human gastrointestinal toxicity: a full in vitro analysis. *Proc Natl Acad Sci USA* 96, no. 13:7563-8.
- 31.Becker-Scharfenkamp, U., and G. Blaschke. 1993. Evaluation of the stereoselective metabolism of the chiral analgesic drug etodolac by high-performance liquid chromatography. *Journal of Chromatography Biomedical Applications* 621, no. 2:199-207.
- 32.Ricote, M., A.C. Li, T.M. Willson, C.J. Kelly, and C.K. Glass. 1998. The peroxisome proliferator-activated receptor-gamma is a negative regulator of macrophage activation. *Nature* 391, no. 6662:79-82.



---

# HIV induces lymphocyte apoptosis by a p53-initiated, mitochondrial-mediated mechanism<sup>1</sup>

DAVIDE GENINI,<sup>\*,†,2</sup> DENNIS SHEETER,<sup>\*,2</sup> STEFFNEY ROUGHT,<sup>\*,‡</sup> JOHN J. ZAUNDERS,<sup>‡</sup>  
SANTOS A. SUSIN,<sup>§</sup> GUIDO KROEMER,<sup>§</sup> DOUGLAS D. RICHMAN,<sup>\*,‡</sup>  
DENNIS A. CARSON,<sup>\*,†</sup> JACQUES CORBEIL,<sup>\*,‡,2</sup> AND LORENZO M. LEONI<sup>\*,†,2,3</sup>

\*Departments of Medicine and <sup>†</sup>The Sam and Rose Stein Institute for Research on Aging, University of California San Diego, La Jolla, California 92093-0663, USA; <sup>‡</sup>San Diego Health Care System and Veterans Medical Research Foundation, San Diego, California 92161, USA; and <sup>§</sup>Centre National de la Recherche Scientifique, UMR1599, Institut Gustave Roussy, F-94805 Villejuif, France

## SPECIFIC AIMS

HIV-1 induces apoptosis and leads to CD4+ T lymphocyte depletion in humans. It is still unclear whether HIV-1 kills infected cells directly or indirectly. In this study we provide a mechanistic view on how HIV-1 induces apoptotic death of infected primary human CD4+ T lymphocytes.

## PRINCIPAL FINDINGS

### 1. HIV damages mitochondria, leading to cytochrome *c* release and caspase activation

The time course of activation of the extrinsic and intrinsic pathways of apoptosis was examined after HIV-1 infection of primary CD4+ T lymphocytes. The percentage of cells undergoing apoptosis was quantified by flow cytometry and measuring the proportion of cells with sub-G1 DNA content and correlating it with HIV p24 production. Caspase activities were measured at multiple time points after infection by using specific fluorometric substrates (**Fig. 1**). The pattern of caspase activation strongly suggested that the intrinsic pathway of apoptosis induction was operational. This suggestion was borne out by the following observations. The catalytic activity of the apical caspase-2 and -9 increased after 2 days, concomitantly with the activation of the executioner caspase-3. Activated caspase-6 was detectable only 72 h after infection. No activity of the death receptor-associated apical caspase-8 was observed during the infection (up to 72 h). Caspase enzymatic activities were corroborated by immunoblotting. Cleavage of the proform of caspase-3 was observed in all samples, but in HIV-1 treated cells the ratio of the cleaved and uncleaved pro-caspase product was increased as early as 24 h and remained elevated up to 72 h relative to the control. The levels of the pro-caspase-9 and -6 products were reduced 48 and 72 h after infection, which suggests processing to their active forms.

### 2. HIV induces p53 phosphorylation and activation

To study the role of p53 in the initiation of the apoptotic pathway during HIV-1 infection, we measured the total level of p53 and its phosphorylation at residue Ser15 by using a phospho-specific antibody. Total and phosphorylated p53 levels increased 24 h after HIV-1 infection. This HIV-triggered phosphorylation of p53 peaked at 48 h and remained detectable for up to 72 h (**Fig. 2**). To confirm that phosphorylation and induction of p53 resulted in the activation of the p53 pathway, we analyzed the protein and mRNA levels of p53-induced genes, p21/CIP1/WAF1 (p21), HDM2, and Bax. Both Bax and p21 levels increased 48 h after HIV-1 infection, and HDM2 increased after 72 h compared to uninfected controls.

### 3. HIV up-regulates Fas ligand but only as a late event

To investigate whether HIV would activate an extrinsic apoptotic pathway involving Fas ligand binding to Fas receptor, we analyzed the expressions of signaling proteins involved in the Fas signaling pathway. In primary cells, the protein levels of Fas receptor and of Fas ligand were not modulated by HIV infection (data not shown), but the expression of surface Fas ligand measured by flow cytometry was increased significantly at 72 h. However, the Fas binding proteins FADD, DAXX, and RIP were all down-regulated, which would be expected to inhibit FasL-Fas-induced apoptosis.

## CONCLUSIONS AND SIGNIFICANCE

We demonstrated that the intrinsic mitochondrial pathway of apoptosis is the primary mechanism that induces

---

<sup>1</sup> To read the full text of this article, go to <http://www.fasebj.org/cgi/doi/10.1096/fj.00-0336fje> To cite this article, use (November 9, 2000) *FASEB J.* 10.1096/fj.00-0336fje

<sup>2</sup> The first two authors contributed equally to the study and the last two authors share senior authorship.

<sup>3</sup> Correspondence: Department of Medicine-0663, University of California, San Diego, 9500 Gilman Dr., La Jolla, CA 92093-0663, USA. E-mail: lleoni@ucsd.edu

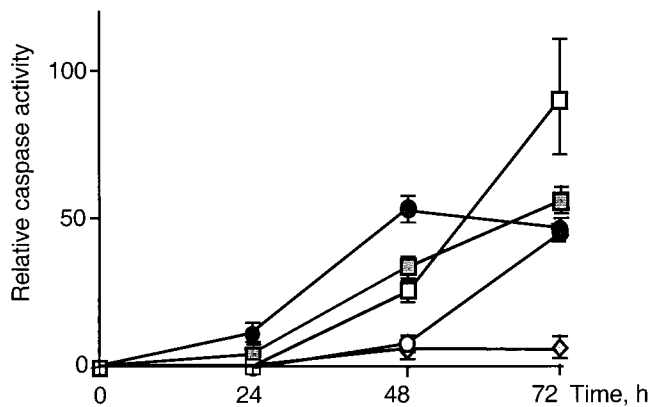


**Figure 1.** Caspase activation in HIV-1-infected CD4<sup>+</sup> T cells. At the times indicated,  $2 \times 10^6$  PBL were washed with PBS and lysed in caspase buffer. A) Caspase activity of 10–20  $\mu$ g of total protein was measured with specific substrates for caspase-2 (■), 3 (□), 6 (○), 8 (◇), and 9 (●) (100  $\mu$ M) after 1 h incubation at 37°C. The cleavage of the fluorometric AMC/AFC was monitored fluorometrically at 400/380 nm excitation and 505/460 nm emission. Activity is represented in relative units to the control without HIV.

CD4<sup>+</sup> T cells to undergo apoptosis. Mitochondrial membrane permeabilization may be a consequence of the activation of the p53 pathway. Once phosphory-

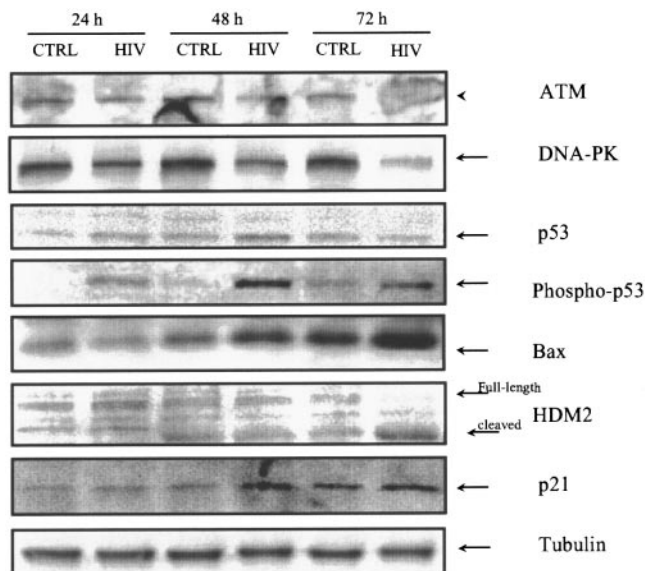


**Figure 2.** Activation of the p53 pathway by HIV-1 infection. Immunoblot analysis was performed on total cell lysates of  $5 \times 10^6$  cells in 100  $\mu$ l lysing buffer as described. The same membranes were stripped and reblotted with specific antibodies, including a tubulin antibody that served as a control for loading.

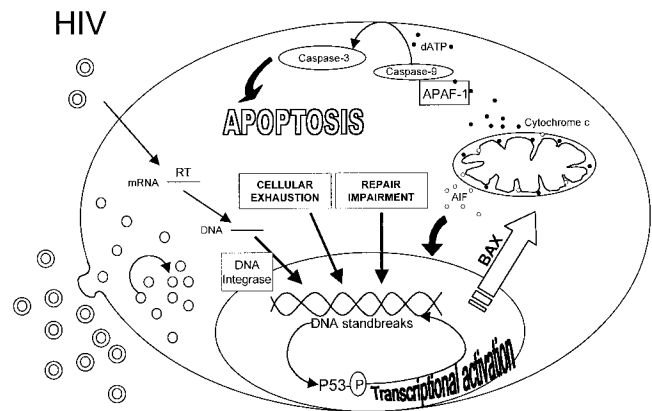


**Figure 3.** HIV-1 enters the cells, and its genome is reverse-transcribed and integrated in host DNA. Less than 24 h after the infection, phosphorylation of p53 at residue Ser15 is observed. This p53 phosphorylation leads to its transcriptional activation, either by increasing its protein levels or by a conformational modification. Activation of the p53 pathway increases the expression of the protein Bax. Bax multimerizes and generates pores in the mitochondrial membranes and allows the release of the pro-apoptotic protein cytochrome *c* and apoptosis-inducing factor (AIF). The released cytochrome *c* will bind to apaf-1 and, in the presence of dATP, sequester and activate caspase-9 and caspase-3, which leads to activation of the caspase proteolytic cascade and results in apoptosis. The released AIF will localize to the nucleus and promote chromatin condensation.

lated, p53 induces up-regulation of Bax, which may translocate to the mitochondrial membrane and promote cytochrome *c* and AIF release.

Furthermore, it appears that the Fas pathway does not play a primary role in HIV-induced apoptosis of CD4<sup>+</sup> T lymphocytes. However, it is possible that Fas ligand might play a role in the depletion of noninfected bystander CD4 cells or CD8<sup>+</sup> T cells by activating caspase-8.

This phenomenon may be especially relevant in primary acute infection when high levels of virus are present and no potent mechanisms of viral control are yet fully operational. The primary infection stage has the highest proportion of CD4 lymphocyte infected during the course of HIV infection. This p53-mediated apoptosis may be responsible for the precipitous drop in CD4<sup>+</sup> T cells seen in primary acute HIV-infected patients, with eventual stabilization of both CD4 and viral loads. These events set the stage for determining the propensity for progression to AIDS. In summary, CD4 T<sup>+</sup> cell death as a result of HIV-1 infection is mediated by the activation of p53 and the intrinsic mitochondrial apoptotic pathway. The mechanism by which HIV mediates this process remains to be further clarified. **[F]**

# Temporal Gene Regulation During HIV-1 Infection of Human CD4<sup>+</sup> T Cells

Jacques Corbeil,<sup>1,5,8</sup> Dennis Sheeter,<sup>2</sup> Davide Genini,<sup>1</sup> Steffney Rought,<sup>1,5</sup> Lorenzo Leoni,<sup>1</sup> Pinyi Du,<sup>1</sup> Mark Ferguson,<sup>1</sup> Daniel R. Masys,<sup>1</sup> John B. Welsh,<sup>2</sup> J. Lynn Fink,<sup>6</sup> Roman Sasik,<sup>3</sup> David Huang,<sup>7</sup> Jorg Drenkow,<sup>7</sup> Douglas D. Richman,<sup>1,2,4,5</sup> and Thomas Gingeras<sup>7</sup>

Departments of <sup>1</sup>Medicine, <sup>2</sup>Pathology, and <sup>3</sup>Physics, University of California San Diego, La Jolla, California 92023, USA; <sup>4</sup>San Diego Veterans Administration Medical Center, San Diego 92161, USA; <sup>5</sup>Veterans Medical Research Foundation, San Diego 92161, USA; <sup>6</sup>San Diego Supercomputer Center, La Jolla, California 92093, USA; <sup>7</sup>Affymetrix, Santa Clara, California, USA

CD4<sup>+</sup> T-cell depletion is a characteristic of human immunodeficiency virus type 1 (HIV-1) infection. In this study, modulation of mRNA expression of 6800 genes was monitored simultaneously at eight time points in a CD4<sup>+</sup> T-cell line (CEM-GFP) during HIV infection. The responses to infection included: (1) >30% decrease at 72 h after infection in overall host-cell production of monitored mRNA synthesis, with the replacement of host-cell mRNA by viral mRNA, (2) suppression of the expression of selected mitochondrial and DNA repair gene transcripts, (3) increased expression of the proapoptotic gene and its gene p53-induced product Bax, and (4) activation of caspases 2, 3, and 9. The intense HIV-1 transcription resulted in the repression of much cellular RNA expression and was associated with the induction of apoptosis of infected cells but not bystander cells. This choreographed host gene response indicated that the subversion of the cell transcriptional machinery for the purpose of HIV-1 replication is akin to genotoxic stress and represents a major factor leading to HIV-induced apoptosis.

The depletion of CD4<sup>+</sup> T cells during human immunodeficiency virus type 1 (HIV-1) infection has been attributed to numerous mechanisms including apoptosis (Ameisen et al. 1991; Laurent-Crawford et al. 1991; Terai et al. 1991). Apoptosis is invariably accompanied by a disruption of inner mitochondrial transmembrane potential (Castedo et al. 1995). This contributes to the release of cytochrome c sequestered in the mitochondrion into the cytosol. In the cytoplasm, cytochrome c combines with APAF-1 and caspase 9 to constitute the apoptosome, which is responsible for the initiation of the caspase cascade triggering the intrinsic apoptosis pathway (Green et al. 1998; Roulston et al. 1999).

To analyze the effects of HIV-1 infection on T-cell transcription, we used a cell line to minimize heterogeneous host-cell responses to infection and to allow the precise enumeration of infected cells. CEM-GFP cells are a CD4<sup>+</sup> lymphoblastoid T-cell line modified to express the green fluorescent protein upon productive HIV-1 infection (Gervaix et al. 1997). When infected by HIV-1, this cell line undergoes characteristic changes including cell-cycle retardation in G2/M, apoptosis, and high levels of virion production.

## RESULTS

CEM-GFP cells were inoculated with HIV-1<sub>LAI</sub> at a multiplicity of infection of 0.5, an inoculum sufficient to ensure that every cell is contacted by virus particles. Aliquots of cells were ob-

tained at 0.5, 2, 4, 8, 16, 24, 48, and 72 h after infection. A mock infection served as a control at each time point, essentially replacing the volume of viral input by an equivalent volume of culture medium from uninfected cells. Each sample was tested on two chips and the average taken. Normalization was done using global normalization and scaling.

At 72 h, HIV-1 transcripts represented more than 30% of all mRNAs present (identical amounts of labeled RNA for control or infected conditions were loaded onto the arrays). This was determined by assessing the level of GAPDH. The average difference value for GAPDH (spanning the whole length of the gene and representing the summation of 198 independent probes) at 30 min in the HIV-infected cells was  $18\,462 \pm 2027$  compared to  $12\,246 \pm 1318$  at 72 h. A similar reduction also was corroborated with  $\beta$ -actin probes. This reduction of mRNA expression is consistent with previously published results (Somasundaran et al. 1988). This intense viral replication was confirmed in the CEM-GFP cells and in primary-activated CD4<sup>+</sup> T lymphocytes as monitored by real-time kinetic RT-PCR. The levels of transcription representative of all doubly and singly spliced (*tat* and *vpr*, respectively) as well as all unspliced (*gag*) messages were measured. Fold increases in the levels of expression of each of these three HIV-1 mRNAs were determined at 48 and 72 h for both infected CEM-GFP cells and primary CD4<sup>+</sup> T cells and compared to that obtained at 24 h. The increased expression was similar in both cell types except that *gag* was expressed at higher levels in the CEM-GFP cells (Table 1). *Tat* was the gene with the greatest increase in expression, being up-regulated 315-fold at 72 h when compared to the level determined at 24 h.

The percentages of CEM-GFP cells productively infected,

<sup>8</sup>Corresponding author.

E-MAIL [jcorbeil@ucsd.edu](mailto:jcorbeil@ucsd.edu); FAX (858) 552-7445.

Article published on-line before print: *Genome Res.*, 10.1101/gr.180201.  
Article and publication are at <http://www.genome.org/cgi/doi/10.1101/gr.180201>.

**Table 1.** Expression of HIV Transcripts

HIV transcript	Cell type	24 h	48 h	72 h
tat	Primary	1	12.9	315.6
	CEM-GFP	1	9.4	211.0
vpr	Primary	1	8.0	35.5
	CEM-GFP	1	26.3	82.3
gag	Primary	1	7.1	21.8
	CEM-GFP	1	23.2	193.6

Real-time PCR quantification of *tat*, *vpr*, and *gag*. The level obtained at 24 h was arbitrarily given a value of 1.

the level of apoptosis, and cell-cycle profiles were assessed and collected at 24, 48, and 72 h after infection using flow cytometry. At 24 h, 29% of the cells were HIV-1-infected as reflected by green fluorescent protein (GFP) expression with ~9% of the cells apoptotic as determined by the proportion of cells with sub-G1 DNA content. At 48 h, 86% of the cells were GFP positive and 22% apoptotic, while at 72 h, 92% were GFP positive and 33% apoptotic (Fig. 1A,B). Orange-fluorescent tetramethylrosamine was used to detect membrane potential changes in mitochondria, a marker of induction of apoptosis. Mitochondrial membrane potential was reduced over time, specifically in HIV-1-infected cells as defined by the intersection of GFP positivity and low orange-fluorescent tetramethylrosamine signal (CMTMRos, bottom right quadrant in Fig. 1B). Uninfected cells in the inoculated culture retained mitochondrial membrane potential, a clear indication that HIV-1 infection altered the membrane potential of mitochondria in infected but not bystander cells. At 72 h, 30% of GFP-positive cells had low mitochondrial transmembrane potential as measured by CMTMRos staining in contrast to <1% of GFP-negative cells (Fig. 1B). To confirm the apoptotic phenotype, caspase activity was assessed. Caspases 2, 3, and 9 but not 6 and 8 were found to be activated in HIV-1 inoculated cell population (Fig. 1C).

Total RNA isolated at each time point for both control and infected CEM-GFP was reverse transcribed, and labeled RNA (cRNA) was generated. cRNA (15 $\mu$ g) was hybridized to HuGeneFL 6800 array. Genes expressed in infected or uninfected cell populations and those common to both were determined for each of the eight time points using GeneChip analysis suite 3.1 and 2HAPI (High-density Array Pattern Interpreter) software packages (Fig. 2). At 30 min after inoculation, 181 genes were expressed only in the HIV-inoculated cells, representing genes that were induced by HIV-1 binding or entry. In contrast, 588 genes were expressed only in the control population, representing genes that are suppressed by exposure to HIV-1. Most of the modulation in gene expression affected genes expressed at lower copy number (the data can be viewed and queried at our 2HAPI web site located at <http://2hapi.ucsd.edu>). A general downregulation of gene expression occurred over time, especially in the HIV-1 infected population. At 72 h, transcripts of 760 genes were called present in the HIV-1-infected cells (summation of genes expressed solely in HIV-infected cells and genes common to both control and HIV-infected cells) and 805 genes were detected in the control cells representing a downmodulation compared to the earlier time points. Two independent processes are operating; in the infected population, the cells are killed by HIV infection and in the control, the culture reaches

confluence. This also was confirmed by the hierarchical cluster analysis expressing ratios of expression of HIV over controls. An impressive shutdown of numerous genes was observed.

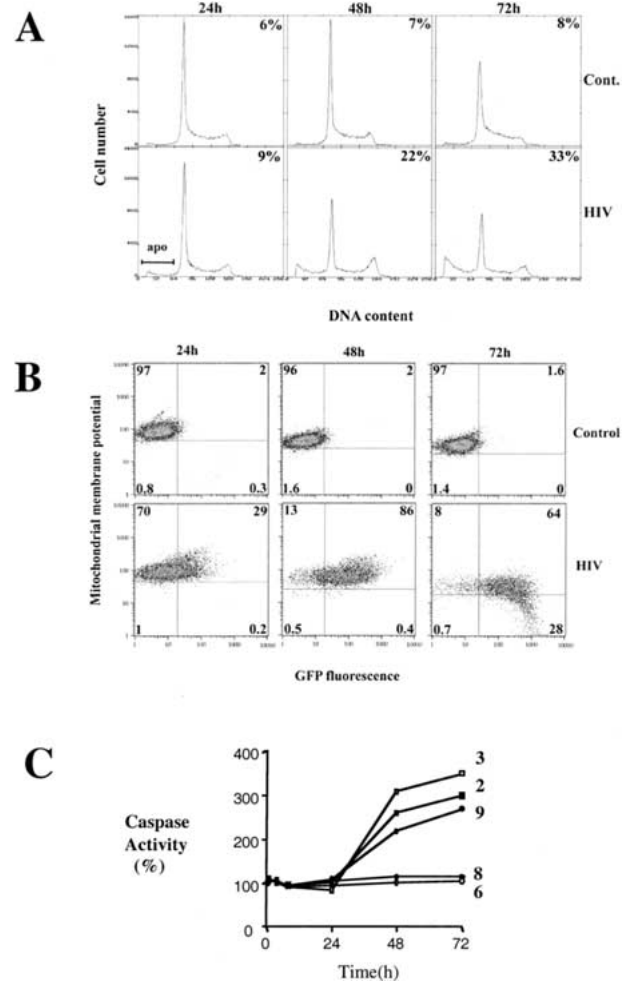


**Figure 1** Analysis of DNA content, cell cycle, percentage of infected cells, mitochondrial membrane potential, and caspase activity. (A) Cell cycle analysis and quantification of apoptosis. Control (mock-infected) and human immunodeficiency virus type 1 (HIV-1)-infected CEM-GFP cells were processed after 24 h, 48 h, and 72 h for DNA content using propidium iodide staining. An assessment of the percentage undergoing apoptosis (upper right corners) was performed by estimating the proportion of cells with subgenomic content of DNA (labeled apo in the figure). The percentages for 24 h, 48 h, and 72 h were 9%, 22%, and 33%, respectively. (B) Determination of the percentage of HIV-infected cells and evaluation of the mitochondrial membrane potential ( $\Delta\psi_m$ ). The percentage of GFP-positive cells (cumulative of the percentage present in top and bottom right quadrants) is an assessment of the number of cells productively infected. The percentages for 24 h, 48 h, and 72 h were 29%, 86%, and 92%, respectively. Cells were gated initially using forward and side scatter criteria to exclude dead cells. Orange-fluorescent tetramethylrosamine was used to assess the mitochondrial transmembrane potential. Gating on live cells only, 28% of cells that were GFP positive (92%) showed reduced staining at 72 h. (C) Cells were infected with HIV-1<sub>LAI</sub> at 0.5 MOI. At the indicated time points,  $2 \times 10^6$  cells were washed with PBS and lysed in caspase buffer. Caspase activity of 10–20  $\mu$ g of total protein was measured with specific substrates for caspase-2 (■), 3 (□), 6 (○), 8 (◆) and 9 (●) (100  $\mu$ M) after 1 h incubation at 37°C.

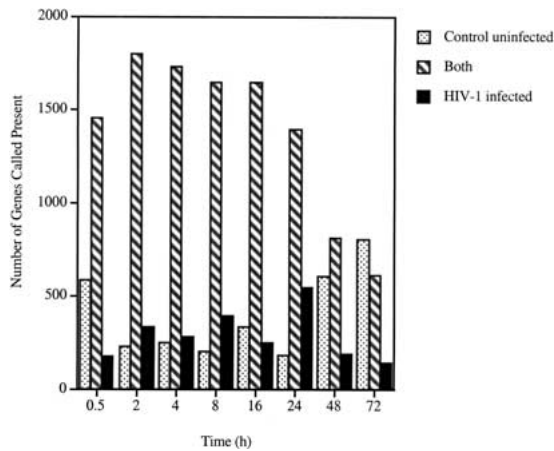


**Figure 2** Genes expressed in control uninfected and HIV-1-infected cells. Stringent criteria were used for calling a gene present (i.e., a gene that can be reliably detected and quantitated with accuracy). A general down-regulation, especially with the HIV-infected population, can be noted. Genes that are expressed in control only increase from 184 at 24 h to 805 at 72 h, while genes specific for HIV-infected cells number 549 at 24 h and 148 at 72 h. Genes expressed in both populations diminish over time as more genes are shut down in the HIV-infected cell population.

Genes expressed early in HIV-1 infection (0.5, 2, 4, and 8 h) included some that were characteristic of cellular defense mechanisms. These included members of the interferon alpha family (accession no. J00212) at 2 h, 4 h, and 8 h, and MxB (accession no. M30818), an antiviral interferon-alpha/beta-inducible protein belonging to the family of large GTPases, at 30' and 2 h (Melen et al. 1996). Genes were grouped in clusters according to patterns of coordinated expression over time (Tamayo et al. 1999). A group of 12 representative clusters represented the best fit with the most distinctive patterns of expression (see supplemental information Fig. A). Cluster 9 shows an impressive increase in later time points for 333 genes. Conversely, cluster 3 represents genes that were down-regulated with time (421 genes).

The similarities present in each cluster group based on the enumeration of Medical Subject Heading (MeSH) keywords were determined using 2HAPI. This approach also revealed a dysregulation in gene expression associated with keywords such as mitochondria (52 genes), apoptosis (75 genes), p53 (18 genes), and repair (38 genes). Genes in the mitochondrial category included mitochondrial 3-ketoacyl-CoA thiolase beta-subunit of trifunctional protein, a gene located in the mitochondrial matrix (D16481), human cytochrome c-1, located in the mitochondrial inter membrane space (J04444), ATP synthase alpha subunit found in the mitochondrion inner membrane (D14710), cytochrome bc-1 complex core protein II localized in the matrix side of the inner mitochondrial membrane (J04973), aconitase (U80040), and porin, which forms a channel through the mitochondrial outer membrane (L08666). All were down-regulated significantly in later time points, indicative of mitochondrial dysfunction. A partial list can be found in Fig. 3. Genes involved in DNA repair and apoptosis also were significantly repressed. These include DNA-PK (U35835), a DNA damage-activated enzyme responsible for phosphorylating p53 (Cuddihy et al. 1999), HSP70 (L12723), a heat-shock protein capable of inhibiting apoptosis, and HHR23A (D21235), which has been shown to bind to

HIV-1 *vpr* (Withers-Ward et al. 1997; Gragerov et al. 1998). In contrast, GADD45 (growth arrest and DNA-damage-inducible protein: M60974) was slightly elevated.

These observations indicated DNA damage or genotoxic stress and prompted an evaluation of the components of DNA repair pathway in the infected cell population at the protein level. p53 was phosphorylated in HIV-1 infected cells (Fig. 4). p53 acts as an inducer of the potent proapoptotic gene Bax (Miyashita et al. 1995; Marzo et al. 1998), which was up-regulated only in HIV-infected cells (Smith et al. 1994). DNA-damage inducible gene Gadd45 also was up-regulated (Zhan et al. 1999). Human mdm2, an inhibitor of p53 function, was down-regulated, possibly leading to an increase in p53 function and GADD45, a repair-sensing protein, was elevated in the infected population (results not shown). This enhanced expression of p53 protein and its stabilization by phosphorylation may be attributable to DNA breaks induced by the integration of the HIV-1 genome into the host genome, the activation of the NFkB pathway (Wu et al. 1994), or the general genotoxic stress induced by HIV-1 infection. The transcription of most genes ultimately was down-regulated by HIV-1 infection. One of the down-regulated genes has been reported previously by Geiss and collaborators (Geiss et al. 2000). The gene prothymosin alpha (M26708) that is expressed to high levels was down-regulated to the same extent in our own experiments. However, we saw a twofold expression enhancement at 30 min after infection. This points out the importance of determining the expression for multiple time points. The general downregulation contrasts with cytomegalovirus infection of primary human fibroblasts (Zhu et al. 1998) for which remarkable amplification of genes resulted from cytomegalovirus infection before the demise of the target cell. Another analysis of the process of HIV infection was performed using differential display by Ryo et al. (2000). Interestingly, they also suggest that HIV exerts a strong cytopathic effect on the host.

Using the cluster and treeview applications of Eisen et al. (1998), we ordered the genes for similarity of expression over time. The resulting ratios of expression for HIV over control were clustered. A section of the hierarchical tree is shown in Figure 5, representing a subset of genes whose expression levels differed by at least fourfold between HIV and control. We focused on a section where expression was increased in HIV-infected cells at the later time point (16 h to 72 h). A selection of these also is shown in supplemental Figure B in our 2HAPI format. Interestingly, several genes were significantly up-regulated.

One such gene identified by the 2HAPI overlap function and the hierarchical clustering was Nuclear Factor I (NFIB-2). This gene was highly expressed at all the later time points (16, 24, 48, and 72 h) during the process of HIV-1 infection. NFIB-2 is part of a family of dimeric DNA-binding proteins with very similar, possibly identical, DNA-binding specificity. These proteins are required for cell-specific transcription of many viral and cellular genes as cellular transcription factors, and as replication factors for adenovirus DNA replication (Qian et al. 1995; Chaudhry et al. 1997). NFIB-2 also has been identified as a recurrent translocation partner gene of high-mobility-group IC (HMGIC) in pleomorphic adenomas (Geurts et al. 1998). This increase in NFIB-2 expression was confirmed using real-time RT-PCR; the values were 3.5-fold greater at 24 h, 10-fold greater at 48 h, and 505-fold greater at 72 h when compared to the mock-infected controls. This increase is remarkable in the face of a general down-regulation

GeneCards Link	Accession # (Entrez link)	UID (PubMed link)	MeSH Term	Relative Expression (HIV- HIV+)	Entrez Description
<a href="#">GeneCard</a>	<a href="#">D16480</a>	<a href="#">94183263</a>	mitochondria		Human mRNA for mitochondrial enoyl-CoA hydratase/3-hydroxyacyl-CoA dehydrogenase alpha-subunit of trifunctional protein, complete cds
<a href="#">GeneCard</a>	<a href="#">L06132</a>	<a href="#">93131931</a>	mitochondria		Human voltage-dependent anion channel isoform 1 (VDAC) mRNA, complete cds
<a href="#">GeneCard</a>	<a href="#">L08666</a>	<a href="#">93280191</a>	mitochondria		Homo sapiens porin (por) mRNA, complete cds and truncated cds
<a href="#">GeneCard</a>	<a href="#">J04444</a>	<a href="#">89109139</a>	mitochondria		Human cytochrome c-1 gene, complete cds

**Figure 3** Selected mitochondrial-associated genes modulated by human immunodeficiency virus (HIV) infection. (Blue) control condition; (red) HIV-infected cells. An additional link to GeneCard, Entrez, and PubMed also are displayed with the Entrez description for the gene. Clicking on the graph itself provides the average difference values and call made by the initial GeneChip analysis suite software. Average difference values of <35 reflects that the gene is not present (includes negative values).

of host-cell mRNA expression in infected cells. Interestingly, expressing this factor constitutively in a Jurkat cell line resulted in decreased production of virus over time as monitored by p24 expression possibly resulting from a reduction in surface expression of the CD4 receptor (data not shown). The role of this factor remains to be fully elucidated in the context of HIV infection. Additionally, this observation was confirmed in primary CD4+ T lymphocytes infected with HIV-1 with a 55-fold increase of this transcript at 24 h (data not shown). Real-time RT-PCR also confirmed that Bax and GADD45 were up-regulated, 2- and 2.1-fold respectively, com-

pared to control cells at 72 h. Bax also was shown to be significantly up-regulated by Western-blot analysis (Fig. 4). Other genes of interest were: SH3GL3, reported to be involved in selective neuronal cell death (Sittler et al. 1998), the type II receptor for interleukin (IL) 1, characteristic of inflammation processes, CD79B (M89957) associated with the immunoglobulin gene superfamily, human pre-T/NK associated protein (CD73) involved in signal transduction associated with increased purine salvage, and the generation of adenosine (Ado) for Ado-receptor signaling (Peola et al. 1996).

## DISCUSSION

This study shows that HIV-1 infection modulates the transcriptional levels of a large number of host genes. Many genes are either suppressed to undetectable levels or are significantly up-regulated very soon after virus inoculation and before the initiation of virus transcription. The changes involved in the culture system (infected and mock infected) are all part of the process encompassing the response of the target cells to productive HIV infection. The mock-infected cells grew normally and cycled normally as seen in Figure 1A, but the HIV-infected cells diverged significantly from the normal cycling phenotype and displayed extensive apoptosis. Fluctuations in gene expression are expected even in normally cycling cells because of differences in proliferation and gen-

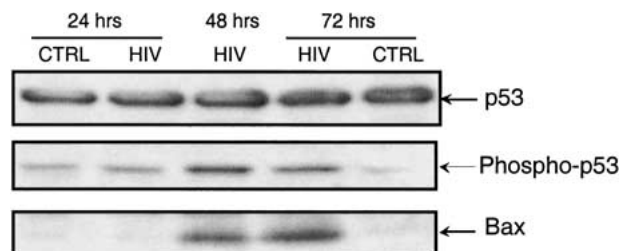


**Figure 4** Western blot for p53, phosphorylated p53, and BAX. p53 concentration remained constant but phosphorylated p53 was markedly increased in HIV 1 at 48 and 72 h, a situation mimicked for BAX.

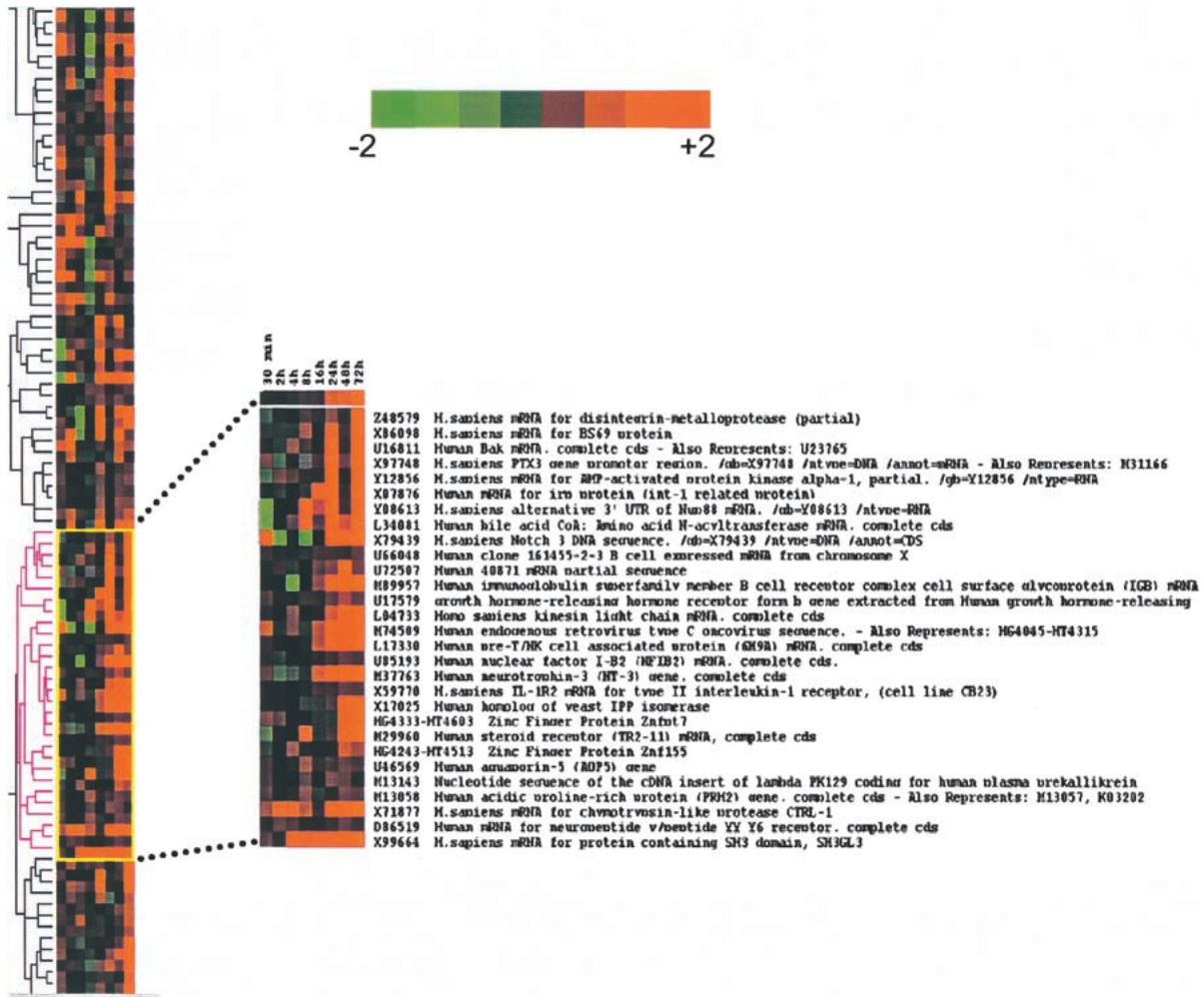


**Figure 5** Hierarchical cluster analysis. We selected genes with average difference values >50 for at least four out of the eight time points. Also, the ratio of the average difference of HIV over control had to be  $\geq 2$  (422 genes met the criteria). The data then were processed using Cluster. The values were log transformed, and self-organizing map was applied (100,000 iterations) prior to generating the hierarchical clusters. The display software Treeview was used to render the figure. Cross section of the tree and magnification of a subset of the hierarchical cluster showing genes that clustered with NFIB-2. These selected genes were overexpressed as compared to control at the later time points. Intensity of color from bright green to bright red (log scale) is shown. (Green) overexpressed in control; (red) overexpressed in HIV-infected population.

eration of different effectors during the course of the experiments. The experiments were done in a cell line expressing the green fluorescent protein, however, we controlled that GFP had little to no impact on the target cell (using cell cycle analysis as in Fig. 1A) compared to the virus by constitutively expressing the protein in the CEM-GFP cell line (results not shown). HIV-1 transcription usurps cellular transcription to such an extent that a marked diminution of host-cell transcription is observed. Changes in transcription include genes that may be essential for mitochondrial function and integrity (Chen et al. 2000) and to DNA repair mechanisms leading directly to the induction of apoptosis of infected cells. This situation applies to productively infected CD4+ T-cell lines and possibly in the acute events following infection in HIV-infected individuals when virus titers are high.

Discovery-driven approaches in genomics using high-density gene expression microarrays have permitted the definition of new avenues of research and the identifica-

tion of pathways and signal transduction events pertinent to the process of HIV-1 infection. High-density microarray interrogation of gene expression represents a powerful tool to dissect the relationships between an infectious agent and its host.

## METHODS

### Cell Culture and Viral Infection

The CEM-GFP CD4+ lymphoblastoid T-cell line was developed as a reporter line to monitor productive HIV infection. A plasmid consisting of the HIV-1 LTR driving the expression of the GFP was introduced in the CEM parental cell line. Upon productive infection, cells express GFP, which can be monitored by flow cytometry. Virus stocks of HIV-1<sub>LAI</sub> were produced and titered in the same cell line and infectivity determined by the method of Karber. CEM-GFP cells were infected at a multiplicity of infection of 0.5 in the presence of polybrene (2  $\mu$ g/mL) added to both mock and HIV-infected cells.

A mock-infected control was processed using supernatant of cultured CEM-GFP cells. All the culture medium (for both mock and infected culture) was removed and replaced with fresh media after the initial 2-h incubation. Aliquots of cells were taken at 0.5, 2, 4, 8, 16, 24, 48, and 72 h after infection for both populations. Cells were washed once with PBS, resuspended in 250  $\mu$ L of PBS to which 750  $\mu$ L of Trizol (Gibco-BRL) was added, and stored at  $-80^{\circ}\text{C}$ .

### CD4+ Lymphocyte Isolation and Infection

CD4+ lymphocytes were isolated from  $\sim 300 \times 10^6$  PBMC using the Vario MACS CD4+ Cell Isolation Kit and Depletion Columns (Miltenyi Biotec) according to the manufacturer's protocol. Purified primary CD4+ T cells were infected with the same strain of HIV-1 at the same multiplicity of infection, two days after stimulation with PHA and addition of IL-2 (20 unit/mL). Aliquots were taken at 2, 24, 48, and 72 h after infection. Cellular and viral messages were quantified using real-time RT-PCR quantification.

### Cell Cycle, Apoptosis, and Mitochondrial Membrane Potential Assays

#### DNA Fragmentation and Cell-Cycle Analysis

Cells ( $2 \times 10^6$ ) were washed in PBS, resuspended in 30% ethanol in PBS, and kept at  $4^{\circ}\text{C}$  until analyzed. Cells then were treated with RNase A (100  $\mu\text{g}/\text{mL}$ ) and stained with 50  $\mu\text{g}/\text{mL}$  of propidium iodide for 1 h at  $37^{\circ}\text{C}$ . Cells were analyzed by flow cytometry as previously described (Telford et al. 1992).

#### Mitochondrial Transmembrane Potential

Cell pellets were resuspended in 100 nM of orange-fluorescent tetramethylrosamine (CMTMRos, Molecular Probes) and incubated at  $37^{\circ}\text{C}$  for 30 min under the normal growth conditions. Cells were washed and fixed in 1% formaldehyde in PBS and analyzed by flow cytometry (Poot et al. 1999).

#### Caspase Activity

Cells were resuspended in caspase buffer (50 mM Hepes, pH 7.4, 100 mM NaCl, 1 mM EDTA, 0.1% Chaps, and 5 mM dithiothreitol) for 10 min at  $4^{\circ}\text{C}$ . Lysates (10–20  $\mu\text{g}$  of total protein) were mixed with 50  $\mu\text{L}$  of HEB buffer (PIPES 50 mM, KCl 20 mM, EGTA 5 mM,  $\text{MgCl}_2$  2 mM, and DTT 1 mM, pH 7), and reactions were initiated by addition of 100  $\mu\text{M}$  of the specific substrate. After 1 h incubation at  $37^{\circ}\text{C}$ , caspase-3-like protease activity was measured by monitoring the digestion of its substrate Ac-DEVD-AMC, caspase-9-like activity using Ac-LEHD-AFC, caspase-6-like protease activity with the substrate Ac-VEID-AMC, caspase-8-like activity with Ac-IETD-AFC, and caspase-2-like activity with Ac-VDVAD-AFC (Calbiochem). Activity was quantified by the release of 7-amino-4-trifluoromethyl-coumarin (AFC) or 7-amino-4-methyl-coumarin (AMC) monitoring fluorescence at excitation and emission wavelengths of 400 and 505 nm, and 380 and 460 nm, respectively, using a fluorimeter (Cytofluor 2000, Millipore).

### Immunoblots

Immunoblot analysis was performed on total-cell lysates of  $5 \times 10^6$  cells in 100  $\mu\text{L}$  RIPA buffer (50 mM TrisHCl, pH 7.4, 50 mM NaCl, 1 mM EGTA, 20 mM glycerophosphate, 0.5% (v/v) Nonidet P-40, 1 mM  $\text{Na}_3\text{VO}_4$ , 1 mM NaF, 1  $\mu\text{g}/\text{mL}$  Aprotinin, 1  $\mu\text{g}/\text{mL}$  leupeptin and 1 mM phenylmethanesulfonyl fluoride (PMSF) at the indicated time points (24, 48, and 72 h). Cell extracts (30  $\mu\text{g}$  per lane) were resolved by SDS-PAGE on 8%–20% gels and transferred on PVDF membranes. The indicated antibodies, p53 and phosphospecific p53(S15) (New England Biolabs, and BAX (N20) (Santa Cruz Biotechnology)

were visualized by alkaline phosphatase-based enhanced chemiluminescence.

### Expression Analysis

The preparation of labeled RNA (cRNA) was performed as described by Affymetrix. The procedure to prepare material for hybridization to the chips involved multiple steps (for more details see our web site at: <http://genomics.ucsd.edu>). We used 10 million cells per time point and condition. Equal amounts of labeled cRNA (15  $\mu\text{g}$ ) were used per GeneChip array. Two chips were used for every time point and condition and the average used for all subsequent analysis. In the case of the HIV-1-infected sample, the viral mRNA contributes significantly to the total RNA loaded into the arrays; however, global normalization and scaling takes account of this contribution. Average difference (intensity of fluorescence) was plotted for duplicate experiments. The variability was within twofold. This was used as our reference for calling a modulation significant (more than twofold). The level of gene expression was normalized for all conditions. The global normalization is a computational technique in which the output of the experimental array is multiplied by a factor (normalization factor) to make the average intensity equivalent to the average intensity of all the other arrays used in the multiple chip experiment. This is based on all probe sets present on the chip. The output yields an intensity of expression and with this and other parameters, a determination of the relative number of copies for a specific mRNA transcript for which an absolute call was made. The data were processed using GeneChip analysis software suite 3.1 (Affymetrix) and then imported into 2HAP1 for further analysis (<http://array.sdsc.edu>).

### Real-Time RT-PCR Quantification

The level of expression of specific transcripts were determined using the Perkin-Elmer ABI Prism 7700 (TaqMan) and Sequence Detection System software. Total RNA was isolated using the TRIzol Method (Gibco-BRL) and then digested with deoxyribonuclease to remove any contaminating genomic DNA. Five micrograms of total RNA was used to generate cDNA using a T7-poly dT oligodeoxynucleotide primer (GGC CAG TGA ATT GTA ATA CGA CTC ACT ATA GGG AGG AGG-T<sub>24</sub>) following the protocol for SuperScript II (Gibco-BRL). Equal amounts of cDNA were used in triplicate and amplified with the Taqman Master Mix provided by Perkin-Elmer. Amplification efficiencies were validated and normalized against GAPDH and fold increases were calculated using the Comparative CT Method for quantitation. The primers and probes used follow: NFIB-2 forward-TCT CAC CAA CGA AGG CTA GGA, reverse-GCT TAT AAA ATG GCT GGC TCA TG probe-CGG CGT CAG AGA TGC TGG GTG A; Bax-alpha forward-CTG ATC AGA ACC ATC ATG GGC, reverse-GAG GCC GTC CCA ACC AC, probe-TCC GGG AGC GGC TGT TGG G, and GADD45 forward-TCT GCA GAT CCA CTT CAC CCT, reverse-GCT GAC GCG CAG GAT GTT, probe-TCC AGG CGT TTT GCT GCG AGA AC. The primers and probes are based on the HIV-1<sub>NL4-3</sub> sequence: tat forward-GCC TTC ATT GCC AAG TTT GTT T, reverse-GTC GCT GTC TCC GCT TCT TC, probe-CAA GAA AAG GCT TAG GCA TCT CCT ATG GCA; vpr forward-GGC AGG AGT GGA AGC CAT AAT A, reverse-CTC TCC TCT GTC GAA TTA TGC CTA T, probe-AAT TCT GCA ACA ACT GCT GTT TAT TCA TTT CAG AA; gag forward-AAA AGA GAC CAT CAA TGA GGA AGC, reverse-TGG TGC AAT AGG CCC TGC, probe-CAG AAT GGG ATA GAT TGC ATC CAG TGC A.

### ACKNOWLEDGMENTS

We thank Drs. Joseph Wong and David Looney for comments and suggestions. This work was supported by the National



Institute of Allergy and Infectious Diseases (AI46237 and AI47703), the Center for AIDS Research Genomics Core laboratory (AI36214), the Universitywide AIDS Research program and the San Diego Veterans Medical Research Foundation (J.C.) as well as NIH grants AI27670, AI38858, AI43638 and AI29164 (D.D.R.) and the San Diego Veterans Affairs Healthcare System.

The publication costs of this article were defrayed in part by payment of page charges. This article must therefore be hereby marked "advertisement" in accordance with 18 USC section 1734 solely to indicate this fact.

## REFERENCES

- Ameisen, J.C. and Capron, A. 1991. Cell dysfunction and depletion in AIDS: The programmed cell death hypothesis. *Immunol. Today* **4**: 102–105.
- Castedo, M., Macho, A., Zamzami, N., Hirsch, T., Marchetti, P., Uriel, J., and Kroemer, G. 1995. Mitochondrial perturbations define lymphocytes undergoing apoptotic depletion *in vivo*. *Eur. J. Immunol.* **25**: 3277–3284.
- Chaudhry, A.Z., Lyons, G.E., and Gronostajski, R.M. 1997. Expression patterns of the four nuclear factor I genes during mouse embryogenesis indicate a potential role in development. *Dev. Dyn.* **208**: 313–325.
- Chen, Q., Gong, B., and Almasan, A. 2000. Distinct stages of cytochrome c release from mitochondrial evidence for a feedback amplification loop linking caspase activation to mitochondrial dysfunction in genotoxic stress induced apoptosis. *Cell Death Differ.* **7**: 227–233.
- Cuddihy, A.R., Wong, A.H., Tam, N.W., Li, S., and Koromilas, A.E. 1999. The double-stranded RNA activated protein kinase PKR physically associates with the tumor suppressor p53 protein and phosphorylates human p53 on serine 392 *in vitro*. *Oncogene* **18**: 2690–2702.
- Eisen, M.B., Spellman, P.T., Brown, P.O., and Botstein, D. 1998. Cluster analysis and display of genome-wide expression patterns. *Proc. Natl. Acad. Sci.* **95**: 14863–14868.
- Geiss, G.K., Bumgarner, R.E., An, M.C., Agy, M.B., van 't Wout, A.B., Hammersmark, E., Carter, V.S., Upchurch, D., Mullins, J.L., and Katze, M.G. 2000. Large-scale monitoring of host cell gene expression during HIV-1 infection using cDNA microarrays. *Virology* **266**: 8–16.
- Gervais, A., West, D., Leoni, L.M., Richman, D.D., Wong-Staal, F., and Corbeil, J. 1997. A new reporter cell line to monitor HIV infection and drug susceptibility *in vitro*. *Proc. Natl. Acad. Sci.* **94**: 4653–4658.
- Geurts, J.M., Schoenmakers, E.F., Roijer, E., Astrom, A.K., Stenman, G., and van de Ven, W.J. 1998. Identification of NFIB as recurrent translocation partner gene of HMGIC in pleomorphic adenomas. *Oncogene* **16**: 865–872.
- Gragerov, A., Kino, T., Ilyina-Gragerova, G., Chrousos, G.P., and Pavlakis, G.N. 1998. HHR23A, the human homologue of the yeast repair protein RAD23, interacts specifically with Vpr protein and prevents cell cycle arrest but not the transcriptional effects of Vpr. *Virology* **245**: 323–330.
- Green, D.R. and Reed, J.C. 1998. Mitochondria and apoptosis. *Science* **281**: 1309–1312.
- Laurent-Crawford, A.G., Krust, B., Muller, S., Rivière, Y., Rey-Cuille, M.A., Bechet, J.M., Montagnier, L., and Hovanessian, A.G. 1991. The cytopathic effect of HIV is associated with apoptosis. *Virology* **185**: 829–839.
- Marzo, I., Brenner, C., Zamzami, N., Jurgensmeier, J.M., Susin, S.A., Vieira, H.L., Prevost, M.C., Xie, Z., Matsuyama, S., Reed, J.C., et al. 1998. Bax and adenine nucleotide translocator cooperate in the mitochondrial control of apoptosis. *Science* **281**: 2027–2031.
- Melen, K., Keskinen, P., Ronni, T., Sareneva, T., Lounatmaa, K., and Julkunen, I. 1996. Human MxB protein, an interferon-alpha-inducible GTPase, contains a nuclear targeting signal and is localized in the heterochromatin region beneath the nuclear envelope. *J. Biol. Chem.* **271**: 23478–23486.
- Miyashita, T. and Reed, J.C. 1995. Tumor suppressor p53 is a direct transcriptional activator of the human bax gene. *Cell* **80**: 293–299.
- Peola, S., Borrione, P., Matera, L., Malavasi, F., Pileri, A., and Massaia, M. 1996. Selective induction of CD73 expression in human lymphocytes by CD38 ligation: a novel pathway linking signal transducers with ecto-enzyme activities. *J. Immunol.* **157**: 4354–4362.
- Poot, M. and Pierce, R.C. 1999. Detection of apoptosis and changes in mitochondrial membrane potential with chloromethyl-X-rosamine. *Cytometry* **36**: 359–360.
- Qian, F., Kruse, U., Lichter, P., and Sippel, A.E. 1995. Chromosomal localization of the four genes (NFIA, B, C, and X) for the human transcription factor nuclear factor I by FISH. *Genomics* **28**: 66–73.
- Roulston, A., Marcellus, R.C., and Branton, P.E. 1999. Viruses and apoptosis. *Annu. Rev. Microbiol.* **53**: 577–628.
- Ryo, A., Suzuki, Y., Arai, M., Kondoh, N., Wakatsuki, T., Hada, A., Shuda, M., Tanaka, K., Sato, C., Yamamoto, M., et al. 2000. Identification and characterization of differentially expressed mRNAs in HIV type 1-infected human T cells. *AIDS Res. Hum. Retroviruses* **16**: 995–1005.
- Sittler, A., Walter, S., Wedemeyer, N., Hasenbank, R., Scherzinger, E., Eickhoff, H., Bates, G.P., Lehrach, H., and Wanker, E.E. 1998. SH3GL3 associates with the Huntingtin exon 1 protein and promotes the formation of polyglutamine-containing protein aggregates. *Mol. Cell.* **2**: 427–436.
- Smith, M.L., Chen, I.T., Zhan, Q., Bae, I., Chen, C.Y., Gilmer, T.M., Kastan, M.B., O'Connor, P.M., and Fornace, Jr., A.J. 1994. Interaction of the p53-regulated protein Gadd45 with proliferating cell nuclear antigen. *Science* **266**: 1376–1380.
- Somasundaran, M. and Robinson, H.L. 1988. Unexpectedly high levels of HIV-1 RNA and protein synthesis in a cytotoxic infection. *Science* **242**: 1554–1557.
- Tamayo, P., Slonim, D., Mesirov, J., Zhu, Q., Kitareewan, S., Dmitrovsky, E., Lander, E.S., and Golub, T.R. 1999. Interpreting patterns of gene expression with self-organizing maps: Methods and application to hematopoietic differentiation. *Proc. Natl. Acad. Sci.* **96**: 2907–2912.
- Telford, W.G., King, L. E., and Fraker, P. J. 1992. Comparative evaluation of several DNA binding dyes in the detection of apoptosis-associated chromatin degradation by flow cytometry. *Cytometry* **13**: 137–142.
- Terai, C., Kornbluth, R.S., Pauza, C.D., Richman, D.D., and Carson, D.A. 1991. Apoptosis as a mechanism of cell death in cultured T lymphoblasts acutely infected with HIV-1. *J. Clin. Invest.* **87**: 1710–1715.
- Withers-Ward, E.S., Jowett, J.B., Stewart, S.A., Xie, Y.M., Garfinkel, A., Shibagaki, Y., Chow, S.A., Shah, N., Hanaoka, F., Sawitz, D.G., et al. 1997. Human immunodeficiency virus type 1 Vpr interacts with HHR23A, a cellular protein implicated in nucleotide excision DNA repair. *J. Virol.* **71**: 9732–9742.
- Wu, H. and Lozano, G. 1994. NF-kappa B activation of p53. A potential mechanism for suppressing cell growth in response to stress. *J. Biol. Chem.* **269**: 20067–20074.
- Zhan, Q., Antinore, M.J., Wang, X.W., Carrier, F., Smith, M.L., Harris, C.C., and Fornace, A.J. Jr. 1999. Association with Cdc2 and inhibition of Cdc2/Cyclin B1 kinase activity by the p53-regulated protein Gadd45. *Oncogene* **18**: 2892–2900.
- Zhu, H., Cong, J.P., Mamtara, G., Gingers, T., and Shenk, T. 1998. Cellular gene expression altered by human cytomegalovirus: global monitoring with oligonucleotide arrays. *Proc. Natl. Acad. Sci.* **95**: 14470–14475.

Received January 18, 2001; accepted in revised form April 2, 2001.



- terotoxin is safe and immunogenic in *Helicobacter pylori*-infected adults. *Gastroenterology* **116**, 804–812 (1999).
4. Gluck, R. *et al.* Safety and immunogenicity of intranasally administered inactivated trivalent virosome-formulated influenza vaccine containing *Escherichia coli* heat-labile toxin as a mucosal adjuvant. *J. Infect. Dis.* **181**, 1129–1132 (2000).
  5. Glenn, G.M., Scharton-Kersten, T., Vassell, R., Matyas, G. & Alving, C.R. Transcutaneous immunization with bacterial ADP-ribosylating exotoxins as antigens and adjuvants. *Infect. Immun.* **67**, 1100–1106 (1999).
  6. Reducing the risk of unsafe injections in immunization programmes: The role of injection equipment. *World Health Organization Expanded Programme on Immunization*. (WHO, Geneva, Switzerland, 1996).
  7. Yu, R., Abrams, D., Alaibac, M. & Chu, A. Morphological and quantitative analyses of normal epidermal Langerhans cells using confocal scanning laser microscopy. *Brit. J. Dermatol.* **131**, 843–848 (1994).
  8. Barry, B.W. Dermatologic formulations. in: *Percutaneous Absorption: Methods, Methodology, Drug Delivery*. (eds. Bronaugh, R.L. & Maibach, H.I.) 33 (Marcel Dekker, New York, 1985).
  9. Kripke, M.L., Dunn, C.G., Jeevan, A., Tang, J. & Bucana, C. Evidence that cutaneous antigen-presenting cells migrate to regional lymph nodes during contact sensitization. *J. Immunol.* **145**, 2833–2838 (1990).
  10. Holmgren, J. *et al.* Antitoxic immunity in experimental cholera: Protection and serum and local antibody responses in rabbits after enteric and parenteral immunization. *Infect. Immun.* **12**, 1331–1340 (1975).
  11. Clemens, J.D. *et al.* Cross-protection by B subunit-whole cell cholera vaccine against diarrhea associated with heat-labile toxin-producing enterotoxigenic *Escherichia coli*: Results of a large-scale field trial. *J. Infect. Dis.* **158**, 372–377 (1988).
  12. Aiba, S. & Katz, S. Phenotypic and functional characteristics of *in vivo* activated Langerhans cells. *J. Immunol.* **145**, 2791–2796 (1990).
  13. Noble, B., Gorfien, J., Frankel, S., Rossman, J. & Brodsky, L. Microanatomical distribution of dendritic cells in normal tonsils. *Acta. Otolaryngol. Suppl. (Stockh)* **523**, S94–S97 (1996).
  14. Glenn, G.M. *et al.* Transcutaneous immunization with cholera toxin protects mice against lethal mucosal toxin challenge. *J. Immunol.* **161**, 3211–3214 (1998).
  15. Glenn, G.M., Scharton-Kersten, T. & Alving, C.R. Advances in vaccine delivery: transcutaneous immunisation. *Exp. Opin. Invest. Drugs* **8**, 797–805 (1999).
  16. Seo, N. *et al.* Percutaneous peptide immunization via corneum barrier-disrupted murine skin for experimental tumor immunoprophylaxis. *Proc. Natl. Acad. Sci. USA* **97**, 371–376 (2000).
  17. Wang, L., Lin J., Hsieh, K. & Lin R. Epicutaneous exposure of protein antigen induces a predominant Th2-like response with high IgE production in mice. *J. Immunol.* **156**, 4077–4082 (1996).
  18. Bouvet, J. & Fischetti, V. Diversity of antibody-mediated immunity at the mucosal barrier. *Infect. Immun.* **67**, 2687–2691 (1999).
  19. Roberts, M.S. & Walker, M. Water, the most natural penetration enhancer. in: *Pharmaceutical Skin Penetration Enhancement* (eds. Walters, K.A. & Hadgraft, J.) 1–30 (Marcel Dekker, New York, 1993).
  20. Cope, R.B. & Colditz, I.G. Effect on systemic antibody concentrations of topical application of cholera toxin to skin of sheep. *Aust. Vet. J.* **78**, 121–123 (2000).
  21. Udey, M.C. Cadherins and Langerhans cells immunobiology. *Clin. Exp. Immunol.* **107** (Suppl. 1), 6–8 (1997).
  22. Bouloc, A., Walker, P., Grivel, J., Vogel J. & Katz, S. Immunization through dermal delivery of protein-encoding DNA: A role for migratory dendritic cells. *Eur. J. Immunol.* **29**, 446–454 (1999).
  23. Scharton-Kersten, T. *et al.* Transcutaneous immunization with bacterial ADP-ribosylating exotoxins, subunits, and unrelated adjuvants. *Infect. Immun.* **68**, 5306–5313 (2000).
  24. Svennerholm, A.-M., Holmgren, J., Black, R., Levine, M. & Merson, M. Serologic differentiation between antitoxin responses to infection with *Vibrio cholerae* and enterotoxin-producing *Escherichia coli*. *J. Infect. Dis.* **147**, 514–522 (1983).
  25. Rudin, A., Riise, G. & Holmgren, J. Antibody responses in the lower respiratory tract and male urogenital tract in humans after nasal and oral vaccination with cholera toxin B subunit. *Infect. Immun.* **67**, 2884–2890 (1999).

## Artificial antigen-presenting cells as a tool to exploit the immune 'synapse'

BERENT PRAKKEN<sup>1</sup>, MARCA WAUBEN<sup>2</sup>, DAVIDE GENINI<sup>3</sup>, RODRIGO SAMODAL<sup>1</sup>, JOELLEN BARNETT<sup>1</sup>, ALBERTO MENDIVIL<sup>1</sup>, LORENZO LEONI<sup>3</sup> & SALVATORE ALBANI<sup>1,4</sup>.

<sup>1</sup>Department of Pediatrics, University of California San Diego, 9500 Gilman Drive, La Jolla, California 92093-0663, USA, <sup>2</sup>Department of Infectious Diseases & Immunology, Utrecht University, Faculty of Veterinary Medicine, PO Box 80165, 3508 TD Utrecht, The Netherlands <sup>3</sup>Department of Medicine, University of California San Diego, 9500 Gilman Drive, La Jolla, California 92093-0663, USA

<sup>4</sup>Androclus Therapeutics, Contrada Torre Allegra, 95030 Catania, Italy  
Correspondence should be addressed to S.A., email: [salbani@ucsd.edu](mailto:salbani@ucsd.edu)

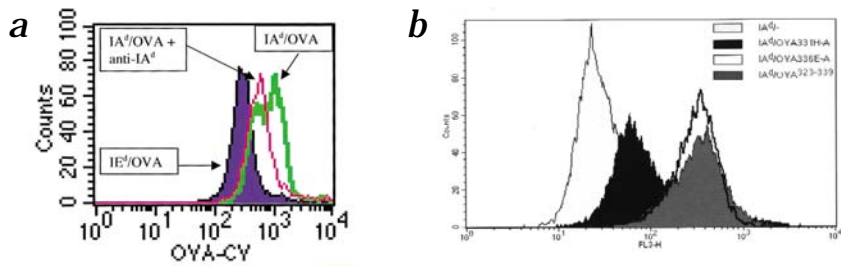
Recent progress in molecular medicine has provided important tools to identify antigen-specific T cells. In most cases, the approach is based on oligomeric combinations of recombinant major histocompatibility complex–peptide complexes fixed to various rigid supports available for binding by the T-cell receptor<sup>1–8</sup>. These tools have greatly increased our insight into mechanisms of immune responses mediated by CD8<sup>+</sup> T cells<sup>1,2</sup>. Examples of the diverse fields of application for this technology include immunization, viral infections and oral tolerance induction<sup>1–6</sup>.

A stable interaction between antigen-presenting cells (APC) and T cells is dependent not only on the absolute affinity between the T-cell receptor (TCR) and its ligand but also on the relative density of molecules available for contact at the interaction site<sup>9</sup>. The proper ligand density is achieved by migration of the relevant molecules toward the initial interaction site, a phenomenon called 'capping', whose outcome is the formation of the immune 'synapse', the machinery required for T-cell signaling<sup>9</sup>. At present, methods for the detection of antigen-specific T cells rely only on absolute affinity between the ligands and do not allow the physiological phenomenon of capping. This may

limit the use of these tools to detection, not manipulation, of antigen-specific T cells. Low-affinity interactions, which may be involved in processes such as autoimmunity, may also be missed<sup>10–14</sup>. So far, examples of successful detection of class II-restricted antigen-specific T cells by oligomeric major histocompatibility complex (MHC)–peptide complexes are also limited<sup>1,2,15–17</sup>.

We have developed a system that mimics the physiological interactions among T cells and APC. We use artificial antigen-presenting cells (aAPC), composed of a liposome, in which MHC class II–peptide molecules are incorporated. The composi-

**Fig. 1** Identification of antigen-specific cells with T-cell capture in a monoclonal TCR population. **a**, OVA<sup>323-339</sup>-IA<sup>d</sup>-specific T-cell hybridoma 8D011B cells were incubated with aAPC in complexes with IA<sup>d</sup> and biotinylated OVA<sup>323-339</sup> and were analyzed by FACS. Before incubation, the hybridoma cells were stained with PE-labeled antibody against CD4, and the aAPC containing IA<sup>d</sup> and biotinylated OVA<sup>323-339</sup> were stained with streptavidin-cychrome. As control for specificity of the binding, 8D011B cells were incubated with aAPC in complexes with IE<sup>d</sup> and biotinylated OVA<sup>323-339</sup>. Binding of hybridoma T cells to aAPC could also be partially inhibited by incubation with monoclonal antibodies against (anti-) IA<sup>d</sup>. Further specificity controls included competition with non-biotinylated peptide during aAPC formation and the use of an irrelevant peptide. Data represent intensity of staining for streptavidin-cychrome (CY) in CD4-gated hybridoma cells (1 experiment of 20). Gates were set on irrelevant isotype controls for CD4, and on binding of cychrome-conjugated streptavidin to T cells-aAPC without biotinylated OVA<sup>323-339</sup>. **b**, OVA<sup>323-339</sup>-IA<sup>d</sup>-specific T-cell hybridoma



DO11.10 cells were incubated with Texas Red-labeled aAPC in complexes with IA<sup>d</sup>-OVA<sup>323-339</sup> (MFI, 373.3) or peptide analogs OVA331H-A (MFI, 77.1) or OVA336E-A and were analyzed by FACS. MHC molecules were preloaded with a 50× molar excess of peptide for 24 h at room temperature and pH 5. Then aAPC were prepared and DO11.10 T-cell hybridomas were incubated with aAPC. As control for specificity of the binding, hybridoma T cells were incubated with aAPC in complexes with IA<sup>d</sup> and HA<sup>126-138</sup>, resulting in low background staining (MFI, 46.9). Data represent intensity of staining for Texas Red (FL3).

tion of these aAPC allows free movement of the MHC-peptide complexes in the artificial membrane. We show here active clustering of TCR-MHC molecules at the immune synapse after interaction between aAPC and T cells. This multivalent system allows identification and stimulation of antigen-specific T cells, thus offering a new tool to study and, in the near future, manipulate immune responses.

#### aAPC as a tool to identify and stimulate T cells

First, we defined optimal conditions for MHC class II-peptide loading and aAPC formation. The size of the aAPC is 60–90 nm and the number of incorporated MHC molecules is 60–160 per aAPC. We evaluated the ability of the aAPC, presenting the synthetic biotinylated peptide ovalbumin consisting of amino acids 323–339 (OVA<sup>323-339</sup>) in the context of MHC class II molecule IA<sup>d</sup>, to allow visualization of the OVA<sup>323-339</sup>-specific, IA<sup>d</sup>-restricted T-cell hybridoma 8D011B, by fluorescence-activated cell sorting (FACS) analysis. The binding to 8D011B was made visible by staining with cychrome-streptavidin-tagged aAPC. We measured 98% binding of the 8D011B hybridoma to the aAPC (Fig. 1a; mean fluorescence intensity (MFI), 821.2). This interaction was specific, as binding was dependent on the presence of the proper MHC-peptide combination (Fig. 1a; mean MFI, 253.6 with MHC class II molecule IE<sup>d</sup>, an ‘incorrect’ MHC), and as it could be partially inhibited by the addition of antibody against MHC (Fig. 1a; mean MFI, 634.3). We achieved 40% reduction in

staining of 8D011B cells when we added equimolar amounts of OVA<sup>323-339</sup> (as a competitive inhibitor) and biotinylated OVA<sup>323-339</sup> (data not shown). Additionally, binding was lost when we replaced biotinylated OVA<sup>323-339</sup> with an irrelevant biotinylated peptide (data not shown).

OVA<sup>323-339</sup> peptide analogs, which have comparable IA<sup>d</sup> binding affinity, differ in activation of DO11.10, an OVA<sup>323-339</sup>-IA<sup>d</sup>-specific T-cell hybridoma<sup>17</sup>. In stimulation assays using spleen cells, peptide analog OVA331H-A seemed to be a weak partial agonist, whereas analog OVA336E-A was a superagonist<sup>17</sup>. The differing responses may have been the result of DO11.10 having different TCR affinity for the IA<sup>d</sup>-peptide analogs. Here, we used aAPC to determine whether these presumed low-affinity TCR-MHC-peptide interactions could be made visible by FACS. DO11.10 hybridoma bound to aAPC with IA<sup>d</sup>-OVA<sup>323-339</sup> complexes (MFI, 373.3) as efficiently as did OVA336E-A-loaded aAPC (Fig. 1b). However, reduced cell-associated fluorescence (MFI, 77.1) resulted when we used OVA331H-A. Binding was lost (MFI, 46.9) when we used irrelevant peptide HA<sup>126-138</sup>. These results indicate that the avidity of the multivalent aAPC is high enough to allow visualization of specific low-affinity TCR interactions.

In related experiments, we stimulated DO11.10 cells with aAPC loaded with OVA<sup>323-339</sup> and measured interleukin (IL)-2 production by intracellular staining by FACS. IL-2 levels were higher than basal production in stimulated cells (MFI for OVA<sup>323-339</sup>, 338.07; basal MFI, 272). We also confirmed this by correspond-

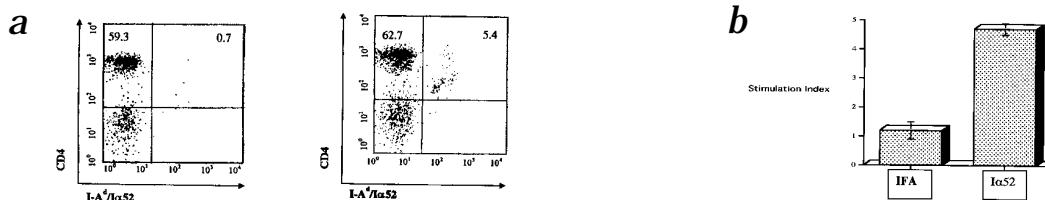
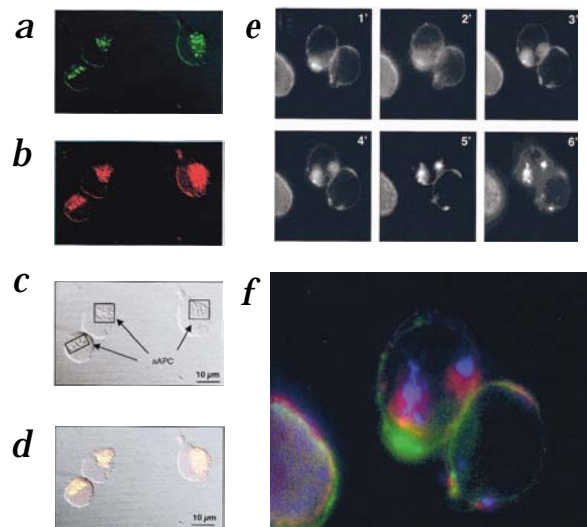


**Fig. 2** Identification by T-cell capture of class II-restricted antigen-specific mouse T cells after immunization. **a**, Increase of IA<sup>d</sup>-α52-specific cells after immunization with α52. Cells were collected from inguinal draining lymph nodes 3 d after the last immunization, stained with PE-labeled antibody against mouse CD4 and incubated with aAPC encompassing IA<sup>d</sup>-biotinylated α52, made visible by the addition of fluoresceinated streptavidin. Left, Mice immunized with incomplete Freund's adjuvant only; right, α52-immunized CD4 cells. Vertical axes, CD4; horizontal axes, aAPC containing IA<sup>d</sup>-α52-

binding T cells. Numbers in upper quadrants represent % of antigen-specific T cells. Conditions: 30× molar excess of α52 peptide:MHC ratio, pH 7.2, 18 h, room temperature. **b**, T-cell proliferation in response to α52 after immunization and *in vitro* expansion. Cells were collected from inguinal lymph nodes and incubated for 3 d with 10 μg/ml α52. No proliferation was detected from cells directly collected from lymph nodes (data not shown). Stimulation index (vertical axis), c.p.m. of stimulated/unstimulated cultures. IFA, incomplete Freund's adjuvant.

**Fig. 3** Interaction of aAPC with T cells induces membrane capping. 8D011B T-cell hybridoma loaded with FITC-CTB, which co-migrates with CD3 molecules (stained in *d* with Alexa-568), were incubated in the presence of aAPC with Ia<sup>d</sup>-OVA<sup>323-339</sup> complexes. **a**, Confocal fluorescence image shows the aggregation of the FITC-CTB in the proximity of the aAPC. **b**, Confocal fluorescence image shows capping of CD3 molecules (detected by binding with Alexa-568 conjugated to antibody against CD3) in exact correspondence with the localization of the CTB. **c**, Nomarsky phase-contrast image of the same cells demonstrates the presence of the aAPC (small circles) on the cell surface, overlapping exactly the capping of the CD3 molecules. **d**, A combined image showing the co-localization of the FITC-CTB, CD3 and aAPC. **e**, Fluorescence images from a time-lapse sequence (1, 2, 3, 4, 5 and 6 min) of FITC-CTB dynamics in T cells interacting with aAPC. There is a progressive increase in fluorescence in the upper cell at about '7 o'clock' and '4 o'clock', followed by an upward movement of the bright fluorescence spots. The lower-right T cell also shows a 'condensation' event at about '6 o'clock'. The cell on the left could be considered a control, as it does not show any visible variations in the diffuse CTB fluorescence. **f**, Three-color overlay of images in *e* to show aAPC-induced membrane capping in T cells. Images at 1, 3 and 5 min were encoded green, red and blue, respectively. The upward shifting of the capping event in the middle cell may be explained by the fact that the cells are not fixed on solid phase, but are embedded in soft agar, and therefore can freely rotate or move.



ing differences in the expression of tyrosine kinases (data not shown).

These preliminary results show that the interaction between aAPC and TCR is essential for the engagement of T-cell activation pathways. Work now in progress will determine whether the addition to the aAPC of co-stimulatory and accessory molecules will provide a fully functional tool to modulate antigen-specific T-cell responses.

To evaluate the efficiency of our aAPC system to identify MHC class II-restricted antigen-specific T cells in a polymorphic population, we studied the expansion *in vivo* of T cells specific for I $\alpha$ 52, a naturally processed, antigenic peptide, presented by IA<sup>d</sup> in BALB/c mice<sup>18,19</sup>. We immunized groups of eight BALB/c mice with either I $\alpha$ 52 in incomplete Freund's adjuvant or with adjuvant alone. Then, 14 days after the last immunization, we collected cells from draining lymph nodes and incubated them with aAPC-presenting IA<sup>d</sup>-biotinylated I $\alpha$ 52 complexes. We found that 5.4% of CD4<sup>+</sup> T cells were I $\alpha$ 52-specific, whereas to I $\alpha$ 52-specific in the immunized mice, whereas only 0.7% of CD4<sup>+</sup> T cells showed staining with the cychrome-streptavidin-tagged aAPC in the mice immunized with incomplete Freund's adjuvant only (Fig. 2a). In contrast, we detected specific T-cell proliferation only when antigen-primed lymph node-derived cells were expanded *in vitro* (Fig. 2b).

#### Interaction of aAPC with T cells allows physiological capping

The immune synapse is the cluster of transmembrane molecules that ensures specific interaction between T cells and APC. The outcome of these interactions is an antigen-specific response by the T cells, mediated by signaling through the TCR. Several factors contribute to the considerable quantitative and qualitative differences in the responses provided by the T cells. These factors include the affinity of the TCR for the MHC-peptide complex and the number of ligands available for interaction<sup>9</sup>. The threshold of response is achieved when enough ligands have migrated to the initial interaction site on the cell surface. aAPC provide hundreds of molecules available for binding by the T cell, and mimic the physiologic interaction between T cell and APC by allowing transmembrane proteins to migrate within the membrane, toward the interaction site. Hence, both high absolute numbers and relative concentrations of interacting molecules

are achieved using aAPC.

We studied the events occurring after the initial interaction between aAPC loaded with IA<sup>d</sup>-OVA<sup>323-339</sup> and the T-cell hybridoma 8D011B. To allow visualization of free movement of the TCR in the T-cell membrane, we used a system in which the migration of sphingolipid cholesterol-rich rafts in the cell membrane is detected with fluorescein isothiocyanate (FITC)-conjugated cholera toxin B (CTB), which binds the GM1 glycosphingolipid<sup>20</sup>. We found co-localization on the cell membrane when we overlapped images of FITC-CTB and TCRs labeled by Alexa-red 568 antibody against CD3, by confocal microscopy (Fig. 3d). The process of TCR-aAPC interaction involved active processes whose outcome was capping, as shown using FITC-CTB to follow the movement of TCR molecules in the T-cell membrane and phase-contrast imaging to allow visualization of the liposomes (<http://medicine.ucsd.edu/albani/movie.mov>). The process of constitution of the immune synapse was completed in approximately 6 minutes, and was strictly aAPC-dependent (Fig. 3e and f). Null MHC-peptide complexes did not bind (data not shown). These data are in full agreement with a report describing the time required by TCR migration to interact with intracellular adhesion molecule 1-MHC-peptide complexes bound to planar membranes<sup>9</sup>. The number of molecular interactions necessary to trigger a T-cell response is estimated to be 200 (ref. 9). Images of T cells at intermediate-to-end stages of capping showed that multiple aAPC were involved in the immune synapse (Fig. 3a-d). Given an average number of 100 MHC-peptide complexes per aAPC, interaction with just a few aAPC may provide the amount of interacting molecules necessary for T-cell activation, when the contact occurs in liquid phase.

In conclusion, we have shown here that aAPC can effectively bind MHC class II-restricted T cells, thus providing an important new tool for the identification and characterization of these cells. aAPC can effectively mimic the physiologic interactions between T cells and APC, particularly in allowing migration of molecules whose accumulation is an essential requirement to induce T-cell activation. This system can be used to study physiological mechanisms of T-cell activation, and, in the near future, to manipulate the intensity and quality of the T-cell response.

## Methods

**Preparation of MHC.** IA<sup>d</sup> and IE<sup>d</sup> molecules were purified from the lysate of B-cell lymphoma A20.11 by immunoaffinity chromatography<sup>21</sup> using monoclonal antibody against IA<sup>d</sup> (MKD6; Pierce, Rockford, Illinois). Affinity-purified MHC molecules were solubilized in a Tris buffer containing 50 mM diethylamine and 2%  $\beta$ -octyl-glucopyranoside (Calbiochem, San Diego, California).

**Peptide loading of MHC class II molecules.** Optimum loading conditions for MHC class II molecules were determined in a MHC class II-peptide-binding assay as described before<sup>22</sup>. Detergent-solubilized MHC class II molecules (3  $\mu$ M) were incubated with a 0.05- to 100-fold molar excess of biotinylated peptide without the addition of protease inhibitors, in the following conditions: pH 5 and pH 7; room temperature and 37 °C; 16, 24 and 40 h of peptide loading; and 0.05-fold, 1-fold, 10-fold, 60-fold and 100-fold molar excess of peptide. MHC-peptide complexes were analyzed using non-reducing SDS-PAGE. After western blot analysis (Highland-ECL; Amersham), the biotinylated peptides were made visible on 'preflushed' films (Hyperfilm; Amersham) through enhanced chemiluminescence (western blot ECL kit; Amersham). Optimum binding conditions were established by evaluation of the density of the spots at the position of the MHC class II dimer-peptide complexes.

**Preparation of lipid solutions.** Phosphatidylcholine (Sigma) and cholesterol (Sigma) were combined in a glass tube at a molar ratio of 7:2. For labeled liposomes, N-(fluorescein-5-thiocarbonyl)-1,2-dihexadecanoyl-sn-glycero-3-phospho-ethanolamine, triethylammonium salt (fluorescein-DHPE) or Texas Red phosphatidylethanolamine (each from Molecular Probes, Eugene, Oregon) was added at a final concentration of 1:1 or 1:2 (molar ratio of fluorescein to phosphatidylcholine), respectively. The solvent was evaporated under an argon stream for 30 min and the lipid film was dispersed at a final concentration of 10 mg/ml in 140  $\mu$ M NaCl and 10  $\mu$ M TrisHCl, pH 8 (buffer A) containing 0.5% sodium deoxycholate. The solution containing mixed micelles was sonicated until it was clear, was separated into aliquots and was stored at -20 °C.

**Preparation of peptides.** Peptide OVA<sup>323-339</sup> (ISQAVHAAHAEINEAGR) and analogs OVA 331H-A (weak agonist; ISQAVHAAAINEAGR) and OVA336E-A (superagonist; ISQAVHAAHAEINAAGR) and peptides HA<sup>126-138</sup> (HNTNGV-TAASSHE) and I $\alpha$ 52 (ASFEAQGALANIADVKA) were synthesized as C-terminal amides and purified by reversed-phase high-performance liquid chromatography. Peptides were N-biotinylated during synthesis (only one biotin molecule/peptide, 100% biotinylation).

**Cell lines.** OVA<sup>323-339</sup>-specific hybridomas 8DO11B and DO11.10 are two different lines from the same clone, using the same TCR (a gift from A. Sette, Epimmune, La Jolla, California).

**T-cell proliferation.** To assess T-cell proliferation in response to I $\alpha$ 52 after immunization and *in vitro* expansion, BALB/c mice 4-6 weeks old (Harlan, Indianapolis, Indiana) were immunized subcutaneously with 100  $\mu$ g I $\alpha$ 52 in complete Freund's adjuvant, followed by immunizations with 100  $\mu$ g I $\alpha$ 52 incomplete

Freund's adjuvant at days 7 and 14 after the initial immunization. Cells were collected from inguinal lymph nodes and incubated for 3 d with 10  $\mu$ g/ml I $\alpha$ 52. Proliferation was measured by thymidine incorporation and is expressed as a stimulation index (c.p.m. of stimulated/unstimulated cultures). T-cell proliferation assays were done on cells directly obtained from lymph nodes or after 3 days of culture with 10  $\mu$ g/ml I $\alpha$ 52. Standard thymidine incorporation techniques were used.

**Preparation of aAPC.** MHC-peptide complexes were added to the lipids in buffer A with deoxycholate at a ratio (weight:weight) of MHC:liposomes of 1:7. Liposomes were formed by detergent removal for 48 h through dialysis at 4 °C against PBS in a 10K Slide A Lyzer (Pierce, Rockford, Illinois), with two changes of solution. When biotinylated peptides were used, the formed aAPC were incubated with streptavidin-cyochrome (PharMingen, San Diego California) for 20 min before the aAPC were added to the cells. For each T-cell capture sample 1  $\mu$ g MHC per 6,000 cells was used.

**Characterization of aAPC by size.** The mean particle sizes of the aAPC were determined both by FACS analysis in comparison with beads of known size, and by dynamic light-scattering analysis with a Malvern 4700 system, using a 25-mW Ne-He laser and automeasure version 3.2 software (Malvern, Herren, Germany)<sup>22</sup>. The particle size distribution as measured by dynamic light-scattering analysis was 63-87 nm.

In the FACS analysis, the size of the FITC-aAPC was compared with the forward scatter of FITC-labeled calibration beads, ranging in size from 40 to 60 nm and from 700 to 900 nm (PharMingen, San Diego, California). This confirmed the mean size of the aAPC as being close to 60 nm.

**Characterization of aAPC by valency.** To allow visualization of MHC incorporation, aAPC were incubated with phycoerythrin (PE)-labeled monoclonal antibodies against MHC class II or PE-labeled isotype controls and were analyzed for PE staining by FACS (ref. 22). MHC incorporation was quantified by the Peterson modification of the Lowry protein assay. To calculate the number of MHC molecules per aAPC, the amount of incorporated MHC (73-100% of the MHC added) and the size of the aAPC, as determined by dynamic light-scattering analysis<sup>22</sup>, were used to convert the amount of incorporated MHC into the number of MHC molecules per aAPC. The number of MHC molecules incorporated in each liposome varied between 60 and 160. The percentage MHC occupancy with a given peptide depended on the peptide used, ranging from 12% to 60% (data not shown).

**Staining of cells for FACS analysis.** Cells were washed twice in standard staining buffer and then incubated at 4 °C for 20 min in FcBlock (PharMingen, San Diego, California). The cells were stained for the surface markers and isotype controls for 20 min at 4 °C, washed twice and resuspended in staining buffer. Monoclonal antibodies against mouse CD3 and CD4, labeled with PE, cyochrome or FITC (PharMingen, San Diego, California), were used.

**T-cell capture.** Cells were incubated with aAPC for 30 min at room temperature. Before acquisition on the FACScalibur (Becton Dickinson, San Jose, California), cells and aAPC were

washed twice (5 min at 500 g) and resuspended in staining buffer. For blocking of binding, aAPC were incubated for 20 min with 50 µg/ml unlabeled antibody against IA<sup>d</sup> (PharMingen, San Diego, California) before being incubated with the cells.

**Stimulation of DO11.10 cells by aAPC and measurement of IL-2 production.** aAPC were prepared as described above. Fresh DO11.10 cells were plated in RPMI with 10% FCS at a density of 60,000 cells/well along with aAPC (10 µg aAPC/well) for 8 h at 37 °C. At the 4-hour time point, monensin (Sigma) was added, at a final concentration of 1 µM. At the 8-hour time point, cells were washed twice and stained for CD3 surface antigen and for intracellular IL-2 (PharMingen, San Diego, California).

**Confocal imaging on fixed cells.** 8DO11B cells were loaded with FITC-CTB (Sigma). Cells (5 × 10<sup>5</sup>/ml; more than 95% viable) and aAPC (0.25 × 10<sup>6</sup> aAPC/ml) were incubated in a volume of 200 µl at room temperature for up to 30 min, placed on ice, and 'cytospun' at 300g for 5 min on poly-L-lysine-coated slides (Sigma). Cells were fixed for 10 min in 4% paraformaldehyde in PBS, washed in PBS, and stained for 1 h at 37 °C with the antibodies against CD3 and IA<sup>d</sup> (PharMingen, San Diego, California) at a concentration of 2 µg/ml in I-Block blocking buffer (Tropix, Bedford, Massachusetts). Alexa 568 (red) secondary antibody (Molecular Probes, Eugene, Oregon) was used to detect the monoclonal antibodies. Images were acquired using a confocal laser-scanning microscope LSM 510 equipped with an argon laser module (Carl Zeiss, Thornwood, New York).

**Time-lapse imaging on fresh cells.** For time-lapse fluorescence on fresh cells, 8DO11B cells were loaded with 8 µg/ml CTB and then layered using a cytospin centrifuge on a glass slide covered with three layers of low-melting-point (42 °C) agarose (0.5%). aAPC (0.25 × 10<sup>6</sup> aAPC/ml) were then gently pipetted over the cells, and a coverslip was added on top of the cells. Fluorescence images were obtained just after the addition of the aAPC every 6 s with a cooled, charged-coupled device camera mounted on a Zeiss Axiophot epifluorescence microscope using a 60 × 1.3-na oil objective (Carl Zeiss, Thornwood, New York).

**Time-lapse imaging on fresh cells.** For time-lapse fluorescence on fresh cells, 8DO11B cells were loaded with 8 µg/ml CTB and then layered using a cytospin centrifuge on a glass slide covered with three layers of low-melting-point (42 °C) agarose (0.5%). aAPC (0.25 × 10<sup>6</sup> aAPC/ml) were then gently pipetted over the cells, and a coverslip was added on top of the cells. Fluorescence images were obtained just after the addition of the aAPC every 6 s with a cooled, charged-coupled device camera mounted on a Zeiss Axiophot epifluorescence microscope using a 60 × 1.3-na oil objective (Carl Zeiss, Thornwood, New York).

*Acknowledgments*

We thank D. Bonnin, D. Schuijffel, S. Nijenhuis and E. Quintela for technical support and assistance. We also thank Nicole Lewon for assistance in editing the manuscript. This study was supported in part by grants NO1-AR40770, NO1-AR44850, NO1-AR72232, NO1-AR41897 and NO1-AR92241. B.P. is supported by the 'Ter Meulenfonds' of the Royal Netherlands Academy of Arts and Sciences and by the Dutch Rheumatoid Arthritis Foundation. M.W. is supported by a fellowship from the Royal Netherlands Academy of Arts and Sciences.

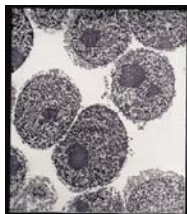
- Altman, J.D. *et al.* Phenotypic analysis of antigen-specific T lymphocytes. *Science* **274**, 94–96 (1996).
- Davis, M.M. *et al.* Ligand recognition by alpha beta T-cell receptors. *Annu. Rev. Immunol.* **16**, 523–544 (1998).
- Lee, P.P. *et al.* Characterization of circulating T cells specific for tumor-associated antigens in melanoma patients. *Nature Med.* **5**, 677–854 (1999).
- Kirsten, J. *et al.* Virus-specific CD8<sup>+</sup> T cells in primary and secondary influenza pneumonia. *Immunity* **8**, 683–691 (1998).
- Mutis, T. *et al.* Tetrameric HLA class I-minor histocompatibility antigen peptide complexes demonstrate minor histocompatibility antigen-specific cytotoxic T lymphocytes in patients with graft-versus-host disease. *Nature Med.* **5**, 839–842 (1999).
- Greten, T. *et al.* Direct visualization of antigen-specific T cells: HTLV-1-specific CD8<sup>+</sup> T cells are activated in peripheral blood and accumulate in CSF from HAM/TSP patients. *Proc. Natl. Acad. Sci. USA* **95**, 7568–7573 (1998).
- Lusembourg, A.T. *et al.* Biomagnetic isolation of antigen-specific CD8<sup>+</sup> T cells usable in immunotherapy. *Nature Biotechnol.* **16**, 281–285 (1998).
- Crawford, F., Kozono, H., White, J., Marrack, P. & Kappler, J. Detection of antigen-specific T cells with multivalent soluble class II MHC covalent peptide complexes. *Immunity* **8**, 675–682 (1998).
- Grakoui, A. *et al.* The immunological synapse: A molecular machine controlling T-cell activation. *Science* **285**, 221–227 (1999).

- Albani, S. *et al.* Positive selection in autoimmunity: Abnormal immune responses to a bacterial dnal antigenic determinant in patients with early rheumatoid arthritis. *Nature Med.* **1**, 448–452 (1995).
- La Cava, A. *et al.* Genetic bias in immune responses to a cassette shared by different microorganisms in patients with rheumatoid arthritis. *J. Clin. Invest.* **100**, 658–663 (1997).
- Anderson, D.E. *et al.* Weak peptide agonists reveal functional differences in B7-1 and B7-2 costimulation of human T-cell clones. *J. Immunol.* **159**, 1669–1675 (1997).
- Nanda, N.K. & Sercarz, E.E. Induction of anti-self-immunity to cure cancer. *Immunity Today* **19**, 495–498 (1998).
- Moalem, G. *et al.* Autoimmune T cells protect neurons from secondary degeneration after central nervous system axotomy. *Nature Med.* **5**, 49–55 (1999).
- Brian, L. *et al.* Use of soluble peptide-DR4 tetramers to detect synovial T cells specific for cartilage antigen in patients with rheumatoid arthritis. *Proc. Natl. Acad. Sci. USA* **97**, 291–296 (2000).
- Rees, W. *et al.* An inverse relationship between T-cell receptor affinity and antigen dose during CD4(+) T-cell responses *in vivo* and *in vitro*. *Proc. Natl. Acad. Sci. USA* **96**, 9781–9786 (1999).
- Janssen, E.M. *et al.* Modulation of Th2 responses by peptide analogues in a murine model of the disease process depends on the Th1 or Th2 skewing characteristics of the therapeutic peptide. *J. Immunol.* **164**, 580–588 (2000).
- Bonnin, D. *et al.* Ontogeny of synonymous T cell populations with specificity for a self MHC epitope mimicked by a bacterial homologue: an antigen-specific T cell analysis in a non-transgenic system. *Eur. J. Immunol.* **29**, 3826–3836 (1999).
- Barton, G.M. & Rudensky, A.Y. Requirement for diverse, low-abundance peptides in positive selection of T cells. *Science* **283**, 67–70 (1999).
- Viola, A., Schroeder, S., Sakakibara, Y. & Lanzavecchia, A. T lymphocyte costimulation mediated by reorganization of membrane microdomains. *Science* **283**, 680–682 (1999).
- Sette, A. *et al.* Effect of pH on MHC class II-peptide interactions. *J. Immunol.* **148**, 844–851 (1992).
- Van Rensen, A.J.M.L., Wauben, M.H.M., Grosfeld-Stulemeyer, M.C., Van Eden, W. & Crommelin, D.J.A. Liposomes with incorporated MHC class II-peptide complexes as antigen presenting vesicles for specific T-cell activation. *Pharm. Res.* **16**, 198–204 (1999).

© 2000 Nature America Inc. • <http://medicine.nature.com>

ON THE MARKET

IN ISOLATION



Nuclei isolation is a snap, says Sigma, with its two new kits.

Easy-to-use nuclei isolation kits are now available from Sigma, which are designed for the reproducible isolation of nuclei with high yield, purity and quality from a variety of mammalian cells and tissues. The Nuclei EZ Prep kit offers a method of nuclei isolation from both suspension and adherent mammalian tissue culture cells. The simultaneous harvest and lysis is said to minimize potential artifacts due to sample handling

time for adherent mammalian cell lines. For more difficult cells, Sigma suggests the Nuclei Pure Prep kit. This kit is designed for the preparation of fragile nuclei and pure nuclei from mammalian cell lines and solid tissues. The protocol incorporates ultracentrifugation through a dense sucrose cushion to protect nuclei and strip away cytoplasmic contaminants. The sucrose cushion concentration can be adjusted to meet





## FUNCTIONAL GENOMIC ANALYSIS OF OSTEOBLASTS CONTACTED BY ORTHOPEDIC IMPLANT PARTICLES

Dominique P. Pioletti<sup>1,6\*</sup>, Lorenzo Leoni<sup>2\*</sup>, Davide Genini<sup>2</sup>, Hiroshi Takei<sup>3</sup>, Pinyi Du<sup>4</sup>, and Jacques Corbeil<sup>4,5+</sup>

Department of Bioengineering<sup>1</sup>, Department of Medicine and The Stein Institute for Research on Aging<sup>2</sup>, Department of Orthopedic<sup>3</sup>, UCSD Center for AIDS Research (CFAR)<sup>4</sup>, University of California, San Diego Veterans Medical Research Foundation<sup>5</sup>, Swiss Institute for<sup>6</sup>

- The authors have contributed equally

Address correspondence to:  
Jacques Corbeil, Ph.D.  
Center for AIDS Research  
University of California San Diego  
9500 Gilman Drive, 0679

La Jolla, CA 92093-0679  
Phone: (858) 552-4339  
Fax: (858) 552-7445  
E-mail: jcorbeil@ucsd.edu

### ABSTRACT

The particles generated from orthopedic implants through a process of wear over years play an essential role in the aseptic loosening of prosthesis. We have investigated the biocompatibility of orthopedic particles on different osteoblast-like cells representative of the different stages of osteoblasts maturation. Particles induced caspase-dependent apoptosis of osteoblasts, immature osteoblasts being the most susceptible. A functional genomic study was performed for the immature osteoblasts in contact to particles. We found that the particles had a profound impact on genes that code for inflammatory cytokines and involved the nucleus architecture. Results from this study suggest that the peri-implant osteolysis following a total joint replacement can be due in part to a decrease of bone formation and not solely to an overstimulation of bone resorption as it is generally proposed. Development of future drugs to control peri-implant osteolysis should promote normal bone formation when particles are present and target osteoblast proliferation to ameliorate the prognosis of patients with orthopedic implants.

### INTRODUCTION

The peri-implant osteolysis following a total joint arthroplasty (TJA) is responsible for the majority of orthopedic implant loosening (1). Failure rates of hip arthroplasty can exceed 30% after 15 years for patients younger than 50 years old (2). A revision surgery where the old implant is replaced by a new one is then performed. Joint disorders treated with TJA can reasonably be expected to give satisfactory results for 20 to 30 years with an initial and revision surgery. After that, no routine procedure exists. The actual trend is to propose TJA to younger patients with the caveat that a second

surgery is likely to be required. Cells response to particles has been identified as a major cause of implant loosening (3). These particles are generated through a process of wear over years. Any of the materials (metallic, polyethylene, methacrylate, ceramic) used for the implants can be involved. In cases of loose titanium implants, the mean concentration of titanium particles retrieved from tissue surrounding the implants could reach 0.1% of the dry tissue weight (4).

A TJA being a mechanical joint, any materials used for the implants will generate wear particles. The solution to the peri-implant osteolysis could reside in the use of drugs that would control the bone remodeling in the surrounding of the implant and therefore prolong its useful life. With this new concept, the etiology of the peri-implant osteolysis induced by wear particles has to be investigated in order to highlight possible targets for drug development.

Normal bone function is assured when an equilibrium between bone formation and bone resorption is maintained. Mostly, the aspect of bone resorption had been studied in relation with wear particles. Macrophages (5), monocytes (6), or giant cells (7) in contact with particles can produce potent osteolytic factors. Effects of implant particles on bone formation has been neglected and should be explored with a particular emphasis toward biocompatibility tests.

Particles from orthopedic implants have been shown to influence the expression of some extracellular matrix proteins in the osteoblasts (8). It has been proposed that biocompatibility tests should include apoptosis studies (9). This is especially important for osteoblasts as apoptosis has been recently shown to be the normal fate for the majority of osteoblasts (10). Moreover, an in vitro study showed that titanium particles can induce apoptosis in osteoblasts (11). The analysis of osteoblast apoptotic pathway and the stimuli that can trigger it warrants investigation, in particular, caspase activity, one of the key enzymes implicated in the induction of apoptosis (12). One important component of the caspase cascade is caspase-3 (13).

The recent advances in molecular biology techniques allow a more comprehensive study of the biological alterations

induced by wear particles in physiologically relevant cells as osteoblasts (14). In this study, we quantified the apoptotic response to titanium (Ti) and polymethylmethacrylate (PMMA) particles in three osteoblast-like cells (human MG-63, rat osteoblast, and human SaOS-2) representative of the different maturation stages of the osteoblasts. The choice of the particles type was based on the fact that titanium is a widely used metal for orthopedic implants and has been demonstrated to generate large amount of particles (4) that can directly interact with the osteoblasts at different stages of their differentiation. PMMA, the bone cement used to seal the orthopedic implant, also generates particles (15) that can be in direct contact with the osteoblasts. A functional genomic study was performed for the immature MG-63 osteoblast-like cells contacted by particles.

Our results demonstrate that implant particles induced and promoted apoptosis especially in immature osteoblasts. Caspase-3 was involved in this process. The particles had a strong effect on gene expression in osteoblasts with an overall trend of gene expression favoring the bone resorption. The results of this study clearly suggest that wear particles from orthopedic implants are involved in the osteolysis not only by favoring the bone resorption as it is generally accepted, but also by inhibiting bone formation and interfering with osteoblasts proliferation. Future drugs developed to control the peri-implant osteolysis should also target the osteoblasts in order to enhance their survival and functions when particles are present.

## MATERIALS AND METHODS

### Particles

Commercially pure titanium particles of -325 mesh nominal diameter were purchased (Aldrich, Milwaukee, WI). The PMMA particles were a gift from Zimmer (Worthington, OH). Particle size distributions were performed by laser diffraction using a Malvern MasterSizer equipment. The values obtained for the different powders are given in Table 1. The particles, sterilized by overnight UV irradiation, were mixed with the culture medium under sterile conditions at a concentration of 0.1% (w/w). This concentration can be considered as representative of the particle concentration found in the surrounding tissue of loose implant in biopsy study (4). The particle solutions were sonicated for 20 minutes in a sealed sterile container to minimize the agglomeration of the particles before being added to the cell culture.

Particles	Density [g/cm <sup>3</sup> ]	d <sub>10</sub> [μm]	d <sub>50</sub> [μm]	d <sub>90</sub> [μm]
Ti	4.5	6.11	18.66	45.57
PMMA	1.1	2.48	48.93	113.69

Table 1. Physical characterizations of the particles used with the size of the Ti and PMMA powders. The size distribution were measured by laser diffraction (Malvern). d<sub>10</sub>, d<sub>50</sub>, d<sub>90</sub> mean that 10%, 50% 90% of the particles have a smaller size than the given size.

### Cell cultures

The gene expression of the osteoblast has been shown to depend on its maturation stage (16). The osteoblast maturation can be evaluated through the production of alkaline phosphatase (17). Three types of osteoblast like cell lines were used to represent three different stages of osteoblast. The human MG-63 osteoblast-like cell (American Type Culture Collection, Rockville, MD) is an immature osteoblast (alkaline phosphatase production: 2.7 μU/μg protein) (18). The rat osteoblast, isolated in our laboratory from neonatal Sprague-Dawley calvaria rat following the procedure of Puelo (17), is a more mature osteoblast (alkaline phosphatase production: 60 μU/μg protein; measurement performed in our laboratory using the Diagnostic kit 245 of Sigma, St.-Louis, MO). Finally, the human SaOS-2 osteoblast-like cell (American Type Culture Collection, Rockville, MD) is a mature osteoblast (alkaline phosphatase production: 5264.4 μU/μg protein) (18). The osteoblasts were seeded at a concentration of 50,000 cells/cm<sup>2</sup> in 50 mm petri dishes and incubated 4 hours to allow adhesion of the cells. The supernatant was removed and 5 ml of particles solution and normal medium was added, defining the time 0. Cells samples were collected at 4 and 24 hours for the genomic study and at 24, 48, and 72 hours for the apoptosis and caspase activity quantification.

### Confocal imaging

MG-63 osteoblast-like cells were cultured 24 hours with 0.1% Ti particles on coverslips. The cells were fixed 10 min. in 4% paraformaldehyde and washed in PBS. To visualize actin filaments, cells were incubated for 1 h at 37°C with Alexa-488-conjugated phalloidin (Molecular Probes, OR); tubulin was visualized using anti-β-tubulin monoclonal antibody, followed by incubation with an Alexa-568 anti-mouse secondary antibody as described in (19) (Molecular Probes, OR). Coverslips were washed successively in PBS and deionized H<sub>2</sub>O for 5 min. and mounted in Fluoromount (Fisher, CA). Images were acquired using a confocal laser scanning microscope LSM 510 equipped with an argon laser module (Carl Zeiss Inc, Thornwood, NY), using a 40x1.3-na oil objective.

### Measurement of DNA fragmentation as apoptosis quantification

The internucleosomal cleavage of genomic DNA has been demonstrated to be a hallmark of apoptosis (20). This fact was used as a quantification of apoptosis induced in the osteoblasts. DNA fragmentation was assessed by flow cytometry. Prior to the analysis, cells were fixed in ice-cold 30% ethanol, and incubated with 100 μg/ml of RNase A and 50 μg/ml propidium iodide for 1 hour at 37°C. FSC/SSC gateway was used to discriminate between particles and cells. Hypodiploid cells were visualized using a Becton-Dickinson FACScalibur, and the program ModFit LT 2.0 (Verity Software House, Topsham).

### Cellular Assay for Caspase Activity

At the indicated time points, cells were washed twice with PBS and the pellet was resuspended in caspase buffer (50 mM HEPES, pH 7.4, 100 mM NaCl, 1 mM EDTA, 0.1% Chaps, and 5 mM dithiothreitol) for 30 min. at 4 °C. Lysates were then stored at -80 °C up to one week. The caspases enzymatic assays were carried out in 96 well plates. Lysates (10-20 µg of total protein) were mixed with 50 µl of caspase buffer, and reactions were initiated by addition of 100 µM of the specific substrate. After 1 hour incubation at 37°C, caspase-3-like protease activity was measured with the substrate Ac-DEVD-AFC. Activity was measured by the release of 7- amino-4-trifluoromethyl-coumarin (AFC) monitoring fluorescence at excitation and emission wavelengths of 400 and 505 nm, respectively.

### Genomic study

The genomic study was performed on the immature MG-63 osteoblast-like cells. We used genefilters (GF211 Research Genetics, Huntsville, AL). We monitored the expression of approximately 4000 genes. The samples (5µg of total RNA per condition) were processed according to the manufacturers recommendations. A duplicate experiment was also performed. The data was analyzed using the pathway software developed by Research Genetics. The 80 genes selected by fold modulation over control were classified in 8 groups (extracellular matrix proteins, cytokines, receptors, enzymes, proteins that regulate nuclear architecture, cell adhesion proteins, apoptosis related proteins, and others) and represented a panel of major genes that are expressed by osteoblasts (16, 21, 22). Three analyses were performed at 4 and 24 hours: control versus Ti, control versus PMMA, and Ti versus PMMA. The difference in gene expression was based on our experimental finding that genes had to be modulated at least 1.5 and 2.5 fold for the 4 and 24 hours experiment, respectively, to be significant in the assay used. There was good concordance between the replicate experiments.

## RESULTS

### Immunocytochemistry

The MG-63 contacted by particles phagocytosed Ti particles present in the culture. View of the osteoblasts at different z-level clearly highlighted that the cytoplasm engulfed the particles. A large number of particles were also found adjacent to the nucleus. The actin filaments organization was profoundly altered when particles were present (Figure 1). Within 24 h, nearly all particles were concentrated in the cytoplasm of the osteoblasts with only a few remaining in the culture wells.

### Apoptosis and caspase-3 activity

The particles were able to induce apoptosis in osteoblast cells as demonstrated by the appearance of hypodiploid DNA-containing cells measured by flow cytometry in permeabilized cells stained with propidium iodide (Figure 2). In addition, the fluorometric measurement of caspase-3-like activity using the

synthetic substrate Ac-DEVD-AFC confirmed the DNA content results (Figure 3). There was a correlation between the presence of hypodiploid cells and caspase activity. The Ti particles had the strongest effect upon immature MG-63 and mature SaOS-2 osteoblast-like cells while the rat osteoblasts appeared more resistant. The PMMA particles were less potent to induce apoptosis than the Ti particles. Control latex particles did not induce any caspase activity despite being phagocytized (results not shown).

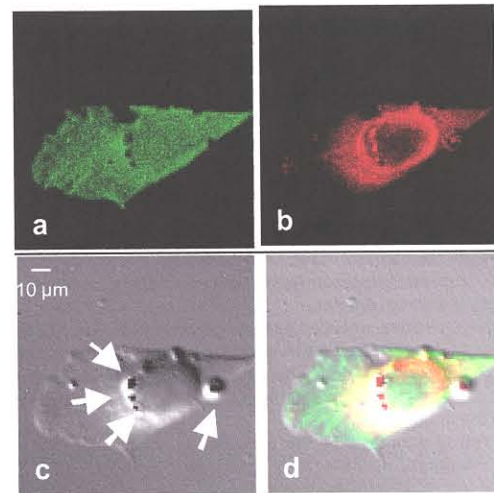


**Figure 1.** Osteoblasts contacted with Ti particles.

MG-63 osteoblast-like cells were cultured 24 hours with 0.1% Ti particles, cells were then fixed and the cytoskeletal alterations visualized by staining with an anti-tubulin antibody (red, microtubules) and FITC-labeled phalloidin (green, actin microfilaments). (a) Confocal fluorescence image shows the distribution of the actin microfilaments of an MG-63 cell. Three dark spots at the center of the cell clearly show the lack of actin filaments in correspondence to the "ingested" titanium particles. (b) Confocal fluorescence image shows the distribution of the microtubules of an MG-63 cell. The three bright red spots at the center of the cells represent the titanium particles that seem to emit strong red autofluorescence. (c) Nomarsky phase contrast image of the same cell demonstrates the presence of the titanium particles ingested by the cell and indicated with the white arrow. (d) A combined image of the figures a, b, and c illustrates the co-localization of the beads with the cytoskeletal alterations.

### Gene expression (MG-63 osteoblast-like cells)

#### Gene modulation after 4 hours co-incubation with Ti particles

After 4 hours co-incubation of Ti particles with MG-63 osteoblast-like cells, 853 genes of the 3964 queried genes had their expression modulated significantly. Of these 853, 32 were found to be of interest with respect to osteoblasts. Twenty one genes were upregulated and 11 downregulated in the Ti group compared to the control group. Little effect on the genetic expression of extracellular matrix proteins (type I collagen, osteonectin, osteopontin, and alkaline phosphatase) was observed, except an upregulation of the fibronectin and osteocalcin genes. The Ti particles had a strong impact on cytokine gene expression with an upregulation of interleukin 1

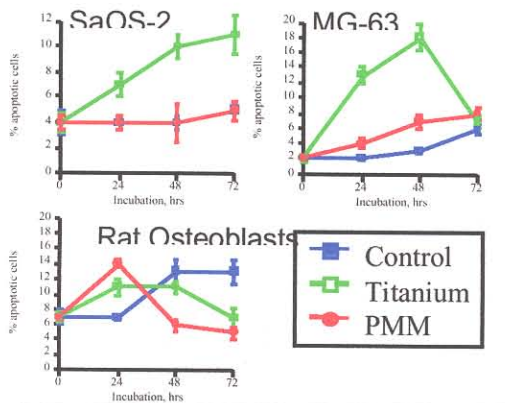


**Figure 2.** Percentage of apoptotic cells in the three osteoblast-like cells used with the two particle types tested. Results are expressed as the means  $\pm$  standard deviation (error bars) and are representative of experiments performed 4 times.

- a) The titanium particles strongly induced apoptosis in the MG-63 osteoblast-like cells while the PMMA particles had a less remarkable effect when compared to control. This trend increased until 48 hours of incubation then no difference was found between the two types of particles and the control.
- b) The induction of apoptosis by the particles was less differentiated for the rat osteoblast. Control cells presented a higher level of apoptotic cells than both particles group after 48 hours of incubation.
- c) The titanium particle was the only one to induce apoptosis in the mature SaOS-2 osteoblast-like cells. This trend increased with longer incubation time.

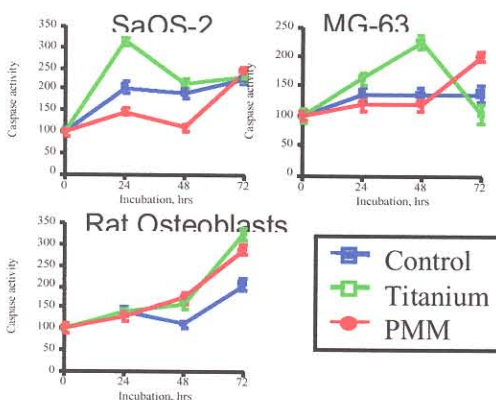


**Figure 3.** Caspase-3-like activity for the three osteoblast cell lines used with the two particle types tested. Results are expressed as the means  $\pm$  standard deviation (error bars) and are representative of experiments performed 4 times.

- a) The caspase activity of immature MG-63 osteoblast-like cells in contact to Ti particles increased over time reaching a peak at 48 hours then returned to the initial level of time  $t=0$ . Unlike for the Ti particles, the caspase activity of osteoblasts in contact to PMMA particles constantly increased with a remarkable increase at 72h. The caspase activity of the control group remained stable for the duration of the experiment.
- b) The rat osteoblasts had a similar caspase activity for the two particles types, that is, a constant increase over time. The control group followed the same pattern with a lower value of caspase activity.

c) The caspase activity of SaOS-2 cells reached a peak after 24h, then decreased and remained stable until 72h. Effect of PMMA particles decreased the caspase activity of SaOS-2 cells when compared to control. However, after 72 hours of incubation, no difference was found between the caspase activity of the SaOS-2 in contact with the two particle types and the control group.

$\alpha$  and  $\beta$  (bone resorption inducer (22)), and TGF  $\beta$  (stimulates osteoblasts growth and differentiation (23)), and a downregulation of fibroblast growth factor (promoter of osteoblast survival (24)) gene. Gene expression for receptors of TNF (bone resorption inducer (22) and proapoptotic agent (24)), interleukin 1 antagonist, insulin-like growth factor (stimulates osteoblast proliferation and differentiation (25)) and tyrosine-protein kinase (stimulate cellular proliferation (26)) were downregulated, while TNF and laminin receptor genes expression were upregulated. A downregulation of the tissue inhibitor of metalloproteinase (TIMP-1) gene expression was detected. This enzyme neutralizes the effect of MMP-1 which can degrade collagen type I (27). The profile of genes modulated in MG-63 osteoblasts by contact with Ti particles appears to favor bone resorption. The Ti particles also had a profound impact on the gene expression of proteins that regulate the nucleus architecture. An upregulation of the Pou and NuMA genes and a downregulation of the HMG and SATB1 genes were observed. These genes belong to the nuclear matrix gene family (21). A downregulation was induced in the actin depolymerizing gene expression as well. The Ti particles also modulated the expression of genes that code for cell adhesion proteins with a downregulation of the integrin  $\beta_1$  ( $\alpha_2\beta_1$  is the major receptor for type I collagen (28)) and an upregulation of laminin  $\gamma_1$ . The apoptosis-related genes p53-binding protein gene was upregulated, the anti-apoptotic BCL2 was downregulated, possibly rendering the cells more prone to undergo apoptotic cell death. The Ti particles had no effect on proliferation genes (c-fos, c-myc, c-jun).

**Gene modulation after 24 hours co-incubation with Ti particles**  
 After 24 hours co-incubation of MG-63 osteoblast-like cells with Ti particles, a less pronounced effect was observed on gene modulation than at the 4 hours time point. Twenty six genes of the 80 initially selected genes had their expression changed. Three genes only were upregulated and 23 downregulated in the Ti group compared to the control group. For the extracellular matrix protein group, no significant effect was observed except a downregulation of collagen type XI. A strong downregulation of TGF  $\beta$  inducible early protein and PDGF was measured. Some changes between the 4 and 24 hours incubation were found in the receptor group with a downregulation of the receptors gene expression of the interleukin 10, colony stimulating factor 3, TGF  $\beta$ , BMP type II, steroid hormone, epidermal growth factor, and tyrosine-protein kinase. The MMP-7 gene expression was downregulated as well as the Pou and YY1 genes. No differences with control were observed for the expression of genes in the adhesion group except for a downregulation of integrin  $\alpha_M$ . The major changes in genes expression as compared to the 4 hours co-incubation results, were found in the cytokines group with a downregulation of the macrophage stimulating 1 and PDGF genes. The proliferation gene c-myc

was downregulated as well as two heat shock protein (1 and 2), fast kinase, and serine/ threonine protein kinase SAK genes.

*Comparison of gene modulation induced by Ti and PMMA particles at both 4 and 24 h.*

After 4 hours co-incubation of MG-63 osteoblast-like cells with particles, we noted no modulation induced by the PMMA particles as compared to the Ti ones for the extracellular matrix group. A downregulation was observed for TGF  $\beta$ , TGF  $\beta$  receptor, steroid hormone receptor, tyrosine-protein kinase receptor, YY1, BCL2, and heat shock protein 1, serine/threonine protein kinase SAK gene expression. An upregulation of macrophage stimulating 1, granulocyte colony-stimulating factor, TNF receptor 1, lamin receptor, integrin  $\beta_1$ , and c-fos genes expression was induced by the PMMA particles compared to the Ti ones. After 24 hours of co-incubation, there was no notable differences in gene expressed by the two types of particles.

## DISCUSSION

Orthopedic implant particles induced apoptosis in osteoblasts in our in vitro model system. This finding extends the results obtained with rat osteoblasts using the terminal deoxynucleotidyl transferase-mediated dUTP-nick end labeling (TUNEL) (11). Caspase-3 was involved in this process. A higher percentage of apoptosis induced by the particles was observed in the immature MG-63 osteoblast-like cells. The increased susceptibility to apoptosis of the immature cells could have important consequences for the bone remodeling. Indeed, if immature osteoblasts prematurely undergo apoptosis as our results indicate, the number of mature osteoblasts which have to synthesize new bone will obviously decrease favoring the resorption process. In addition, it has been shown that Ti particles strongly decreased the osteoblasts viability (11). Particle-induced apoptosis in osteoblast may thus be partly responsible for the osteolysis surrounding orthopedic implants.

The relevance of cell shape and the adherence to substratum in modulating the process of apoptosis has been demonstrated (29). In our case, the particle size may have also played a relevant role in the biological response. The PMMA particles showed a larger size distribution than the Ti particles (c.f. Table 1.). It can be surmised that the higher apoptosis rate induced by the Ti particles may be related to the chemical composition of the particles, but the greater shape changes of the osteoblasts which attached to small particles may also be a contributing factor. This hypothesis requires further testing.

Ti particles had a stronger effect on transcriptional induction of genes in immature MG-63 osteoblast-like cells than the PMMA particles. The effect of particles on gene expression

was rapid as highlighted by the up or down regulation of many genes after 4 hours of being subjected to particles. However, after 24 hours no notable differences were found between the two particle types. It can be speculated, that the initial contact to particles sets the stage for the responses of the cells.

A profound effect of particles on genes that regulate the nuclear and cell architecture was noted. This observation was confirmed by immunocytochemistry which demonstrated a reorganization of the actin filament when particles were present. The effect of particles on osteoblast genes architecture could be explained by the fact that particles phagocytosed by osteoblasts imposed new deformations on the cytoskeleton. In turn these deformations can modulate the expression of genes involved in controlling the architecture of the cell as previously reported (29).

The most striking effect of particles was on the modulation of cytokine genes noticeable after only 4 hours of exposure to particles. It is difficult to interpret the resulting effect of this cytokine genes modulation on potential bone formation. However, there was a trend toward downregulation of cytokines or cytokine receptors involved in bone formation (FGF, TIMP-1, ILGF) and an upregulation of cytokines involved in bone resorption (IL 1 $\alpha$ , IL 1 $\beta$ , TNF). Thus, it is likely that the contact of particles with osteoblasts would favor the bone resorption in vivo.

Interestingly, this study showed that the expression of one major integrin responsible for osteoblast adhesion were downregulated. Because osteoblasts are anchorage-dependent cells, downregulation of adhesion proteins can be responsible for a dysfunction of the cell. Especially for immature osteoblasts, it has been shown that during early maturation stage the osteoblast adhesion proteins are usually upregulated (16). The downregulation of integrin could explain the recent finding that the adhesion strength of osteoblasts in contact with particles was decreased (30). The following succession of events when osteoblasts are in contact with particles can therefore be proposed: osteoblast-particle contact, phagocytosis of particles, decrease of cell adhesion, induction of apoptosis. However, this hypothetical schema needs further validation.

Our study demonstrate the undeniable impact of orthopedic implant particles on osteoblasts. The peri-implant osteolysis following a total joint replacement could be in part attributed to a decrease of bone formation and not only to an overstimulation of bone resorption as it was generally believed. Consequently, development of future drugs designed to control peri-implant osteolysis should target the osteoblasts by promoting their survival by increasing adherence, by favoring the production extracellular bone matrix, and by decreasing the synthesis of osteolytic cytokines.

Research Foundation and UCSD Center for AIDS Research Genomics Core Laboratory.

## ACKNOWLEDGMENTS

This work was supported by Swiss Biology and Medicine Foundation Grant, NIH Grant #GM23200, and the Veterans Medical

## REFERENCES

1. Clarke, I. C., Campbell, P. & Kossovsky, N. (1992) in *Particulate debris from medical implants: mechanisms of formation and biological consequences*, ASTM STP 1144, ed. St. John, K. R. (American Society for testing and materials, Philadelphia), pp. 7-26.
2. Amstutz, H., Dorey, F. J. & Finerman, G. A. M. (1998) in *Total hip arthroplasty outcomes*, eds. Finerman, G. A. M., Dorey, F. J., Grigoris, P. & McKellop, H. A. (Churchill Livingstone, New York), pp. 55-63.
3. Friedman, R. J., Black, J., Galante, J. O., Jacobs, J. J. & Skinner, H. B. (1993) *J Bone Joint Surg* **75-A**, 1086-1109.
4. Salvati, E. A., Foster, B. & Doty, S. B. (1993) *Clin Orthop* **293**, 160-173.
5. Glant, T. T. & Jacobs, J. J. (1994) *J Orthop Res* **12**, 720-731.
6. Lee, S. H., Brennan, F. R., Jacobs, J. J., Urban, R. M., Ragasa, D. R. & Glant, T. T. (1997) *J Orthop Res* **15**, 40-49.
7. Goodman, S. B. & Fornasier, V. L. (1992) in *Particulate debris from medical implants: mechanisms of formation and biological consequences*, ASTM STP 1144, ed. St. John, K. R. (American Society for Testing and Materials, Philadelphia), pp. 27-37.
8. Yao, J., Cs-Szabo, G., Jacobs, J. J., Kuettner, K. E. & Glant, T. T. (1997) *J Bone Joint Surg* **79-A**, 107-112.
9. Eloy, R. & Weill, N. (1997) in *Biocompatibility assessment of medical devices and materials*, ed. Braybrook, J. H. (John Wiley & Sons, London), pp. 124-128.
10. Jilka, R. L., Weinstein, R. S., Bellido, T., Parfitt, A. M. & Manolagas, S. C. (1998) *J Bone Miner Res* **13**, 793-802.
11. Pioletti, D. P., Takei, H., Kwon, S. Y., Wood, D. & Sung, K.-L. P. (1999) *J Biomed Mat Res* **46**, 399-407.
12. Salvesen, G. S. & Dixit, V. M. (1997) *Cell* **91**, 443-446.
13. Rotonda, J., Nicholson, D. W., Fazil, K. M., Gallant, M., Gareau, Y., Labelle, M., Peterson, E. P., Rasper, D. M., Ruel, R., Vaillancourt, J. P., Thornberry, N. A. & Becker, J. W. (1996) *Nature Structural Biology* **3**, 619-625.
14. Puelo, D. A., Preston, K. E., Shaffer, J. B. & Bizios, R. (1993) *Biomaterials* **14**, 111-114.
15. Horowitz, S. M. & Gonzales, J. B. (1996) *Calc Tissue Int* **59**, 392-396.
16. Stein, G. S., Lian, J. B., Stein, J. L., Van Wijnen, A. J. & Montecino, M. (1996) *Physiol Rew* **76**, 593-629.
17. Puelo, D. A., Holleran, L. A., Domerus, R. H. & Bizios, R. (1991) *J Biomed Mater Res* **25**, 711-723.
18. Rifas, L., Fausto, A., Scott, M. J., Avioli, L. V. & Welgus, H. G. (1994) *Endocrinology* **134**, 213-221.
19. Sanders, M. C. & Wang, Y. L. J. (1990) *J Cell Biol* **110**, 359-365.
20. Enari, M., Sakahira, H., Yokoyama, H., Okawa, K., Iwamatsu, A. & Nagata, S. (1998) *Nature* **391**, 43-50.
21. Bidwell, J. P., Alvarez, M., Feister, H., Onyia, J. & Hock, J. (1998) *J Bone Miner Res* **13**, 155-167.
22. Gowen, M. (1994) in *Bone and Mineral Research*, eds. Heersche, J. N. M. & Kanis, J. A. (Elsevier Science, Vol. 8, pp. 77-114.
23. Roodman, G. D. (1993) *Calcif Tissue Int* **53**(Suppl 1), S94-S98.
24. Hill, P. A., Tumber, A. & Meikle, M. C. (1997) *Endocrinology* **138**, 3849-3858.
25. Chevalley, T. H., Rizzoli, R., Manen, D., Caverzasio, J. & Bonjour, J.-P. (1998) *Bone* **23**, 103-109.
26. Siddhanti, S. R. & Quarles, L. D. (1994) *J Cell Bioch* **55**, 310-320.
27. Takagi, M., Santavirta, S., Ida, H., Ishii, M., Mandelin, J. & Konttinen, Y. T. (1998) *Clin Orthop* , 35-45.
28. Xia, G., Wang, D., Bensar, M. D. & Karsenty, G. (1988) *J Biol Chem* **273**, 32988-32994.
29. Chen, C. S., Mrksich, M., Huang, S., Whitesides, G. M. & Ingber, D. E. (1997) *Science* **276**, 1425-1428.
30. Kwon, S. Y., Takei, H., Pioletti, D. P., Lin, T., Ma, Q. J., Akeson, W. H., Wood, D. J. & Sung, K. L. P. (2000) *J. Orthop. Res.* in press.

## ***EPILOGUE***

Many drugs commonly used for the treatment of diseases induce apoptosis. The most common signaling pathway we found activated in our experiments was the intrinsic pathway of apoptosis. This resulted in the release of cytochrome c from mitochondria and activation of the complex Apaf-1 and caspase-9. The execution of the pathway appeared to be the same induced by different drugs as well as for HIV-induced CD4+ depletion. On the other hand the triggering events were distinct. In two of the studied systems we observed p53 activation, but the signaling pathways leading to the cytosolic release of cytochrome c were different. Bcl-2 family members were modulated to shift the equilibrium to the pro-apoptotic side in all the cases studied. It appears that, depending on the cell type and on the apoptosis-inducing stimuli, various Bcl-2 family members can modulate the regulation of apoptosis. So far, a lot is known about the execution of apoptosis, but much more has to be discovered about its initiation. Often, anti-cancer drugs target the signaling events upstream of cytochrome c release, and it is clear that understanding this signaling pathway is fundamental to optimize the drugs ability to induce cell death in cancer cells. This will allow the selection of new specific drugs able to target desired cell types and cell pathways, increasing the toxicity for the neoplastic cells and reducing the side effects on the healthy cells. For this reason the development of new drugs and the study of their mechanism of action is crucially important.

Understanding the biology of a cell provides a basis to interpret how a disease appears in the human body and may help prevent its development. The aim of the lab where I worked the last three years is to synthesize new drugs, to understand how they work in the cell, to identify their molecular targets and to select more potent and selective analogs. My thesis was situated perfectly in this context, in fact the results herein reported help elucidate how nucleoside analogs, the new drug indanocine, and the non-steroidal anti-inflammatory etodolac induce apoptosis in B-CLL cells. Hopefully these results will soon be translated into clinical application for better treatment of cancers.





## REFERENCES

1. Datta, S. R., Brunet, A., and Greenberg, M. E. Cellular survival: a play in three Akts, *Genes and Development*. 13: 2905-27, 1999.
2. Kerr, J. F., Wyllie, A. H., and Currie, A. R. Apoptosis: a basic biological phenomenon with wide-ranging implications in tissue kinetics, *Br J Cancer*. 26: 239-57, 1972.
3. Coucouvanis, E. and Martin, G. R. Signals for death and survival: a two-step mechanism for cavitation in the vertebrate embryo, *Cell*. 83: 279-87, 1995.
4. Brison, D. R. and Schultz, R. M. Apoptosis during mouse blastocyst formation: evidence for a role for survival factors including transforming growth factor alpha, *Biol Reprod*. 56: 1088-96, 1997.
5. Nossal, G. J. Negative selection of lymphocytes, *Cell*. 76: 229-39, 1994.
6. Thompson, C. B. Apoptosis in the pathogenesis and treatment of disease, *Science*. 267: 1456-62, 1995.
7. Raff, M. C., Barres, B. A., Burne, J. F., Coles, H. S., Ishizaki, Y., and Jacobson, M. D. Programmed cell death and the control of cell survival: lessons from the nervous system, *Science*. 262: 695-700, 1993.
8. Shi, L., Nishioka, W. K., Thing, J., Bradbury, E. M., Litchfield, D. W., and Greenberg, A. H. Premature p34cdc2 activation required for apoptosis [see comments], *Science*. 263: 1143-5, 1994.
9. Ploegh, H. L. Viral strategies of immune evasion, *Science*. 280: 248-53, 1998.
10. Isacson, O. On neuronal health [see comments], *Trends Neurosci*. 16: 306-8, 1993.
11. Choi, D. W. Excitotoxic cell death, *J Neurobiol*. 23: 1261-76, 1992.
12. Yoshida, Y. Hypothesis: apoptosis may be the mechanism responsible for the premature intramedullary cell death in the myelodysplastic syndrome, *Leukemia*. 7: 144-6, 1993.
13. Fiers, W., Beyaert, R., Declercq, W., and Vandenabeele, P. More than one way to die: apoptosis, necrosis and reactive oxygen damage, *Oncogene*. 18: 7719-30, 1999.
14. Collin, R. Recherches cytologiques sur le developement de la cellule nerveuse, *Nevraxe*. 8: 181-307, 1906.
15. Horvitz, H. R., Chalfie, M., Trent, C., Sulston, J. E., and Evans, P. D. Serotonin and octopamine in the nematode *Caenorhabditis elegans*, *Science*. 216: 1012-4, 1982.
16. Ellis, R. E., Yuan, J. Y., and Horvitz, H. R. Mechanisms and functions of cell death, *Annu Rev Cell Biol*. 7: 663-98, 1991.
17. Vaux, D. L. and Korsmeyer, S. J. Cell death in development, *Cell*. 96: 245-54, 1999.
18. Hengartner, M. O. and Horvitz, H. R. *C. elegans* cell survival gene *ced-9* encodes a functional homolog of the mammalian proto-oncogene *bcl-2*, *Cell*. 76: 665-76, 1994.
19. Steller, H. Mechanisms and genes of cellular suicide, *Science*. 267: 1445-9, 1995.
20. Fadok, V. A., Bratton, D. L., Rose, D. M., Pearson, A., Ezekewitz, R. A., and Henson, P. M. A receptor for phosphatidylserine-specific clearance of apoptotic cells [see comments], *Nature*. 405: 85-90, 2000.
21. Fadok, V. A., Voelker, D. R., Campbell, P. A., Cohen, J. J., Bratton, D. L., and Henson, P. M. Exposure of phosphatidylserine on the surface of apoptotic lymphocytes triggers specific recognition and removal by macrophages, *J Immunol*. 148: 2207-16, 1992.
22. Trump, B. F., Berezsky, I. K., Chang, S. H., and Phelps, P. C. The pathways of cell death: oncosis, apoptosis, and necrosis, *Toxicol Pathol*. 25: 82-8, 1997.
23. Wyllie, A. H. Cell death: a new classification separating apoptosis from necrosis. *In*: I. D. Bowen and R. A. Lockshin (eds.), *Cell Death in Biology and Pathology*, pp. 9-34. London: Chapman & Hall, 1981.
24. Wynford-Thomas, D. Cellular senescence and cancer, *J Pathol*. 187: 100-11, 1999.
25. Brenner, S. The genetics of *Caenorhabditis elegans*, *Genetics*. 77: 71-94, 1974.
26. Horvitz, H. R., Shaham, S., and Hengartner, M. O. The genetics of programmed cell death in the nematode *Caenorhabditis elegans*, *Cold Spring Harb Symp Quant Biol*. 59: 377-85, 1994.
27. Yuan, J. Y. and Horvitz, H. R. The *Caenorhabditis elegans* genes *ced-3* and *ced-4* act cell autonomously to cause programmed cell death, *Dev Biol*. 138: 33-41, 1990.
28. Thornberry, N. A., Bull, H. G., Calaycay, J. R., Chapman, K. T., Howard, A. D., Kostura, M. J., Miller, D. K., Molineaux, S. M., Weidner, J. R., Aunins, J., and et al. A novel heterodimeric cysteine protease is required for interleukin-1 beta processing in monocytes, *Nature*. 356: 768-74, 1992.

29. Yuan, J., Shaham, S., Ledoux, S., Ellis, H. M., and Horvitz, H. R. The *C. elegans* cell death gene *ced-3* encodes a protein similar to mammalian interleukin-1 beta-converting enzyme, *Cell*. 75: 641-52, 1993.
30. Howard, A. D., Kostura, M. J., Thornberry, N., Ding, G. J., Limjuco, G., Weidner, J., Salley, J. P., Hogquist, K. A., Chaplin, D. D., Mumford, R. A., and et al. IL-1-converting enzyme requires aspartic acid residues for processing of the IL-1 beta precursor at two distinct sites and does not cleave 31-kDa IL-1 alpha, *J Immunol*. 147: 2964-9, 1991.
31. Miura, M., Zhu, H., Rotello, R., Hartweg, E. A., and Yuan, J. Induction of apoptosis in fibroblasts by IL-1 beta-converting enzyme, a mammalian homolog of the *C. elegans* cell death gene *ced-3*, *Cell*. 75: 653-60, 1993.
32. Nicholson, D. W., Ali, A., Thornberry, N. A., Vaillancourt, J. P., Ding, C. K., Gallant, M., Gareau, Y., Griffin, P. R., Labelle, M., Lazebnik, Y. A., and et al. Identification and inhibition of the ICE/CED-3 protease necessary for mammalian apoptosis [see comments], *Nature*. 376: 37-43, 1995.
33. Van de Craen, M., Vandenabeele, P., Declercq, W., Van den Brande, I., Van Loo, G., Molemans, F., Schotte, P., Van Criekinge, W., Beyaert, R., and Fiers, W. Characterization of seven murine caspase family members, *FEBS Lett*. 403: 61-9, 1997.
34. Humke, E. W., Ni, J., and Dixit, V. M. ERICE, a novel FLICE-activatable caspase, *J Biol Chem*. 273: 15702-7, 1998.
35. Hu, S., Snipas, S. J., Vincenz, C., Salvesen, G., and Dixit, V. M. Caspase-14 is a novel developmentally regulated protease, *J Biol Chem*. 273: 29648-53, 1998.
36. Mittl, P. R., Di Marco, S., Krebs, J. F., Bai, X., Karanewsky, D. S., Priestle, J. P., Tomaselli, K. J., and Grutter, M. G. Structure of recombinant human CPP32 in complex with the tetrapeptide acetyl-Asp-Val-Ala-Asp fluoromethyl ketone, *J Biol Chem*. 272: 6539-47, 1997.
37. Thornberry, N. A., Rano, T. A., Peterson, E. P., Rasper, D. M., Timkey, T., Garcia-Calvo, M., Houtzager, V. M., Nordstrom, P. A., Roy, S., Vaillancourt, J. P., Chapman, K. T., and Nicholson, D. W. A combinatorial approach defines specificities of members of the caspase family and granzyme B. Functional relationships established for key mediators of apoptosis, *J Biol Chem*. 272: 17907-11, 1997.
38. Ashkenazi, A. and Dixit, V. M. Death receptors: signaling and modulation, *Science*. 281: 1305-8, 1998.
39. Green, D. R. Apoptotic pathways: the roads to ruin, *Cell*. 94: 695-8, 1998.
40. Wang, S., Miura, M., Jung, Y. K., Zhu, H., Li, E., and Yuan, J. Murine caspase-11, an ICE-interacting protease, is essential for the activation of ICE, *Cell*. 92: 501-9, 1998.
41. Salvesen, G. S. and Dixit, V. M. Caspase activation: the induced-proximity model, *Proc Natl Acad Sci U S A*. 96: 10964-7, 1999.
42. Tachias, K. and Madison, E. L. Converting tissue-type plasminogen activator into a zymogen, *J Biol Chem*. 271: 28749-52, 1996.
43. Muzio, M., Stockwell, B. R., Stennicke, H. R., Salvesen, G. S., and Dixit, V. M. An induced proximity model for caspase-8 activation, *J Biol Chem*. 273: 2926-30, 1998.
44. Yamin, T. T., Ayala, J. M., and Miller, D. K. Activation of the native 45-kDa precursor form of interleukin-1-converting enzyme, *J Biol Chem*. 271: 13273-82, 1996.
45. Yang, X., Chang, H. Y., and Baltimore, D. Essential role of CED-4 oligomerization in CED-3 activation and apoptosis [see comments], *Science*. 281: 1355-7, 1998.
46. Stennicke, H. R., Jurgensmeier, J. M., Shin, H., Deveraux, Q., Wolf, B. B., Yang, X., Zhou, Q., Ellerby, H. M., Ellerby, L. M., Bredesen, D., Green, D. R., Reed, J. C., Froelich, C. J., and Salvesen, G. S. Pro-caspase-3 is a major physiologic target of caspase-8, *J Biol Chem*. 273: 27084-90, 1998.
47. Yang, X., Stennicke, H. R., Wang, B., Green, D. R., Janicke, R. U., Srinivasan, A., Seth, P., Salvesen, G. S., and Froelich, C. J. Granzyme B mimics apical caspases. Description of a unified pathway for trans-activation of executioner caspase-3 and -7, *J Biol Chem*. 273: 34278-83, 1998.
48. Darmon, A. J., Nicholson, D. W., and Bleackley, R. C. Activation of the apoptotic protease CPP32 by cytotoxic T-cell-derived granzyme B, *Nature*. 377: 446-8, 1995.
49. Huang, B., Eberstadt, M., Olejniczak, E. T., Meadows, R. P., and Fesik, S. W. NMR structure and mutagenesis of the Fas (APO-1/CD95) death domain, *Nature*. 384: 638-41, 1996.
50. Chou, J. J., Matsuo, H., Duan, H., and Wagner, G. Solution structure of the RAIDD CARD and model for CARD/CARD interaction in caspase-2 and caspase-9 recruitment, *Cell*. 94: 171-80, 1998.

51. Eberstadt, M., Huang, B., Chen, Z., Meadows, R. P., Ng, S. C., Zheng, L., Lenardo, M. J., and Fesik, S. W. NMR structure and mutagenesis of the FADD (Mort1) death-effector domain, *Nature*. 392: 941-5, 1998.
52. Zou, H., Li, Y., Liu, X., and Wang, X. An APAF-1-cytochrome c multimeric complex is a functional apoptosome that activates procaspase-9, *J Biol Chem*. 274: 11549-56, 1999.
53. Martin, S. J. and Green, D. R. Protease activation during apoptosis: death by a thousand cuts?, *Cell*. 82: 349-52, 1995.
54. Cryns, V. and Yuan, J. Proteases to die for [published erratum appears in *Genes Dev* 1999 Feb 1;13(3):371], *Genes Dev*. 12: 1551-70, 1998.
55. Rheaume, E., Cohen, L. Y., Uhlmann, F., Lazure, C., Alam, A., Hurwitz, J., Sekaly, R. P., and Denis, F. The large subunit of replication factor C is a substrate for caspase-3 in vitro and is cleaved by a caspase-3-like protease during Fas-mediated apoptosis, *Embo J*. 16: 6346-54, 1997.
56. Enari, M., Sakahira, H., Yokoyama, H., Okawa, K., Iwamatsu, A., and Nagata, S. A caspase-activated DNase that degrades DNA during apoptosis, and its inhibitor ICAD [see comments] [published erratum appears in *Nature* 1998 May 28;393(6683):396], *Nature*. 391: 43-50, 1998.
57. Liu, X., Zou, H., Slaughter, C., and Wang, X. DFF, a heterodimeric protein that functions downstream of caspase-3 to trigger DNA fragmentation during apoptosis, *Cell*. 89: 175-84, 1997.
58. Cohen, G. M. Caspases: the executioners of apoptosis, *Biochem J*. 326: 1-16, 1997.
59. Takahashi, A., Alnemri, E. S., Lazebnik, Y. A., Fernandes-Alnemri, T., Litwack, G., Moir, R. D., Goldman, R. D., Poirier, G. G., Kaufmann, S. H., and Earnshaw, W. C. Cleavage of lamin A by Mch2 alpha but not CPP32: multiple interleukin 1 beta-converting enzyme-related proteases with distinct substrate recognition properties are active in apoptosis, *Proc Natl Acad Sci U S A*. 93: 8395-400, 1996.
60. Xue, D. and Horvitz, H. R. *Caenorhabditis elegans* CED-9 protein is a bifunctional cell-death inhibitor, *Nature*. 390: 305-8, 1997.
61. Cheng, E. H., Kirsch, D. G., Clem, R. J., Ravi, R., Kastan, M. B., Bedi, A., Ueno, K., and Hardwick, J. M. Conversion of Bcl-2 to a Bax-like death effector by caspases, *Science*. 278: 1966-8, 1997.
62. Chinnaiyan, A. M., O'Rourke, K., Tewari, M., and Dixit, V. M. FADD, a novel death domain-containing protein, interacts with the death domain of Fas and initiates apoptosis, *Cell*. 81: 505-12, 1995.
63. Stanger, B. Z., Leder, P., Lee, T. H., Kim, E., and Seed, B. RIP: a novel protein containing a death domain that interacts with Fas/APO-1 (CD95) in yeast and causes cell death, *Cell*. 81: 513-23, 1995.
64. Hsu, H., Xiong, J., and Goeddel, D. V. The TNF receptor 1-associated protein TRADD signals cell death and NF-kappa B activation, *Cell*. 81: 495-504, 1995.
65. Hsu, H., Shu, H. B., Pan, M. G., and Goeddel, D. V. TRADD-TRAF2 and TRADD-FADD interactions define two distinct TNF receptor 1 signal transduction pathways, *Cell*. 84: 299-308, 1996.
66. Boldin, M. P., Goncharov, T. M., Goltsev, Y. V., and Wallach, D. Involvement of MACH, a novel MORT1/FADD-interacting protease, in Fas/APO-1- and TNF receptor-induced cell death, *Cell*. 85: 803-15, 1996.
67. Takeuchi, M., Rothe, M., and Goeddel, D. V. Anatomy of TRAF2. Distinct domains for nuclear factor-kappaB activation and association with tumor necrosis factor signaling proteins, *J Biol Chem*. 271: 19935-42, 1996.
68. Saraste, M. Oxidative phosphorylation at the fin de siecle, *Science*. 283: 1488-93, 1999.
69. Newmeyer, D. D., Farschon, D. M., and Reed, J. C. Cell-free apoptosis in *Xenopus* egg extracts: inhibition by Bcl-2 and requirement for an organelle fraction enriched in mitochondria [see comments], *Cell*. 79: 353-64, 1994.
70. Liu, X., Kim, C. N., Yang, J., Jemmerson, R., and Wang, X. Induction of apoptotic program in cell-free extracts: requirement for dATP and cytochrome c, *Cell*. 86: 147-57, 1996.
71. Bossy-Wetzell, E., Newmeyer, D. D., and Green, D. R. Mitochondrial cytochrome c release in apoptosis occurs upstream of DEVD- specific caspase activation and independently of mitochondrial transmembrane depolarization, *Embo J*. 17: 37-49, 1998.
72. Li, P., Nijhawan, D., Budihardjo, I., Srinivasula, S. M., Ahmad, M., Alnemri, E. S., and Wang, X. Cytochrome c and dATP-dependent formation of Apaf-1/caspase-9 complex initiates an apoptotic protease cascade, *Cell*. 91: 479-89, 1997.

73. Li, K., Li, Y., Shelton, J. M., Richardson, J. A., Spencer, E., Chen, Z. J., Wang, X., and Williams, R. S. Cytochrome c deficiency causes embryonic lethality and attenuates stress-induced apoptosis, *Cell*. *101*: 389-99, 2000.
74. Bredesen, D. E. Neural apoptosis, *Ann Neurol*. *38*: 839-51, 1995.
75. Susin, S. A., Zamzami, N., Castedo, M., Hirsch, T., Marchetti, P., Macho, A., Daugas, E., Geuskens, M., and Kroemer, G. Bcl-2 inhibits the mitochondrial release of an apoptogenic protease, *J Exp Med*. *184*: 1331-41, 1996.
76. Susin, S. A., Lorenzo, H. K., Zamzami, N., Marzo, I., Brenner, C., Larochette, N., Prevost, M. C., Alzari, P. M., and Kroemer, G. Mitochondrial release of caspase-2 and -9 during the apoptotic process, *J Exp Med*. *189*: 381-94, 1999.
77. Du, C., Fang, M., Li, Y., Li, L., and Wang, X. Smac, a mitochondrial protein that promotes cytochrome c-dependent caspase activation by eliminating IAP inhibition [In Process Citation], *Cell*. *102*: 33-42, 2000.
78. Verhagen, A. M., Ekert, P. G., Pakusch, M., Silke, J., Connolly, L. M., Reid, G. E., Moritz, R. L., Simpson, R. J., and Vaux, D. L. Identification of DIABLO, a mammalian protein that promotes apoptosis by binding to and antagonizing IAP proteins [In Process Citation], *Cell*. *102*: 43-53, 2000.
79. Hay, B. A., Wassarman, D. A., and Rubin, G. M. Drosophila homologs of baculovirus inhibitor of apoptosis proteins function to block cell death, *Cell*. *83*: 1253-62, 1995.
80. Kaiser, W. J., Vucic, D., and Miller, L. K. The Drosophila inhibitor of apoptosis D-IAP1 suppresses cell death induced by the caspase drICE, *FEBS Lett*. *440*: 243-8, 1998.
81. Wang, S. L., Hawkins, C. J., Yoo, S. J., Muller, H. A., and Hay, B. A. The Drosophila caspase inhibitor DIAP1 is essential for cell survival and is negatively regulated by HID, *Cell*. *98*: 453-63, 1999.
82. Petit, P. X., Susin, S. A., Zamzami, N., Mignotte, B., and Kroemer, G. Mitochondria and programmed cell death: back to the future, *FEBS Lett*. *396*: 7-13, 1996.
83. Marzo, I., Brenner, C., Zamzami, N., Susin, S. A., Beutner, G., Brdiczka, D., Remy, R., Xie, Z. H., Reed, J. C., and Kroemer, G. The permeability transition pore complex: a target for apoptosis regulation by caspases and bcl-2-related proteins, *J Exp Med*. *187*: 1261-71, 1998.
84. Vander Heiden, M. G., Chandel, N. S., Williamson, E. K., Schumacker, P. T., and Thompson, C. B. Bcl-xL regulates the membrane potential and volume homeostasis of mitochondria [see comments], *Cell*. *91*: 627-37, 1997.
85. Antonsson, B., Montessuit, S., Lauper, S., Eskes, R., and Martinou, J. C. Bax oligomerization is required for channel-forming activity in liposomes and to trigger cytochrome c release from mitochondria, *Biochem J*. *2*: 271-8, 2000.
86. Schendel, S. L., Xie, Z., Montal, M. O., Matsuyama, S., Montal, M., and Reed, J. C. Channel formation by antiapoptotic protein Bcl-2, *Proc Natl Acad Sci U S A*. *94*: 5113-8, 1997.
87. Shimizu, S., Narita, M., and Tsujimoto, Y. Bcl-2 family proteins regulate the release of apoptogenic cytochrome c by the mitochondrial channel VDAC [see comments], *Nature*. *399*: 483-7, 1999.
88. Matsuyama, S., Xu, Q., Velours, J., and Reed, J. C. The Mitochondrial F0F1-ATPase proton pump is required for function of the proapoptotic protein Bax in yeast and mammalian cells, *Mol Cell*. *1*: 327-36, 1998.
89. Harris, M. H., Vander Heiden, M. G., Kron, S. J., and Thompson, C. B. Role of oxidative phosphorylation in Bax toxicity, *Mol Cell Biol*. *20*: 3590-6, 2000.
90. Luo, X., Budihardjo, I., Zou, H., Slaughter, C., and Wang, X. Bid, a Bcl2 interacting protein, mediates cytochrome c release from mitochondria in response to activation of cell surface death receptors, *Cell*. *94*: 481-90, 1998.
91. Scaffidi, C., Fulda, S., Srinivasan, A., Friesen, C., Li, F., Tomaselli, K. J., Debatin, K. M., Kramer, P. H., and Peter, M. E. Two CD95 (APO-1/Fas) signaling pathways, *Embo J*. *17*: 1675-87, 1998.
92. Green, D. R. Apoptotic Pathways: Paper Wraps Stone Blunts Scissors, *Cell*. *102*: 1-4, 2000.
93. Yonish-Rouach, E., Resnitzky, D., Lotem, J., Sachs, L., Kimchi, A., and Oren, M. Wild-type p53 induces apoptosis of myeloid leukaemic cells that is inhibited by interleukin-6, *Nature*. *352*: 345-7, 1991.
94. Hansen, R. and Oren, M. p53; from inductive signal to cellular effect, *Curr Opin Genet Dev*. *7*: 46-51, 1997.
95. Evan, G. and Littlewood, T. A matter of life and cell death, *Science*. *281*: 1317-22, 1998.

96. Debbas, M. and White, E. Wild-type p53 mediates apoptosis by E1A, which is inhibited by E1B, *Genes Dev.* 7: 546-54, 1993.
97. Graeber, T. G., Osmanian, C., Jacks, T., Housman, D. E., Koch, C. J., Lowe, S. W., and Giaccia, A. J. Hypoxia-mediated selection of cells with diminished apoptotic potential in solid tumours [see comments], *Nature.* 379: 88-91, 1996.
98. Wagner, A. J., Kokontis, J. M., and Hay, N. Myc-mediated apoptosis requires wild-type p53 in a manner independent of cell cycle arrest and the ability of p53 to induce p21waf1/cip1, *Genes Dev.* 8: 2817-30, 1994.
99. Shieh, S. Y., Ikeda, M., Taya, Y., and Prives, C. DNA damage-induced phosphorylation of p53 alleviates inhibition by MDM2, *Cell.* 91: 325-34, 1997.
100. Xu, Y. and Baltimore, D. Dual roles of ATM in the cellular response to radiation and in cell growth control [see comments], *Genes Dev.* 10: 2401-10, 1996.
101. Mayo, L. D., Turchi, J. J., and Berberich, S. J. Mdm-2 phosphorylation by DNA-dependent protein kinase prevents interaction with p53, *Cancer Res.* 57: 5013-6, 1997.
102. Freedman, D. A. and Levine, A. J. Nuclear export is required for degradation of endogenous p53 by MDM2 and human papillomavirus E6, *Mol Cell Biol.* 18: 7288-93, 1998.
103. Buckley, C. D., Pilling, D., Henriquez, N. V., Parsonage, G., Threlfall, K., Scheel-Toellner, D., Simmons, D. L., Akbar, A. N., Lord, J. M., and Salmon, M. RGD peptides induce apoptosis by direct caspase-3 activation [see comments], *Nature.* 397: 534-9, 1999.
104. Thornberry, N. Caspases and Granzymes. *In: American Association for Cancer Research, San Francisco, CA, April 1-5, 2000 1999, pp. 138.*
105. Tsujimoto, Y., Cossman, J., Jaffe, E., and Croce, C. M. Involvement of the bcl-2 gene in human follicular lymphoma, *Science.* 228: 1440-3, 1985.
106. Vaux, D. L., Cory, S., and Adams, J. M. Bcl-2 gene promotes haemopoietic cell survival and cooperates with c-myc to immortalize pre-B cells, *Nature.* 335: 440-2, 1988.
107. Hockenbery, D., Nunez, G., Milliman, C., Schreiber, R. D., and Korsmeyer, S. J. Bcl-2 is an inner mitochondrial membrane protein that blocks programmed cell death, *Nature.* 348: 334-6, 1990.
108. Oltvai, Z. N., Milliman, C. L., and Korsmeyer, S. J. Bcl-2 heterodimerizes in vivo with a conserved homolog, Bax, that accelerates programmed cell death, *Cell.* 74: 609-19, 1993.
109. Yin, X. M., Oltvai, Z. N., and Korsmeyer, S. J. BH1 and BH2 domains of Bcl-2 are required for inhibition of apoptosis and heterodimerization with Bax [see comments], *Nature.* 369: 321-3, 1994.
110. Borner, C., Martinou, I., Mattmann, C., Imler, M., Schaerer, E., Martinou, J. C., and Tschopp, J. The protein bcl-2 alpha does not require membrane attachment, but two conserved domains to suppress apoptosis, *J Cell Biol.* 126: 1059-68, 1994.
111. Chittenden, T., Flemington, C., Houghton, A. B., Ebb, R. G., Gallo, G. J., Elangovan, B., Chinnadurai, G., and Lutz, R. J. A conserved domain in Bak, distinct from BH1 and BH2, mediates cell death and protein binding functions, *Embo J.* 14: 5589-96, 1995.
112. Muchmore, S. W., Sattler, M., Liang, H., Meadows, R. P., Harlan, J. E., Yoon, H. S., Nettesheim, D., Chang, B. S., Thompson, C. B., Wong, S. L., Ng, S. L., and Fesik, S. W. X-ray and NMR structure of human Bcl-xL, an inhibitor of programmed cell death, *Nature.* 381: 335-41, 1996.
113. McDonnell, J. M., Fushman, D., Milliman, C. L., Korsmeyer, S. J., and Cowburn, D. Solution structure of the proapoptotic molecule BID: a structural basis for apoptotic agonists and antagonists, *Cell.* 96: 625-34, 1999.
114. Chou, J. J., Li, H., Salvesen, G. S., Yuan, J., and Wagner, G. Solution structure of BID, an intracellular amplifier of apoptotic signaling, *Cell.* 96: 615-24, 1999.
115. Minn, A. J., Velez, P., Schendel, S. L., Liang, H., Muchmore, S. W., Fesik, S. W., Fill, M., and Thompson, C. B. Bcl-x(L) forms an ion channel in synthetic lipid membranes, *Nature.* 385: 353-7, 1997.
116. Antonsson, B. and Martinou, J. C. The Bcl-2 protein family, *Exp Cell Res.* 256: 50-7, 2000.
117. Adams, J. M. and Cory, S. The Bcl-2 protein family: arbiters of cell survival, *Science.* 281: 1322-6, 1998.
118. Desagher, S., Osen-Sand, A., Nichols, A., Eskes, R., Montessuit, S., Lauper, S., Maundrell, K., Antonsson, B., and Martinou, J. C. Bid-induced conformational change of Bax is responsible for mitochondrial cytochrome c release during apoptosis, *J Cell Biol.* 144: 891-901, 1999.

119. Eskes, R., Desagher, S., Antonsson, B., and Martinou, J. C. Bid induces the oligomerization and insertion of Bax into the outer mitochondrial membrane, *Mol Cell Biol.* 20: 929-35, 2000.
120. Jurgensmeier, J. M., Xie, Z., Deveraux, Q., Ellerby, L., Bredesen, D., and Reed, J. C. Bax directly induces release of cytochrome c from isolated mitochondria, *Proc Natl Acad Sci U S A.* 95: 4997-5002, 1998.
121. Shimizu, S., Eguchi, Y., Kamiike, W., Funahashi, Y., Mignon, A., Lacronique, V., Matsuda, H., and Tsujimoto, Y. Bcl-2 prevents apoptotic mitochondrial dysfunction by regulating proton flux, *Proc Natl Acad Sci U S A.* 95: 1455-9, 1998.
122. Hockenbery, D. M., Oltvai, Z. N., Yin, X. M., Millman, C. L., and Korsmeyer, S. J. Bcl-2 functions in an antioxidant pathway to prevent apoptosis, *Cell.* 75: 241-51, 1993.
123. Kane, D. J., Sarafian, T. A., Anton, R., Hahn, H., Gralla, E. B., Valentine, J. S., Ord, T., and Bredesen, D. E. Bcl-2 inhibition of neural death: decreased generation of reactive oxygen species, *Science.* 262: 1274-7, 1993.
124. Krajewski, S., Tanaka, S., Takayama, S., Schibler, M. J., Fenton, W., and Reed, J. C. Investigation of the subcellular distribution of the bcl-2 oncoprotein: residence in the nuclear envelope, endoplasmic reticulum, and outer mitochondrial membranes, *Cancer Res.* 53: 4701-14, 1993.
125. Chadebech, P., Brichese, L., Baldin, V., Vidal, S., and Valette, A. Phosphorylation and proteasome-dependent degradation of Bcl-2 in mitotic-arrested cells after microtubule damage, *Biochem Biophys Res Commun.* 262: 823-7, 1999.
126. Dimmeler, S., Breitschopf, K., Haendeler, J., and Zeiher, A. M. Dephosphorylation targets Bcl-2 for ubiquitin-dependent degradation: a link between the apoptosome and the proteasome pathway, *J Exp Med.* 189: 1815-22, 1999.
127. Maundrell, K., Antonsson, B., Magnenat, E., Camps, M., Muda, M., Chabert, C., Gillieron, C., Boschert, U., Vial-Knecht, E., Martinou, J. C., and Arkinstall, S. Bcl-2 undergoes phosphorylation by c-Jun N-terminal kinase/stress-activated protein kinases in the presence of the constitutively active GTP-binding protein Rac1, *J Biol Chem.* 272: 25238-42, 1997.
128. Yamamoto, K., Ichijo, H., and Korsmeyer, S. J. BCL-2 is phosphorylated and inactivated by an ASK1/Jun N-terminal protein kinase pathway normally activated at G(2)/M, *Mol Cell Biol.* 19: 8469-78, 1999.
129. Chinnaiyan, A. M., O'Rourke, K., Lane, B. R., and Dixit, V. M. Interaction of CED-4 with CED-3 and CED-9: a molecular framework for cell death [see comments], *Science.* 275: 1122-6, 1997.
130. Pan, G., O'Rourke, K., and Dixit, V. M. Caspase-9, Bcl-XL, and Apaf-1 form a ternary complex, *J Biol Chem.* 273: 5841-5, 1998.
131. Green, D. R. and Reed, J. C. Mitochondria and apoptosis, *Science.* 281: 1309-12, 1998.
132. Metivier, D., Dallaporta, B., Zamzami, N., Larochette, N., Susin, S. A., Marzo, I., and Kroemer, G. Cytofluorometric detection of mitochondrial alterations in early CD95/Fas/APO-1-triggered apoptosis of Jurkat T lymphoma cells. Comparison of seven mitochondrion-specific fluorochromes, *Immunol Lett.* 61: 157-63, 1998.
133. Zhou, Q., Krebs, J. F., Snipas, S. J., Price, A., Alnemri, E. S., Tomaselli, K. J., and Salvesen, G. S. Interaction of the baculovirus anti-apoptotic protein p35 with caspases. Specificity, kinetics, and characterization of the caspase/p35 complex, *Biochemistry.* 37: 10757-65, 1998.
134. Crook, N. E., Clem, R. J., and Miller, L. K. An apoptosis-inhibiting baculovirus gene with a zinc finger-like motif, *J Virol.* 67: 2168-74, 1993.
135. Yang, Y., Fang, S., Jensen, J. P., Weissman, A. M., and Ashwell, J. D. Ubiquitin protein ligase activity of IAPs and their degradation in proteasomes in response to apoptotic stimuli, *Science.* 288: 874-7, 2000.
136. Deveraux, Q. L. and Reed, J. C. IAP family proteins--suppressors of apoptosis, *Genes Dev.* 13: 239-52, 1999.
137. Thornberry, N. A. and Lazebnik, Y. Caspases: enemies within, *Science.* 281: 1312-6, 1998.
138. Levi-Montalcini, R. The nerve growth factor 35 years later, *Science.* 237: 1154-62, 1987.
139. Clark, E. A. and Brugge, J. S. Integrins and signal transduction pathways: the road taken, *Science.* 268: 233-9, 1995.
140. Yao, R. and Cooper, G. M. Requirement for phosphatidylinositol-3 kinase in the prevention of apoptosis by nerve growth factor, *Science.* 267: 2003-6, 1995.

141. Bellacosa, A., Testa, J. R., Staal, S. P., and Tsichlis, P. N. A retroviral oncogene, akt, encoding a serine-threonine kinase containing an SH2-like region, *Science*. 254: 274-7, 1991.
142. Cardone, M. H., Roy, N., Stennicke, H. R., Salvesen, G. S., Franke, T. F., Stanbridge, E., Frisch, S., and Reed, J. C. Regulation of cell death protease caspase-9 by phosphorylation, *Science*. 282: 1318-21, 1998.
143. Zha, J., Harada, H., Yang, E., Jockel, J., and Korsmeyer, S. J. Serine phosphorylation of death agonist BAD in response to survival factor results in binding to 14-3-3 not BCL-X(L) [see comments], *Cell*. 87: 619-28, 1996.
144. Gordon, M. S., Kato, R. M., Lansigan, F., Thompson, A. A., Wall, R., and Rawlings, D. J. Aberrant B cell receptor signaling from B29 (Igbeta, CD79b) gene mutations of chronic lymphocytic leukemia B cells [In Process Citation], *Proc Natl Acad Sci U S A*. 97: 5504-9, 2000.
145. Lowe, S. W., Ruley, H. E., Jacks, T., and Housman, D. E. p53-dependent apoptosis modulates the cytotoxicity of anticancer agents, *Cell*. 74: 957-67, 1993.



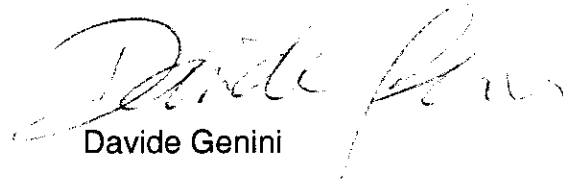


## ***APPENDIX***



I declare that all the data and results contained in this thesis are from my original work and all the collaborations are mentioned in the papers.

Sincerely



Handwritten signature of Davide Genini in black ink, written in a cursive style.

Davide Genini



CURRICULUM VITAE of:

DAVIDE GENINI

of: LEARDO GENINI and ROSANNA GENINI (ENRILE)  
birthdate: 21.21.1971 in BELLINZONA  
Nationality: CH, 6705 CRESCIANO

Current address:  
1665 1/2 Grand Ave.  
San Diego CA 92109 - USA  
Tel. (619) 483 7814

Professional address:  
Department of Medicine  
The Sam and Rose Stein Institute  
University of California San Diego  
Gilman Drive  
La Jolla CA 92093  
Tel. 619 534 53 77  
Fax. 619 534 53 99  
dgenini@ucsd.edu

Permanent address:  
6705 Cresciano TI - CH  
Tel. (091) 863 1503

Elementary school:  
"SCUOLA ELEMENTARE CANTONALE" in CRESCIANO From 1977 to  
1982

Secondary school:  
"SCUOLA MEDIA CANTONALE" in LODRINO from 1982 to 1986

High school: "LICEO CANTONALE" in Bellinzona from 1986 to 1990

Military in Airolo (CH) Sommer 1990

Bachelor: Zürich, 13. November 1996, in Natural science, Biochemistry

College, University:  
EIDGENÖSSISCHE TECHNISCHE HOCHSCHULE ZÜRICH from  
1991 to 1996

Thesis title: "Development of an Assay for Long Term Culture on Stroma and in Liquid Culture for the Pre-clinical Testing of Anticancer Agent's Hematotoxicity" carried out in the Laboratory of Oncology at the "Ospedale regionale di Locarno" directed by Prof. F. Cavalli, under the supervision of Dr. Michele Ghielmini (Ospedale San Giovanni Bellinzona) and Prof Dr. K. H. Winterhalter (ETHZ)



Phd: November 1997- November 2000  
Ph.D. Obtained with honors at Universite de Fribourg, but carried out at the University of California San Diego.

Grants/fellowships:

November 1997, Graduate student fellowship from the Swiss National Foundation section Ticino, 33250.- SFr  
November 1998, Graduate student fellowship from the Swiss National Foundation section Ticino, 16000.- SF  
From April 1999, sponsored by UCSD

Job: Ten months (January-October) 1997 in the Laboratory of Oncology at the "Ospedale regionale di Locarno" directed by Prof. F. Cavalli, in the Molecular Biology unit

Scientific interests:

Drugs and pro-drugs for cancer treatment, drug-induced cellular apoptosis, cellular differentiation mechanism, signal transduction in metabolic regulation, hematology. HIV-induced cell death.

Responsibilities:

UCSD, Students instruction

Further personal data:

unmarried

professional skills: Standard and advanced molecular and cellular biology techniques including: mammalian cell culture, transfection, cytotoxicity assay, proliferation assay, immunoblotting, colony forming assays, long-term culture, immunohistochemistry, flow cytometer, electrophoresis, protein purification, photoaffinity labeling, fluorimetric assays, immunoprecipitation, gene expression analysis, cloning, sequencing, PCR-based techniques; Data collection, analysis and presentation, electronic data evaluation, knowledge of specialized literature, knowledge of the who's who in the field of apoptosis

languages: Italian, English, German, French

hobbies: Sports, Snowboard & ski instructor, Graffiti painting

Persons of reference:

Prof. Dr. Franco Cavalli  
Servizio Oncologico Cant.  
Ospedale San Giovanni  
6500 Bellinzona - CH  
Tel (091) 820 9111  
Fax (091) 820 9044  
oncosg@siak.ch

Prof. Dr. Dennis A. Carson  
Department of Medicine  
School of Medicine  
9500 Gilman Drive  
La Jolla, Ca 92093-0663  
Tel (619) 534 5408





Fax (619) 534 5399  
dcarson@ucsd.edu

Prof. Dr. Kaspar H. Wintherhalter  
Laboratorium für biochemie  
ETH-Zentrum  
Universitätstrasse 16  
CH-8092 Zürich  
Tel (01) 632 3131  
Fax (01) 632 1121  
[kaspar.winterhalter@bc.biol.ethz.ch](mailto:kaspar.winterhalter@bc.biol.ethz.ch)

Prof. Dr. Sandro Rusconi  
Institute of Biochemistry  
Science faculty, UNIFR  
Perolles, 1700 Fribourg-CH  
Tel +41 26 300 8656  
Fax +41 26 300 9735  
[sandro.rusconi@unifr.ch](mailto:sandro.rusconi@unifr.ch)